Department of Cell and Developmental Biology
University College London
London

Directional Migration of the Neural Crest:

an interplay between Contact Inhibition of Locomotion and Co-attraction.

Carlos Carmona Fontaine

A thesis submitted to UCL
in fulfilment of the requirements for the degree of
Doctor of Philosophy

November 2010

Abstract

Collective cell migration is recognised as a common feature of cell movement *in vivo*. Despite its importance for both morphogenesis and malignant progression, little is known about how directional and coordinated cell movements are regulated collectively. An interesting example of collective migration *in vivo* is the migration of Neural Crest (NC) cells. NC cells are highly migratory and multipotent embryonic cells, which migrate with remarkable directionality and coordination. In this thesis it is proposed that a mayor force in allowing NC collective directionality is given by local cell-cell interactions. Two main interactions, a repulsive and an attractive one, are identified here and their role in NC migration is analysed. First, it is shown that Contact Inhibition of Locomotion (CIL) is essential for NC migration. These cells collapse their protrusions upon contact with others and polarise towards cell-free regions leading to cell dispersion. Also, it is shown that the non-canonical Wnt signalling is crucial in this process as its members localise at the site of contact. This leads to activation of RhoA and inhibition of cell protrusions in this region. These results provide one of the first examples of CIL *in vivo* and establish a novel role for non-canonical Wnt signalling. Second, a longer-range attractive interaction is also described here in a novel mechanism termed coattraction. It is shown *in silico*, *in vitro* and *in vivo* that when CIL is combined with coattraction, directional collective movements emerge instead of the simple dispersion allowed by CIL. Surprisingly, it was found that the anaphylatoxin/chemoattractant C3a and its receptor C3aR mediate NC coattraction. Finally, it is proposed that CIL and coattraction act together to allow cell collectives, such as the NC, to self-organise allowing a more efficient response to external signals such as chemoattractants and restrictive cues.

I declare that all this work has been done by myself unless otherwise indicated.

Acknowledgements

"Jadis, si je me souviens bien, ma vie était un festin où s'ouvraient tous les cœurs,
où tous les vins coulaient."
Une saison en enfer. Arthur Rimbaud

To my family and everyone who has supported me during this time. Also to the daughters of Mnemosyne, especially to Terpsichore, Calliope, Erato, Euterpe and Urania; and to Parthenope.

I am in debt of the people who has also contributed to this work. Dr. Roberto Mayor for supervision and also for experimental help and collaboration. Dr. Helen Matthews for contributions to the first part of this work, specially in all the experiments regarding Syndecan4 where my contribution was focused to the statistical and image analysis. Dr. Mauricio Moreno for help in molecular biology in general and cloning in particular. I also want to thank Dr. John Lambris and Apostolia Tzekou for essential reagents such as the peptides and blocking antibodies, Dr. Maddy Parsons for FRET analysis, Chaudhary F. Riaz for SEM images and all the people in Mayor's lab for constant help, comments and support. I am also thankful of my second supervisor, Dr. Claudio Stern, for his unconditional support and feedback in the course of this work. In addition, I have to thank Dr. Les Dale, Dr. Ben Steventon and July Carter for critically reading the first draft of this thesis. This thesis would have not been possible without the generous support from Boehringer Ingelheim Fonds and a ORS scholarship.

On a different note, I would like thank Ben, Claudio, Leo, Lorena, Mauricio and Yama for metascientific and metaphysic companion in the lab and its surroundings.

Contents

List of Figures

List of Tables

Abbreviations

ANF: Anterior Neural Fold.

BMP: Bone Morphogenetic Protein.

CoA: Coatraction.

CIL: Contact Inhibition of Locomotion.

CFP: Cyan Fluorescent Protein.

DAPI: 4',6-diamidino-2-phenylindole (nuclear staining).

DIC: Differential Interference Contrast (microscopy illumination technique).

Dsh: Dishevelled. PCP gene.

EMT: Epithelial to Mesenchymal Transition.

EST: Expressed Sequence Tag.

FDX: Fluorescein Dextrane.

FGF: Fibroblast Growth Factor.

FRET: Förster Resonance Energy Transfer or Fluorescence Resonance Energy Transfer.

Fz7: Frizzled 7. G-coupled (Wnt) receptor.

GDNF: Glial-Derived Neurotrophic Factor.

GFP: Green Fluorescent Protein.

H2B: Histone 2B (used for nuclear labells).

IHC: Immunohistochemistry.

MAC: Membrane Attack Complex.

MBL: Mannose-Binding Lectins.

MO: Morpholino antisense Oligo. Plural: MOs.

NC: Neural Crest. Plural: NCs.

ON: Over Night.

PCP: Planar Cell Polarity.

Pk1: Prickle1. PCP intracellular protein.

RDX: Rhodamine Dextrane.

RA: Retinoic Acid.

RFP: Red Fluorescent Protein.

SDF1: Stromal cell-Derived Factor 1.

SEM: Scanning Electron Microscopy.

Syn4: Syndecan 4.

Stb: Strabismus. PCP membrane protein.

VEGF: Vascular Endothelial Growth Factor.

YFP: Yellow Fluorescent Protein.

Part I

Introduction

Chapter 1

Introduction

1.1 Complexity and embryology

> "Indeed, it is evident that we will not truly understand genes and chromosomes until we understand the gene-specified interactions that take a seed, or a fertilized egg, to a mature organism. In short we will not understand life and living organisms until we understand emergence."
>
> Holland (1998)

1.1.1 Complexity

The Greek *Thaumazein*, the philosophical wonder and the astonishment produced by this contemplation, is the origin of all philosophy and knowledge (Schrödinger, 1964). However, phenomena are difficult to attain and to rationalise. Heraclitus said "The one is the many", a contradictory statement that may be interpreted as *The one*, the whole, is too complex to be understood and calculated because in reality *is many* (Nietzsche, 1873). To make problems more comprehensible, they are divided into units, fundamental laws and composing particles that could help to understand the whole. Western epistemology[1] was actually funded in this principle. The atomist school in ancient Greece is a clear, although not unique, case of this. Early pre-Socratic philosophers were searching for *the* element that constitutes all things. Thales of Miletus proposed that everything was derived

[1] from Greek *episteme*, "knowledge" and *logos* "study", thus theory or study of knowledge.

from water, whereas Anaximenes, postulated that it was air. Anaximander, also from the Milesian school proposed that the essential element was the *Apeiron*, an abstract unlimited and undefined element that was at the core of everything, one of the first attempts to decompose matter in something not tangible or evident for the senses. Another interesting idea was that the world is formed by the combination of four elements (earth, wind, water and fire) proposed by Empedocles. Later on, in its dialogue *Timaeus,* Plato integrated these ideas with geometry and the atomism of Leucippus and his student Democritus, into one of the first theories the nature of the physical world (Garcia Morente, 1939). As a common feature, all these philosophers, were trying to *reduce* the complexity of the world to its simplest form, *i.e.* they were reductionists.[2]

Reductionism refers to an approach to knowledge by breaking complex phenomena into simpler parts. Current epistemology, especially in scientific research, is strongly influenced by this reductionist approach. The search of the ultimate *a-tomic* particle, as the one that cannot be further divided and the search of the *gene*, as the unit of inheritance are examples of ongoing large research programs advocated to the problem of *the particle*. For example, consider the amount of resources designated to sequence the human genome or the efforts put into the Large Hadron Collider at CERN or in the Tevatron to provide experimental evidence of the existence, or non-existence, of the Higgs boson. Natural phenomena are complex and intermingled with the environment and perception. This makes virtually any scientific research, or at least its ultimate aim, amazingly complex and sometimes unattainable. Thus, science looks for simpler problems, elements that can be handled to try to understand the problem as a whole. To understand matter, science looks for atoms; to understand heredity, science looks for genes. In other words, is an attempt to try to understand the whole by knowing its conforming particles.

One of the greatest examples of successful reductionism in science is the work of Isaac Newton. His monumental work brought, and still brings, huge advances to our understanding of the physical world by identifying the essential laws that govern motion and mechanics in general. Importantly, it seemed that the same fundamental laws that ruled the inter-

[2]It must be said that their motivations were not only epistemological but there were also important metaphysical and specially ontological aims in these ideas.

actions of everyday things were the still valid when comes to the interactions of celestial bodies. According to Prigogine and Stengers, early in the XIX century, the French mathematician and astronomer Pierre-Simon Laplace announced the dusk of physics: there was no possibility for another Newton because a second world will not exist. To him, Newtonian mechanics were the ultimate explanation of our physical environment and the role of physics then, was only to polish this gem. However, few years earlier, people such as Immanuel Kant would not agreed with Laplace. Indeed, Kant had a much better premonition of the future of science. He stated that living beings were essentially different to unanimated bodies as they *self-organise* and *self-reproduce* (Kant, 1790; Keller, 2007). He questioned the validity of approaching biology with same methods used in classical physics and suggested the necessity for a new kind of science (Karsenti, 2008). By the XXth century, it was evident that even some physical phenomena were not easy to understand in a reductionist way, or even more problematic, the well-defined fundamental laws studied at the particle level, are broken when extrapolated to higher scales (Anderson, 1972). This posed another problem: is the whole just the sum of the parts? As Anderson pointed out, this is typically answered affirmatively but is a common misleading notion. Reductionism does not imply *constructivism*. In other words, *"the ability to reduce everything to simple fundamental laws does not imply the ability to start from those laws and reconstruct the universe."* (Anderson, 1972).

Many phenomena in nature are *non-linear, i.e.* systems whose output is not directly proportional to its input. For example, if we carefully open the water tap, the liquid will run smoothly and we may be able to establish a linear relation between the flux and how much we have opened the tap. However, if we continue to open the tap (assuming there is high pressure in the neighbourhood), the flux will soon become turbulent and not proportional to the turns we have given the tap. Now the system is more complex to understand because it is chaotic. Interestingly, in some irreversible (in the thermodynamic sense) and chaotic processes, such as dissipative systems, order and patterns can *emerge* (Prigogine and Stengers, 1977). A simple but illustrative example is a hot cup of tea cooling down to room temperature. Although the trajectory of its temperature can be complex and modified by random environmental perturbations, its outcome is certain: the

temperature of the room. It is usually said that these systems have an attractor or an attractive state (Milnor, 1985). A more technical example, where patterns emerge due the non-linearity of the system, are Belousov-Zhabotinsky reactions. These reactions are far from the equilibrium and an oscillatory change in the colour of the solution can be observed until it reaches the equilibrium. Amazingly, if these reactions are performed in shallow recipients and looked from the top, the oscillations can be seen as spots, which then grow into a series of expanding concentric rings. These emerged patterns are difficult to explain from the reductionist-constructivist point of view. Moreover, they emerged spontaneously, thus it can be said that this system is self-organised (Nicolis and Prigogine, 1977).

The concept of *self-organisation* is often used to explain phenomena such as dissipative or any other system were new properties emerge from within. Using this concept, scientist such as John Holland, John Von Neumann and Stuart Kauffman, contributed to form the idea of what is known as "complex adaptive systems" or simply *Complexity*. However, their motivation was more biological (and sociological) and computation was their preferred methodology (Holland, 1998). They model complex problems as composed by particles, or agents that interact under some defined rules or properties. They showed that in many situations, a non-linear behaviour emerged from these interactions. Behaviours that were not a simple extrapolation of the interactions at the particle scale. Thus, self-organisation is the *spontaneous* emergence of a global pattern from local interactions among agents or forming particles. Interestingly, agents usually interact only locally *i.e.* with their immediate spatial or temporal neighbours.[3] This concept of local interactions will have a special importance later in this thesis. Importantly, in self-organising systems, there is no "controlling" agent responsible for its organisation. This makes a self-organising process essentially decentralised (non-hierarchical) and collective. In other words, the behaviour of the group is a property that unfolds from the relation of its units and not from any feature of a particular unit or agent. Although this approach may still be considered reductionist, it has some essential differences with the constructivist approach. Instead of looking for principles that govern the behaviour of particles, this approach is looking for simple rules of interactions that may allow the emergence of general principles and complex patterns.

[3]The neighbouring concept may be further expanded to, and not only to, information or energetic neighbours.

Although complexity has been applied to all kinds of phenomena, from oscillatory chemical reactions to weather forecast, biology is probably one of its favourite subjects and as Kant predicted, biology is the new passion for mathematicians and physicists (Cohen, 2004). Complexity has been used to study biology at all scales ranging from animal population dynamics to attempts to decode the outstanding amount of noise in processes such as gene expression (Nowak and Sigmund, 2004; Rao et al., 2002) or in cytoskeleton dynamics (Karsenti et al., 1984). Also, the collective behaviour of insects (Camazine et al., 2001), the firing patterns of the brain (Babloyantz et al., 1985; Ikegaya et al., 2004), and the synchronisation of fireflies in their flashing frequencies (Camazine et al., 2001); are other examples of self-organising problems studied by complexity. Despite the complexity of living beings, the outcome of all these processes is highly reproducible and ordered, showing the robustness of life.

1.1.2 Embryology and Morphogenesis

A fundamental problem in biology is the emergence of functional forms, *i.e.* the emergence of structures and their function and how these two mutually influence each other. In the field of evolution, for example this is an essential topic (see for example Gould, 1977, Chapter 2). Also in cell biology, the control and genesis of the right number, size and disposition of organelles, *i.e.* the form of the cell, is a good example of self-organising complexity (Rafelski and Marshall, 2008).

As Waddington stated, from all the branches of biology, embryology is probably the one that it is most concerned with structure and form (Waddington, 1956, pg. 4). Moreover, from all the complex systems we may be interested to study; arguably one of the most astonishing ones is the formation of an embryo. It is a system where a simple set of initial conditions of entangled components, has the utmost complex outcome: the emergence of the being. The embryological process is a source of endless surprise, a saucerful of secrets, far from being fully understood. Probably as surprisingly as development itself, is the robustness of embryonic development as its outcome is incredibly constant despite its complexity.

The chemical *versus* the physical nature of embryology

> "[...] trying to bridge the current chasm between *Entwicklungsmechanic*, the developmental mechanics of our embryogenesis forefathers, and the modern movement of molecular developmental biology."
> Beloussov and Gordon (2006)

The ultimate aim of embryology is to explain how relations among genetic, epigenetic and environmental factors, unfurl a whole organism. Thus, it is essentially a problem of emergence. In its strict meaning, morphogenesis literally means the generation or production of form. The morphogenetic process has been usually considered a more physical process, separated from the molecular or chemical component of embryology (Wolpert, 1969). For example, when Waddington defines the concept of *Individuation*[4], he separates it into the spatial distribution of the "substances"[5] generated in the cellular differentiation process; and the spatial disposition of cell masses (Waddington, 1956, Chp. XX). Thus, he distinguished the chemical from the physical nature of individuation. In the chemical component, or pattern formation, no actual change of shape is necessarily occurring. In contrast, in morphogenesis, the physical component, the action of forces takes place to change the shape and distribution of cells. Although this separation is sometimes useful, we must be aware of its interrelation (Wolpert, 1969).

Historically, the great and constant advance of molecular biology has biased embryology towards a more chemical, or molecular, approach to development. As Johannes Holtfreter clearly stated:

> "The problem of induction with its chemical implications over-shadowed everything else. Yet the principle of induction is only one of the many devices employed in the process of organizing the egg material. [...] It has become obvious that in order to answer these and similar questions a more thorough knowledge of the physical phenomena involved in morphogenetic processes is needed."
> Holtfreter (1943)

Holtfreter is calling for an equal treatment for two aspects of the same phenomena. In many ways, the physical and chemical natures of embryology are not two different problems, or

[4] A secondary phase in induction that follows *evocation*. It may be thought as the complex response of a tissue after being exposed to a an evoking signal.

[5] Gene, proteins, and he would probably include *plasmagene* products.

not even two linked problems, but two representation of the very same phenomenon. To facilitate the study of the embryo, these aspects may be experimentally dissociated, as say for example, in cultures of isolated migratory cells or in inductive assays performed in tissues, such as *Xenopus* animal caps or chick's extra-embryonic regions. These assays are not very informative of what is happening *in* the embryo but they are useful to test experimental hypothesis. It is important to maintain this dissociation at the experimental level only but not at the conceptual one. As Wilhelm His stated a long time ago:

> "To think that heredity will build organic beings without mechanical means is a piece of unscientific mysticism"
> His, 1888, quoted in Beloussov and Gordon (2006)

Embryology and morphogenesis should be studied from both, its chemical and its physical components. Therefore, in this thesis the problem of morphogenesis will be considered as a whole, as a complex problem where its physical dimension is mapped onto its chemical one. The question about how patterns emerge will be more important than which approach is taken to answer it. This thesis will actually deal with cell migration, a "typical" morphogenetic problem as it involves translocation of cells and thus, change of -cellular and tissular- shapes. Of course, to study cell migration we need to quantify and measure some parameters to obtain a description of the physical aspect of the problem: the spatial displacement of a body over time. Nonetheless, aspects belonging to the chemical nature of cell migration will be also studied here and hopefully both will be integrated. Before going to the subject of this thesis, a brief introduction to cell migration will be presented. An emphasis will be put on topics important for this work such as, cell directionality and polarity, collective migration and the particular cell type this thesis deals with: the Neural Crest.

1.2 The Neural Crest

1.2.1 NC Induction I: patterning the ectoderm.

The neural crest (NC) is an embryonic cell population characteristic of vertebrates that gives rise to a variety of cell types, including neurons and glial cells of the peripheral nervous system, connective tissues of the craniofacial structures and pigment cells of the skin (LeDouarin and Kalcheim, 1999). From studies in chick, amphibian and zebrafish embryos, some of the signals involved in the induction of the NC have been identified, including BMPs, Wnts, FGFs, Notch and RA (reviewed in Knecht and Bronner-Fraser, 2002; Aybar and Mayor, 2002). The traditional model of NC specification stated that at early stages of crest induction an intermediate level of BMP was necessary, neither so high as to specify ventral epidermis nor so low as to specify neural tissue (LaBonne and Bronner-Fraser, 1998; Marchant et al., 1998). Subsequently, the so called "posteriorising signals", coming from the back of the embryo (but also from the underlying mesoderm), such as Wnts, FGFs and RAs completed NC induction (LaBonne and Bronner-Fraser, 1998; Aybar and Mayor, 2002). This two-step induction process would then control the transcription of genes that are gradually restricted to the NC region.

However, the process of NC induction is likely to be more complex. Steventon et al. 2005 proposed a more functional two-step model of NC development. First, there is an inductive process *per se*, involving cell signalling, and cell specification. Then, there is a maintenance process characterised by the up-regulation of survival signals and effector genes (Steventon et al., 2005). A similar mechanism has been proposed by other authors (Sauka-Spengler and Bronner-Fraser, 2008).Steventon et al. 2009 showed that the signalling process, previously underscored as an initial step, is required through all NC development giving an interesting turn to the model. The work also shows that the tissues responsible for this sequence of signals change as their relative position to the NC is modified over time (Steventon et al., 2009). This emphasis in timing of signals and in the precise identification of neighbouring tissues, allows a sequential model of NC induction (Steventon, 2008). First, there is a primordial patterning of the ectoderm where the

neural tissue starts to differentiate from non-neural ones. At their interface, the neural plate border is formed, a process that requires high levels of RA and FGF but surprisingly, low Wnt levels. Neural border formation probably occurs by late blastula and/or early gastrula stages and thus, it precedes the steps described above. This formed neural plate border is the region competent for NC *evocation*, the first step of induction (Waddington, 1956). NC evocation requires high Wnt and intermediate BMP levels. Also, during this process, FGF signalling is maintained while RA signalling seems to be lowered. Finally, signals coming from the underlying intermediate mesoderm support a stage of maintenance, or individuation. This later process seems to require high BMP, Wnt, FGF and RA levels (Steventon, 2008).

This sequential model fits better with the experimental data available. For example, it explains why the NC does not develop at the anterior neural fold (ANF). It has been shown that the interaction between the neural plate and the non-neural ectoderm is sufficient to induce NC cells (Moury and Jacobson, 1990; Selleck and Bronner-Fraser, 1995; Mayor et al., 1997). Nonetheless, it is well established that no NC are formed at the ANF, where a neural plate/non-neural ectoderm border also exists. Interestingly, analysis of the expression of some of the earliest NC markers, such as *snail* and *pax3*, showed a transient expression at the ANF, which disappears at the early neurula stage, suggesting that the NC is transiently specified at the ANF (Carmona-Fontaine et al., 2007). Based on this observation, it was shown that as gastrulation goes on, a strong inhibitory signal precludes NC formation to more posterior regions. This is mediated by the diffusible Wnt-inhibitor Dkk1 produced by the prechordal mesoderm (Carmona-Fontaine et al., 2007). Thus, the initial conditions required to form the neural plate border, seem to be present at the prospective ANF during early gastrulation. However, the inhibition of Wnt signalling by the prechordal mesoderm, halts or inhibits NC evocation and possibly redirects the differentiation of these cells towards a placodal fate (Litsiou et al., 2005; Carmona-Fontaine et al., 2007).

1.2.2 NC Induction II: formation of a tissue competent for migration.

The link between these inductive mechanisms and the acquisition of a migratory identity is not clear. However, the process of NC induction leads to the formation of a tissue capable of migration. For example, the ANF can be transformed into NC cells via the activation of Wnt signalling (Carmona-Fontaine et al., 2007). Surprisingly, these transformed cells migrate as normal NC cells. Thus, in the process of NC induction, an otherwise epithelial cell population acquires all the features required for cell migration. Which are the molecules and transcription factors required for this to occur?

It is known that one of the first steps for NC migration is a transition from an epithelial and relatively static tissue configuration to a mesenchymal cell population. This is also an important mechanism for the metastasis and migration of cancer cells and it is known as Epithelial Mesenchymal Transition (EMT). Genes from the *snail* family have an essential role in this process (Barrallo-Gimeno and Nieto, 2005; Thiery et al., 2009). Interestingly, these genes were first described in the NC were they also control EMT (Nieto et al., 1992, 1994; Mayor et al., 1995). During EMT, molecules such as cadherins are differentially regulated. For example, the activity of E-cadherin, is usually down-regulated during cancer EMT and it is known that Snail1 and Snail2 are key factor in this repression (Cano et al., 2000; Bolos et al., 2003). A similar event occurs in the NC where it is known that *cadherin-6B*, which is strongly expressed in premigratory NC cells, is down-regulated at the onset of migration (Nakagawa and Takeichi, 1995, 1998) in a Snail2-dependent manner (Taneyhill et al., 2007). Other events that occur during neural crest EMT such as the up-regulation of cadherin-7 (Nakagawa and Takeichi, 1995, 1998) and connexin-43 (Lo et al., 1997), are likely to be controlled by the same or other "NC-specific" transcription factors.

Migratory cells are subject to more stress, or *anoikis*.[6] Interestingly, cancer cells develop an intrinsic resistance to *anoikis* (Simpson et al., 2008). NC cells express many genes related with cell survival such as anti-apoptotic and proliferation factors (Kelsh et al., 2000; Trbulo et al., 2004; Bonano et al., 2008). These genes have been involved in the

[6] Literally, Greek word for *"Homelessness"*.

maintenance of the NC population but it is possible that they can also be playing a role in protection from *anoikis*.

Many more mechanisms are likely to be required for cell migration in general and for NC migration in particular. To understand these mechanisms better, an introduction to cell migration, followed by a small description of NC migration, are now presented.

1.3 Cell Migration

Cell migration is a process ubiquitous in nature. Even some of the simplest organisms such as prokaryotes, show complex and robust biochemical networks that allow them to migrate. Moreover, they can sense the chemical composition of their environment to follow gradients of nutrients and other molecules (Barkai and Leibler, 1997; Alon et al., 1999). Similarly, cell migration is essential for unicellular eukaryotes such as amoebae and *Chlamydomonas*. Interestingly, it has been recently shown that the active motility of *Chlamydomonas* is essential for their distribution along water columns, which have great impact in marine ecosystems (Durham et al., 2009). Multi-cellular organisms, of course, do not use cell migration as a mechanism of locomotion. However, it is a central process in their formation and subsistence.

From the quest of the sperm for the egg to the neuronal wiring occurring in the developing brain, cell migration is required throughout the complete embryological process. Likewise, during adult life, cell migration is responsible to a great degree for the maintenance of the body. Vasculogenesis (and regeneration of the vascular network after injury), immune responses and wound healing, are typical mechanism dependent on cell migration. Cell migration must be tightly regulated. In fact, disregulation in the control of cell migration can lead to, or exacerbate, human diseases such as cancer, atherosclerosis and chronic inflammatory pathologies. Thus, cell migration can be considered then as an essential mechanism of cell organisation and coordination.

1.3.1 General mechanisms of cell migration

How is cell migration regulated in eukaryotes? Several years ago, Lauffenburger and Horwitz proposed a widely accepted cyclic model of cell migration (see also Ridley et al., 2003; Friedl and Wolf, 2003; Rafelski and Theriot, 2004; Vicente-Manzanares, 2005). The first step is the -morphological and molecular- polarisation of the cell. This polarisation generates a cell that has a front and a rear end. Second, a ruffling membrane extension propelled by dynamic cytoskeletal machinery is formed at the front end. Lamellipodia, flat lamella-shaped membrane processes, are typical examples of these membrane protrusions. Other typical membrane protrusions are filopodia, actin-rich rod shaped membrane extensions generally considered to help the cell to sense the environment (Mattila and Lappalainen, 2008).

A third step consists of the formation and stabilisation of attachments to the substrate in these ruffling protrusions. These cell-substrate adhesions, at least *in vitro*, adopt a punctuated distribution called focal contacts (Curtis, 1964; Abercrombie and Dunn, 1975; Izzard and Lochner, 1976). Most of these focal complexes are not stable and they are quickly disassembled. However, some of these adhesion points mature into larger structures referred as called focal adhesions. The cytoskeleton is also crucial in this stage but its protagonism is now shared with adhesion molecules such as integrins and adaptor proteins that join the cytoskeleton to the molecules that provide the physical adhesion to the substrate molecules. Also, actin microfilaments can form structures associated with myosin motors, called stress fibres, which probably help in intracellular trafficking and, because they can attach to focal adhesions, they can execute force. Once the front of the cell has attached to the substratum, it is able to render forces of traction and contraction. The first one will produce the actual displacement movement by reaction while the second one will contract the cell allowing it to recover it initial size increased after the extension step (Lauffenburger and Horwitz, 1996; Ridley et al., 2003; Friedl and Wolf, 2003; Vicente-Manzanares, 2005).

The rear end of migratory cells is also strongly attached to the substrate. The fact that only specific regions of the cell are attached gave strong support to the idea that the

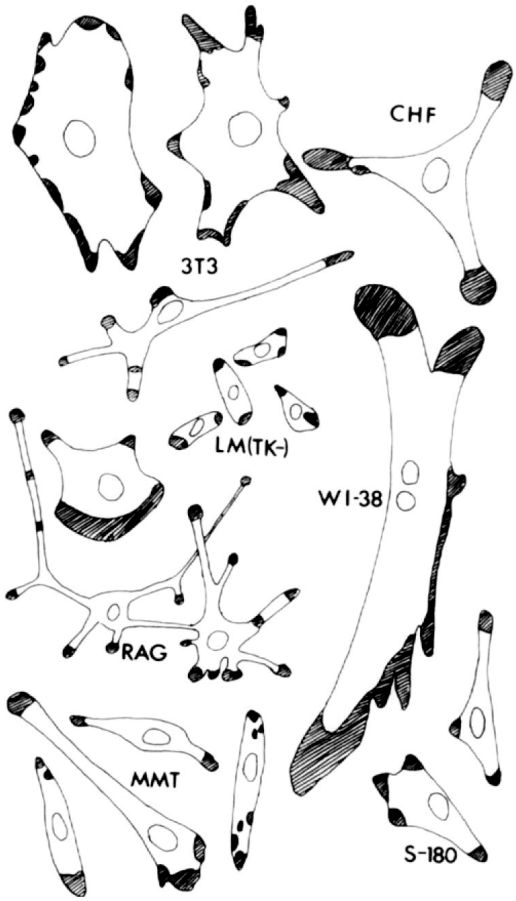

Figure 1.1: **Points of adhesion in different cell types.** Reprinted from Harris 1973, with permission from Elsevier.

distribution of molecules in the cell body was spatially regulated. A figure from one of the first publications that showed this is reproduced here (Figure 1.1, reproduced from Harris, 1973). To be able to contract the rear edge, focal adhesions in this region must be disassembled first, a mechanism that is not well understood.

This model is a conceptualisation rather than a description of cell migration as all these mechanisms overlap. Probably the time-lapse photography approach, typically used to study cell migration, is one of the reasons why this cyclic and fragmented view of cell locomotion has prevailed. Nonetheless, it was proposed as a way to integrate the large number of molecules involved in cell migration. In addition, it is didactic and integrates both, the temporal and spatial regulation of molecular dynamics in migratory cells (Lauf-

fenburger and Horwitz, 1996). Some aspects of cell migration, relevant to this thesis, will be treated with greater detail in further sections. In particular, how a cell is polarised and how is migration regulated in groups of cells.

1.3.2 Polarisation in cell migration.

Cell polarity and directional migration

A keystone of directional cell migration is cell polarisation (Ridley et al., 2003). The model presented in Lauffenburger and Horwitz 1996 aims to give a comprehensive view of cell migration. However, it does not explain how a cell is polarised at the first instance and how this polarity is maintained in directional migration.

To polarise a cell its initial symmetry must be broken. Interestingly, cells are capable of spontaneous polarisation (Sohrmann and Peter, 2003; Wedlich-Soldner et al., 2003; Altschuler et al., 2008). This spontaneous polarisation is thought to relay in positive feedback loops that amplify small differences in the concentration of signalling molecules in the cytoplasm. These types of mechanisms, have been shown to be sufficient to obtain cells with a single and stable point of polarisation (Altschuler et al., 2008). However, cells usually migrate towards specific regions and targets. Thus, this spontaneous mechanism of polarisation needs to be integrated or may be overridden by a polarity mechanism relaying on external cues.

External spatial cues, including chemoattractants and chemorepellents, are usually considered to explain the persistent orientation of cell polarity that leads to directional migration. However, the extracellular matrix and other topological features of the migratory space are also important (Petrie et al., 2009). The molecular bases of these mechanisms have been widely studied and reviewed elsewhere (see for example Kay et al., 2008; Petrie et al., 2009). In brief, the consensus is that small changes in the environment are amplified and reshaped to form an intracellular gradient. For example, it is known that *Dictyostelium* cells can follow gradients of cyclic-AMP (cAMP), even when these gradients are very shallow (Kay et al., 2008; King and Insall, 2009). The key component of this response is that

small differences in the activation levels of the cAMP receptor, are amplified to generate an heterogeneous distribution of molecules such as PI3K at the front of the cell and high levels of PTEN at the back (Ridley et al., 2003; Kay et al., 2008). Importantly, the distribution of these and other molecules, such as Rho-GTPases (Heasman and Ridley, 2008), members of the PCP pathway (Veeman et al., 2003; Simons and Mlodzik, 2008) and PAR proteins (Macara, 2004), have profound effects on cell structures and processes such as the cytoskeleton, cell trafficking and membrane activity. In addition, these molecules are known to mutually regulate each other allowing a coherent cell response and polarisation (Ridley et al., 2003; Petrie et al., 2009). In some ways, this transduction mechanism proposed for chemotaxis, is not too different to the one described for spontaneous cell polarisation. It seems that cells are able to amplify subtle cytoplasmic differences and that this amplification mechanism can be triggered spontaneously or biased by external cues.

The PCP pathway and the role of Rho-GTPases will be briefly reviewed, as they are relevant for this thesis.

The PCP pathway

The Planar Cell Polarity (PCP) or non-canonical Wnt signalling pathway was first described in *Drosophila,* where a number of mutations were linked with the disruption of bristles and hairs on the adult cuticle (Gubb and García-Bellido, 1982). In the *Drosophila,* wing, epithelial cells are highly polarized, with a single hair outgrowth forming at the distal end of each cell. Mutations in PCP genes cause loss in cell polarity in this tissue, with hairs forming in a disorganized pattern (Veeman et al., 2003; Simons and Mlodzik, 2008). In vertebrates, PCP signalling also regulates cell polarity during a number of different developmental processes including neural tube closure, cochlear hair orientation and ciliogenesis (Wang and Nathans, 2007; Simons and Mlodzik, 2008).

The precise description of the members of the PCP pathway is not simple. First, it is also known as non-canonical Wnt signalling. Both, canonical and non-canonical Wnt signalling, involve the binding of a Wnt ligand to its cognate receptor Frizzled (Figure 1.2).

However, different Wnts and co-receptors determine if the concomitant signalling cascade will be canonical or non-canonical. The problem is that there is not one, but many "non-canonical" Wnt signalling (Semenov et al., 2007). The main components studied in this thesis are depicted in Figure 1.2. The second source of confusion is related with the PCP itself. As mentioned above, "PCP molecules" or genes were identified in polarity mutants in *Drosophila* epitheliums. A big proportion of the pathway has been constructed based in genetic rather than biochemical interactions. Thus, it is possible that there is more than one "PCP pathway", which may even compete (Lawrence et al., 2007; Chen et al., 2008).

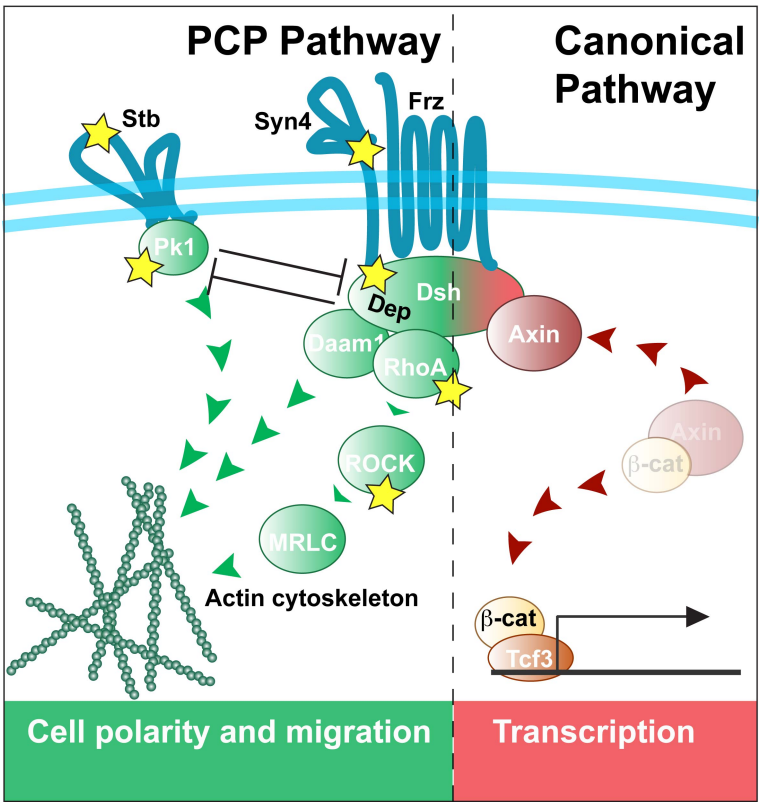

Figure 1.2: **The PCP pathway.** A simplified version of the PCP pathway based on (Montcouquiol et al., 2006; Semenov et al., 2007; Lawrence et al., 2007; Vladar et al., 2009). Stars represent members of the pathway relevant for this work. See main text for further details.

A simple and conservative model of the PCP is presented here (Figure 1.2) and is based in models proposed elsewhere (Montcouquiol et al., 2006; Semenov et al., 2007; Lawrence et al., 2007; Vladar et al., 2009). First, a "non-canonical" Wnt, Wnt11 for example, binds to a Frizzled receptor such as Frz7. This binding recruits a key component of the pathway,

Dishevelled (Dsh), to the membrane. Dsh is also involved in the canonical pathway, but only when Fz is interacting with specific co-receptors such as LRP5/6 (Montcouquiol et al., 2006). A recently described transmembrane modulator of the non-canonical Wnt pathway is Syndecan4 (Muñoz et al., 2006). Dsh contains a DEP domain, which is essential for its function in the non-canonical pathway (Tada and Smith, 2000). This domain activates directly and indirectly many other proteins such as Daam1 and RhoA (see Figure 1.2). Other proteins that interact with Dsh include PARs and PKCγ proteins. Many of these activated proteins influence cell polarity, independently of transcription via modulation of the cytoskeleton (Figure 1.2). In the next section, the case of RhoA is treated in greater detail.

Strabismus (Stb) is a transmembrane protein that modulates PCP in *Drosophila* by competing with Fz for the interaction with another PCP protein, Flamingo (Semenov et al., 2007; Chen et al., 2008). It is not clear whether a similar regulation occurs in vertebrates but it is known that vertebrate-homologues of these proteins are also involved in PCP-dependent mechanisms such as in fish gastrulation (Carreira-Barbosa et al., 2009).

Rho-GTPases in cell migration.

Directional cell migration is achieved by the polarised formation of cell protrusions at the front and the contraction of stress fibres at the trailing edge (Figure 1.3). The typical Rho GTPases - RhoA, Rac1 and Cdc42 - play a critical role in controlling cell polarity. These three Rho-GTPases regulate different aspects of cytoskeleton dynamics. Cdc42 has been shown to be involved in controlling the actin cytoskeleton present in protrusions known as filopodia (Gupton and Gertler, 2007; Mattila and Lappalainen, 2008). Rac1 promotes the formation of lamellipodia by regulating actin polymerization (Jaffe and Hall, 2005). The three Rho isoforms - RhoA, RhoB and RhoC - can induce stress fibre formation (Wheeler and Ridley, 2004). The general view is that in polarized cells Rac1 and Cdc42 are active at the front where they promote the formation of cell protrusions, while RhoA is active at the back where it controls cell contraction. In addition, a clear mutual inhibition between Rac1 and RhoA has been established (Rottner et al., 1999). However, recent studies

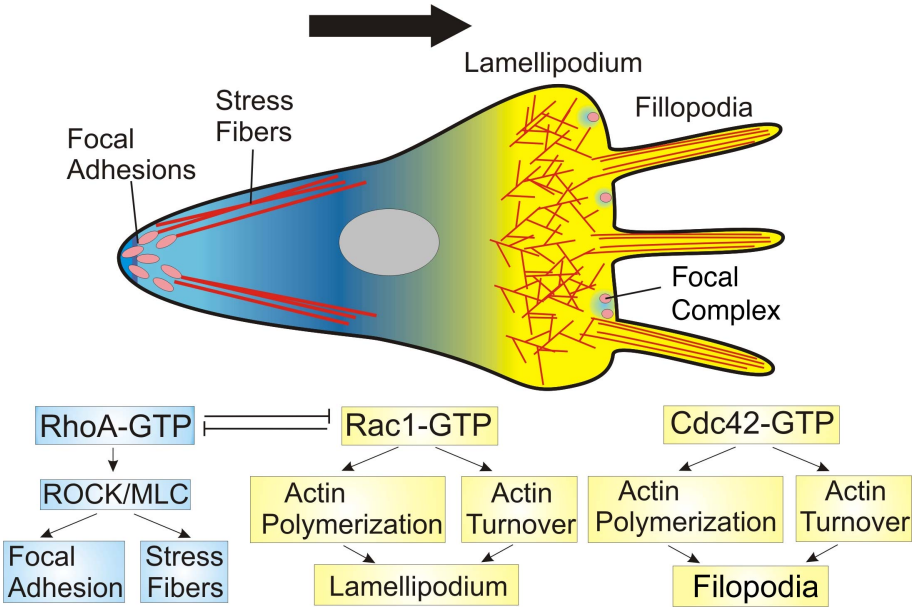

Figure 1.3: **Rho GTPases and cell protrusion control.** Reprinted from Mayor and Carmona-Fontaine 2010, with permission from Elsevier.

have shown that all three GTPases can be activated at the front of migrating cells, where RhoA has a role in the initial events of protrusion formation, whereas Rac1 and Cdc42 are involved in reinforcement and stabilization of newly expanded protrusions (Pertz et al., 2006; Machacek et al., 2009).

In addition to their role in actin dynamics, the Rho GTPases also control polarized adhesion to the substratum during directional migration. Small focal complex structures are localized in the lamellipodia of most migrating cells, and are important for the attachment of the extending lamellipodium to the extracellular matrix (Lauffenburger and Horwitz, 1996). It has been shown that Rac1 is required for focal complex assembly (Nobes and Hall, 1995; Rottner et al., 1999). Focal complexes can be disassembled as the cell lamella moves over them or can mature into focal adhesions induced by RhoA (Rottner et al., 1999).

For many cells the final step of the cell migration cycle is the retraction of the back in order to move forward. This cell body contraction is dependent on actomyosin contractility and can be regulated by RhoA via ROCKs (also known as Rho-kinases) to affect

Myosin Light Chain (MLC) phosphorylation, both by inhibiting MLC phosphatase and by phosphorylating MLC (Kaibuchi et al., 1999).

1.3.3 Collective Migration

An emerging concept in the field of cell migration is the idea that most cells do not move as isolated entities *in vivo* but they interact with their neighbours during migration. Even cells of the immune system that can migrate singly must interact with other non-motile cells along their migratory paths. Thus, cells must have their locomotory machinery adapted to these constant interactions. This has prompted scientists for decades to try to investigate the "social behaviour of cells" (Abercrombie and Heaysman, 1953). However, exactly how cells interact during migration remains to be understood. This is a central issue in this thesis; therefore, the different types of collective migration will be outlined.

Types of collective migration

In multicellular organisms, cells often move in groups rather than as singular cells. Cell migration in loosely or closely associated groups has been called collective cell migration (reviewed in Friedl and Wolf, 2003; Montell, 2008; Friedl and Gilmour, 2009; Rørth, 2009; Weijer, 2009). Collective cell migration is now a widely recognized mode of migration during embryogenesis and cancer.

There is a wide variety of collective cell migration, from a sheets of migrating cells found in carcinomas and in head mesoderm of amphibian embryos (Figure 1.4a, Winklbauer et al., 1992; Bell and Waizbard, 1986; Nabeshima et al., 1998), to closely associated clusters of cells such as the migration of the lateral line in zebrafish, border cells in *Drosophila* embryos and melanomas (Figure 1.4b, Haas and Gilmour, 2006; Day et al., 1981). Other cells are organized in chains such as *Drosophila* myoblasts and squamous cell carcinoma (Figure 1.4c, Richardson et al., 2007; Gaggioli et al., 2007). Another example of this, is the migration of endothelial cells during sprouting in angiogenesis. Another mode of collective cell migration has been called streaming (Figure 1.4d), and has been found in

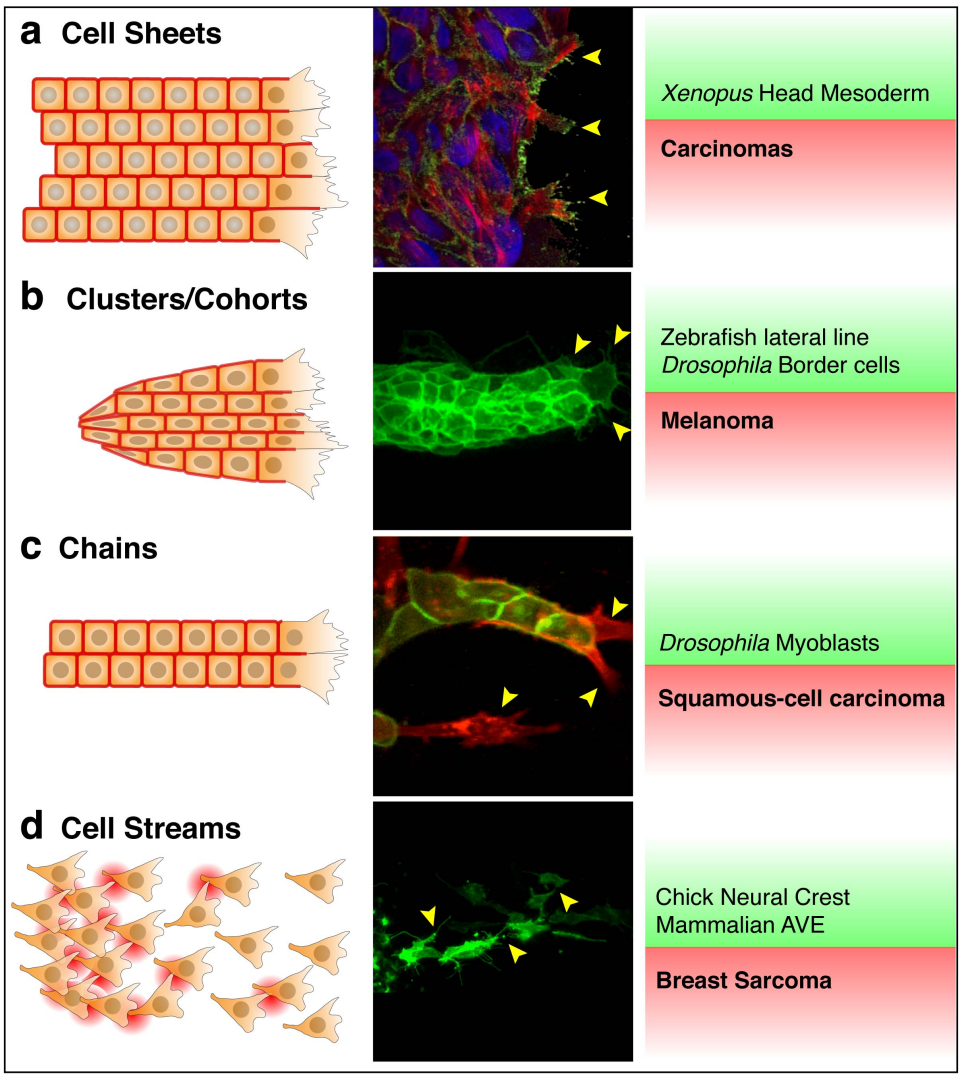

Figure 1.4: **Examples of collective cell migration** First column: schematic representation of different migratory types. The regions where cells are interacting are depicted as a red border. Second column: examples. (a) Intestinal epithelial cells. (b) Zebrafish lateral line. (c) Fibroblast-leaded squamous cell carcinoma invasion. (d) Avian Neural Crest. Yellow arrowheads show localized protrusion formation. Third column: examples of these different types of migration in health (green background) and disease (red background). AVE: Anterior Visceral Endoderm. Reprinted from Mayor and Carmona-Fontaine 2010, with permission from Elsevier.

the migration of neural crest cells, mammalian endoderm and possibly in some breast carcinomas (Teddy and Kulesa, 2004; Matthews et al., 2008b; Carmona-Fontaine et al., 2008b; Hegerfeldt et al., 2002). In this kind of migration, the cells move as a loose cluster in which individual cells can be identified but are constantly interacting with each other.

Despite the diversity within collective migration, there is a common theme through all of them: they all have major protrusions at the leading edge and show a high degree of organization and coordination during migration. The degree of inhibition of cell protrusions between cells is variable and in some cases, cryptic protrusions are observed between cells (Farooqui and Fenteany, 2005; Vasilyev et al., 2009). However, it is tempting to speculate that there is a mechanism of inhibition of protrusions in cell clusters during collective cell migration. Moreover, these cell collectives are capable of directional migration. How is cell polarity and directionality regulated in cell groups? Is there any link in between the inhibition of protrusions and cell polarity?

An important part of this thesis is dedicated these to these questions. Which mechanism may account for the inhibition of protrusions during collective migration and how is this connected with cell polarity. Here it is proposed that Contact Inhibition of Locomotion is an important player in these processes.

1.3.4 Contact Inhibition of Locomotion

The concept of Contact Inhibition of Locomotion (CIL) describes the observation that a cell changes the direction of its movement after contacting another cell. It gradually emerged from the work of Abercrombie and Heaysman starting in 1953. They aimed to study how the behaviour of a cell is influenced by other cells, *i.e.* their *"social behaviour"*.

Heaysman and Abercrombie observed what happened when two embryonic chicken heart explants were placed in close proximity. Collisions occur between fibroblasts migrating from opposing explants. At the time they started their experiments, they could not perform detailed microscopic observations. Instead, they carried out careful macroscopic measurements obtaining statistical parameters to describe cell behaviour. Nonetheless, they made at least two crucial observations. First, they observed that fibroblasts will lower their speed in proportion to the number of cells they encounter. Thus, contact with or the proximity to other cells will reduce cell motility (Abercrombie and Heaysman, 1953). Moreover, they observed that at the region where the two explants encountered each other, the fibroblasts would never clump on top of each other. Instead, they will halt their mi-

gration or disperse elsewhere (Abercrombie and Heaysman, 1954). They concluded that a cell would preferentially adhere to the substrate rather than to its neighbouring cell. They called this restriction CIL and proposed that the tendency of alignment between neighbouring cells and the monolayering of explants were outcomes of CIL too (Abercrombie and Heaysman, 1954). This last observation was probably the first description of collective cell polarity.

Later on, with improved observation tools, Abercrombie and colleagues, added important cellular details to the process such as the retraction of the cell protrusion after contact (Abercrombie and Dunn, 1975) and that the ruffling activity of the membrane will be restarted elsewhere in the cell perimeter (Abercrombie and Ambrose, 1958). Thus, CIL will more often lead to the redirection of colliding fibroblasts than to stop their movement (Abercrombie and Ambrose, 1962; Abercrombie, 1970). All these observations were integrated into a more complete definition of CIL as: *"the phenomenon of a cell ceasing to continue moving in the same direction after contact with another cell"* (Abercrombie, 1979).

During the following years, different degrees of CIL were found in a large number of healthy and cancerous cell types (reviewed in Abercrombie, 1979). Efforts were exerted to try to observe CIL *in vivo* with only limited success (Bard et al., 1975; Bard and Hay, 1975). At the same time, the implications of CIL in migration and morphogenesis were disputed (Davis and Trinkaus, 1981; Erickson and Olivier, 1983; Trinkaus, 1985). On the other hand, important advances in the field of cell migration were made with the identification of several molecular components that allowed the generation of models of cell polarization and chemotaxis (Lauffenburger and Horwitz, 1996; Ridley et al., 2003; Kay et al., 2008; King and Insall, 2009). These important new discoveries on directional cell migration were unmatched by a sufficiently detailed molecular understanding of CIL. Thus, two main issues about CIL remained unsolved and are dealt with in this thesis: do cells exhibit CIL *in vivo*, and what are the molecular basis of CIL.

1.4 Neural Crest Migration

The migration of the NC is one of the most remarkable examples of coordinated cell migration. It comprises a large cell population that, from the dorsal neural tube, populates almost the entire embryo. This emigration from the neural tube is accomplished with a delicate order and cell coordination.

Depending on their original position along the anterior-posterior axis, the NC is subdivided into cranial, cardiac, vagal, trunk and sacral regions. These NC subpopulations adopt different migratory routes and they trend to produce different derivatives. Whether NC cells depart the neural tube already specified or they leave the tube as undifferentiated progenitors that will acquire their respective fate at the final destination, is still a controversial issue. Either way, NC migration is an essential mechanism that bridges the specification of these cells with their final and diverse roles along the whole body.

Cephalic NC cells migrate in three streams, mandibular, hyoid and brachial, that colonise the branchial arches to form most of the skeletal, muscular and connective tissues of the head, including odontoblasts (Kontges and Lumsden, 1996). In addition, together with the paraxial mesoderm, they form the neck and shoulders (Matsuoka et al., 2005). Moreover, they contribute to the cranial sensory ganglia, the thymus and the cornea (Sadaghiani and Thibaud, 1987).

Cardiac NC cells can be considered a sub-region of the cranial NC as they are initially located in between the otic placode and the third somite in avian embryos (Kirby and Waldo, 1990). However they are studied separately because they form other derivatives such as melanocytes and, notoriously, the connective and muscular components of mayor arteries and the septum in the heart.

Trunk NC cells migrate through two main pathways that define also their derivatives. The first one, is a route tangential to the surface of the embryo, *i.e.* beneath the epidermis. This NC subpopulation mainly differentiates into melanocytes and other pigmented cells (LeDouarin and Kalcheim, 1999). A second subpopulation adopts a deeper pathway in between the somites and the neural tube. These NC cells form the sensory and sympathetic

ganglia, Schwann and chromaffin cells (LeDouarin and Kalcheim, 1999).

The enteric nervous system, formed mostly by parasympathetic ganglia, is a complex and autonomous nervous system that controls the behaviour of the digestive tract. This system is formed when vagal NC cells (originating from the neck region) meet sacral NC cells (originating from the sacral region). Failures in this process can result in serious congenital problems such as the Hirschsprung's disease (Heanue and Pachnis, 2007).

This thesis will focus on the migratory mechanisms of cranial NC cells both, *in vivo* and *in vitro*. However, the accent of this work will be in general migratory properties rather than in particularities of cranial NC migratory pathways or derivatives. Some of the main questions that will be asked in this work are, how is directional NC migration controlled? How does a group of NC cells find its migratory route? Do cell-cell interactions influence their migration? However, before answering these questions, we shall briefly review what is known about NC directional migration so far.

1.4.1 Molecular landscapes in NC migration

As mentioned in Section 1.2.2, NC specification, can be seen from two points of view. First, is a process that, by patterning the ectoderm, locates the NC at a defined and specific region of the embryo. However, it is also a process that takes a group of static epithelial cells into a mesenchymal migratory population (Figure 1.5a-c). By the end of the induction, a NC cell is a highly migratory mesenchymal cell. Still, they will only migrate when in a permissive substrate and environment.

NC migration must be finely tuned in order to direct the correct number of cells to the right destination. Moreover the migratory routes are very well defined and their migration is highly persistent. The definition of these paths may be mechanic, *i.e.* the NC cells migrate through the free spaces available in between surrounding structures such as brachial pouches. This is probably an important factor but is not sufficient to restrict the migratory pathways. Strong evidence show that the extracellular matrix in conjunction with signals from neighbouring tissues create a molecular landscape that defines the route

taken by a NC cell.

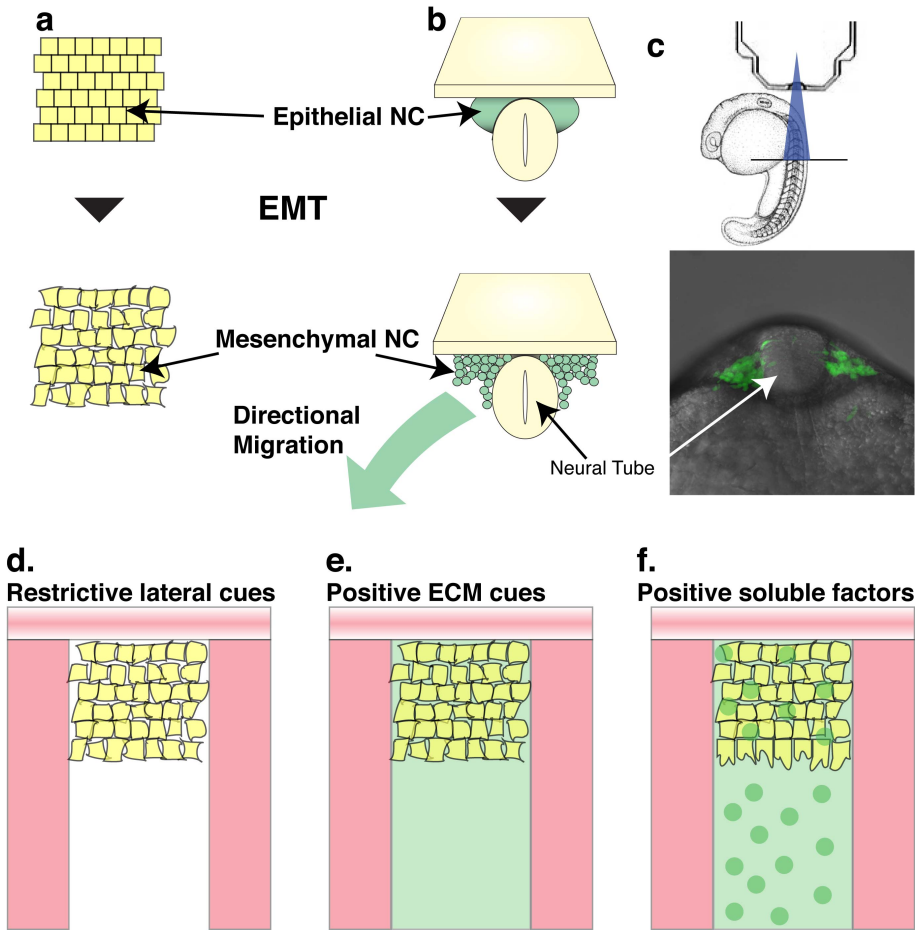

Figure 1.5: **Key factors in NC migration** a. EMT is the first step in NC migration. It transforms an epithelium of cells into a mesenchymal-like population. b. The process of EMT is schematised with respect to the neural tube to highlight the origin of NC cells. c. NC cells visualised *in vivo* after EMT. Top panel shows the orientation of the embryo to allow an optical transverse section as shown below. NC cells are labelled in green. d-f. External factors important for NC directional migration *in vivo*. d. Restrictive lateral cues (red areas). e. Permissive elements of the ECM (green area). f. Chemotactic and/or chemokinetic factors that promote NC migration (green dots).

Definition of a migratory territory. Restrictive lateral cues.

It is known that areas surrounding the normal pathway of NC migration have repulsive cues that restrict their migratory space. These signals include semaphorines, ephrines and neuropilin for which NC cell have the specific cognate receptors. These signals provide

a corridor-like space in which NC streams migrate (Figure 1.5d). Interestingly, these repulsive cues are differentially expressed along the body axis and NC receptors seem to change accordingly. Thus, there seems to be a code in these molecules that may help to the correct direction of different NC subpopulations to their different targets (see Kuriyama and Mayor, 2008, for a review).

Definition of a migratory territory. Positive ECM cues.

Most of the evidence for the role of the extracellular matrix (ECM) in NC migration comes from studies using the trunk NC of avian embryos. ECM proteins such as fibronectin, collagen, laminin and vitronectin have been involved in trunk NC migration (reviewed in Perris and Perissinotto, 2000). Migration on these substrates depends on the expression of adhesion molecules such as integrins in NC cells (Perris and Perissinotto, 2000). These factors provide a permissive substrate in which NC can migrate (Figure 1.5e). More recently, it has been shown a similar mechanism for cranial NC in amphibian embryos (Alfandari et al., 2003). However, in this case only fibronectin has been shown to be permissive as integrin $\alpha 5 \beta 1$, present in NC cells, binds to it (Alfandari et al., 2003).

A contrary ECM component is aggrecan, which seems to act as a repulsive cue in NC cells. Interestingly, aggrecan is expressed in regions complimentary to the permissive ECM elements (Perissinotto et al., 2000). Thus, its function is also likely to be related with limiting the territories for NC migration (Perris and Perissinotto, 2000; Perissinotto et al., 2000).

Positive soluble factors.

There is a long history and debate about the existence of chemoattractants for the NC or not (see for example, Erickson, 1985; Perris and Perissinotto, 2000; Kuriyama and Mayor, 2008). This is why in this section they have been called positive soluble factors (Figure 1.5f). Nonetheless, recent evidence supports the possibility of NC chemoattractants. For example, Jiang et al. 2003 showed that enteric NC cells express the Netrin receptor, DCC,

and that submucosal and pancreatic ganglia express Netrins. Either these tissues or pure Netrins can attract enteric NC cells. However, they also showed an effect of this protein in NC survival making difficult to dissect the contribution of chemoattraction (Jiang et al., 2003). Similarly, it was shown that GDNF is a paracrine factor that attracts NC cells to the digestive tube (Young et al., 2001).

A recent work in chick cranial NC cells, show a role for VEGF in directing NC migration. Again, this work shows *in vitro* NC attraction towards a source of VEGF or towards the endogenous source of it (the second branchial arch McLennan et al., 2010). Another factor that has been studied as a potential NC attractant is Sdf1 (or CXCL12) as NC cells express its receptor CXCR4. For example, Sdf1 signalling is required for the formation of dorsal root ganglia (Belmadani et al., 2005). However, chemoattraction was not tested directly in this work. Similarly, studies in zebrafish have shown a role for Sdf1 in NC migration affecting craniofacial development (Killian et al., 2009) and melanophore patterning (Svetic et al., 2007). Again, although these works show an important role for Sdf1 in NC migration, they do not show it actually acts as a chemoattractant.

More recently, a work in *Xenopus* cranial NC, showed that Sdf1 attracts these cells *in vitro* (Theveneau et al., 2010). An interesting observation of this work is that NC cells will respond efficiently to Sdf1 only when in a group. This observation, together with this thesis and a publication related to it (Carmona-Fontaine et al., 2008b), lead to the conclusion that CIL is required for collective chemotaxis (Theveneau et al., 2010). Nevertheless, the problem whether Sdf1 actually acts as a chemoattractant *in vivo* remains unresolved. Some evidence suggest the contrary as Sdf1 mRNA seems to be distributed in all the ectoderm surrounding the NC and not as a gradient (Theveneau et al., 2010), although is still possible that there is a gradient at the protein level. More importantly, under some conditions, NC cells *in vivo* can migrate in the opposite direction *i.e.* going against the alleged gradient (this thesis, Figure 4.9).

In conclusion, NC *in vivo* migrate directionally because of their mesenchymal features given by EMT (Figure 1.5a-c), in combination with the mechanical and molecular restrictions of the surroundings that form a "corridor" (Figure 1.5d), where ECM permissible

and soluble positive (maybe chemotactic) factors, lead to the directional polarisation of NC cells (Figure 1.5e,f). However, NC also can migrate directionally *in vitro*, where more of these signals are absent (Matthews et al., 2008b; Carmona-Fontaine et al., 2008b, this thesis). Thus, there must be some intrinsic features of migratory NC cells allowing directional migration *in vitro*. The problem of autonomous directionality in NC migration constitutes the main topic of this thesis. Therefore, in the next section, some of the intrinsic molecular properties of NC cells will be outlined.

1.4.2 Molecular features of migratory NC cells.

Adhesion molecules in NC migration.

Adhesion molecules are essential for NC migration. First, many of them provide the adhesive force required to adhere to the substrate. Moreover, most, if not all, adhesion molecules are also able to transduce signalling hence, they can also be considered receptors. For example, integrins $\alpha5\beta1$ adhere to fibronectin but this mechanical adhesion also triggers a conformational change that is in turn transduced into a signal required for NC migration (Shattil et al., 2010; Alfandari et al., 2003). Similarly, molecules with weak adhesive properties such as ephrins may be playing an important role in signalling by segregating NC subpopulations and restricting their paths of migration (Drescher, 1997).

Cadherins are also important in NC migration. As mentioned before, several cadherins need to be downregulated for the transition from a stratified epithelium to a mesenchymal cell population. Classic cadherins are usually subdivided into type I cadherins, expressed preferentially in stable cell assemblies; and type II cadherins, expressed in less cohesive mesenchymal cells (DeLuca et al., 1999). Accordingly, many type I cadherins are downregulated at the onset of NC migration at the same time that some type II cadherins are up-regulated (Kuriyama and Mayor, 2008). A notorious example is the expression of Cadherin11 in migratory NC cells (Hadeball et al., 1998). A recent report shows that Cadherin11 is required for NC migration as it regulates cell-cell and cell-substrate adhesion via interaction with Trio, a Rho-GTPase regulatory protein (Kashef et al., 2009).

It seems that the right balance between Cadherin11-dependent adhesion and signalling, is achieved via ADAM13, a metalloprotease that cleaves Cadherin11 extracellularly and thus, it inhibits adhesion but not Trio-dependent signalling (McCusker et al., 2009; Kashef et al., 2009).

The PCP pathway in NC migration.

The role of the PCP in NC migration has been extensively studied in *Xenopus* and zebrafish embryos (De Calisto et al., 2005; Gessert et al., 2007; Matthews et al., 2008b,a; Shnitsar and Borchers, 2008; Carmona-Fontaine et al., 2008b). First, De Calisto et al. 2005 described the essential role of this pathway by showing that PCP downregulation in *Xenopus* embryos inhibits NC migration. In addition, via detailed cellular observations, these authors concluded that the PCP was necessary for the correct polarisation of NC cells (De Calisto et al., 2005). In addition, in *Xenopus*, it was shown that Pescadillo, a possible nuclear non-canonical Wnt component, is required for NC migration (Gessert et al., 2007).

A further understanding of this problem was contributed by Matthews et al. 2008b, were the role of the PCP in NC migration was extended to zebrafish embryos. Using both species the authors showed that Syn4 interacts with the PCP pathway to control NC polarity in migration (Matthews et al., 2008b). Moreover, they showed that both, PCP and Syn4 play a synergic (but different) role in controlling Rho-GTPases activity. Namely, Syn4 inhibits Rac1, whereas the PCP pathway activates RhoA, who in turn happens to inhibit Rac1 in these cells (Matthews et al., 2008b). The number of PCP molecules that regulate NC migration has increased, helping to get a better picture of the process. For example, the differential and complimentary role of two Wnt ligands, Wnt11 and Wnt11R, was shown (Matthews et al., 2008a). In addition, it is known that Dsh is translocated to the membrane upon PCP activation (Witzel et al., 2006; Matthews et al., 2008b). Shnitsar and Borchers showed that PTK7 kinase, forms a complex with Frz7 and Dsh; and it is required for the recruitment of Dsh to the membrane. Furthermore, PTK7 inhibition blocks PCP signalling and inhibits NC migration (Shnitsar and Borchers, 2008). A later

work (Carmona-Fontaine et al., 2008b), showed the role of PCP signalling in NC cell-cell interactions but it will not be described here as it comprise a major part of this thesis.

The Complement system in NC migration.

The complement system is a cascade of enzymatic reactions essential for innate immunity in vertebrates. It can be triggered by several stimuli to produce inflammation, opsonization[7] of antigens (and microorganisms) and damage in the membrane of pathogens by the formation of the membrane attack complex ((MAC) Walport, 2001a,b). There is no evidence in the literature for a role of the complement in NC migration, however a recent publication showed the expression of several of its member in the migrating NC (McLin et al., 2008). In this thesis, a crucial role for some of its members is described and as such, the system will be shortly described here.

There are mostly three pathways for complement activation, all of which converge to catalyse the cleavage of C3 into C3b and a small peptide called C3a (Figure 1.6). The **classical pathway** was the first pathway to be discovered and start with the activation of the C1-complex triggered by antigen-bound antibodies. This complex catalyses the cleavage of C4 into C4b and C4a, the former being a co-factor of C2a, to form C2aC4b. This binary complex is a C3 convertase as it catalyses the lysis of C3 into C3b and C3a (Janeway et al., 2001).

The **alternative pathway** was the second pathway to be discovered although is older in phylogenetic terms (Zarkadis et al., 2001). This pathway also ends up in the cleavage of C3 but the convertase and the initial trigger is rather different. This pathway takes advantage of the spontaneous C3 hydrolysis into form C3a and C3b. Then, C3b can covalently bind to the surface of pathogenic agents if in close proximity. Although spontaneous, the cleavage is relatively rare and, if C3b is not quickly bound, the products are deactivated. If bound, C3b can form a binary complex with Factor B known as C3bB. When factor B is in this complex is liable to the action of factor D that produces factor Bb (that remains bound to C3b) and factor Ba. The remaining complex, now denominated C3bBb is another C3

[7] A process of "tagging" antigens to facilitate and enhance its recognition by phagocytic agents.

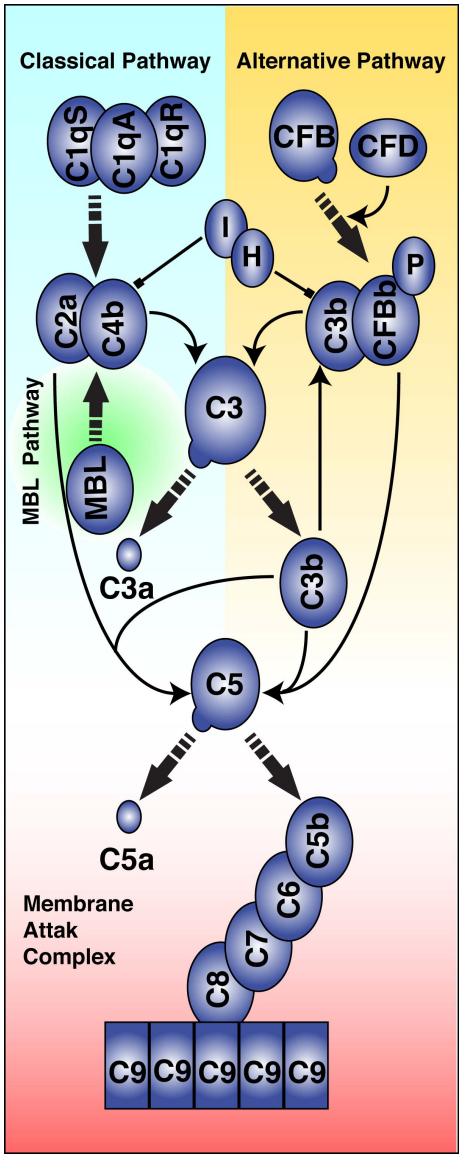

Figure 1.6: **The Complement Pathway**

convertase and thus, it can start an amplificatory positive loop of C3a and C3b production (Janeway et al., 2001).

The **Mannose-binding lectin pathway** is similar to the classical pathway but it is triggered the binding of mannose-binding lectins (MBL), to mannose residues on the pathogen surface. This activates MBL-associated serine proteases, such as MASP-1, and MASP-2 that cleave C4 and C2 to form C2aC4b, the C3 convertase.

As mentioned before these pathways converge at the cleavage of C3. This is the core of the complement as its C3b fragment continues a cascade of reactions until the formation of a liposoluble multiprotein complex, known as MAC, which can perforate the membrane of pathogens. At the same time, the small peptide C3a is an anaphylatoxin with potent chemotactic properties in cells that express its specific receptor, C3aR (Sahu and Lambris, 2001; Schraufstatter et al., 2009). C3 in general, and C3a in particular, have an important role in this thesis.

1.5 Aim and Structure

1.5.1 Aim

In summary, cell migration plays a major role in embryonic development. Usually migration in morphogenesis involves the movement of a large cell population that needs to coordinate its cell movements and orchestrate a unified cell polarity. The NC is an excellent example of this type of migration as it is a large population of mesenchymal cells that stream in a very coordinated and directional manner *in vivo* (Figure 1.7). Some important factors for this collective NC migration were discussed in this chapter. Astonishingly, under some circumstances, NC cells are capable of a similar degree of coordination in collective migration *in vitro*. Thus, something *in* NC cells or *in their interactions* is at the core of directional collective migration.

In this thesis, the problem of directional collective cell migration will be addressed. More specifically, this thesis will deal with the role of local cell-cell interactions during NC migration both, *in vitro* and *in vivo*. The orchestration of a coordinated and directed cell movement is a complex but crucial process. A simple observation under a microscope will reveal that cells migrate in a very tenacious way, almost without hesitation but in a continuous movement towards their destination. Hence, one of the main questions we can ask about cell migration is how cells acquire directionality, and how this directionality is coordinated in a large group of cells. Again, the emphasis of this thesis will be on how cell the behaviour of one cell is influenced by, and influences the, behaviour of others. Ergo,

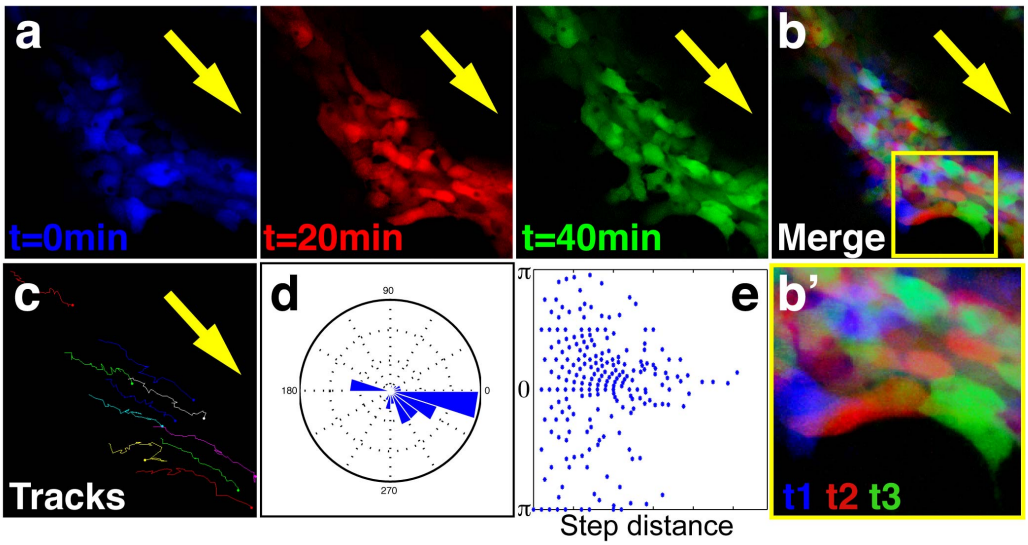

Figure 1.7: **Coherence in collective NC migration *in vivo*.** a. Three consecutive frames of a time-lapse movie separated by 20 mins. The images were differently pseudo-coloured. b. Overlay of the three images in a. showing the coherent migration of NC cells as the blue-red-green sequence can be clearly identified (see detail in b'). c. Tracks of selected cells exhibiting nearly parallel paths of migration. d. Migration angles are clustered towards a narrow region of the circle. e. Angle *versus* displacement plot showing that cells only take large displacements when in the appropriate direction.

it will emphasise the role of *social* cell interactions in NC migration. In this thesis, two interactions, one repulsive corresponding to CIL, and the other been a mutual attraction, termed here *coattraction*; are shown to be essential for NC collective migration *in vitro* and *in vivo*. Moreover, the integration of both is sufficient to generate collective migration, highlighting the importance of cell-cell interactions.

1.5.2 Structure

First, materials and procedures used in this thesis will be described. They have been divided in two chapters. The first one deals with the experimental procedures, most used routinely in cell and developmental biology laboratories. The second chapter contains descriptions of the analytical and computational tools used in this work. They are not particularly difficult but some of them have not been previously used. Thus, this description is intended for who may be interested in applying similar methods to their own

research. Neither of these chapters is required to read the rest of the thesis, so they can be skipped if desired.

In the results part (four chapters), two NC social interactions and their implications for migration are highlighted. The first two chapters deal with CIL in NC cells *in vitro* and *in vivo*. Most of this work can also be found in a recent publication (Carmona-Fontaine et al., 2008b). The other two chapters deal with an interaction that has not been described before in metazoan cells: coattraction, a mutual cell attraction among NC cells. This mutual attraction, is regulated by the complement fragment C3a and its receptor C3aR.

These results are discussed in one general discussion followed by an appendix of the publications to which this thesis has contributed. This is to provide a quick guide to this thesis and to recognise the invaluable contribution of many other colleagues and collaborators to the results and conclusions of this thesis. A list of the references follows this appendix.

Part II

Experimental and Analytical Procedures

Chapter 2

Experimental Procedures, Methods and Solutions

2.1 Animal manipulation and embryological procedures

2.1.1 Obtaining *Xenopus* embryos

Mature *Xenopus laevis* females were pre-primed by subcutaneous injection of 100 units of Serum Gonadotrophin (Intervet) 2 to 5 days before use. To stimulate ovulation, pre-primed females were injected with 500 units of choronic gonadotrophin (Intervet) 12-15 hours before the planned fertilization (usually Over Night, ON). Frogs were then placed in Egg-laying medium (1x MMR solution, see the solutions section), at $\sim$17°C, which maintains the naturally laid mature oocytes inactivated until collection. Adult male *Xenopus* were terminally anaesthetised in a solution of 0.5% Tricaine (Ethyl 3-aminobenzoate methanesulfonic acid) and the testes were dissected and stored in Leibovitz L-15 medium (Invitrogen) after antibiotic addition (Gentamycin 50μg/mL). For *in vitro* fertilisation, a small piece of testis was macerated in distilled H_2O and the resulting sperm suspension was mixed with the oocytes in a dry Petri dish. After cortical rotation, the dish was flooded with H_2O. At the 2-8 cell stage, the jelly was removed from embryos by gentle

agitation in a solution of 2% L-cysteine (pH 8.2) and embryos were raised in 1/10 normal amphibian media (NAM). Embryos were staged using standard tables (Nieuwkoop and Faber, 1967).

2.1.2 Obtaining Zebrafish embryos

Zebrafish (*Danio rerio*) strains were maintained and bred according to standard procedures (Westerfield, 2000). Embryos were obtained from natural spawning of an AB wild-type colony. Transgenic Sox10-GFP embryos were obtained from crosses of identified heterozygous sox10-7.2:GFP carriers (Carney et al., 2006). Embryos were raised in fish water at 28.5°C and were staged using standard tables (Kimmel et al., 1995).

2.1.3 Morpholino and mRNA microinjection in *Xenopus* and Zebrafish

Micro-injections were carried out using a Narishige IM300 Microinjector under a Leica MZ6 or a Nikkon SMZ645 dissecting microscope. Borosilicate capillaries (Intrafil, 0100106) were pulled to make thin needles with a Narishige PC-10 puller. The puller was set to the two-step mode with both steps adjusted at the 69.5% of its capacity. The needle was filled with mRNA or morpholino solution and calibrated using an eye piece graticule to inject 10nl in *Xenopus* or 4nl in Zebrafish. *Xenopus* injections were carried out in a dish of ficoll. *Xenopus* embryos were injected at the 2, 8, 16 or 32-cell stage and cultured in ficoll until the onset of gastrulation, at which point they were transferred to NAM1/10. For injections specifically targeted to the neural crest, embryos were injected in the animal ventral blastomere at the 8-cell stage or into blastomeres A2 or B2 at the 32-cell stage. Zebrafish embryos were injected dry at the 1 or 2-cell stage, with the injection targeted through the yolk and into the cell. Zebrafish embryos were then allowed to develop in fish water at 28.5°C. In some cases, the temperature was modified to change the speed of development.

2.1.4 *Xenopus* NC transplantation

Neural crest grafts were carried out according to (Carmona-Fontaine et al., 2008b). Neural crests from embryos injected with 10ng of fluorescein-dextran (FDX, Invitrogen, D1820) for labelling. Then, they were dissected at stage 17-18 and transferred to wildtype host embryos, which had their neural crest removed. Embryos were then cultured in NAM 3/8 until stage 26, and neural crest migration was followed using fluorescent microscopy (Leica MZFLIII).

2.1.5 *Xenopus* NC culture for *in vitro* migration assays

Neural crest explants were cultured in fibronectin coated glass or plastic surfaces.

NC culture in glass:

Glass coverslips for neural crest culture were sterilised in ethanol washes and dried under flame. They were then incubated for 1 hour at 37°C with a solution of 50-100$\mu g/mL$ fibronectin (Sigma) in PBS. Coverslips were then washed with PBS and blocked with 0.1% bovine serum albumin (BSA)/PBS for 1/2 hour at 37°C before being transferred to Danilchick's solution (DFA). Neural crests were dissected from embryos at stage 17-20 as previously described (Alfandari et al., 2003). Dissection was carried out in NAM 3/8 and once removed, neural crests were transferred to an agarose coated dish containing DFA. The neural crests were then transferred to the coated coverslips immersed in DFA and kept stationary at room temperature until the cells attached to the fibronectin. Cultures were then kept at 18°C. For neural crest culture of dissociated cells, neural crests were initially placed on the coverslip containing a 500μL drop of dication-free DFA ($Ca^{2+}, Mg^{2+}-$free). After the cells had dissociated, the coverslip was flooded with DFA and the cells were allowed to attach to the coverslip and then transfered to 18°C.

NC culture in plastic:

The procedure was essentially the same. In this case small petri dishes (Falcon, 351006) were coated with fibronectin in the same way as described but a ten times diluted fibronectin solution (*i.e.* $10\mu g/mL$) was used. When the explants were attached to the coated surface, the dish was fully covered with DFA, closed (making sure that no air bubble is left inside) and inverted.

2.1.6 Preparation and graft of protein coated beads

Two slightly different protocols were used for bead preparation depending on the nature of the beads. Affi-Gel Blue beads (100-200 mesh, BioRad, 1537302) were washed in 100% EtOH for two or three times and then air-dried after removing most of the EtOH. Subsequently, beads were rehydrated with the desired protein/inhibitor solution for two to three hours at room temperature or overnight at 4°C. Heparin beads (Sigma, H5263) were washed thoroughly with filtered or sterile PBS, then dried and finally flooded in the protein solution (usually diluted in PBS).

To perform the bead grafts *in vivo*, embryos were immobilised in an agarose coated dish filled with NAM 3/8 or ficoll (See Solutions section). A small incision was performed in the ectoderm close to the neural crest region and one bead per embryo was gently placed with the aid of forceps. Embryos were kept immobilised until the wound was healed. Beads were also used *in vitro* for the chemotatcic bead assay. A small line of silicon grease (VWR, 6366082B) was drawn over a fibronectin-coated plastic dish (see 2.1.5) and quickly after, the DFA was added. Then, the beads were careully located under the silicone grease and immobilised at its border. Subsequently, NC explants were cultured in front of each bead.

2.1.7 Patterned-fibronectin surfaces

To make stripes of high levels of fibronectin we used silicon matrices as described in (Vielmetter et al., 1990). Briefly, a matrix with channels of 90μm was filled with a fibronectin (50ng/mL) and fluorescein (for visualization, 1ng/mL) solution. By capillarity, this will form high level of fibronectin stripes, separated by stripes of lower level of fibronectin. This system allows to provide a preferential rather than restricted area for NC migration. The stripes are not visible in movies because we used the same channel to visualise the cells nucleus whose fluorescence was much higher. However, at time 0 these stripes were photographed to be able to draw the stripes in movies and figures.

2.1.8 Cell-substrate and cell-cell adhesion assays

To measure the cell-substrate adhesion, cell cultures were performed as normal but flipped-over after 10, 20, 30 or 40 minutes. Then the percentage of explants that remained attached was scored. Experiments were done in triplicate. Differences of cell-cell adhesion were determined using a cell-sorting assay as described in (Ninomiya et al., 2004) with some minor modifications. The main modification was that cells from differently labelled donors were separately dissociated in Ca^{++}- Mg^{++}-free DFA instead of the 50% Ca^{++}-Mg^{++}-free PBS supplemented with 0.1% BSA (1/2 PBSB) previously used. Then cells were mixed and re-suspended with the pipette and then left to re-aggregate in agarose-coated wells under gentle agitation. After one hour the aggregates were completely mixed in all conditions. Finally, they were cultured at 14.5°C for 24hrs and then analysed. Experiments were done in triplicate.

2.2 Biochemical and Molecular Biology Procedures

2.2.1 Obtaining and stocking DNA clones

Small amounts of (plasmid) DNA clones were usually obtained either spotted on a filter paper or as a small colony of transformed bacterias. If on paper, the spotted region was cut out the paper and resuspended in H_2O for several minutes. Then, $5\mu L$ were taken and added to $100\mu L$ of competent Dh5α E. coli and left on ice for 20 to 30 minutes. After this, a brief heat shock (45" at 42°C) was given to the bacteria tubes and then they were returned to ice to chill. After a minute, $600\mu L$ of distilled water was added to the bacteria and mix. $100\mu L$ were then platted on LB agar plates containing an antibiotic for selection (typically ampicillin or kanamycin) and left Over Night (ON) at 37°C and the presence of colonies was expected by the next morning. With a sterile micro-pipette tip one isolated colony was picked and grown ON in ∼100mL of LB in an agitating chamber at 37°C. At the next day, the bacteria were pelleted by centrifugation (10 min, 8500 rpm) and the supernatant discarded. The amplified DNA was extracted from the bacteria using the Plasmid Midi kit (Qiagen, 12143). Concentration was measured using the NanoDrop Spectrophotometer (ND-1000) and DNA quality was estimated by agarose gel electrophoresis.

2.2.2 Enzymatic DNA restriction

Ten μg of plasmid DNA containing the gene of interest was cut at a 3' restriction site (for mRNA) or at a 5' restriction site (for antisense probes) with an appropriate restriction endonuclease. Enzymes, buffers and BSA were obtained from Promega. Typically a $100\mu L$ reaction was used with $10\mu L$ of the appropriate 10x buffer, $1\mu L$ of BSA (supplied with the enzyme) and $1\mu L$ of enzyme in H_2O. The digestion was left for 3 hours or ON and the reaction efficiency was assessed by agarose gel electrophoresis.

Linearised (digested) plasmid DNA was purified with chlorophorm extraction and EtOH precipitation. To do that, the sample volume was doubled (to $200\mu L$) with DEPC-water. The same volume ($200\mu L$) of Phenol:Chloroform:Isoamyl alcohol (25:24:1) was added,

mixed by vortexing and centrifuged at 4°C for 10 minutes at 13,000 rpm. Carefully, the top layer was removed and placed in a new 1.5 mL eppendorf tube. Two volumes of 100% EtOH ($400\mu L$) and 1/10 of the total volume ($60\mu L$) of 3M Sodium Acetate were added. The mixture was incubated at -20°C for at least 1 hour but it was usually left ON. Subsequently the samples were centrifuged at 4°C for 30 minutes at 13,000 rpm. The supernatant was carefully removed and the samples were cleaned with $350\mu L$ of 70% EtOH and centrifuged at 4°C for 15 minutes at 13,000 rpm. Again, the supernatant was carefully removed and the samples were air-dryed. When all the EtOH has been eliminated, the samples were resuspended in $20\mu L$ of H_2O. The efficiency of the purification can be assessed by agarose gel electrophoresis.

2.2.3 Synthesis of mRNA/morpholinos for microinjection

mRNA:

Two μL of 3' linearised and purified plasmid DNA containing the gene of interest were mixed with transcription mixture. Synthetic capped mRNA was synthesised using the SP6 mMessage mMachine kit (Ambion) following maufactorers instructions. mRNA was purified using the RNeasy kit (Qiagen, 74104) and resuspended in molecular biology H_2O. Concentration was measured using the nanoDrop spectrophotometer.

Morpholinos:

Oligo-morpholinos were designed as recommended by GeneTools or using previously reported morpholinos. The following morpholinos were used during this thesis: Wnt11R (Garriock et al., 2005), xSyn4 (Muñoz at al, 2006), zebrafish Syndecan-4 (zSyn4, 5'-CGGACAACTTTATTCACTCGGGCTA-3') and Complement C3 (C3mo, 5'-ACTGGACAATGTGCAAACTTTGAAT-3'). The latter two morpholinos were designed against the 5'-UTR region of the respective genes. A standard control morpholino, 5'-CCTCTTACCTCAGTTACAATTTATA-3', was used to asses the toxicity of equimolar concentration of experimental morpholinos. Injection of this control Mo in wild-type zebrafish or *Xenopus*

embryos causes no defective phenotype.

2.2.4 Synthesis of antisense RNA probes for *in situ* hybridisation

Two μL of 5' linearised and purified plasmid DNA containing the gene of interest were mixed with transcription mixture.*In vitro* transcription of antisense RNA was carried out using either T3, T7 or SP6 RNA polymerase (Promega) using conditions suggested by the manufacturer. The NTP-mix used for the reaction contained 0.35mM digoxigenin-labelled UTP, resulting in the production of a digoxigenin-labelled RNA. RNA was purified using the RNeasy kit (Qiagen, 74104) and the DNA was degraded using the alternative step contained in this kit. Concentration was measured using the nanoDrop spectrophotometer. Probes were diluted in hybridisation buffer to working concentrations (empirically determined, usually between 0.1 to 1 $ng/\mu L$).

2.2.5 DNA construction to make the *sox-10*-membrane-GFP transgenic fish

A *sox-10* reporter construct was generated by driving the expression of membrane GFP under the control of the *sox-10* promoter. To do this, a 7 kb DNA fragment corresponding to the genomic region 5' to the zebrafish *sox-10* gene, was cloned upstream a to membrane-bound-GFP gene (Carney et al., 2006). This DNA region was obtained from the p-7.2sox10:egfp plasmid (kindly donated by R Kelsh). 40 to 80 pg of DNA linearised with NotI was injected into 1-cell zebrafish embryo to generate the transgenic fishes.

2.2.6 Zebrafish Wnt11 dominant-negative and zWnt11-RFP generation

Xenopus and zebrafish Wnt11 proteins are highly conserved. Thus, a C-terminally truncated dominant-negative zebrafish wnt11 construct was generated according to the *Xenopus* version (Tada and Smith, 2000). PCR amplification was performed using the primers 5'-GGTCCAGGATCCATGACAGAATACAGGAACT-3' and 5'-GGTCCAGAATTCGTA-

ATCCGGTGAGCTGACCA-3'. The PCR fragment was then cloned into the BamHI and EcoRI sites of pCS2+ vector. This construct comprises aminoacids 1-281 lacking the cysteine-rich region (Figure2.1 a, b). mRNA injection of this dominant negative of Wnt11 produces the expected phenotypes for the loss of function of Wnt11 (Figure 5.6).

The Wnt11-RFP fusion protein was constructed as a C-terminal fusion of zebrafish wnt11 cDNA and RFP. The YFP region of Wnt11-YFP11 was swapped with a modified version of RFP (cherry-RFP). A linker sequence of nine aminoacids (GSSEFSIDG) was introduced between Wnt11 and RFP. The Wnt11-RFP fusion cDNA was cloned into pCS2+ between the BamHI and XbaI polylinker sites.

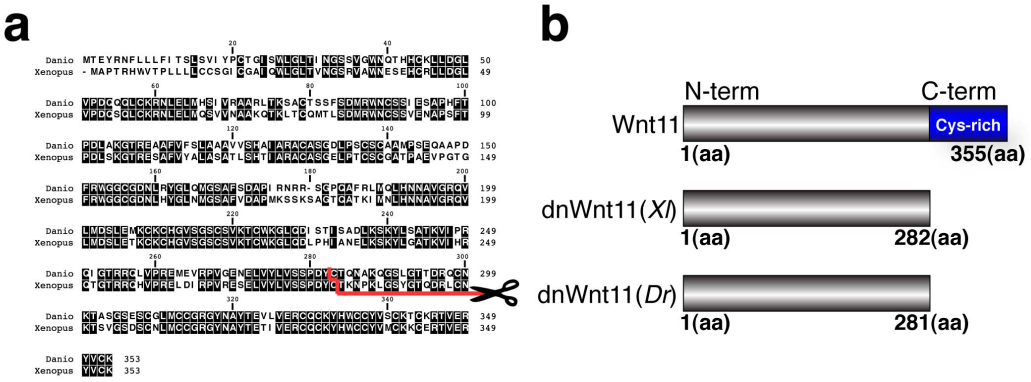

Figure 2.1: **Generation of a zebrafish dnWnt11.** a. Alignment of *Xenopus* Wnt11 and zebrafish Wnt11 proteins. The C-terminus region of zebrafish Wnt11 was deleted to generate a similar construct to *Xenopus* dnWnt11 (red line, Tada and Smith, 2000). b. Schematic representation of full length Wnt11, *Xenopus* dnWnt11 and the new zebrafish dnWnt11.

2.2.7 Peptides, proteins and chemical inhibitors usage

Peptides Synthesis and antibody production

Peptides used in this study were synthesized in an Applied Biosystem peptide synthesizer (model 431A, Foster City, CA) using Fmoc-based chemistry (Atherton and Sheppard, 1989). All peptides were HPLC purified to 95% purity, and the identity of the peptides was confirmed by laser desorption mass spectrometry (MALDI).

Antibodies against synthetic peptides were made in rabbits by subcutaneous injections of the synthetic peptides coupled to keyhole limpet hemocyanin by glutaraldehyde (Reichlin, 1980) and m-Maleimidobenzoyl-N-hydroxysuccinimide ester (peptides containing free cysteine) (Kitagawa and Aikawa, 1976). The rabbit immunoglobulin was fractionated from other serum proteins by ammonium sulfate precipitation and the specific antibody was purified by affinity chromatography on the corresponding peptide column. See the table below for the sequences of peptides and antigens used to develop antibodies.

Name	**Sequence**
C3a peptide (C-terminus representing the active site of C3a)[1]	H-RYYEKKREAEKLSKDDDTLGR-COOH
C3a-DesArg peptide[2]	H-RYYEKKREAEKLSKDDDTLG-COOH
Control Peptide	H-EAYKQRYEDRLELRIELIG-COOH
C3a Antigen (C-terminus of anaphylatoxin)	H-CRYYEKKREAEKLSKDDDTLGR-COOH
C3aR Antigen (extracellular loop 1)	H-ELLHYKWPSDLVSCKLLPS-$CONH_2$

1. (Hugli, 1990)
2. Ibid.

Table 2.1: Sequence of peptides and antibodies

Peptide and antibody treatments in embryos and cell cultures

Treated cell cultures were performed in the same way than untreated ones but peptides, chemicals or antibodies were directly diluted in the DFA solution. Working concentrations are as follow.

Compound	**[Concentration]**
C3a	0.7μM
C3aDesArg	0.7μM
Control Peptide	0.7μM
anti-C3a	1μg/mL
antiC3aR	1μg/mL
SB290157*	20μM **.C3aR inhibitor (Calbiochem). Stock solution diluted in DMSO. Final DMSO concentration in working solution: 0.2%*

Table 2.2: Chemicals: working concentration

2.2.8 Whole Mount *in situ* hybridisation

In situ hybridisation proceure was adapted from stardad protocols (Harland, 1991). To avoid RNAase contamination, which can degrade the RNA probe, all solutions (up to and including post hybridisation washes) were made using diethyl pyrocarbonate (DEPC) treated water. Embryos were fixed in MEMFA for 1hr at room temperature and transferred to 100% methanol for indefinite storage at -20°C. Embryos were rehydrated with successive washes of: 75% methanol, 50% methanol, 25%methanol and PBT. Embryos were then bleached in bleaching solution under light for 10 minutes, washed thoroughly in PBT and re-fixed for 30 minutes in 4%paraformaldehyde (PFA) in PBS or MEMFA. After further washing in PBT, embryos were transferred to hybridisation buffer and incubated for 3-6 hours at 62°C. The digoxigenin labelled probe was then added and incubated with embryos overnight at 62°C. After hybridisation embryos were washed in a series of Formamide/SSC solutions (see Solutions section) for 10 minutes each at 62°except form the last one (Washing Solution 5) which lasted 30 minutes. Embryos were then rinsed with PBT, maleic acid buffer (MAB) and then blocked in 2% BMBR (Boehringer Mannheim blocking reagent; Roche) in MAB for 2 hours at room temperature. Embryos were incubated overnight at 4°C with an anti-digoxigenin-alkaline phosphatase (AP) conjugated antibody (Roche) diluted in 2% BMBR/MAB. Excess antibody was removed by six 30 minute washes with MAB at room temperature with gentle agitation. Embryos were then transferred to AP buffer (see Soluitons) where the AP colour reaction was developed using $75\mu g/mL$ BCIP (5-bromo-4-chloro-3-indoyl-phosphate; Roche) and $150\mu g/mL$ NBT (4-nitro blue tetrazolium chloride; Roche) at 37°C. Embryos were then washed with 100% Methanol to remove any background staining and transferred to 4%PFA for storage.

When it was necessary to visualise the expression of two genes in one embryo, double *in situ* hybridisation was carried out. Double *in situ* hybridisation uses the protocol described above, with a few minor alterations; a mixture of two RNA probes were added, one labelled with digoxigenin as described and one labelled with UTP-fluorescein. After finishing the *in situ* hybridisation, embryos were transferred back to 2%BMBR/MAB and incubated overnight at 4C with an anti-flourescein-AP antibody (Roche). Embryos were then washed

in MAB and transferred to AP buffer. For the AP colour reaction, BCIP only was added, giving a pale blue colour, which is distinguishable from the dark blue of the first in situ hybridisation. Alternatively, in some cases a BCIP/INT (Roche) reactive was used to give a red/brown colour.

2.2.9 Western Blots

Four to five whole embryos were frozen at stage of interest until Western Blot was performed. Approximately 60μL of homogenisation buffer were added to the samples (with phosphatase inhibitor if requiered). Homogenizated with the tip of a micro-pippette, and spun several times replacing the tube in each cycle. Then the samples were centrifugated for 10mins at 13,000rpm at 4°. The supernants were recovered and placed in new tubes. Protein concentration was measured and uniformed among different samples. To run the gel, the sample was diluted to the desired concentration and mixed with running buffer (Solutions or Invitrogen, NP0007) and β-mercaptoethanol (final concentration of %2.5). Then the mixture was boiled for 5 mins. The electrophoretic chamber was filled with running buffer (Solutions or Invitrogen, NP0002), the gel (Invitrogen, NP0322BOX) was assembled and the samples loaded (typically 10-20μL to load a total amount of 10μg of protein). To estimate the weight of the bands obtained, a protein standard ladder (Invitrogen, LC5925) was used. Electrophoresis was performed at 200V for 40-60 mins. Immediatelly after, proteins were transferred to a PDVF membrane (Amersham Hybond-p) using a semi-dry blotter. Transfer was performed at 15V for 30-60 mins. Transference efficiency may be assessed by stainig the gel (with coomasie blue) and/or the membrane (with ponceau red). The membrane was then blocked overnight in 5% Marvel/TSBT at 4°C or 2-4 hours at RT. Following, the membrane was incubated ON at 4°C or 2-3 hours at RT in a primary antibody solution (diluted to the desired concentration in 5% Marvel/TSBT). The membrane was then extensivelly washed with TSBT and incubated in a secondary antibody solution. After extensive washes, the bands were visualised using a luminol/peroxidase chemoluminescent reaction. Briefly, equal volumes of the two peroxidase detection solutions (see Solutions) were applied to the membrane for 5 minutes in the dark. Then the excess of solution was removed form the membrane, wrapped in cling

film (to avoid the membrane drying up) and placed on an signal amplification cassette. In the dark, X-ray films (Fuji, Film superRX) were introduced in the cassette and developed in a X-OGraph machine.

2.2.10 RT-PCR

Obtaining total mRNA

To obtain total mRNA from *Xenopus* embryos, the RNeasy kit (Qiagen, 74104) was used. Three to five embryos were placed in the *RNAlater* solution of the kit and stored at -20°C until continuing with the extraction. Manufacturer's recommendation were followed and the quality of the extraction was estimated by the intensity and sharpness of the two rRNA bands in an agarose gel electrophoresis. mRNA concentration was measured using the NanoDrop spectrophotometer.

Reverse Transcription (RT)

cDNA libraries of embryos at different developmental stages were constructed from extracted total mRNA using Oligo-dT primers. Enzymes, buffers, nucleotides, salts and Olido-dT primers were obtained form Promega (C1101). A typical ($30\mu L$) reaction mixture is detailed in table 2.3.

RT-mix	
mRNA	$\sim 1.5\mu g$
5x Buffer	$6\mu L$
Oligo-dT	$1.5\mu L$
dNTPmix	$3\mu L$
$MgCl_2$	$3\mu L$ (to get a final $2.5\mu M$)
	H_2Oup to 28.5μL
Enzyme mix	
RT polymerase	$1.35\mu L$ (13.5 U)
RNAsin	$0.15\mu L$

Table 2.3: Typical RT mixture conditions

The RT-mix was heated at 65°C for three minutes to denaturate the mRNA and then the samples were chilled on ice for 1 minute. At room temperature the enzyme mix was added

to the RT-mix and the reaction was left for 1 hour at 42°C.

Polymerase Chain Reaction (PCR)

PCRs were performed in a Eppendorf "Mastercycle Personal" or "Gradient" thermocycler. Enzymes, buffers, nucleotides and salts were obtained form Promega. Primers were designed by different methods and synthesised by a commercial provider (Invitrogen). A typical ($100\mu L$) reaction mixture is detailed in table 2.4 and a typical PCR sequence is detailed in table 2.5.

RT-mix	
RT product	$\sim 10\mu L$ (10% total vol.)
5x Buffer	$20\mu L$
dNTPmix	$5\mu L$
$MgCl_2$	$10\mu L$ (to get a final $2.5\mu M$)
100 μM Forward primer	$1\mu L$
100 μM Reverse primer	$1\mu L$
Taq polymerase	$2.5\mu L$ (12.5 U)
	H_2Oup to $100\mu L$

Table 2.4: Typical PCR mixture conditions

	Temperature (°C)	Time
Initial denaturation	94	1min
Denaturation	94	15s
Annealing	50-60*	30s
Extension	72	1min
	repeat 25-30 times	
Final extension	72	5min
Chill	4	indef.
	**primer specific*	

Table 2.5: Typical PCR cycle

2.2.11 Cloning of *c3aR*

Production of a *c3aR* EST to make an antisense probe

The cloning of *c3aR* was required as neither annotated *Xenopus laevis c3aR* was available on gene databases such as Pubmed nor whole genome sequence is available for *X. laevis*.

Furthermore, no homologous EST (expressed sequence tag) was found for this gene with the method described in section 3.1. Hence, degenerated nested primers were designed against highly conserved regions among *c3aR* orthologues in different species. Two forward primers, 5'-GAATTCGTGTGCYGAYYTNATYTGYTGYTTRTC-3' and 5'-GAATTC-ATGTTYGCNAGYGTNTT-3' were used. Only one reverse primer, 5'-GAATTCTTG-AAGTCYYTGCCCATRAARACRTA-3', was designed. Y denotes any pyrimidine (C or T), R any purine (A or G) and N stands for any base. The initial GAATTC of all these primers corresponds to a EcoRI restriction site used in further steps. A PCR, using the first forward primer was performed using as a template cDNA obtained from total mRNA of a stage 30 embryo. A further nested PCR was performed to the PCR product using the second forward primer. Special conditions were used for these two PCR cycles:

	Temperature (°C)	Time
Initial denaturation	94	1min
Denaturation	94	15s
Annealing	52	30s
Extension	72	1min
		repeat 10 times
Denaturation	94	15s
Annealing	57	30s
Extension	72	1min + 10s/cycle
		repeat 25 times
Final extension	72	5min
Chill	4	indef.

Table 2.6: PCR conditions used to clone *c3aR*.

Moreover, a higher primer concentration was used (2.5μM). The obtained sequence (c3aRdraft 652bp) was purified form the agarose gel using the Min Elute kit (Qiagen, 28606) according manufacturer's instructions. The purified product was then digested with EcoRI to obtain a "sticky" ended DNA fragment which was purified by precipitation. This product was cloned into a pBluescriptSK+ vector also previously digested with EcoRI. A normal ligation protocol was used using T4 ligase (Promega, M1801). Two successfully ligated clones were obtained and an antisense probe labelled mRNA probe was synthesised from them to address the gene expression pattern.

Amplification of the 5' cDNA end (5' RACE)

The sequence obtained by the method described above yield an EST correspoding to the central region of the *Xenopus laevis c3aR*. Thus, no information to design an antisense oligo morpholino was obtained. To obtain the sequence around the initiation codon region, a 5' RACE protocol was performed. From the c3aRdraft sequence, four reverse primers were designed: SP0 5'-CAGCACGATAGCAATGACCA-3', SP1 5'-AGAGGCAAGAAAAAGCCAAA-3', SP2 5'-AACACGGGGAGGCACAAC-3' and SP3 5'-AGGACACCAGCCAGATGAAC-3' . These are consecutive nested primers with SP3 the most internal one. The 5'/3' RACE kit was used (Roche, 03353621001) essentially according the manufacturer's instructions. The main change is that an additional nested primer was designed (SP3) to perform a third round of amplification aiming to reduce non-specific bands and increase the DNA yield. According the kit's recommendation, PCRs were performed using the Expand High Fidelity PCR System (Roche, 1132641001). Several sequences were obtained, almost all of them, were the expected 5' region to the c3aR draft. Their difference was their extension form the starting point (SP3 region).

2.3 Solutions

2.3.1 Mediums and buffers for animal and embryonic maintenance

Modified Ringer Solution (MMR) (10x)

1M	$NaCl$
20mM	KCl
10mM	$MgSO_4$
20mM	$CaCl_2$
50mM	HEPES
1mM	Disodium-EDTA
	Adjust pH to ~ 7.6

Normal Amphibian Medium A

1.1M	$NaCl$
20mM	KCl
10mM	$Ca(NO_3)_2$
10mM	$MgSO_4$
1mM	Disodium-EDTA
	Sterilse by autoclaving

Normal Amphibian Medium B

20mM	NaH_2PO_4
	Adjust pH to ~ 7.5
	Sterilise by autoclaving

Normal Amphibian Medium C

100mM	$NaHCO_3$
	Sterilise by millipore filtration

Working concentrations for NAM (1L)

	NAM A	NAM B	NAM C
NAM 1/10	10mL	10mL	1mL
NAM 3/8	37mL	37mL	1mL
NAM 3/4	75mL	75mL	1mL
	Add 1mL Streptomycin (50 mg/ml)		
			H_2O *up to 1L.*

Tricaine Solution

Ethyl 3-aminobenzoate methanesulfonate	5g
	H_2O *up to 1L.*

Ficoll

3% Polysucrose	in NAM3/8

Fish water

60 mg "Instant Ocean"	per litre H_2O.

Danilchick's Solution (DFA)

53mM	$NaCl$
5mM	Na_2CO_3
4.5mM	K-Gluconate
32mM	Na-Gluconate
1mM	$MgSO_4$
1mM	$CaCl_2$
0.1%	BSA
pH 8.3	(adjusted with 1M Bicine)
50μg/ml	Streptomycin

Di-cation-free Danilchick's Solution

53mM	$NaCl$
5mM	Na_2CO_3
4.5mM	K-Gluconate
32mM	Na-Gluconate
0.1%	BSA
pH 8.3	(adjusted with 1M Bicine)
50μg/ml	Streptomycin

2.3.2 General Use solutions

DEPC-water

0.1%	DEPC (Diethylpyrocarbonate)

Leave in agitation ON. Autoclave twice.

PBS and PTW

137mM	$NaCl$
2.7mM	KCl
4.3mM	Na_2HPO_4
1.4mM	KH_2PO_4
	Adjust pH t0 7.3

Use DEPC water if for molecular biology.

Add 0.1% Tween-20 to make PTW

mRNA NTP-mix (10x)

10mM	GTP
10mM	ATP
10mM	UTP
10mM	CTP

2.3.3 *In situ* Hybridisation Solutions

MEMFA

MEM salts (10x)	
1M	MOPS
10mM	$MgSO_4$
20mM	EGTA
	In DEPC-water

To make MEMFA:

1vol	MEM salts
1vol	37-40% paraformaldehyde
8 vol	DEPC-water

SSC (20x)

3M	NaCl
0.3M	Tri-sodium citrate
Adjust pH to	7.0

Bleaching Solution

20%	H_2O_2 (20 vol)
5%	Formamide
2.5%	20x SSC
	in DEPC-water

Hybridisation Buffer

50%	Formamide
5x	SSC
1x	Denhardt's Solution
1mg/ml	Ribonucleic acid
100μg/ml	Heparin
0.1%	CHAPS
10mM	EDTA
0.1%	Tween-20
Adjust pH to	5.5

Labeled NTP-mix (10x)

10mM	GTP
10mM	ATP
10mM	CTP
6.5mM	UTP
3.5mM	Dig/Fluo-UTP

Probe washing solutions (100mL)

Solution	Formamide	SSC 20x
1	50mL	10mL
2	25mL	10mL
3	12.5mL	10mL
4	-	10mL
5	-	1mL
		Add 0.1mL Tween
		DEPC-water up to 100mL.

Maleic acid buffer (MAB)

100mM	Maleic acid
150mM	$NaCl$
0.1%	Tween-20

Alkaline Phosphatase Buffer

10% M	Maleic acid
10%M	$NaCl$
10%M	$NaCl$
0.1%	Tween-20
	Complete volume with H_2O.

2.3.4 Western Blot Solutions

Homogenisation Buffer

1M Tris-HCL (pH7.6)	2mL
1M NaCl	10mL
1% TritonX-100	1mL
Add distilled water up to	100mL

Dissolve a protease inhibitor pill (Roche 11836153001) in to 10mL. Aliquot & freeze

Sample Buffer
to be used instead of NP0007

1M Tris-HCl, pH 6.8	1mL
Glicerol	1.6mL
10% SDS	3.2mL
Bromophenol Blue	0.4mL
β-Mercaptoethanol	0.8mL
H_20	9mL

Protein Buffer (10x, 1L.)

Tris	3027g (250mM)
Glicine	144,2 g (1921mM)
	Adjust pH to ~ 8.3

Running Buffer (1x)
to be used instead of NP0002

Protein Buffer (to 1x)	10%
SDS	0.1%p/v

Transfer Buffer (1x)

Protein Buffer (to 1x)	10%
Methanol	20%
SDS (Optional)	$<$ 0.1%p/v (usually 0.03%)

For 1L

100mL	10x Protein Buffer.
200mL	Methanol.
0.03%	SDS
Up to 1L with H_2O	

TBS and TBST

Peroxidase detetection reagent storage

Reagent	**Dilution and storage**
Luminol (SigmaA8511-5G)	250 mM in DMSO (keep aliquots in dark @ -20°)
Coumeric acid (Sigma C9008-5G)	90 mM in DMSO (keep 0.44mL aliquots in dark @ -20°)
Tris-HCl	1M pH 8.5
Hydrogen Peroxide	30% v/v

Peroxidase detetection Stock solutions

Solution 1

Luminol	0.5mL	1mL
Coumeric acid	0.22mL	0.44mL
Tris-HCl	5mL	10mL
Distilled water	up to 50mL	up to 100mL

Solution 2

Hydrogen Peroxide	32μL	64μL
Tris-HCl	5mL	10mL
Distilled water	up to 50mL	up to 100mL

Store both solutions @ 4°for not longer than a few weeks

Coomasie Blue

0.2%	Coomasie blue (Fluka 27816)
10%	Acetic Acid
45%	MetOH

Use to stain gel. Wash with the same solution but without the coomasie blue.

Poinceau Red

0.1%	Ponceau Red (Sigma P35041)
5%	Acetic Acid

Use to stain the membrane. Wash with the H_2O or TSBT.

Chapter 3

Analytical Procedures

3.1 Phylogenetical Analysis

3.1.1 Identification of *Xenopus laevis* ortholog genes

For some of the genes used in this thesis, no *Xenopus laevis* ortholog were described in the literature. Particularly, most of the members of the complement cascade were not described when our study began. To obtain these sequences the usual approach taken here was to identify possible candidates from ESTs databases. To do this, a blast search using as a query the protein sequence of the mammalian ortholog of the gene of interest was performed against the therapod node of the Metazome database. This search provides clusters of supposed ortholog genes along the different known genomes known in this node. From these clusters, the gene sequence of the animal closer, in phylogenetical terms, to *Xenopus laevis* was obtained. It usually was a *Xenopus tropicalis* sequence. This aminoacid sequence was processed with the *tblastn* algorithm from the NCBI Blast server (http://blast.ncbi.nlm.nih.gov/) using the *Xenopus laevis* EST sequences as a target. Highly homologous ESTs were ordered to synthesise an antisense RNA probe as described before. Their expression pattern was assed by *in situ* hybridisation.

Genes identified in this way include the complement members C2, C4, C5, C6, C7, C8α,

C8β, C8γ , Factor H and Factor I. A notable exception to this approach was C3aR since no *Xenopus laevis* EST showed a significant homology to the *X. tropicalis* gene. Given the importance of that gene in this project its PCR cloning was required as described before.

3.1.2 Sequence alignments and phylogentical tree drawing

Sequence alignments were usually performed using the clustal algorithm (Higgins and Sharp, 1988) using the default parameters of the clustal webpage (http://align.genome.jp/). Alignments were graphically edited using either Jalview (www.jalview.org) or CLC Sequence Viewer (CLC bio A/S, www.clcbio.com). The same alignment file (*.aln) generated with the clustal algorithm was used to draw a tree in Phylodendron (http://iubio.bio.indiana.edu/-treeapp/treeprint-form.html). Typically unrooted radial trees were used.

To predict transmembrane helices in proteins, a method based on a hidden Markov model was used (TMHMM Server v. 2.0, http://www.cbs.dtu.dk/services/TMHMM/, described in Krogh et al., 2001).

3.2 Image Analysis

3.2.1 Standard and Time-Lapse Photography of *Xenopus* and Zebrafish embryos.

Photography of fixed embryos

Embryos were immobilised in an agarose coated dish and photographed with a Leica DFL420 camera attached to a Leica MZFLIII dissecting microscope using the IM50 software (Leica).

Time-Lapse photography of *Xenopus* and Zebrafish embryos NC *in vivo*

Sox10 -7.2: GFP (Carney et al., 2006) transgenic zebrafish embryos were used to analyze NC migration *in vivo*. Each embryo was staged according to the number of somites and only embryos with equal numbers were compared. The embryos were dechorionated, inserted into a drop of 0.2% agarose in fish water (Westerfield, 2000) and mounted in a custom-built chamber. Control and experimental embryos were mounted side to side in the same chamber. A compound (Leica DM5500) or a confocal (Leica SP2-DMRE) microscope was used for time-lapse imaging. Digital images were typically collected at 30 to 90 second intervals for a period between 1 and 14 h. After 6 to 8 h time lapse of 20 somites embryos, cephalic NC migrate between 500-800μm in the anterior-posterior axis, between 40-60μm in the dorso-ventral axis and between 7 and 9μm of depth. Therefore, during cell track analysis it was assumed that most of NC cell migration occurs in a two-dimensional curved plane. Imaging was usually performed orthogonally to this plane. Sequences of images were quantitatively analyzed using NIH ImageJ (http://rsb.info.nih.gov/ij) and Matlab (R14b, Mathworks) software. Briefly, cells were tracked over time and from those x, y, t values different migratory parameters such as speed, persistence and angle of migration were estimated. Similarly, cell protrusions and cell dipersion were analysed with custom made scripts.

Two-plane confocal image

For the analysis of cell protrusions shown, for example, in Figure 5.2, a two plane confocal image was performed. Here, the plane just above the fibronectin layer was set as plane 1 and given an arbitrary colour. This plane corresponds to the protrusions plane. A second plane through the center of the cell was defined as plane 2 and a different colour was assigned to it. This plane corresponds to the shape of the cell. Both planes were overlapped to illustrate the desired comparison.

3.2.2 Fluorescence (Förster) Resonance Energy Transfer (FRET) analysis

Plasmid DNA encoding FRET probes; Raichu-Rac1, Raichu-Cdc42 (Itoh et al., 2002) and RhoA biosensor (Pertz et al., 2006) were subcloned in vectors suitable for mRNA *in vitro* transcription as described in (Carmona-Fontaine et al., 2008b). Synthesised mRNA's were injected directly into *Xenopus* embryos at the 8-cell stage together with a (red) cell tracker (usually membrane-Cherry). Fluorescence could be detected from stage 14 onwards. Neural crests expressing the FRET probes were dissected at stage 17 and cultured on fibronectin-coated coverslips for 5-7 hours as previously described. Cells were then fixed for 30 minutes in 4%PFA/PBS at room temperature and then mounted in glycerol/PBS for observation. Samples were imaged using a Zeiss lSM 510 META laser scanning confocal microscope and a 63 x Plan Apochromat NA 1.4 Ph3 oil objective. The CFP and YFP channels were excited using the 405 nm blue diode laser and the 514 nm argon line respectively. The two emission channels were split using a 545 nm dichroic mirror, which was followed by a 475-525 nm bandpass filter for CFP and a 530 nm longpass filter for YFP. Pinholes were opened to give a depth of focus of 3 mm for each channel. Scanning was performed on a line-by-line basis with zoom level set to two. The gain for each channel was set to approximately 75% of dynamic range (12-bit, 4096 grey levels) and offsets set such that backgrounds were zero. Time-lapse mode was used to collect one pre-bleach image for each channel followed by bleaching with 50 scans of the 514 nm argon laser line at maximum power (to bleach YFP). A second post-bleach image was then collected for each channel. Pre- and post-bleach CFP and YFP images were then imported into Mathematica (Wolfram) for processing. Briefly, images were smoothed using a 3 x 3 box mean filter, background subtracted and post-bleach images fade compensated. A FRET efficiency ratio map over the whole cell was calculated using the following formula,

$$FRET_{efficiency} = CFP_{postbleach} - CFP_{prebleach}/CFP_{postbleach}. \tag{3.1}$$

Ratio values were then extracted from pixels falling inside the bleach region as well as an

equally sized region outside of the bleach region and the mean ratio determined for each region and plotted on a histogram. The non-bleach ratio was then subtracted from the bleach region ratio to give a final value for the FRET efficiency ratio. Data from images were used only if YFP bleaching efficiency was greater than 70%.

3.3 Analysis of cell shape and protrusions

3.3.1 Identification and orientation of lamellipodia

To analyse cell protrusions, the cells were labelled with a membrane-bound fluorescent dye (GFP or RFP). The shape of individual cells was analyzed using ImageJ. First, a threshold was set to generate binary images of the migratory cells. The outline/analyze particles function was used to draw the contour of each cell at different time points, which were overlapped maintaining the original XY positions. Cell extensions, were defined as the new positive area between two consecutives frames (separated by the shortest time of 1 minute in the time-lapse analysis). Because during the course of one minute, the body (centroid[1]) of the cell does not move significantly, it can be assumed that the new area generated corresponds to lamellipodia. It is unlikely that new areas correspond to filopodia since they move faster and the intensity of their fluorescence is weaker, thus probably escape to this analysis. Nontheless, if desired, the temporal parameters and fluorescence sensitivity can be easily modified to detect and analyse filopodia. Using ImageJ, two different colours were assigned to two consecutive binary images of a cell. Then the images were subtracted generating a new 3-colour-code image. The area only present at the second time point (new) has a distinctive colour and it was considered the cell extension. Similarly, old areas (present only at the first time point) and static areas (present at both time points) can be easily distinguished as they also get differently coloured. Then, the area and other parameters of the protrusion can be measured. The orientation of the protrusion was estimated by tracing a vector from the centroid of the cell and the centroid of the new area (the protrusion).

[1]Defined as the average of the x and y coordinates of all the cell pixels.

3.3.2 Cell smoothness: a novel method to quantify protrusive activity

A second method to estimate cell protrusions was used. It is based on the premise that the more protrusion a cell have, the more its perimeter increases with respect to is area. Therefore, the perimeters of the cells were compared with the perimeter of the ellipse that will better describe that cell. A ratio to quantify this deviation from a perfectly elliptical perimeter, Cell Smoothness (CS), was defined:

$$CS = \frac{P_e}{P_c} \tag{3.2}$$

with P_e and P_c the ellipsis and cell perimeter, respectively. Smooth cells (with no or small protrusive activity) will have a CS value close to one whereas more protrusive cells will trend to decrease their CS value. As the CS index is a ratio, it does not depend on the cell size or circularity.

To obtain the parameters required for this quantification images of migratory cells were imported into ImageJ. Similarly to the previous method, cells were labelled with a membrane-bound fluorescent dye, and a threshold was set to generate binary images of them. The analyse particles function was used to draw obtain the outlines of each cell and measure their perimeter. The same function was used again but this time it was set to obtain and measure the perimeter of the best-fit ellipse for each cell. These correspond to the P_e and P_c values required to calculate CS. A detailed guide to how to this analysis is include as an Appendix to this thesis.

3.4 Analysis of migratory behaviour

3.4.1 Cell tracking

Time-lapse image series of individual migratory cells were manually tracked using the MTrackJ plug-in of ImageJ. A 2-D cell tracking was preferred because of the characteristics of the cell culture used *in vitro* and the characteristics of the NC migration *in vivo* described

in 3.2.1. This method requires a manual identification of each cell at each time point. Because usually a low magnification and relatively long time distance in between frames were used in these analysis, there was no need to identify the cell centroid or any specific landmark to locate the cells accurately. If tracks were performed at higher temporal and/or spatial resolution, the centroid of the cell or the nuclei was determined and used for tracking. Matrices containing the x,y data of each cell at each time point were imported to Matlab were a script was written to analyse them.

3.4.2 General Parameters: Distance, Speed, Persistence Directionality and others

Either manually or with the aid of the Matlab script described above, different parameters of the tracks could be estimated. Euclidean geometry was always assumed. The distance advanced by a cell between different time points can be calculated with the changes of their position values (δx and δy) using Pythagoras' theorem. The distance from the origin can be calculated in the same way. The total length of the path will be the summation of the advances at all the time points. The "instantaneous" speed can be estimated as the distance advanced at a particular time point, divided by the time difference among frames (δt). A more important average speed can be estimated as the total length of the path divided by the total migratory time or, what is the same to $\delta t \times$ *numbers of frames*.

An important parameter of migratory cells is their persistence. This gives an account of the efficiency or commitment towards a direction of a cell during its migration. It was calculated as the distance form the origin at the end of the migration divided by the total length of the past. A very committed cell will have a total length of migration similar to its distance from the origin and thus, its persistence value will trend to the unit. On contrary, a cell with no directionality will have a long but convoluted migratory path with no big net advance and thus its persistence value will approach to zero.

The orientation of the cell at each time with respect to an external parameter (the *x-axis* for example) or to its previous orientation can be calculated. First, the angle with respect to the *x-axis* is calculated using:

$$\theta = \arctan \sqrt{\frac{\delta y^2}{\delta x^2}} \tag{3.3}$$

Then, the new angle is calculated (the external parameter, the next time step, etc...) also with respect to the *x-axis*. The angular difference is then calculated using their dot product. The population of angles was usually represented using a rose histogram.

Analysis of cell collisions

Cell collisions were analysed by determining the acceleration vector associated to them similarly to what has been performed before (Dunn and Paddock, 1982; Paddock and Dunn, 1986). Colliding cells were treated as particles centered on its own nuclei and then tracked. When the analysis was performed *in vivo* cells were centred differently as the nuclei is rarely visible. Consecutive images were pseudo-coloured (differently) and blended obtaining a color-coded image, similar to the one described in Section 3.3. Here, it is possible to distinguish the areas in both frames (null areas) from the areas in the first frame only (negative area) and from the areas in the second frame only (positive areas). Negative areas are considered retractions and positive areas are considered protrusions. Tracks were made from sequences of these combined areas. Colliding cells were tracked and their positions were imported to Matlab. Mean velocities were measured before and after the collision and the corresponding acceleration was calculated according previous works (Dunn and Paddock, 1982; Paddock and Dunn, 1986). The resulting vector was orientated in relation with the initial velocity as described in the same work. Finally, acceleration vectors from several collisions of cells under the same conditions were depicted together in a compass plot.

Chemotactic index

To calculate the Chemotactic Index (CI), the coordinate system was rotated to have the y-axis passing through the source of the chemoattractant at the top and the cells at the bottom. Then the CI will correspond to the cosine of the angle between the displacement

of the cell and the y-axis (Kay et al., 2008). A CI value of 1 (angle value 0) means that the cell is directly going towards the chemoattractant.

3.4.3 Group level parameters

3.4.4 Average path

To calculate the average path, the Cartesian positions of the tracked cells were averaged at each time point. With this, the angle between the displacement of each cell and the direction of the average displacement can be obtained for each time step. This angle reflects the alignment between cells as lower values will indicate aligned cells and higher values will indicate that cells are departing from the general directional trend. To do this, θ was calculated using,

$$\theta = \arccos\left(\frac{c_i \bullet c_a}{|c_i||c_a|}\right) \tag{3.4}$$

where, c_i is the displacement vector for the cell i and c_a is the average displacement vector at a particular time point, $c_i \bullet c_a$ is the dot product between those two vectors and $|c_i| = \sqrt{c_i \bullet c_i}$.

3.4.5 Quantification of Invasion

To quantify Invasion in confronted explants, an invasion index, similar to the one that has been previously used (5; see below), was devised. To do this, colliding cell populations were obtained form embryos labelled with different fluorescent dyes (GFP and RFP). Colour channels were imported separately to ImageJ, thresholded and masked. For each confrontation, both masks were pseudocolored (different colors) and then blended. The resulting blended image has a different color for the overlapping area. Invasion Index (ι) was estimated by measuring the overlapping or invasion area (IA) between the two different explants standardised by the initial surface of the invaded explant (R_i). The initial

area was used for standardisation instead of the more intuitive final one because the area of NC explants increases notoriously while other cells populations do not change significantly their size. Ri did not show any significant variation neither among nor between groups. Areas were normally distributed and thus One-way ANOVA was used to compare the resulting ι values.

3.4.6 A novel method to quantify cell dispersion via a Delaunay triangulation of neighbours

When trying to measure the dispersion of groups of cells several problems arise. Because it is sometimes difficult to control exactly the initial number of cells, especially with primary cultures, simply measuring the final surface covered for the explant can be very misleading. Also, the ratio between the initial and the end explant surface can be misleading because the explant may dissociate in a heterogeneous way and thus, differences may be averaged out. To overcome these difficulties, a way to measure dispersion based in more local differences rather in global differences was devised. It consists in the simple idea that in situations where there is more dispersion, neighbouring cells will be more distant from each other. To determinate the nearest neighbours, Matlab/Qhull Delaunay triangulation (Barber et al., 1996) algorithm was used in 2D. For a set P of points on a plane, this triangulation requires that no point in P is inside the circumscribed circle (circumcircles) of any triangle of the triangulation. In the following figure a visual explanation of how the algorithm works is provided for clarity (panel a).

Once the triangulation was obtained, the areas of the triangles were calculated in Matlab. Finally, triangles were depicted in a colour-coded fashion where the colour is proportional to their areas. To compare different treatments or to analyse repetitions of the same experiment areas were statistically compared. The natural logarithm of the area values was used to have the data normally distributed (figure below, panel b and c, normal probability plot and histograms, panel d). Colours represent different arbitrary treatments. Then, the logarithm of the areas was analysed, using one-way ANOVA and depicted in box plots (panel e).

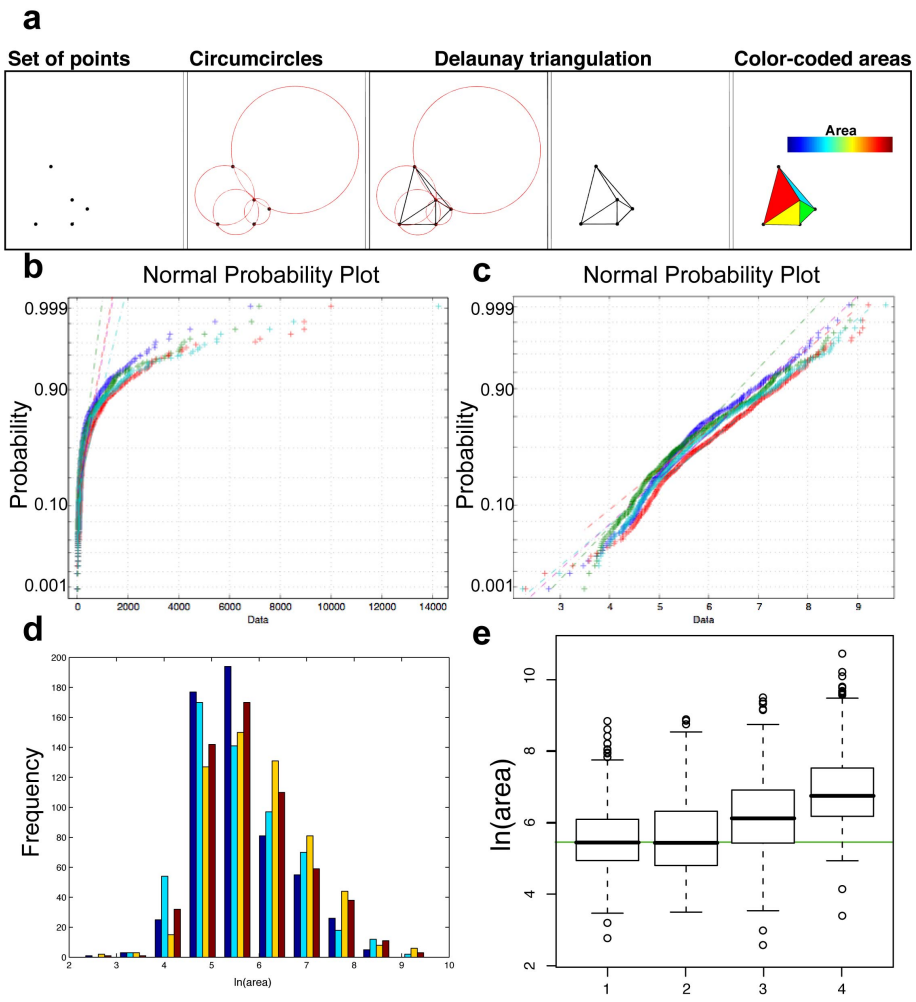

Figure 3.1: **Method to calculate cell dispersion via Delaunay triangulation.**

3.4.7 Acoustic and visual representation of harmonic cell movements

To represent harmonic cell movements the deviation of each cell from the average path was used. In order to do this, an arbitrary sequence of notes (in Hertz, Hz) was given to the average path. In the case presented here C major scale (up and down) was used so if a cell would go exactly over the average path, it will play C4 (middle C, 261.6 Hz), D4(293.7 Hz), E4(329.6 Hz), F4(349.2 Hz) G4(392.0 Hz), A4(440 Hz), B4(493.9 Hz), C5(523.2), B4 and so on. However as no cell takes the average path this sequence was never played but each cell will play a version of it shifted according the deviations from the average path.

The alignment angle θ, calculated as mentioned above, was the main considered parameter although the speed also had a minor influence. This angle needed to be transformed to a shift in musical pitch. Thus, θ was directly mapped onto cents using, $\Delta cent = \theta(600/\pi)$. To take into account the speed of the cells the sign of $\Delta cent$ was determined by it using,

$$sign = \frac{v_i - v_a}{abs\,(v_i - v_a)} \tag{3.5}$$

with v_i the speed of a cell i at a particular time point and v_i the average speed of the group at that time point. Thus, cells that would be faster than the average will have a positive $\Delta cent$ whereas slower cells will have a negative $\Delta cent$. Then $\Delta cent(sign)$ values were added/subtracted to the corresponding note b using,

$$a = b \times 2^{\frac{\pm \Delta cent}{1200}}, \tag{3.6}$$

where a is the resulting note. For example, if the cell number 3 at the 6th time point should play A4 (440Hz) and its $\Delta cent(sign)$ was 50, the note it would play would have a frequency of ∼427.5Hz, *i.e.* it would be in an slightly lower pitch than the expected 440Hz. This was repeated for each cell at each time point. With that, a *cell x time* matrix of Hertz values was generated that can be visualised by simply using the *imagesc* function in Matlab. We called this diagrams harmony maps. Harmonic groups of cells will have the same/similar Hz values which will be reflected in horizontal stripes of the same colour. To transform this matrix to sound, a MIDI toolbox for Matlab was used (Lartillot et al., 2008) but other software such as csound (csounds.com) may also be used. Briefly, Hertz values were transformed to MIDI data taking advantage of the microtonality feature of MIDI using,

$$p = 69 + 12 \times \log_2 \left(\frac{f}{440} \right), \tag{3.7}$$

where f is the frequency to be transformed into a MIDI value p. The reference number 69 is the MIDI value of A4.

3.5 Directional Statistics

3.5.1 Circular mean and variance

These parameters were calculated following Mardia and Jupp 2000. In brief, directional vectors were considered unit vectors. Then, the mean orientation $\overline{\theta}$, corresponds to of centre of mass (with Cartesian coordinates $(\overline{C}, \overline{S})$) with respect to the origin (0,0). $\overline{C}$ and $\overline{S}$ correspond to the average $\cos(\theta)$ and $\sin(\theta)$, respectively. The distance between the pairs $(\overline{C}, \overline{S})$ and (0,0) correspond to the *mean resultant length*, $\overline{R}$.

Then, when $\overline{R} > 0$,

$$\overline{\theta} = \begin{cases} \arctan(\overline{C}/\overline{S}) & \text{if } \overline{C} \geqslant 0, \\ \arctan(\overline{C}/\overline{S}) + \pi & \text{if } \overline{C} < 0. \end{cases} \tag{3.8}$$

The, value of $\overline{R}$ ranges from 0 to 1 and is an important parameter as the closer it is to 1, the more clustered the angles are and *vice versa*. Then the simplest measurement of dispersion in circular statistics, the circular Variance (V) is:

$$V = 1 - \overline{R} \tag{3.9}$$

3.5.2 A statistical method to test deviation from random orientation

Statistical Analysis was done by custom-made functions and scripts in Matlab to implement the modifications by Moore to the Rayleigh's test (Moore, 1980). This approach was specifically developed to test non-random distribution of vectors and thus, it is ideal for our analysis. As recommended, we used a two-tailed version of this test (Moore, 1980). The graphic outcome of this analysis was processed either in Matlab itself or exported as a post-script file and edited in Adobe Illustrator (v.13.0, Adobe).

3.6 Modelling

3.6.1 The biological scenario

A 2D-model of moving particles was design to test if collisions between particles may improve their efficiency to disperse and to eventually to reach a target. The situation attempted to be modelled was the *in vivo* cranial NC migration. A simplified explanation of what we know about this is described below:

The NC cell population is initially localized at the dorsal midline from where it delaminates and migrates ventrally. Although the NC cells migrate in a 3D space, we have assumed a 2D space. This assumption is based in the following observations. Z-stack analysis performed in preliminary experiments established how deep the NC migrates in the zebrafish embryo. After 6 to 8 h time lapse of 20 somites embryos, we found that cephalic NC migrate between 500-800μm in the anterior-posterior axis, between 40-60μm in the dorso-ventral axis and between 7 and 9μm in the periphery-center axis. In consequence, it is possible to assume that most of the cell migration is performed in two dimensions, while the third dimension (in the Z axis when the embryo has a lateral orientation) can be neglected. In addition, it was observed that migration of cephalic NC is highly directional from dorsal to ventral, and it is known that they follow specific pathways which are flanked by negative signals (for a review see, Kuriyama and Mayor, 2008).

3.6.2 Model description I: Contact Inhibition of Locomotion only

In our model, the particles (cells) are initially localized at the top (dorsal) of a surface (a 2D lattice) laterally limited by regions where the cells cannot migrate (as in the embryo). At the bottom (ventral), there is a region were cells stop their migration (target). When running the model, cells were prompted to move as random walkers.

In one or two-dimensional manifolds, it can be proven that as the number of steps in a random walk approaches infinity, the probability of reaching the origin (and thus any other position) equals the unity (Weisstein, 2007). This means that in theory, all cells in the

model will eventually reach the target. The question was if it was possible to significantly reduce the number of steps required to reach the target, by including a contact inhibition variable.

The model was run under two different conditions: with and without the contact inhibition parameter (CIL). Cells with contact inhibition were asked to rotate in $180°\pm\theta$ (being θ an arbitrary angle defined before running the model) after the collision. Cells without contact inhibition are not affected by the collision.

The *Step* parameter was defined as the number of iterations a cell (with or without contact inhibition) will continue moving in the same direction before rotating randomly. The *Step* parameter allows the migration of a cell in non-random manner for a small fixed number of iterations (Step), and therefore, it helps to distinguish the effect on migration produced by the collision during contact inhibition from the random migration at the end of the *Step*. If the Contact inhibition parameter is considered, at any time that the cell collides, *Step* is reset, thus the cell will continue for a *Step* number of iterations in the new direction given by the collision (unless it collides again). It is shown that even small *Step* numbers, are sufficient to generate a strong difference on the directionality of cells with or without contact inhibition (Figure 5.10).

The model was implemented as a particle-based (agent) approach using NetLogo (Wilensky, 1999). Some of the features were modified from Random Balls Model (Wilensky, 1998). Then, experiments were simulated and variables were calibrated using Mathematica (Mathworks, Mathematica J/link toolkit, Bakshy and Wilensky, 2007).

3.6.3 Model description II: Adding coattraction

The conditions for the model that includes both CIL and coattraction are essentially the same but in, two noteworthy modifications. First, collisions included an intrinsic alignment which consisted in that colliding cells will migrate in the same direction for an arbitrary length of time, after which they will move away with the angle θ described above. The length of the alignment was defined by *AlN* but this parameter can be as short as one

without changing the global behaviour of the system (Figure 6.1).

The major modification was the inclusion of the coattraction parameter *per se*. For this aim, an interaction radius rCoA was defined fro each particle. Particles will sense particles within this radius but only when the internal clock (given by *Step*) has the maximum value. If these conditions are met, the particle will move towards the centre of mass of all the particles within this radius $\pm$ a noise ζ.

Part III

Experimental Results

Chapter 4

NC cells exhibit Contact Inhibition of Locomotion

4.1 A role for cell-cell contacts in polarisation and directionality

Xenopus Neural Crest (NC) cells migrate with high directionality and persistence in their normal embryonic pathways (See section 1.4 for details and references). Interestingly, these cells can also display persistent and directional motion when cultured *in vitro*, where embryonic guidance cues are absent. This indicates that to a certain degree, NC migratory features are autonomous. Thus, the study of NC migration *in vitro* may help to elucidate the intrinsic capabilities of these cells for directional migration alongside the influence of external signals.

The establishment of a polarised cell is essential for directional migration (Lauffenburger and Horwitz, 1996; Ridley et al., 2003). Cells in fixed NC explants visualised with SEM reveal a striking heterogeneity in their polarisation. Leader cells (the cells at the border of the explant), show pronounced polarisation with clear lamellipodia at their front (arrowheads in Figure 4.1a). Conversely, trailing or internal cells show discrete polarisation

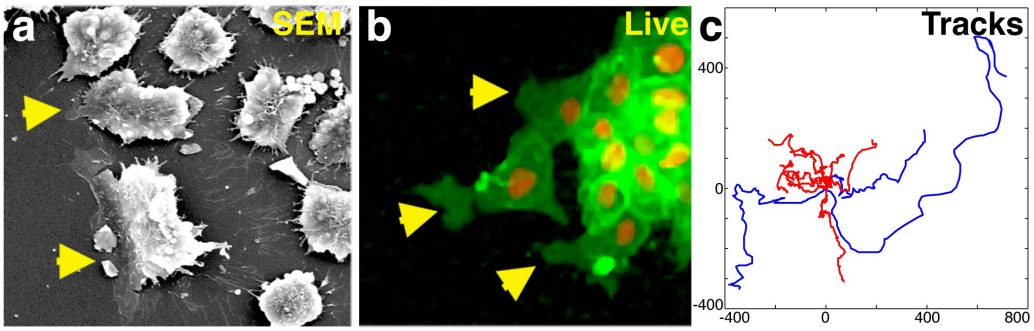

Figure 4.1: **Only leader NC cells are polarised and move directionally.** a. SEM image showing that leader but not trailer cells show clear polarisation, evidenced by large lamellipodia (yellow arrowheads). b. Image of a live NC explant labelled with membrane-GFP and nuclear-cherry (Red). c. Tracks of leading (blue) and trailing cells (red) showing that strong polarisation correlates with higher directionality.

with smaller membrane processes and no lamellipodia (Figure 4.1a). As expected, the same difference between leader and trailer cells can be observed in live cells labelled with membrane-GFP (Figure 4.1b). Importantly, this differential polarity is also reflected in differences in the directionality of migration. Leader cells have directional path, with a greater net displacement and persist in the same direction. In contrast, trailer cells make little progression and have low persistence (Figure 4.1c).

Differences between trailing and leader cells appear to be dynamic rather than reflecting an intrinsic cell difference or the presence of two distinct cell populations. Figure 4.2 (and Movie 4.1[1]) shows the temporal evolution of a cell migrating in a cluster. Top panels illustrate that when this cell is at the centre of the cluster, it has no clear polarization and exhibited undirected motion (Figure 4.2a). However, once this cell has a free edge, it becomes polarised and begins migrating directionally (Figure 4.2b). Furthermore, dissociated and then re-aggregated NC cells, so that their initial positions are randomised, maintain the leader *versus* non-leader difference. For example, a small re-aggregated group is shown in Figure 4.3a. Each of these cells is at the edge of the small cluster and thus they are polarised and leave the group with strong directionality.

Additional confirmation of the ability of all the cells to polarise if exposed to a free edge

[1]Please find a CD attached to this thesis containing the cited movies.

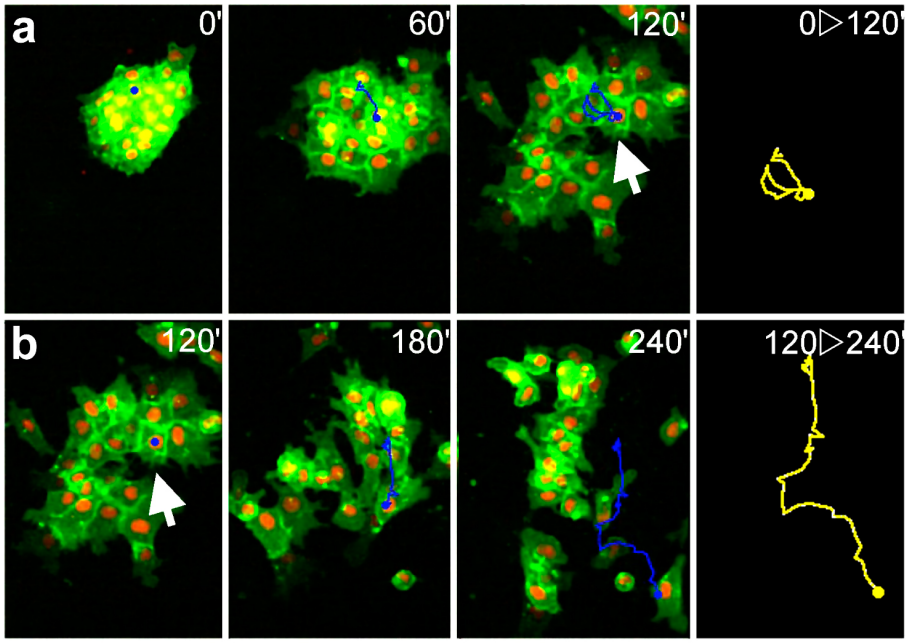

Figure 4.2: **Leader or trailer cell behaviour is dynamic and not intrinsic.** a. Selected frames of a time-lapse movie and track of a trailer cell. White arrow shows the moment when that cell is exposed to a free edge. b. Selected frames of a time-lapse movie and track the same cell but now behaving as a leader cell due exposure to the free edge of the explant. Time in minutes in upper-right corner.

comes from the experiment shown in Figure 4.3b-h. An intact NC migratory explant will show polarised cells with clear lamellipodia along its periphery (Figure 4.3c). If such an explant is cut as shown in Figure 4.3b, non-polarised cells will be exposed to the free edge (Figure 4.3e,f). As expected, these cells, which displayed little directional migration prior to cut (Figure 4.3d, quickly produce lamellipodia and polarise towards the cell free region, beginning directional migration (Figure 4.3g-i).

Two possible mechanisms may account for the described behaviour of NC cells in culture. Firstly, NC cells receive their polarity from the cell-free zone itself. A second possibility is that NC cells will spontaneously polarise in all directions but cell-cell contacts restrict this polarisation. Thus, cells will be polarised only at the cell-free zone because this is the region where polarisation is not been inhibited. The comparison between the behaviours of single and leader cells allows for discrimination between these two possibilities. As described above, leader cells show directional and persistent movement. These features

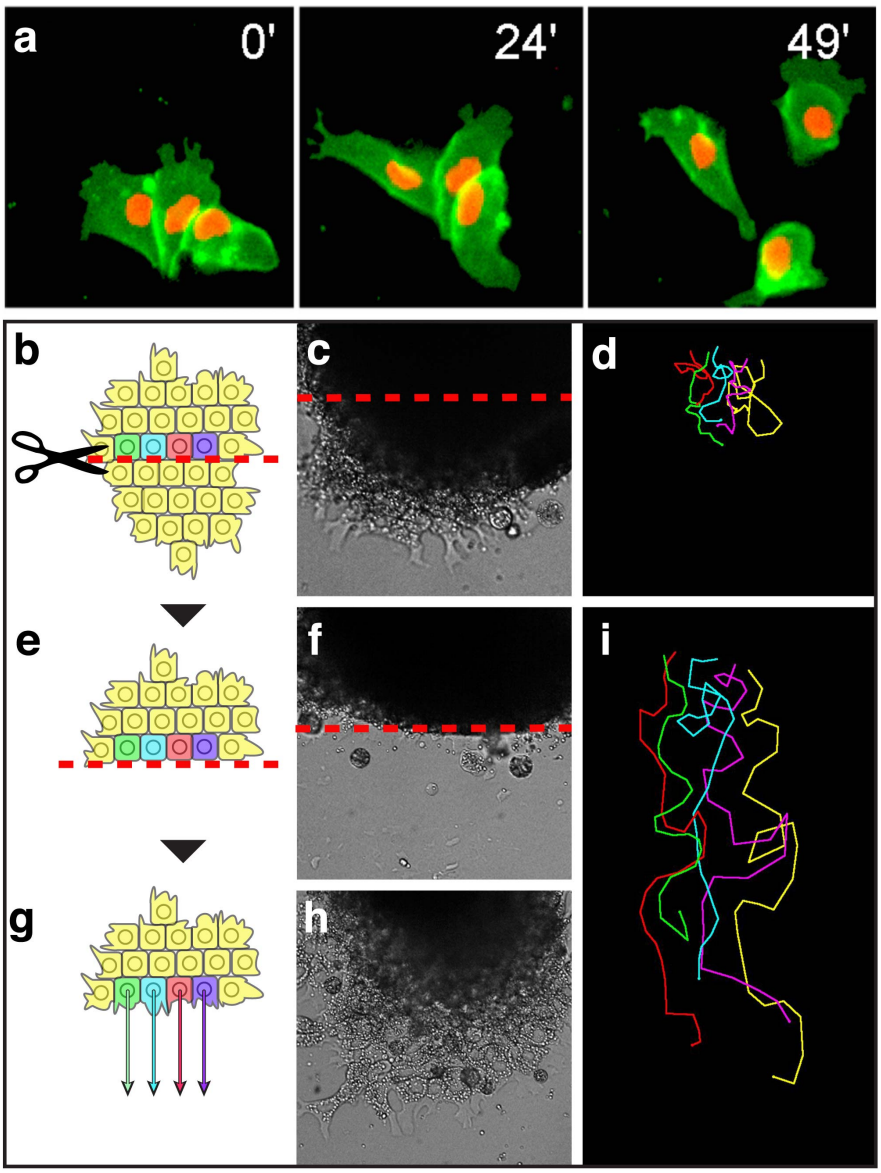

Figure 4.3: **Cell position reshuffling and cut-explants experiments further support that there is no intrinsic difference between leader and trailer cells.** a. Small NC group re-aggregated after dissociation showing that all cells can polarise. b. Scheme of c. c. NC explant where its internal cells have no directional migration and only cells at the explant edge have clear protrusions. d. Tracks of the cells in c. e. Scheme of f. f. Cut-explant showing non-polarised (no protrusions) cells at the edge. g. Scheme of h. h. Cells exposed to the cell-free zone quickly polarise and start directional migration as shown in i. Time in minutes in upper-right corner.

can be appreciated in the temporal projection shown in Figure 4.4a and Movie 4.2. The temporal projection consists of five superimposed consecutive images of the same visual

field showing the displacement of a leader cell (positions at each frame are marked with a number). On the contrary, a similar depiction of a migratory single cell shows a lack of directionality (Figure 4.4b, Movie 4.2). Detailed observation of the polarity of this cell reveals a high rate of spontaneous polarity in all directions. Quantification of this persistence in both conditions confirms this clear difference (Figure 4.4c). Interestingly, individual cells have a much higher speed in migration than leader cells highlighting the dissociation between directional migration and the rate of displacement of a cell and supporting an inhibitory role for cell contact (Figure 4.4d). These experiments show that the contact itself, rather than the cell-free space, is responsible for stable cell polarity.

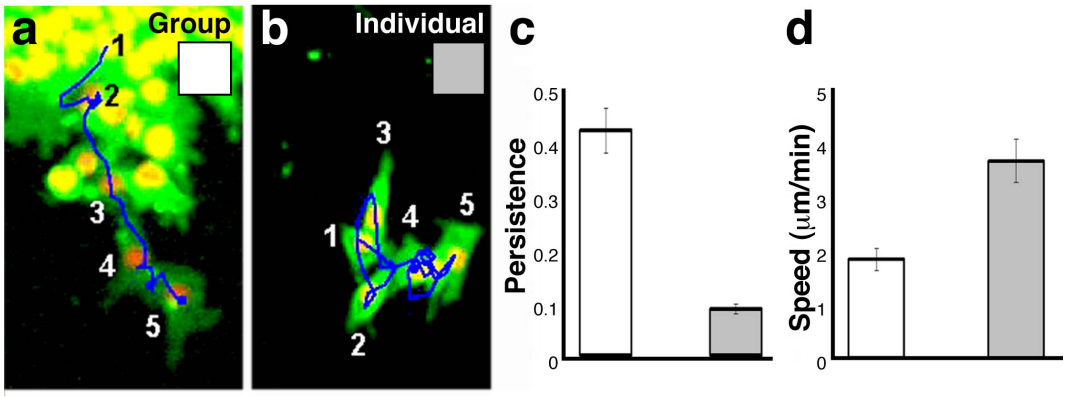

Figure 4.4: **Cell-cell contacts are required for polarisation and directional migration.** a. Temporal projection of five frames showing the migration of a leader cell in a group. Numbers indicate the consecutive positions of the cell. b. Temporal projection of five frames showing the migration of a single cell. c. Leading cells in a group have higher persistence than single cells. d. Cells in groups have migrate slower than single cells, thus speed and directionality are not always linked.

Together, these results indicate that the directional migration of cultured NC cells is dependent on cell-cell contact, which is likely to inhibit the formation of cell protrusions leading to cell polarisation. Also, these results show that cell speed diminishes when cells have more neighbours. These features of NC cells are highly reminiscent of the features reported for cell types exhibiting Contact Inhibition of Locomotion (Abercrombie and Heaysman, 1953; Winklbauer et al., 1992; Abercrombie, 1979).

4.2 Contact Inhibition of Locomotion in NC cells

4.2.1 *In vitro* studies

One of the main characteristics of cells exhibiting Contact Inhibition of Locomotion (CIL) is that cells will collapse their protrusion upon contact and reset their direction of migration. If a cell is contacted all around its periphery it will stop migrating. In contrast, if a cell lacks CIL it will continue its motion invading neighbouring cells (see section 1.3.4 and references therein for more details). An explant confrontation assay has been usually used to assess the presence of CIL (Abercrombie and Heaysman, 1953; Abercrombie, 1979). In this assay, two NC explants were cultured in close proximity such that their leading cells would encounter cells from the other explant migrating in the opposite direction (Figures 4.5 and 4.6).

When two NC explants are confronted, they start dispersing radially. However, when they encounter the outgrowth of the other explant they stop dispersing in that direction and a clear sharp border at the interface of the two explants can be observed (Figure 4.5a; Movie 4.3). Overlapping cells can be detected because cells of different explants are labelled with different colours. However, in this condition cells almost never overlap (Figure 4.5b,e,g; Movie 4.3), a clear indication of *homotypic* (same cell type) CIL among NC cells.

In order to reach their target regions, NC cells need to invade structures such as the head mesoderm during normal embryonic development. Thus, it is unlikely that NC cells will exhibit CIL against the cells conforming these structures, as it would impede their normal migration. Accordingly, NC explants aggressively invade mesodermal (Figure 4.5c) explants, a clear suggestion that NC do not exhibit CIL against this other cell type. This lack of *heterotypic* (between different cell types) CIL is also evident if the overlapping region is measured. While two NC cell populations barely overlap, there is a significant increase in the area of overlap in NC and mesodermal confrontations (Figure 4.5d,f,g). Proper invasion should include cells at the core of the explant as well as others engulfing it, however this would be difficult to observe with a two-dimensional visualisation.

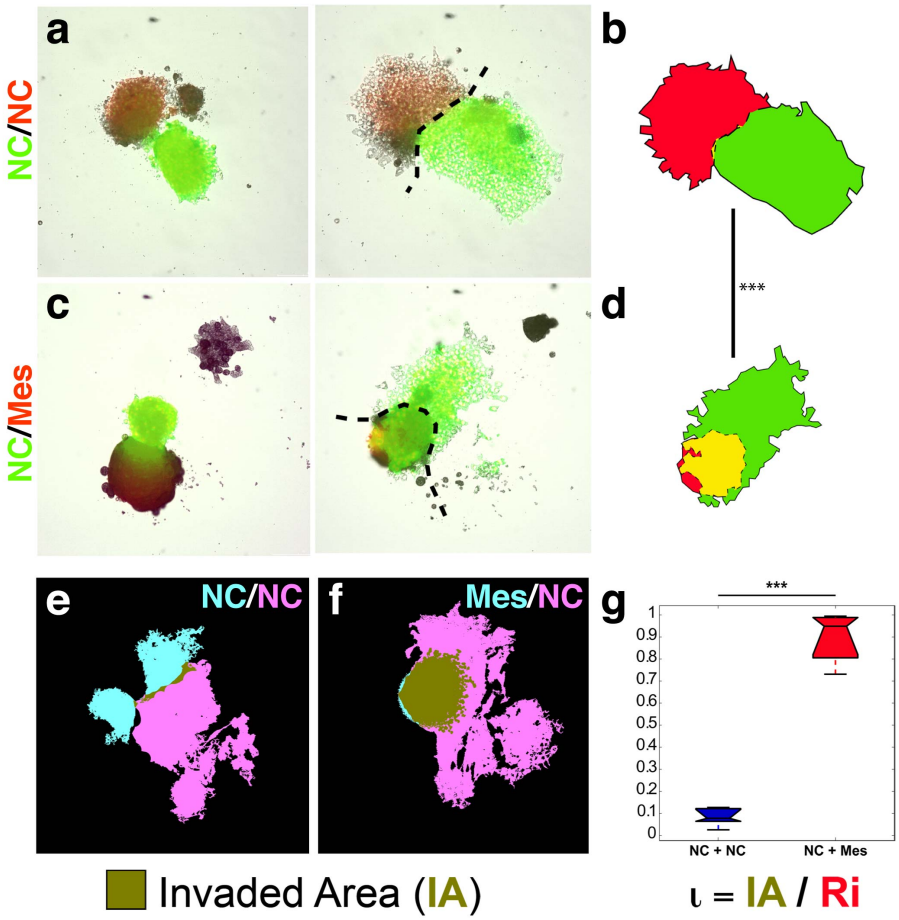

Figure 4.5: **NC cells have homotypic CIL.** a. Initial and final frames showing two confronted NC explants. b. Representation of the overlap between the two cell populations (in yellow). c. Initial and final frame showing a NC explant (green) confronted to en explant of head mesoderm. d. Representation of the overlap between the two cell populations (in yellow). e-g. Quantification of cell overlaps. e. Overlapped masks of two NC explants. f. Overlapped masks of a NC and a mesodermal explant. g. Box plot of measured confrontations. *** $p < 0.001$.

Two-photon confocal microscopy has a high depth of visualisation and allows three-dimensional reconstruction of samples. Thus it is an excellent tool to analyse NC invasion into the mesoderm. As a control, it can be seen that NC/NC confrontation results in two non-overlapping cell monolayers (Figure 4.6a-c). The two NC cell populations can be distinguished because they are differently labelled (red nuclei/green membrane or green nuclei/red membrane). On the contrary, NC cells completely engulfed mesodermal explants as shown in Figure 4.6d,d'. The scheme in Figure 4.6e shows the paths of NC

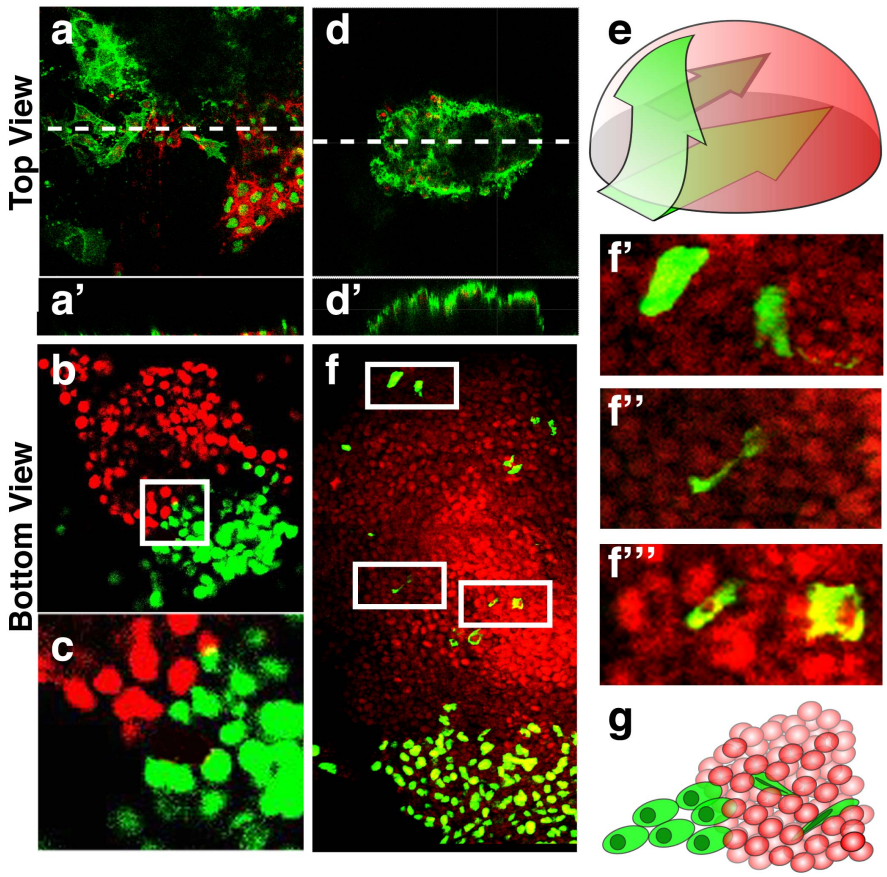

Figure 4.6: **NC cells can invade other structures such as head mesoderm.** a. Confocal image at the interface between two NC explants (red and green). a. z-section through the dashed line shown in a. b. Similar to a. but with cells with only nuclear staining. c. Magnification of the squared region indicated in b. d. Confocal image at of a group of NC cells (green) over mesoderm (unlabelled). d. z-section through the dashed line shown in d. e. Schematic representation of the invasion paths of NC cells. f. Mesodermal explant (red) invaded by NC cells. f'-f"'. Detailed view of nuclei shown in f. Note the distorted morphology of invading nuclei. g. Schematic representation of f-f"'.

invasion. The middle arrow indicates that NC cells can penetrate, in addition to migrate under and over, the mesoderm cluster as shown in Figure 4.6f-g. Interestingly, invading NC have their nuclei deformed (Figure 4.6f'-f"'), a phenomenon also observed in invading cancerous cells (Wolf et al., 2007).

These experiments strongly support the idea that NC exhibit homotypic CIL. However, a detailed analysis of cell-cell collisions is required to properly demonstrate CIL (Dunn and

Paddock, 1982; Paddock and Dunn, 1986). Cell collisions can be observed in the explant-confrontation assay but now focusing at the cell level. When, a NC cell comes into contact with a cell from the opposite group, its lamellipodium collapses and the direction of its migration changes (Figure 4.7a; Movie 4.4). This is described precisely by Abercrombies definitive definition of CIL:

> "the phenomenon of a cell ceasing to continue moving in the same direction after contact with another cell."
> (Abercrombie, 1979)

It is important to distinguish the effect of cell collisions on cell direction from just random changes in cell movement. Accelerations, by definition, are the change of velocity over time and they have been successfully used to analyse CIL statically (Dunn and Paddock, 1982; Paddock and Dunn, 1986). The velocities of analysed collisions are shown in Figure 4.7b and corresponding accelerations in Figure 4.7c. A random vector distribution will be uniformly (not normally) distributed, *i.e.* their vectorial addition will not be far from zero (Mardia and Jupp, 2000). As it can be observed, the distributions of accelerations are far from random as they show a strong directional bias. Directional statistics are required to test the significance of this clustering. An excellent test to assay circular uniformity is the Rayleigh's test (Mardia and Jupp, 2000). However, this test only takes into account the directional component of vectors (all vectors are assumed to be unit vectors). An improved version of this test, which considers the length of vectors, is then the optimal test to use in this situation (Moore, 1980). Acceleration vectors after collisions resulted to have a highly significant deviation form a random distribution (Moore's test: $p < 0.001$), another demonstration of homotypic CIL in NC cells.

Altogether, the results presented in the last two sections show that cell-cell contact is essential for NC polarisation and directional migration *in vitro*. They also show, for the first time, that NC cells exhibit homotypic CIL, mechanism that mediates contact-dependent cell polarity and directional migration. Importantly, CIL is cell-specific and thus not just a mechanical response to collisions as NC cells can invade other tissues such as mesoderm.

4.2.2 *In vivo* studies

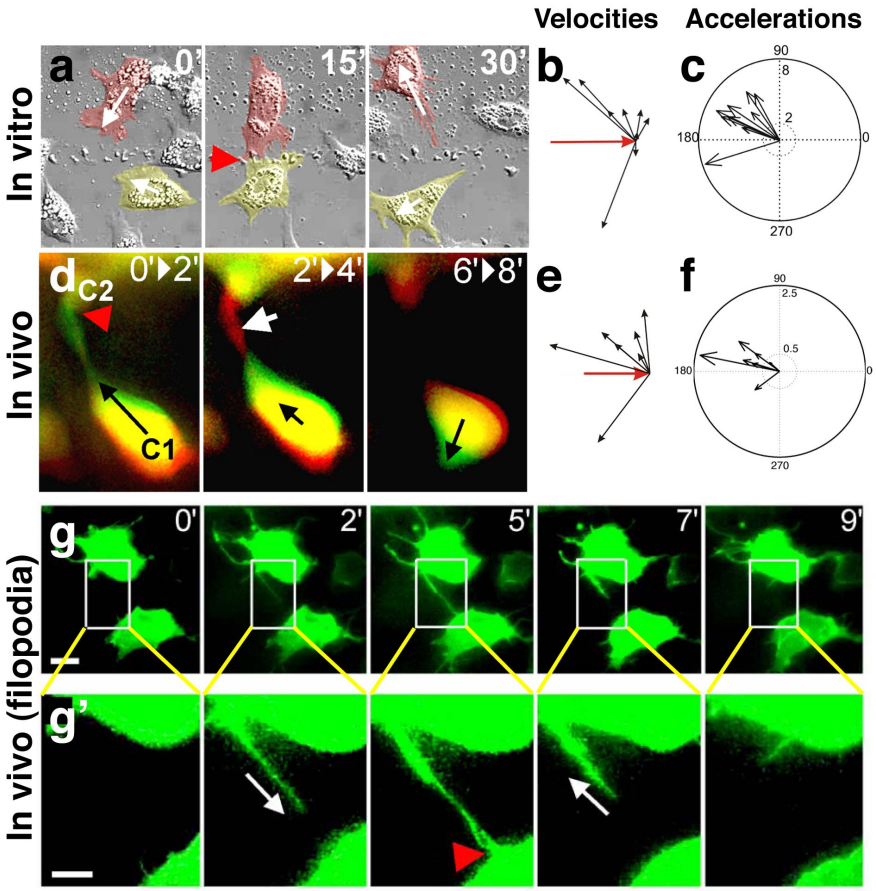

Figure 4.7: **Analysis of cell collisions demonstrate that NC cells exhibit CIL *in vitro* and *in vivo*.** a. Selected frames of a time-lapse movie showing two colliding NC cells *in vitro* (pseudocoloured in red and yellow). b. Aligned velocities of collisions. Red velocity: Initial velocity. Black velocities: velocity after collision standardised by the initial ones. c. Compass plot showing that acceleration vectors are highly clustered after collisions ($p < 0.001$). d. Selected frames of a time-lapse movie showing the collision of two NC cells *in vivo*. Each image corresponds to the superposition of two consecutive frames (indicated in upper corner) to show cell progression (green) and cell retraction (red). e. Aligned velocities. f. Acceleration vectors ($p < 0.001$). g. Selected frames of a time-lapse movie of NC migration *in vivo* using the *sox10*:membrane-GFP transgenic zebrafish. Membrane-GFP is only expressed in NC cells allowing the visualisation of filopodia dynamics during collisions. g. Detail of g. Time in minutes in upper-right corner. White arrows: direction of movement. Red arrowheads collision points.

To date, CIL has mostly been described *in vitro* with very few attempts to demonstrate it *in vivo* due, at least in part, the difficulties of observing cell migration *in vivo* (Mayor and Carmona-Fontaine, 2010). Recent advances in microscopy (such as confocal imaging)

and in cell labelling (such as development of transgenic animal lines) are allowing scientist to overcome the technical limitations of *in vivo* imaging. Zebrafish embryos present several advantages for cell imaging such as an almost complete transparency of their body. Moreover, transgenic lines -where GFP is transcribed under the control of cell-line specific promoters- allow specific cells to be followed. Here, two *sox10*:-GFP transgenic zebrafish lines were used: one that expresses GFP in the cytoplasm (Carney et al., 2006), and the other in the membrane of NC cells (see section 2.2.5 for details). *In vivo* NC migration of these animals can be visualised and analysed using fluorescent and confocal imaging. Similar to the observations *in vitro*, whenever two NC cells make contact, they change their direction of migration and their protrusions collapse (Figure 4.7d; Movies 4.5 and 4.6). Importantly, the velocities and accelerations derived from these collisions were also measured and analysed. Large changes in the direction of cell migration are seen after each cell collision as shown in the velocity vectors (Figure 4.7e). The change of the velocities was again highly clustered and thus, significantly different form a uniform (random) distribution (Acceleration vectors in Figure 4.7f). Therefore, NC cells exhibit CIL *in vitro* as well as *in vivo*.

So far, the analysis of NC cell behaviour shown here has centred in the dynamics of large protrusions such as lamellipodia. It is known that chick NC cells migrating *in vitro* establish long and transient contacts with neighbouring cells mediated by thin processes or filopodia (Teddy and Kulesa, 2004). Interestingly, these connections may mediate some kind of cell-cell communication, as they seem to influence cell directionality (Teddy and Kulesa, 2004). These contacts have a variable duration but how and when this retraction is controlled remains unknown. Taking advantage of the *sox10*:membrane-GFP transgenic line, the detailed morphology of migrating NC cells was observed *in vivo*. As reported for chick NC cells *in vitro*, zebrafish NC cells also showed long filopodia connections with neighbouring cells *in vivo*. Moreover, it seems that CIL is also affecting these protrusions as they quickly retract after contacting neighbours (Figure 4.7g,g', Movie 4.7).

It is tempting to speculate that CIL could play a role in guiding the migration of NC cells in normal development. *In vitro* CIL has an important role in two aspects, directionality and invasive potential, and these can be tested *in vivo* for the migratory NC. Labelled

Xenopus NC cells transplanted onto an unlabelled host embryo integrate with endogenous NC cells and migrate directionally (Figure 4.8a-d). If CIL has a role in this process, the directionality of these cells will depend on cell density. Conversely, if direction of migration is dictated by external cues independently of cell contacts, NC cells will remain migrating directionally regardless of the cell density. To test this, a similar graft of labelled NC cells was transplanted onto an embryo whose own NC cells have been previously removed (Figure 4.8e). In this case, where the final cell density is much lower, NC directional migration is almost completely lost (Figure 4.8e-h). This experiment shows that the directionality of NC migration depends on interactions with other NC cells and supports the conclusion that CIL is required for normal NC migration *in vivo*.

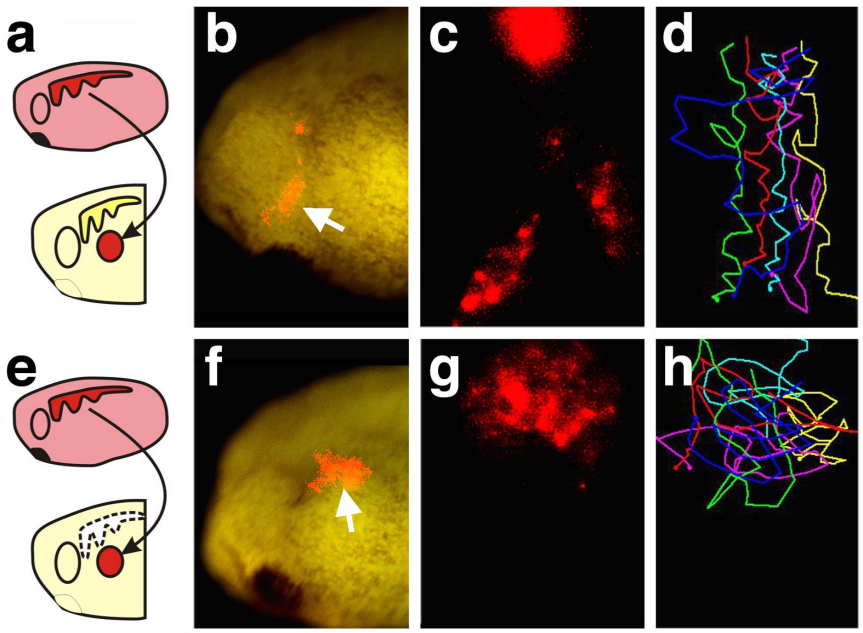

Figure 4.8: **CIL is required for NC directional migration *in vivo*.** a-d. Transplantation of labelled NC onto a normal, unlabelled embryo. a. Schematic representation of the procedure. b. Overlay of bright field and fluorescent pictures of the host embryo, 12 hours after transplantation. c. Close up of b. but only showing the fluorescent channel. d. Tracks of grafted cells. e-h. Transplantation of labelled NC onto an embryo whose endogenous NC have been previously removed. e. Schematic representation of the procedure. f. Overlay of bright field and fluorescent pictures of the host embryo 12 hours after transplantation. g. Close up of f. but only showing the fluorescent channel. h. Tracks of grafted cells. Note the poor net displacement of NC cells if their number is low (as there are no endogenous NC cells).

The study of the invasive potential of NC cells *in vivo*, may lead to interesting conclusions. To study this, an *in vivo* or "sandwich" invasion assay was specifically developed (Figure 4.9a). Figure 4.9b shows that *Xenopus* labelled grafts of NC can efficiently migrate towards ventral regions. However, this ventral migration is halted when NC cells encounter an opposed (or "sandwiched") embryo (Figure 4.9c). Interestingly, NC cells were perfectly able to continue migrating and invade an opposed embryo when the NC have been removed from the latter (Figure 4.9d). In this case labelled NC did not encounter NC cells from the opposed embryo but were confronted with its head mesoderm which NC are able to invade *in vitro* (Figures 4.5, 4.6). These results confirm the invasive potential of NC but now *in vivo*. Perhaps more importantly, they also show that NC can migrate backwards (from ventral to dorsal) in the region where they invade the sandwiched embryo (yellow region in Figure 4.9d). This last observation further supports the role of CIL in directional NC migration and shows that any external directional cue may be overridden by the action of cell-cell contacts.

It has been proposed that "population pressure" may be a major force in directing NC migration from the dorsal neural tube to ventral regions (Barlow et al., 2008). This idea basically states that NC cells will move from more high to low cell density regions. The results presented here, especially the ones in Figures 4.8 and 4.9, are in agreement with the idea of population pressure and CIL may give a mechanistic explanation to this observation.

In summary, NC cells trend to spontaneously and transiently polarise, leading to unstable polarisation and random migration in individual cells (Figure 4.4). However, cell-cell contacts locally restrict the formation of protrusions. This means that internal cells in a cluster will have little polarisation whereas peripheral or leader cells will be strongly polarised and show more directional migration (Figures 4.1, 4.2 and 4.4). Importantly, these differences are not intrinsic but determined by cell contacts (Figures 4.2 and 4.3). NC cells exhibit CIL *in vitro* and *in vivo*, and this is most likely the mechanism by which protrusion are inhibited. First, NC cannot invade regions populated by other NC cells but they can when confronted to other cell types ruling out a pure mechanical impediment for invasion (Figures 4.5, 4.6, 4.9). Detailed observation of CIL *in vitro* and *in vivo*, shows

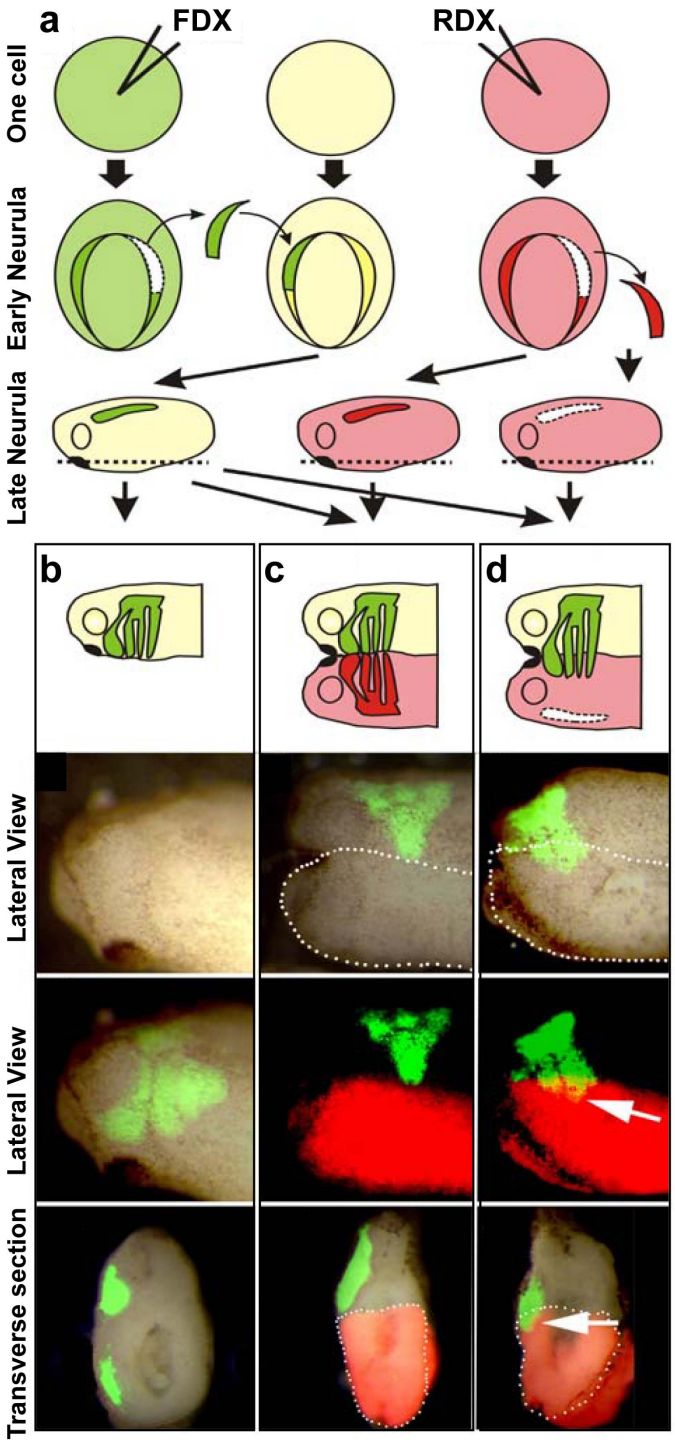

Figure 4.9: **Invasive potential of NC cells *in vivo*** a. Experimental design. *Xenopus* embryos are fluorescently labelled by injection of FDX (green) or RDX (red) at the 1-cell stage. At the early neurula stage (48hrs after injection) NC are taken from a FDX injected embryo and grafted onto an unlabelled embryo. At the same stage, NCs are removed from some of the RDX embryos. Then, the ventral region of the embryo (dashed line) is removed and two embryos are *sandwiched* together as shown below. b-d Analysed conditions. Top panels are cartoons of the situations shown below. Bottom panels are transverse sections of embryos shown in middle panels. Control embryo with FDX-labelled NC. c. Sandwich of FDX NC embryo with a normal RDX embryo. d. Sandwich of FDX NC embryo with a RDX embryo in which the NC has been removed. Dotted line enclose sandwiched embryos.

that NC cells retract their protrusions after contact (Figure 4.7). This can explain how NC cells only polarise and emit protrusions towards cell-free zones. Importantly cell density seems to be essential for directional migration *in vivo* supporting the critical role of CIL

in this process.

Chapter 5

Molecular bases of Contact Inhibition of Locomotion

5.1 PCP controls directionality in cell groups

In the previous chapter, the importance of cell-cell contacts and CIL in both, *in vitro* and *in vivo* NC migration was shown. The molecular mechanisms of CIL are barely understood and thus, NC migration provides an excellent model system to study this problem. *Xenopus* and zebrafish embryos are relatively easy to genetically manipulate and there are several signalling pathways already known to be crucial for NC migration (see Section 1.4 for more details).

One of these pathways, the Planar Cell Polarity (PCP) pathway, is an especially good candidate to be involved in CIL. First, it is a well-known regulator of collective movements and morphogenetic rearrangements such as mesodermal convergent extension (Keller, 2002), NC migration (De Calisto et al., 2005), and neural tube formation (Tawk et al., 2007). Second, and more importantly, its main cellular role is to control polarity (see 1.3.2, 1.4.2, and references therein for more details). In fact, the inhibition of this pathway does not have an effect in the *in vitro* migration of individual cells. DshDep+ is a mutant form of Dishevelled (Dsh) that inhibits the PCP pathway (Tada and Smith, 2000). Individual

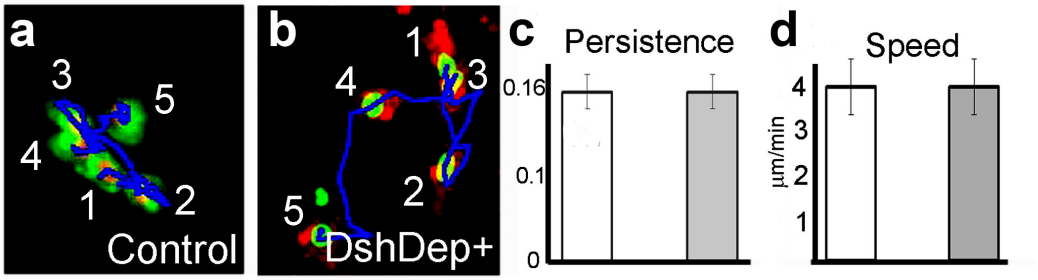

Figure 5.1: **Inhibition of PCP pathway does not affect the motility of single NC cells.** a. Temporal projection of five frames showing the migration of a single control NC cell. Numbers indicate the consecutive positions of the cell. Blue line: path of the tracked cell. b. Temporal projection of five frames showing the migration of a DshDep+ cell. c. Persistence of control (white bar) and DshDep+ (grey bar) cells. d. Speed of control (white bar) and DshDep+ (grey bar) cells. No significant differences were found either in the persistence or in the speed of these cells ($p > 0.05$).

DshDep+ NC cells do not show any appreciable difference with control NC cells (Figure 5.1, Movie 5.1). However, it is known that this very same treatment disrupts NC migration *in vivo* (De Calisto et al., 2005; Matthews et al., 2008b). Interestingly, these works suggested that the main effect of the PCP pathway was in cell polarity more than in motility. Altogether these observations position the PCP pathway as an excellent candidate to direct NC migration through the control of cell polarity, possibly via CIL.

As shown in the previous chapter, clusters of migratory NC cells show polarised cells at the leading edge, lamellipodia formation only at the periphery of the cluster and almost no protrusions in between cells (Figure 4.1 and 5.2a,b). On the contrary, the same DshDep+ treatment, which showed no effect in individual cells, strongly disrupts the organization in NC clusters. SEM analysis revealed that these cells produce lamellipodia in any direction even in between cells (Figure 5.2c,d). To further confirm this, live membrane-GFP-labelled NC clusters where imaged using confocal microscopy. Two focal planes were taken, one at the substrate level to image cell protrusions and the other higher up to image cell-cell boundaries. This allows a clear visualisation of the organisation of the cluster. As shown in Figure 5.2d,e; control cells only produce lamellipodia in cell-free regions whereas DshDep+ produce protrusions everywhere, even in between cells. These results are a clear suggestion that the mechanism of protrusion inhibition at the cell-cell contact is being disrupted by PCP downregulation.

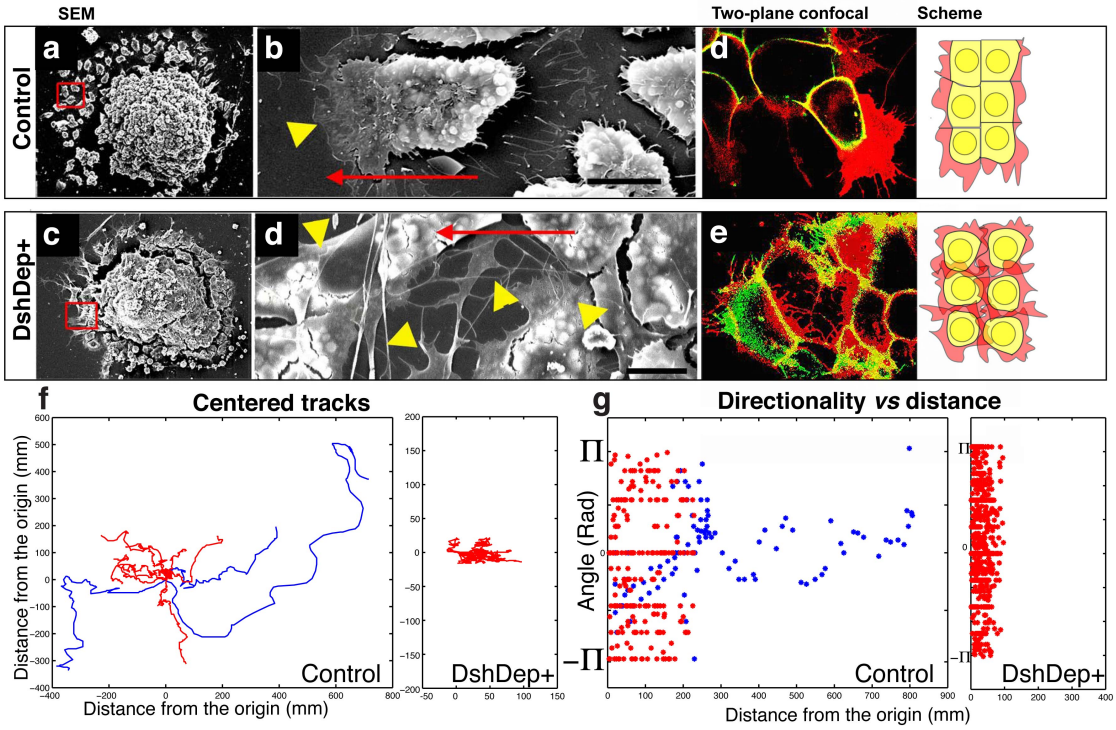

Figure 5.2: **Inhibition of PCP pathway dramatically affects the polarity and directionality in groups of NC cells *in vitro*.** a-f. Inhibition of PCP *in vitro*. a. Control NC explant visualised by SEM. b. Detail of NC explant visualised by SEM. Note clear polarisation of leader cell. Red arrow: direction of migration. Yellow arrowhead: lamellipodia. c. DshDep+ NC explant visualised by SEM. b. Detail of DshDep+ NC explant visualised by SEM. Note the formation of protrusions in between NC cells. d. Two-plane confocal image (left) and schematic representation of the result (right) of control a control NC clusters. Red image is at the minimum z-value *i.e.* at the substrate level and shows membrane processes. Green image correspond to a z-plane 10 μm higher to show cell boundaries. e. Similar to d. but for a DshDep+ NC cluster. f. Tracks of NC cells. In control plot (left), leader cells are in blue and trailing cells in red. In DshDep+ plot (right), all cells are in red as all behave like trailing cells. g. Change of direction *versus* distance from the origin. In control plot (left), angles of leader cells correspond to blue asterisks and trailing cells to red ones. In plot DshDep+ (right), all angles are as red asterisks as all cells behave like trailing cells.

An important conclusion from the previous chapter is that the polarity of NC cells is correlated with their persistence. For example, if the tracks of leader cells are plotted together with tracks of trailing cells, a clear difference in the net displacement can be appreciated (Figure 5.2f; left). However, all DshDep+ cells showed the behaviour of internal cells, regardless of where in the explant were located (Figure 5.2f; right). Similarly, control leader cells have a small angular dispersion, rarely moving backwards but trailing

cells move randomly. This is shown in Figure 5.2g where the angles are plotted against the distance from the origin. Again, all DshDep+ behaved like trailing cells taking angles uniformly distributed from -180°($-\pi$ rad) to 180°(π rad). Thus, the inhibition of the PCP pathway *in vitro* via injection of DshDep+ results in disrupted collective cell polarity and a consequent effect in cell directionality.

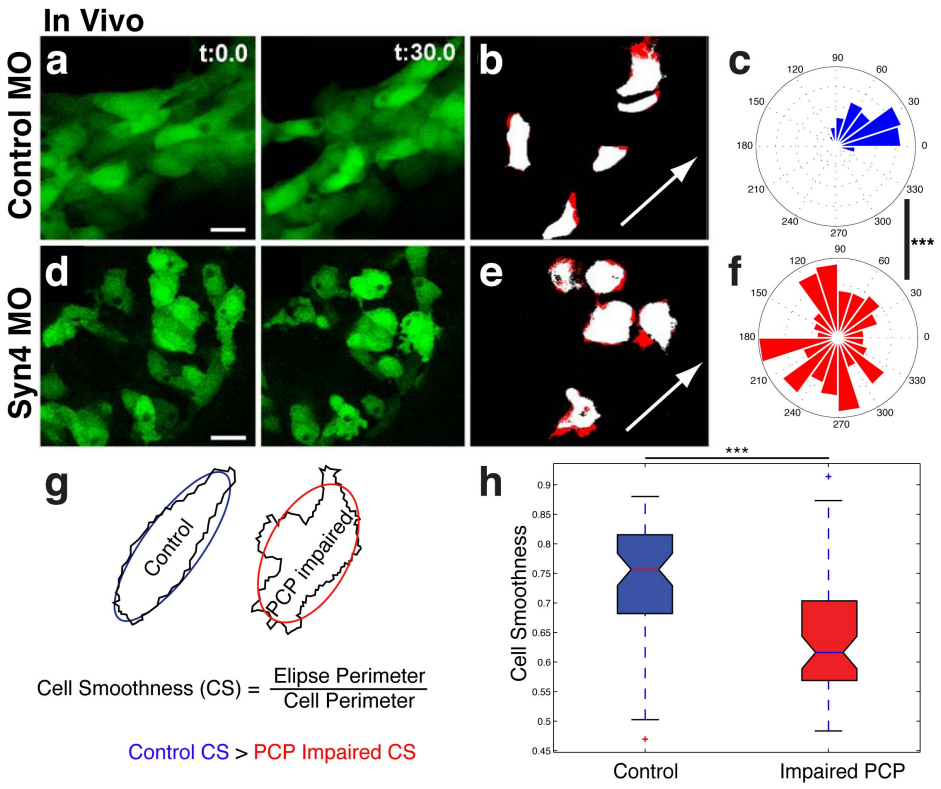

Figure 5.3: **PCP inhibition greatly disturbs the organisation of NC migration *in vivo*.**a. Consecutive positions of control NC cells migrating *in vivo*. b. The new areas covered by NC cells during migration can be obtained by the difference between the images shown in a. (red areas). White arrow: direction of migration. c. Rose plot of the new areas covered by control NC cells (blue). Note the clustering in the direction of migration. d. Consecutive positions of DshDep+ NC cells migrating *in vivo*. e. New areas covered by DshDep+ NC cells during migration (in red). f. Rose plot of the orientation of new areas covered by DshDep+ cells (red). g. Method to calculate cell smoothness. Quantification of cell smoothness in control and PCP impaired-NC cells migrating *in vivo*. *** $p < 0.001$.

A recent publication showed an effective way of blocking the PCP pathway in zebrafish embryos *in vivo*. This consists in the injection of a morpholino against the proteoglycan Syndecan4 (Syn4), which is specifically expressed in NC cells and positively modulate

the PCP pathway (Matthews et al., 2008b; Muñoz et al., 2006). Thus, the injection of Syn4 MO provides an effective tool to inhibit the PCP pathway specifically in the NC. Observation of NC migration in Syn4 MO embryos showed that the effect of PCP inhibition *in vivo* is very similar to its effect *in vitro*. Because the resolution of SEM cannot be achieved *in vivo*, it is more difficult to univocally identify lamellipodia. However, by comparing the displacement of cells in consecutive time steps, newly formed regions can be identified (frames in Figure 5.3a,d new regions in Figure 5.3b,e). The orientation of these new areas, corresponding to cell displacement and new protrusions, can be quantified to compare the two conditions. In control embryos, these areas are strongly based towards the direction of migration whereas they are randomised in Syn4 MO embryos (Figure 5.2c,f). Another feature of Syn4 MO cells is that they seem to produce more protrusions and thus, to have a more roughed contour than control cells. To analyse this, the *cell smoothness* can be measured (Figure 5.3g, see section 3.3.2 for more details). As expected, control cells in average have smoother contours than DshDep+ cells (Figure 5.3h). This is in agreement with the idea that cell contacts inhibit the formation or maintenance of protrusions in control cells (thus they are smoother) and that this inhibition mechanism is lost when the PCP pathway is downregulated. In other words, the PCP pathway is required for the inhibition of cell protrusions in between cells.

5.2 The role of the PCP pathway in CIL

The data presented in the previous section, strongly suggest that the PCP pathway may have a role in CIL during NC migration. Collision assays can be used to assess this directly. First, collisions were visualised and analysed *in vitro*. As shown in the previous chapter, control NC cells exhibit CIL. After collision, they withdraw the protrusions that are in contact with other cells resetting a lamellipodium elsewhere and thus, significantly changing the direction of movement (Figure 4.7, 5.4a). Surprisingly, when two DshDep+ cells encounter each other, they keep their respective direction of migration or remain together without showing the repulsion shown by cells exhibiting CIL. A typical collision of DshDep+ cells is shown Figure 5.4b. In addition, the velocity and acceleration plots

are depicted showing no significant CIL in these cells (Figure 5.4b). Wnt11, is a ligand that triggers the PCP pathway and known to be required for NC migration. Interestingly, inhibition of Wnt11 (via a dominant negative form, dnWnt11), depletes CIL from NC cells (Figure 5.4c). These results show that the PCP pathway is required for CIL *in vitro*.

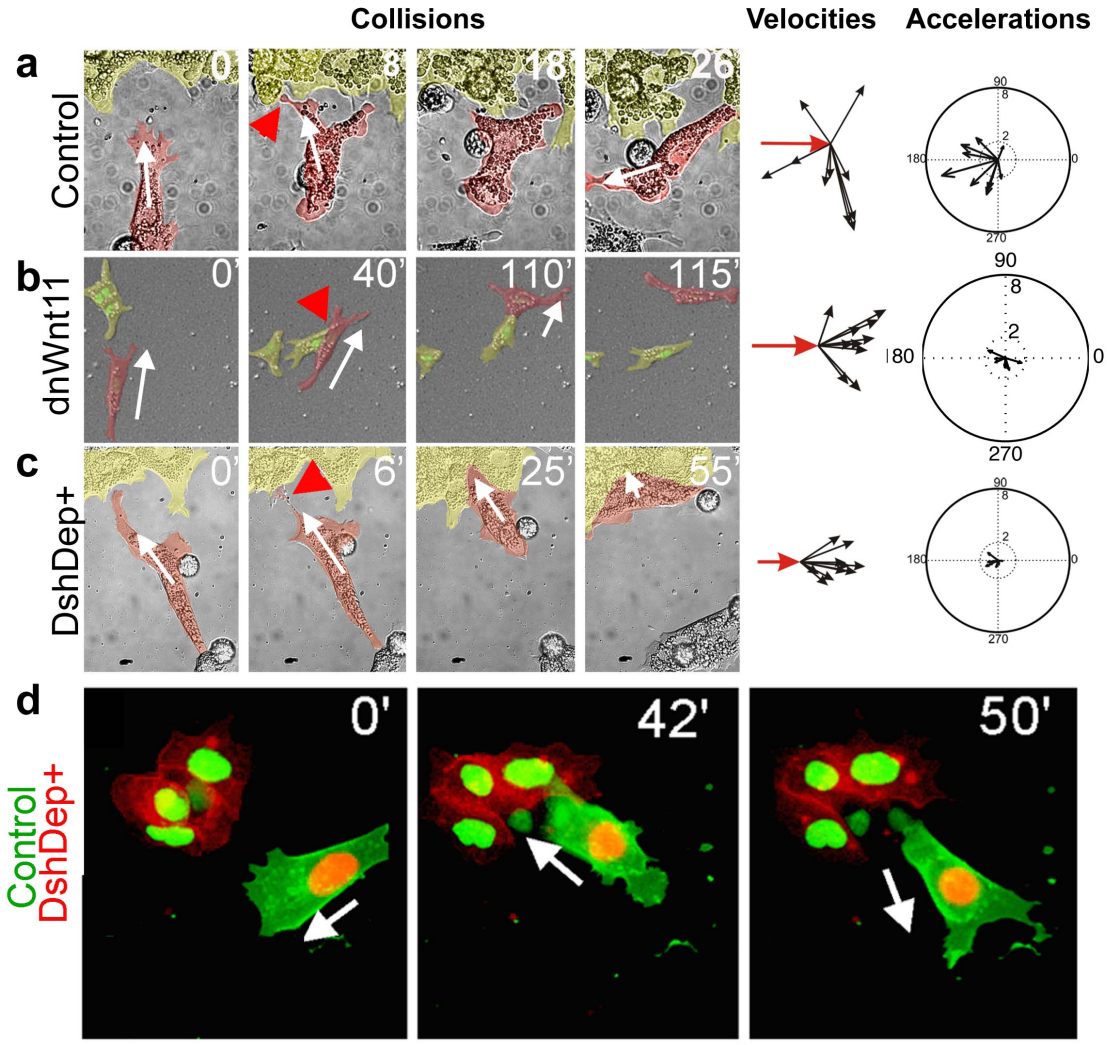

Figure 5.4: **PCP pathway is required for CIL *in vitro*.** a-c. Effect on CIL of PCP pathway inhibition. Selected frames of a time-lapse movie show cell collisions of pseudo-coloured NC cells (red and yellow). White arrow: direction of migration. Red arrowhead: collision point. Time in minutes in upper-right corner. Also velocity and acceleration vectors are shown for each condition. a. Control NC cells showing CIL ($p < 0.001$). b. dnWnt11. The effect of collisions seem not to be different from random, thus there is no CIL ($p > 0.05$). c. DshDep+, again not showing significant CIL ($p > 0.05$). d. When control (green) cells collide with DshDep+ (red) cells, only the first one exhibit CIL, thus PCP is required for CIL response.

CIL is a complex process, and is likely to be composed of a sequence of smaller steps controlled by different molecular pathways. For example, during CIL cells need to be able to perceive the contact with another cell. This requires that cells exhibiting CIL are signalling to contacting cells and, at the same time, they perceive signals from their neighbours. To investigate if PCP signalling is involved in both or in one of these processes, co-cultures of control and PCP inhibited cells can be used. The rationale behind co-culture experiments is to see what happens in collisions between control and treated cells. In this case the use of DshDep+ is preferred as this is a cell autonomous inhibition. Surprisingly, when control NC cells collide with DshDep+ cells, they exhibit normal CIL (Figure 5.4d, Movie 5.2). This suggests that PCP signalling is required to perceive a colliding cell but not to signal to others as DshDep+ cells are still able to signal to control cells, which exhibit normal CIL to the former cells.

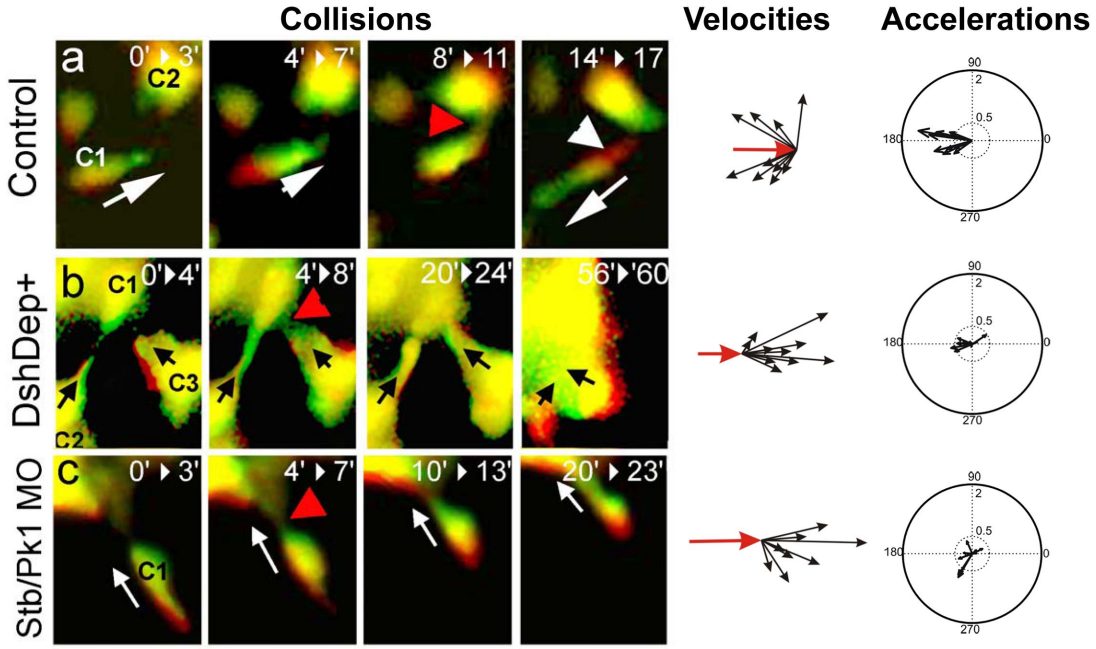

Figure 5.5: **PCP pathway is required for CIL *in vivo*** For each condition, collisions are shown as the difference between two consecutive frames (times shown in upper right corner). Green areas: regions where the cell has moved on. Red areas: regions left by the cell. C1, C2: colliding cells. White or black arrows: direction of migration. Red arrowhead: collision point. Also velocity and acceleration vectors are shown for each condition. a. Control showing CIL ($p < 0.001$). b. DshDep+ not showing CIL ($p > 0.05$). c. A combination of Stb and Pk1 MOs, not showing significant CIL ($p > 0.05$).

The possibility to visualise cell collisions *in vivo*, using the *sox10*:GFP transgenic embryos, permits the analysis of the role of the PCP pathway in CIL in a more natural context. In Figure 5.5a the normal behaviour of control cells is shown. As in the *in vitro* situation, injection of DshDep+ resulted in a significant reduction of CIL (Figure 5.5b; Movie 5.3). Similarly, the inhibition of other components of this pathway such as Stb and Pk1 also resulted in lost of CIL for NC cells (Figure 5.5c).

Wnt11 is an important regulator of NC migration *in vivo* and its inhibition resulted in NC cells that did not exhibit CIL *in vitro*. The previously used Wnt11 inhibitor (dnWnt11) was developed for *Xenopus* but *in vivo* analysis of NC migration is better done in zebrafish. Thus, to study the role of Wnt11 *in vivo*, a similar construct but designed for zebrafish, was made (Figure 5.6a,b). As expected, embryos injected with this construct showed typical PCP-inhibition phenotypes. They developed with problems in gastrulation and NC migration resulting in shorter body axis, smaller eye separation and reduced NC migration and derivatives (Figure 5.6c-e). Importantly, when NC cell collisions were analysed in *sox10*:GFP embryos injected with the zebrafish dnWnt11, a significant loss of CIL was found (Figure 5.6f,g). Altogether the results in this section show a critical role for the PCP pathway in CIL both, *in vitro* and *in vivo*. The role of this pathway in NC migration was already described (De Calisto et al., 2005; Matthews et al., 2008b; Gessert et al., 2007; Carmona-Fontaine et al., 2008a) but these results give a mechanistic explanation to previous findings and underscore the critical role of CIL in cell migration *in vivo*.

5.3 Linking cell contact with molecular signalling

Cell-cell contact and the local collapse of cell protrusions, and thus CIL, can be considered physical problems. How is it then that a biochemical pathway, such as the PCP controls it? There must be a link in between these apparently dissociated physical and chemical natures of CIL.

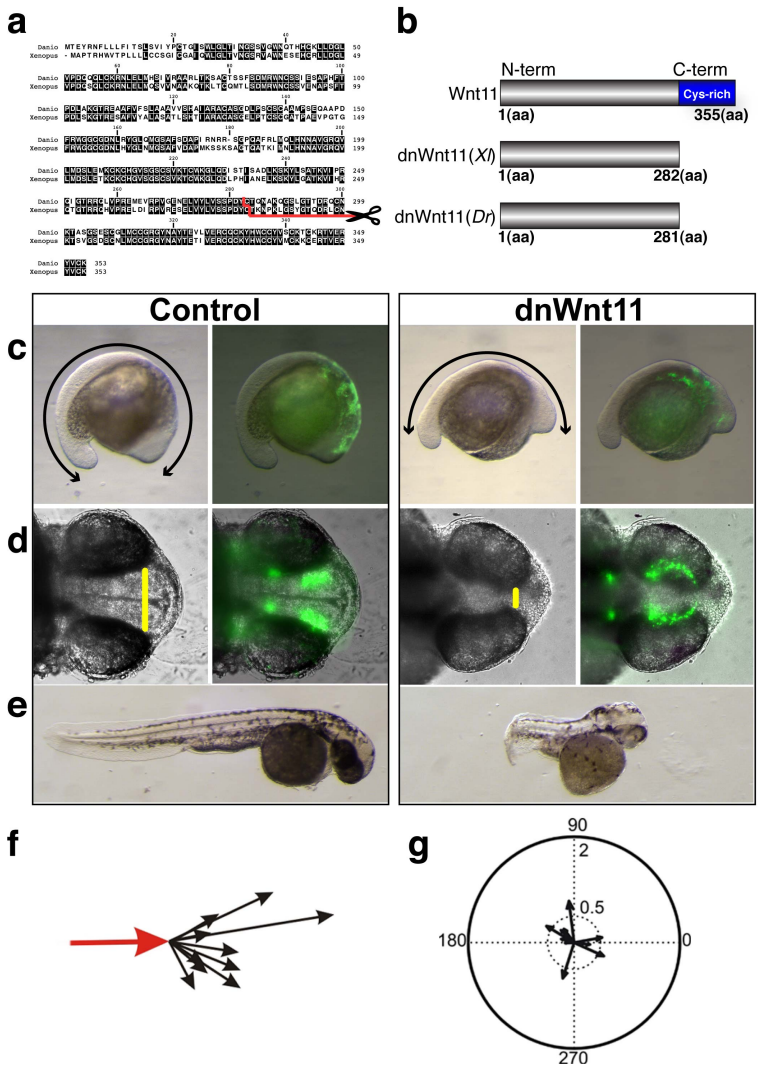

Figure 5.6: **Generation and effect *in vivo* of a zebrafish dnWnt11.** a. Alignment of *Xenopus* Wnt11 and zebrafish Wnt11 proteins. The C-terminus region of zebrafish Wnt11 was deleted to generate a similar construct to *Xenopus* dnWnt11 (red line, Tada and Smith, 2000). b. Schematic representation of full length Wnt11, *Xenopus* dnWnt11 and the new zebrafish dnWnt11. c-e. Zebrafish embryos treated with dnWnt11 show typical PCP inhibition phenotypes. c. Convergent extension is affected (black arrow indicates body length). d. Eye distance is reduced (yellow line). e. At later stages the reduction of the body axis and the diminution of NC derivatives, such as melanocytes, are evident. f-g. dnWnt11 inhibits CIL. f. Velocity vectors. g. Acceleration vectors ($p > 0.05$).

5.3.1 Subcellular localization of PCP members during CIL

There is accumulating evidence showing that effective signal transduction requires the accumulation of receptors and other pathway components in the vicinities of the cell

membrane (reviewed in Scott and Pawson, 2009; Groves and Kuriyan, 2010). In addition, it has been recently shown that key components of the PCP pathway colocalise at the cell membrane *in vivo* (Witzel et al., 2006). The ligand Wnt11, the receptor Fz7, and the key downstream component Dsh, show enhanced membrane localisation when the pathway was active. Interestingly, this accumulation was in cells that were in close contact to others. Thus, it was proposed that the cell contact is locally activating PCP components (Witzel et al., 2006). This conclusion may provide the link in between the molecular and the mechanical component of CIL.

Fluorescently tagged PCP components can be injected in embryos, together with a membrane label and see if they preferentially localise at this region. As shown in Figure 5.7a, Wnt11, Fz7 and Dsh localise in the membrane of NC cells *in vitro*. Note that cells are in contact with others NC cells. A similar approach can be taken *in vivo* but because NC cells are expressing GFP, PCP proteins need to be tagged with RFP. As shown in Figure 5.7b again PCP members seem to be preferentially localised at the cell-contact regions. To test this idea further, two additional improvements were made. First, differentially labelled probes were used for Wnt11 and Fz7 component to allow simultaneous imaging and co-localisation (Wnt11-YFP and Fz7-CFP). Second, cells at the leading edge of a cluster were analysed to estimate the role of cell-cell contact in PCP localisation. As seen in Figure 5.7c, PCP members co-localise but only at the cell-cell contact region and not in membranes facing cell-free zones. All this suggests that the contact may be localising PCP members leading to CIL. However, if this is really the mechanism by which CIL is acting, PCP members should get localised during cell collisions too. In Figure 5.7d, the collision of two Dsh-GFP labelled NC cells, is shown. As it can be observed, there is a clear accumulation of Dsh at the cell contact region during collisions, showing that PCP is also activated in collisions and thus during CIL (Figure 5.7d and Movie 5.4).

5.3.2 Activation of RhoA via cell contact and through the PCP pathway

The experiments shown in Figure 5.7 help to understand how the cell contact can induce local activation of the PCP pathway. However, it is not clear how this activation results

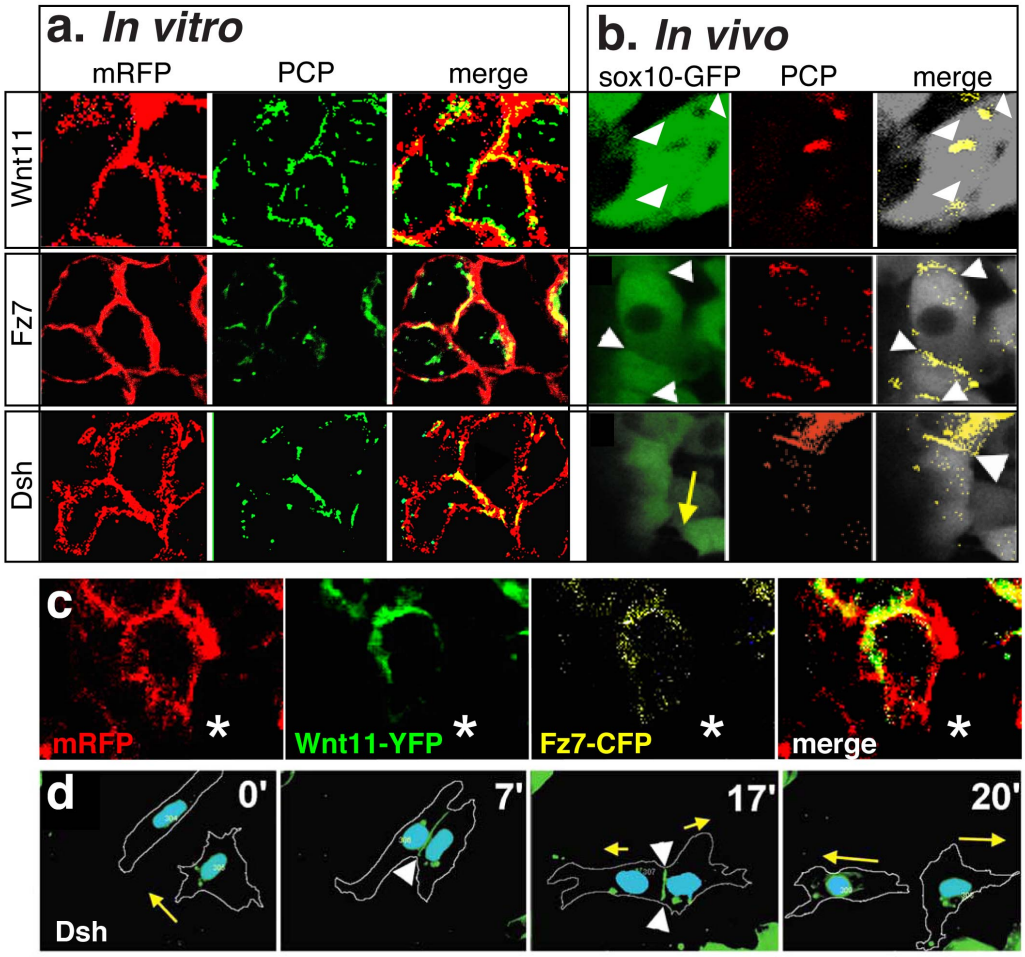

Figure 5.7: **PCP members localise at the cell-cell contact *in vitro* and *in vivo*.** a. Subcellular localization of several PCP (green) members in NC cells *in vitro*. Note the accumulation in membranes (red) at the cell-cell contact region. mRFP: membrane-RFP. b. Subcellular localization of several PCP (red) members in NC cells *in vivo*. Green shows sox10/GFP^{+} cells, thus only NC. c. Membrane localization of PCP members is restricted to cell-cell contact regions and not to the leading edge (cell-free, white asterisk). d. Selected frames of a cell collision (outlined in white) showing that PCP members (Dsh) get localised at the collision region. Yellow arrow: direction of migration. Time in minutes on upper-right corner.

in the morphological changes observed in CIL. These changes include a molecular and morphological repolarization, most notably reflected in the collapse of protrusions after contact. Members of the family of small Rho-GTPases, are heterogeneously distributed in polarised cells and are critical regulators of cellular cell polarity during cell migration (Ridley et al., 2003). One of them, RhoA inhibits cell protrusions and is known to antagonise Rac1, which in turn helps to maintain large membrane processes such as

lamellipodia (Worthylake and Burridge, 2003). Thus, RhoA may be a good candidate to induce the collapse and withdrawal of cell protrusions. Interestingly, it has been recently shown that in migratory NC cells the PCP is a key positive regulator of RhoA (Matthews et al., 2008b). Thus, during CIL, contact-dependent PCP localisation may induce local activation of RhoA, which will inhibit Rac1 and lead to the collapse of cell protrusions.

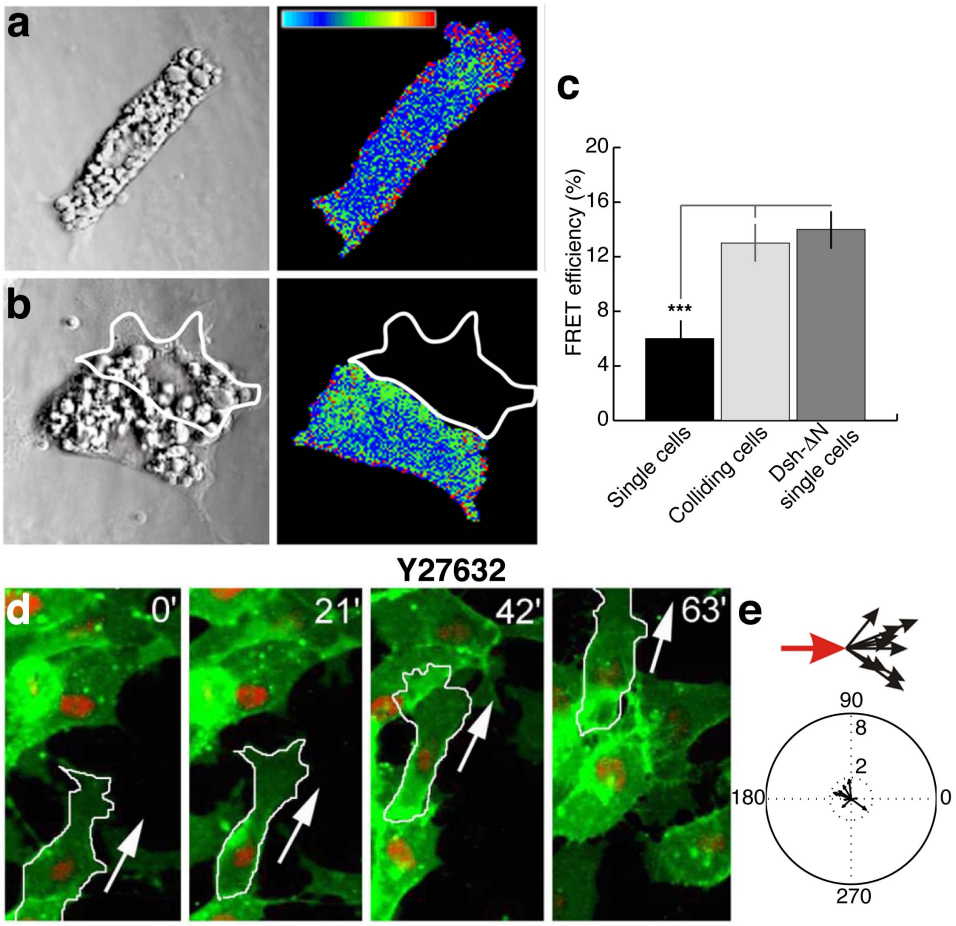

Figure 5.8: **RhoA is activated in cell collisions and is required for CIL.** a. DIC image of a single NC cell (left) and FRET image (right) of the same cell showing RhoA activity. b. DIC image of a colliding pair of NC cells (left) and FRET image of one of them (right, the other one is outlined in white). c. Quantification of FRET efficiency of the treatments shown in a. and b. and also for single NC cells whose PCP activity has been enhanced (via injection of DshΔN). d. Frames of a time-lapse movie showing NC cells treated with a chemical inhibitor of ROCK (Y27632), a downstream target of RhoA. Note that colliding cell (outlined in white) does not change its direction (white arrow) after collision. Time in minutes on upper-right corner. e. Velocity and acceleration vectors showing that there is no CIL in NC cells treated with Y27632 ($p > 0.05$).

Following Matthews et al., 2008b; FRET was used to determine the activity of RhoA. First, the activity of this GTPase was measured and compared in single *versus* colliding cells. While single cells presented moderated RhoA activity (measured as FRET efficiency, see section 3.2.2), colliding cells presented a significant increase in this activity (Figure 5.8a-c). Although at the resolution these experiments were performed, is difficult to draw detailed spatial conclusions, it seems that the highest RhoA activity is localised at the region of contact (Figure 5.8b). To link these results with the previous findings about the relation between PCP and RhoA activities, the PCP was upregulated in single cells and then the activity of RhoA was monitored. Single cells injected with Dsh-ΔN, a strong PCP activator (Tada and Smith, 2000), showed increased RhoA activity. Interestingly, this increase was of the same order of magnitude than the increase due cell-cell contact (Figure 5.8c).

These results establish a clear correlation between cell contact, PCP and RhoA activation. Thus, RhoA is an excellent candidate to be an effector and key regulator of CIL. To directly test its role in this process, NC cells were treated with a chemical inhibitor of ROCK (Y27632), a downstream target of RhoA, and its effect in cell collisions was analysed. Cells treated with Y27632 did not stop their migration nor did they significantly changed their direction of migration after colliding with other NC cells (Figure 5.8d and Movie 5.5). Hence, these cells did not show a significant CIL response (Figure 5.8e, $p > 0.05$).

5.4 A summary and a model

5.4.1 Summary

The results presented in this and in the previous chapter, allow to propose a mechanism for directional NC migration. This mechanism, CIL, may help us to understand problems like how NC can migrate directionally *in vitro* (where external cues are absent), why leader cells behave differently to trailing cells and how cell polarity is established in a large group of migratory cells. CIL is unlikely to be sufficient to explain all the features of NC migration but it highlights the essential role of local cell-cell interactions in the global

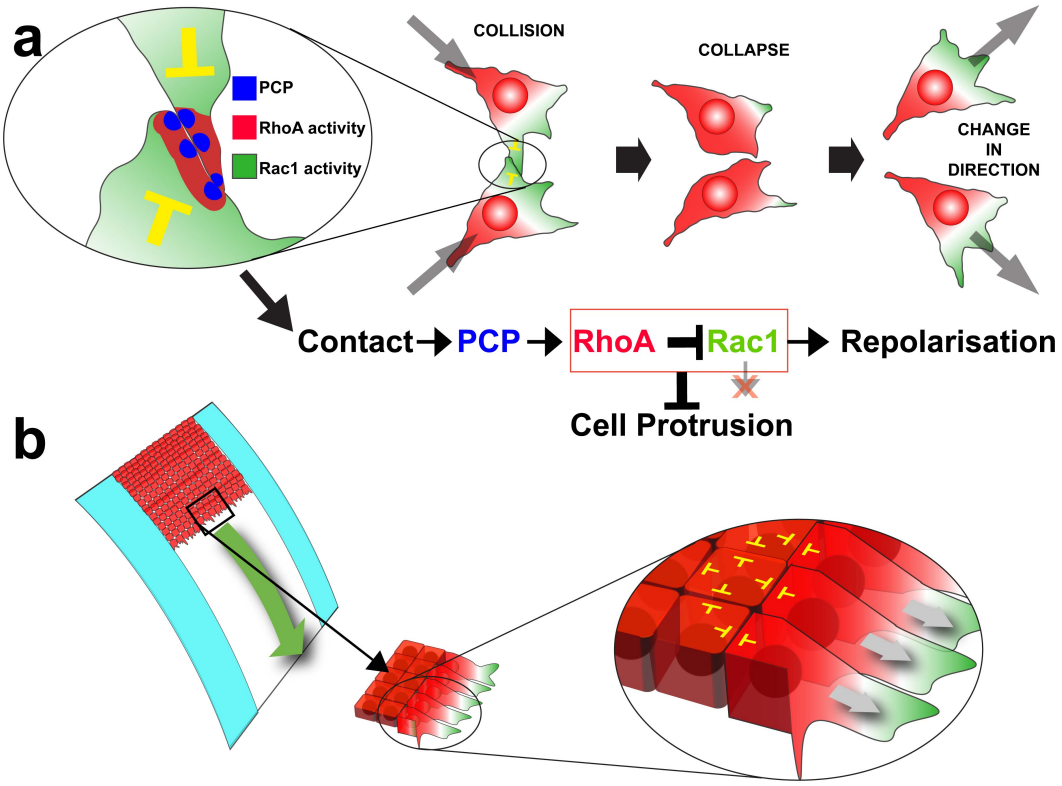

Figure 5.9: **Summary: Molecular basis of Contact Inhibition of Locomotion.** a. CIL in cell collisions. Polarised cells have high Rac1 (green) activity at the front and high RhoA (red) activity levels at the back. However, cell-cell collisions localise PCP members (blue) at the contact region where they locally activate RhoA. This leads to inhibition of cell protrusions as RhoA can inhibit Rac1, a crucial positive regulator of lamellipodia formation and maintenance. b. CIL in collective migration. A similar molecular mechanism may operate during NC collective migration. Cells in contact will have their protrusions inhibited by the high levels of RhoA and low levels of Rac1 triggered by the PCP pathway. Thus only cells at the leading edge will be polarised. Red cells: NC cells. White area: region of migration (limited by regions in cyan). Yellow "Ts": CIL.

behaviour of the migratory NC. The molecular bases of CIL are also proposed here.

Typically, migratory cells are morphologically polarised presenting, among other features, a large protrusion at their leading edge. This polarity is also evident at the molecular level where specific proteins show preferential localisation either at the front or at the back of the cell (see section 1.3.2 and references therein for details). Rho-GTPases such as RhoA and Rac1 are one of these heterogeneously distributed proteins. The model presented here starts with polarised NC cells. They have large frontal lamellipodia with high levels of

Rac1 and high levels of RhoA at the back of the cell body (Figure 5.9a). During cell collisions, PCP members become localised and activated at the contact region (detailed region in Figure 5.9a). PCP activation is then transduced into RhoA activation, which, via ROCK and Rac1 inhibition, leads to the collapse of cell protrusions. Because NC cells spontaneously trend to polarise (Figure 4.4), a new protrusion is readily set elsewhere changing the direction of migration of the cell (Figure 5.9a). These are the proposed molecular basis of Contact Inhibition of Locomotion. The same idea can be extrapolated to densely packed mesenchymal cells such as NC clusters. In this case, internal cells will be under the effect of CIL all around their periphery, idea that matches with the PCP localisation and the absence of major cell protrusions. In contrast, cells at the leading edge will be exposed to a cell-free region. This local relief from CIL, leads them to emit protrusions only to the front where high Rac1 are permitted (Figure 5.9b). When the first row of cells advances, then the next row of cell will be exposed to a cell-free region, polarise, move forward, and so on. It is proposed here that CIL, in theory, could lead to a more efficient and more directional displacement of NC cells.

5.4.2 A simple model of NC migration based in CIL.

A simple computational model was built in order to test if CIL may indeed increase the efficiency and directionality of NC cells (particles in the model). Model details are described in section 3.6. Briefly, a population of self-propelled particles[1] are set at the top of a two-dimensional rectangular region and asked to move randomly following some simple rules. In the simplest condition, particles will deflect from all borders but the bottom one in which they stop (or *differentiate*). The parameter *Step* is an internal clock that defines the number of iterations a particle will move in one direction before changing it randomly. In this condition particles ignore each other and they can overlap. This is the condition without CIL (-CIL or no CIL). To add a CIL-like behaviour, particles were given the same rules than before with one additional routine. When particles collide with others, they will move away form each other with an angle θ and reset the internal clock *Step*.

[1] Particles have intrinsic motion and constant speed.

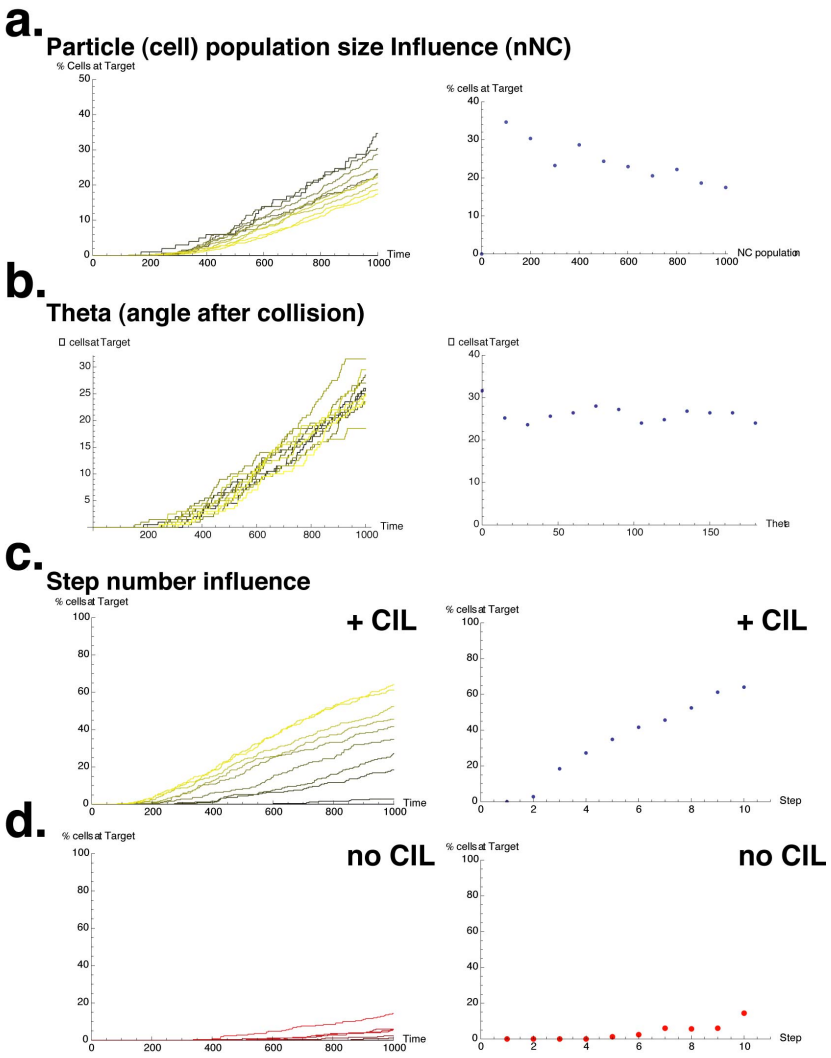

Figure 5.10: **A simple model to estimate the role of CIL I: The parameters.** a-c. The model, where randomly moving particles had a CIL-like behaviour, was run for 1000 iterations using different values for selected parameters. Left plots: time *versus* % of cells at the target region. Coloured lines represent low (dark) to high (clear yellow) parameter values. Right plots: parameter value *versus* % of cells at the target region at the end. a. Influence of cell population size. b. Influence of angle θ. c. Influence of *Step*. d. Influence of *Step* in a model where particles behave exactly the same but do not have CIL. Note the diminished influence of *Step* in this condition.

Before testing the effect of CIL in the models, different parameter values were tried. Because this is mostly a qualitative model, the ideal situation is that none of the parameters has dramatic effects if its values are slightly changed. In other words a more robust model is desired. The effect of the number of particles, the angle θ and the *Step* was tested in the +CIL model. The percentage of differentiated cells was scored and used as an efficiency

measure. None of them showed an abrupt effect in the model while their values were changing (Figure 5.10a-c). Nonetheless, the *Step* parameter showed an steady increase in the efficiency of the model (Figure 5.10c). This was expected as it defines how long a particle will remain in the same direction. Also expected, this parameter has a smaller effect in the no CIL model because here cell collisions do not reset the value of *Step* (Figure 5.10c). To keep the model robust, small *Step* values were used for the rest of the simulations.

Having shown that the parameters that can be used did not have dramatic effects, the two models (-CIL and +CIL) were run under the same conditions (Population: 250, angle θ: 45°, *Step:* 4). As shown quantitatively in Figure 5.11a, the +CIL model was significantly more efficient than the -CIL (this is also shown visually in Figure 5.11b and in Movie 5.6). For example, when half of the population has *differentiated, i.e.* reached to the final destination in the +CIL model less than 1% have done it the no CIL one. Correspondingly, when about 40% of the particles have *differentiated* in the -CIL model, almost all the particles have *differentiated* when they have CIL (Figure 5.11a,b).

The model shows that in theory, CIL is sufficient to increase the efficiency in the dispersion of particles. In a figurative way, this is not too different to the influence of collisions in the dispersion of gas molecules. Moreover, in the model with CIL, particles in average have more directional paths (Figure 5.11c). This is consistent with the empirical observations that CIL can increase the persistence of NC cells (Chapter 4). Thus, cell-cell contacts, via the local activation of PCP/RhoA, trigger CIL in NC cells. This behaviour is essential to establish the polarity in single cell collisions and also to coordinate the polarity in multicellular arrays such as NC clusters *in vitro* and NC streams *in vivo*. Moreover, CIL is essential for the efficiency and directionality of NC cell migration.

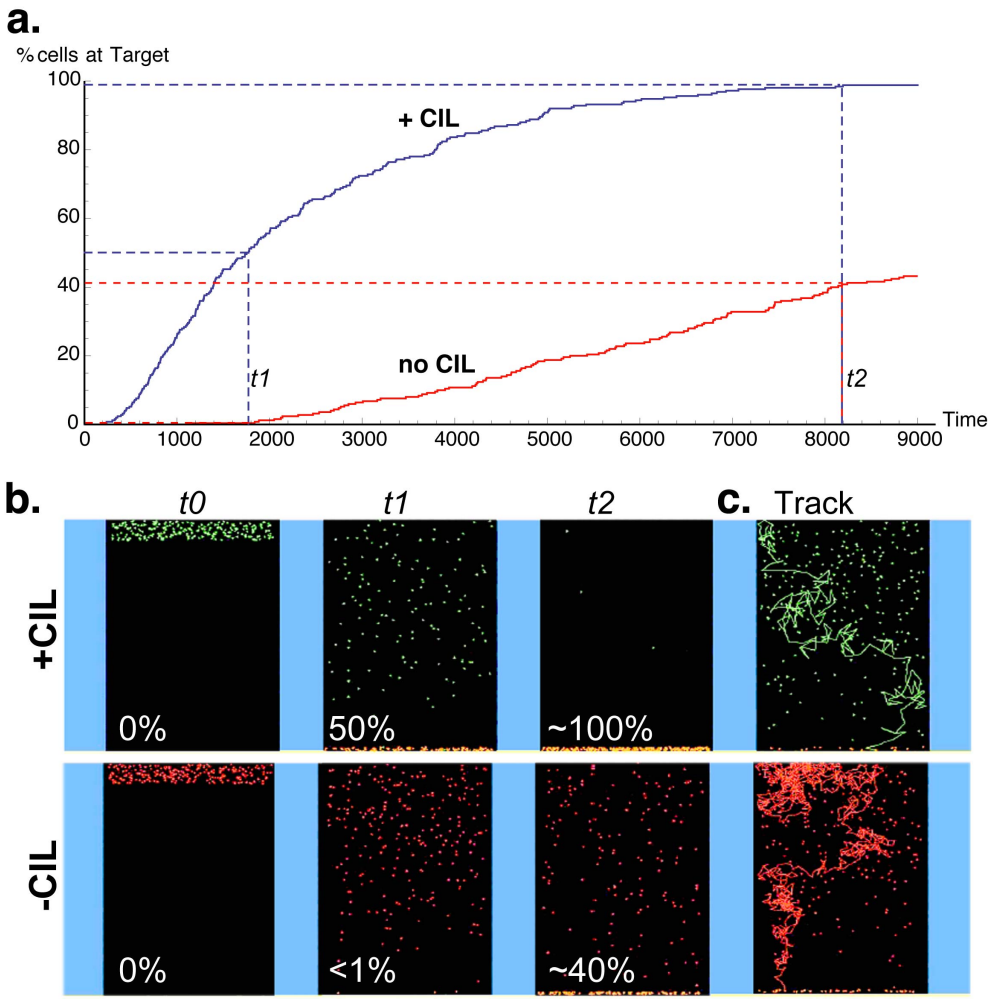

Figure 5.11: **A simple model to estimate the role of CIL II: The results.** a. Time *versus* % of cells at the target region plot to quantitatively compare the effect of CIL. Parameters in both conditions, +CIL (blue) and no CIL (red), have the same values (Cell population: 250, angle θ: 45°, *Step:* 4). b. Selected frames of the visual output of the results shown in a. Panels correspond to time 0 (*t0*), the time when 50% of the particles reached the target in the +CIL condition (*t1*, see plot in a. as well) and the time when almost all particles reached the target in the same condition (*t2*, see plot in a. as well). c. Path of a randomly chosen cell in each condition. CIL greatly improves directionality.

Chapter 6

Coattraction is essential for NC collective migration

6.1 Mutual attraction and CIL may explain NC behaviour

As presented in the previous two chapters, CIL is essential for NC migration. It not only controls the polarity and behaviour of these cells but also it increases the directionality and efficiency in migration. As predicted by the computer model, CIL increases the capacity of the cell population to disperse on a restricted space (Figures 5.10, 5.11). Nonetheless, NC migration *in vivo* shows a high degree of coherence, something the model fails to reproduce. For example, NC cells *in vivo* move with high persistence and maintain contact with their neighbours for extended periods of time (Figure 6.1a). This denotes that their movement is not simple dispersion. Surprisingly, NC explants cultured *in vitro*, can also adopt collective directional migration in the absence of external attractive or repulsive cues (Movie 6.1). The frequency of this behaviour is increased when explants are cultured in corridors to maintain high cell density. These corridors can be mechanical (*i.e.* there is a physical barrier for cell migration, Movie 6.1) or by providing alternating stripes of high and low fibronectin (Fig. 6.1b, Movie 6.2). This indicates that interactions between NC within a cluster are sufficient to generate collective migration. In other words, NC cells

can self-organize to migrate as a collective cluster.

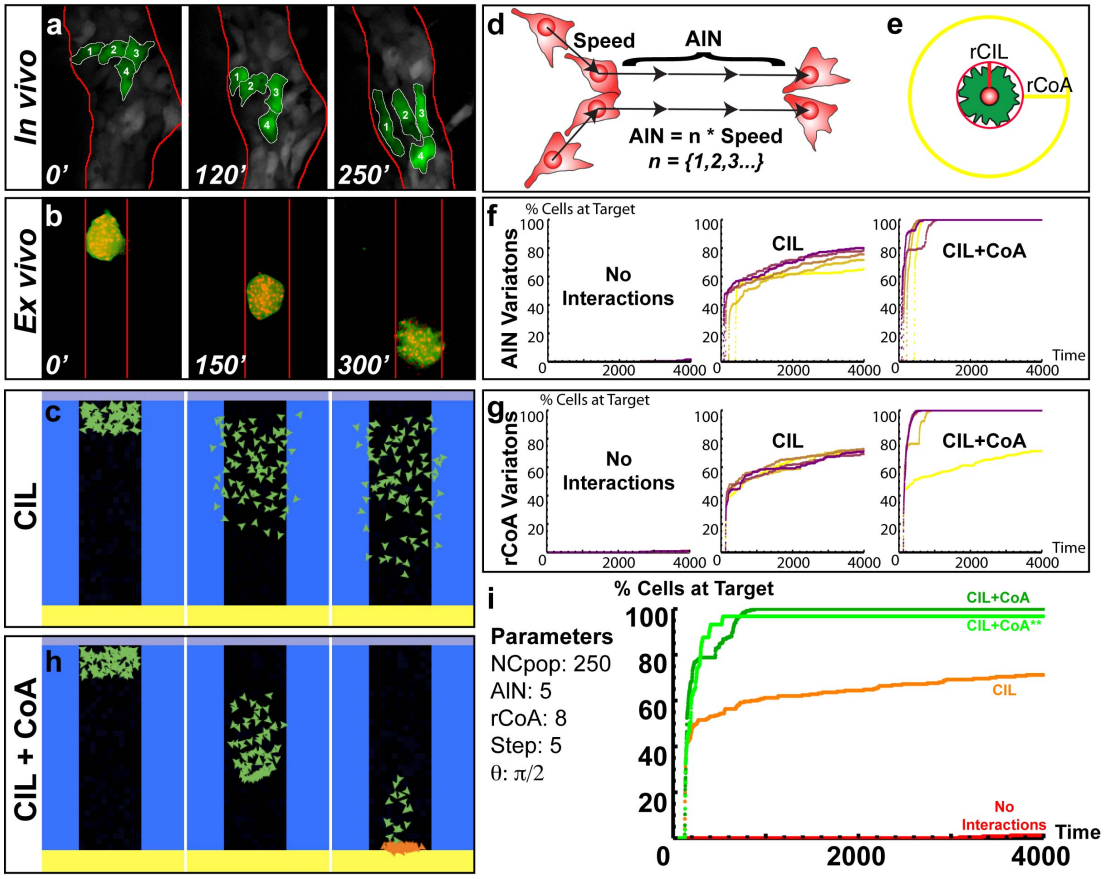

Figure 6.1: **NC self-organisation in collective migration suggests the existence of coattraction.** a. Frames showing NC migration *in vivo* in a zebrafish embryo (time in minutes indicated in frames). Cells were coloured to show that they maintain their neighbour relations during migration *in vivo*. Red lines: migratory path. b. *In vitro* NC cultured on a surface with stripes of different levels of fibronectin (high/low) show directional migration. Red lines: border of high fibronectin levels. c. Screen shots of the development of an agent based model where particles move randomly and change their direction after collision (CIL). d. Detailed description of how particles behave in collisions. e. Schematic representation of a particle/cell and its two interaction radii with rCIL = particle size and rCoA > rCIL. f,g. Parameter sweep for the three types of models: no interactions (left), CIL only (middle) and CIL+CoA. Efficiency is measured as % of cells at the target over time. f. Different values of AlN (see d.) do not change the outcome of the model dramatically. (Yellow = 1, Purple = 10). g. Different values of rCoA do not change the outcome of the model dramatically. (Yellow = 1, Purple = 10). h. Screen shots of the development of an agent based model where particles have both, CIL and CoA. Frames are at equivalent times to c. Orange Particles: particles at the target. i. Summary of all treatments. CoA: Coattraction

Careful observations of collisions in NC and other cells reveal that upon contact, cells align their directions for a usually short but variable time interval (Winklbauer et al.,

1992; Stramer et al., 2010). A possibility is that including in the model a transient and local alignment may result in a better simulation of NC migration. Thus, this transient alignment during collisions was included in a new version of the model, presented in Section 5.4.2 (Figure 6.1c,d, see methods for details). As shown in Figure 6.1c, this alignment is not sufficient to reproduce the collective and cohesive movement of NC cells (Figure 6.1a,b).

An alternative hypothesis is that in order to maintain a cluster conformation, an attractive interaction might counterbalance cell repulsion caused by CIL. To test this, a new routine was integrated to the model. Particles have a repulsion radius, rCIL, that represents their size. In addition to this radius, a longer-range attraction radius rCoA, was added (Figure 6.1e). It means that a particle will be attracted to all the cells within this radius. Surprisingly, adding this simple rule to the existing CIL-like repulsion resulted in the emergence of coherent group behaviour (Figure 6.1h). Importantly, this model was also robust, as its outcome was not dramatically affected by small changes in parameters. For example, the value of AlN, that establish how long cells are aligned after collision (Figure 6.1d), did not change the behaviour of particles significantly (Figure 6.1f). Similarly, the length of the attraction radius rCoA was also not a determinant of the behaviour of the group (Figure 6.1g). The only exception was that when rCoA was set to zero (meaning that there was no attraction) the particles behaved as in the condition with repulsion only (yellow line in Figure 6.1g). Hereinafter, this hypothetical mutual cell attraction will be referred as coattraction or CoA.

The plot in Figure 6.1i summarises the results obtained in the model. Particles with no interaction showed very poor efficiency (measured as the percentage of particles that reach the bottom region) whereas particles with CIL showed a dramatic increase in the migration efficiency. However, the addition of coattraction makes the particles not only more efficient but also makes them move cohesively. In these models particles at the target can still influence the behaviour of motile particles. If this influence is eliminated, the behaviour of the particles is virtually the same with the exception of a small group of particles that is left behind (condition CIL+CoA** in Figure 6.1i). This demonstrates that coattraction may be an essential cell interaction in collective migration.

6.2 NC cells exhibit Coattraction.

The model presented in the previous section suggests that coattraction may help to understand NC migration. Interestingly, models of the collective movement of animals, such as bird flocks, fish schools and locusts among others, have also shown that mutual attraction is essential for the emergence of swarming behaviour (Grégoire et al., 2003; Grégoire and Chaté, 2004; Buhl et al., 2006; Sumpter et al., 2008; Torney et al., 2009). However, the biological evidence for coattraction in animal cells is missing.

Interestingly, examination of NC migration *in vivo* and *in vitro*, revealed that NC cells occasionally migrate out of the cluster but rapidly correct their trajectory re-join the migratory stream (Figure 6.2a,b). It would be difficult to explain this behaviour with cells moving randomly or having only CIL. On the contrary, it may actually support the idea of some kind of mutual attraction between NC cells. More suggestive, when labelled NC cells are grafted onto a host embryo in non-NC regions, grafts will migrate and integrate to the endogenous NC (Figure 6.2c,d). However, if the NC is removed from the host embryo, the graft will remain close to its original location (Figure 6.2c,e). This suggests that is the endogenous NC, and not the surrounding area, what attracts NC cells. Finally, if two clusters of NC are grafted in a host embryo they trend to migrate towards each other (Figure 6.2c,f). These results, although not conclusive, support the idea of coattraction in between NC cells.

NC explants cultured alone typically disperse radially. However, when two explants were cultured at close proximity ($\sim$500μm) they move toward each other with high directionality (Figure 6.3a,a'; Movie 6.3). To quantify this behaviour, explant displacement vectors were calculated (Figure 6.3b). This analysis shows that these vectors have a significantly non-random distribution and that are strongly biased towards the confronted explant (Figure 6.3d). In contrast, no directional bias is observed when NC explants are confronted to other tissues such as lateral epidermis (Figure 6.3c). These results show that there is mutual attraction, or coattraction, between NC cells and that this attraction is cell type-specific. This conclusion leads to the intriguing hypothesis that NC cells may produce a chemoattractant that is sensed at some distance by other NC cells. Whatever the

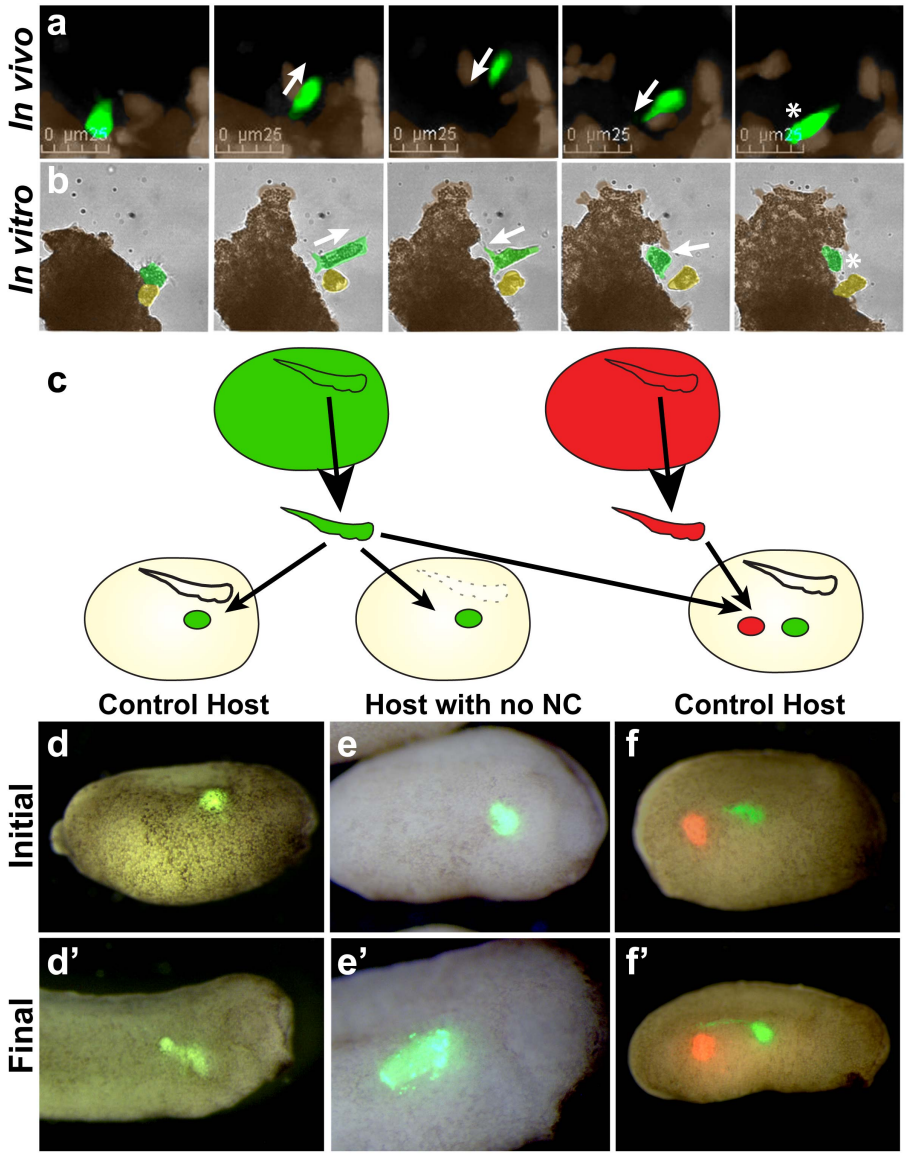

Figure 6.2: **Behaviour of NC cells *in vitro* and *in vivo* suggest that they may exhibit CoA.** a,b. Typically, if a single NC leaves the group it quickly returns to it. a. Frames of a time-lapse movie showing this *in vivo*. b. The same but *in vitro*. c-f. The behaviour of grafted labelled NC cells, suggest CoA. c. Experimental design. d,d'. Labelled NC grafted onto a normal host trend to join the endogenous stream of NC migration. e,e'. However, if endogenous NC are removed, grafted cells do not integrate to the NC stream. f,f'. Two grafts of NC cells trend to migrate towards each other.

attractant, it must be expressed by NC, along with its receptor, and be able to function at a distance (Figure 6.3e).

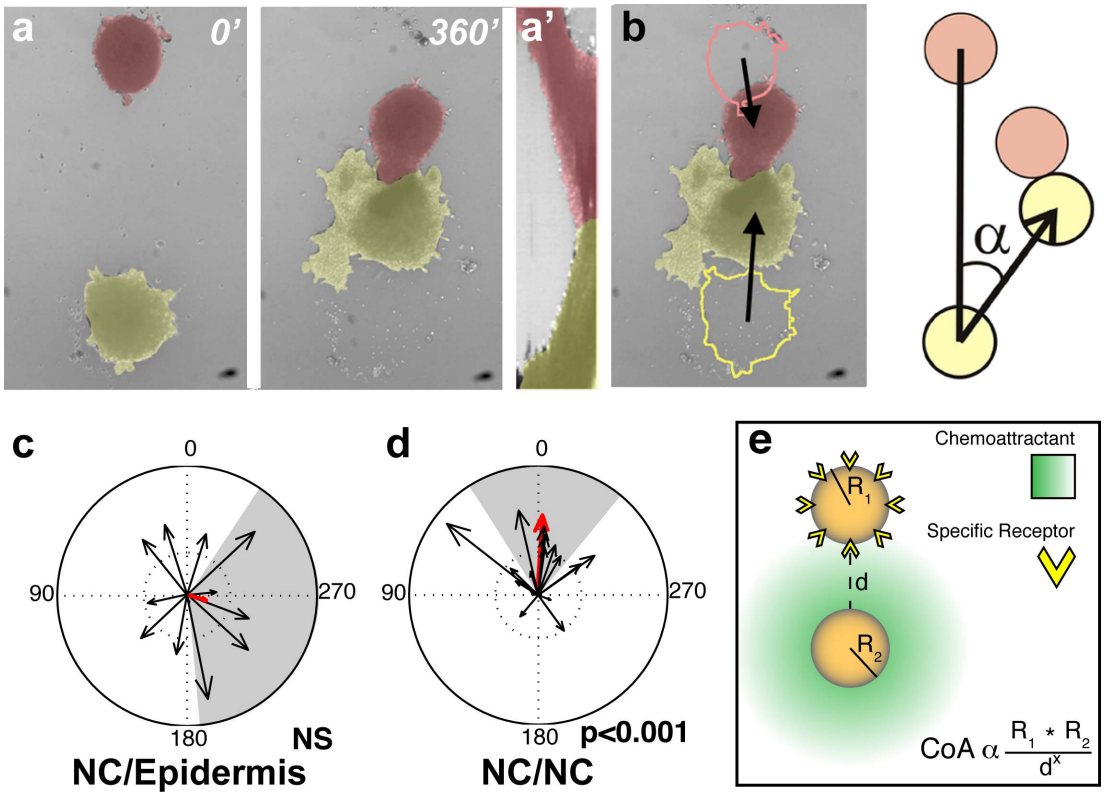

Figure 6.3: **NC cells exhibit Coattraction.** a. Initial and final positions of two NC explants (pseudo-coloured in red and yellow for clarity). Note how they migrate towards each other. a'. Kymograph of a. b. Method to determine the displacement vectors. c. Displacement vectors of NC confronted to epidermis grafts are randomly distributed (NS, $p > 0.05$). d. Displacement vectors of NC confronted to other NC grafts are significantly clustered towards each other ($p < 0.001$). e. A proposed mechanism of CoA involving a chemoattractant released and sensed by NC cells. For clarity, in the scheme one graft is releasing the attractant and the other has the receptor but the two actions should be in both grafts.

6.3 Looking for a chemotactic ligand/receptor pair to mediate Coattraction.

To look for candidate molecules for coattraction, genes encoding secreted proteins and expressed in the NC were searched for in publicly available *in situ* hybridisation databases (Sahu and Lambris, 2001; Hugli, 1990). This search revealed ten candidates molecules. Amongst which was C3, a central component of the complement pathway, initially synthesized as a large protein (∼180kDa) but then cleaved to produce C3a and C3b (see Section 1.4.2). C3a is a small anaphylatoxin with known chemotactic properties in the

immune system and signals through its receptor, C3aR (Sahu and Lambris, 2001). The *Xenopus* homologue of C3 is highly conserved and possesses all the functional domains of mammalian C3a (Grossberger et al., 1989). However, there is no evidence for a function of complement proteins during early development; especially as at these embryonic stages the circulatory system has not yet formed. The presence of these proteins could reflect an unexplored role for complement and an exciting coattraction mechanism.

To study the possible role of C3/C3a in NC migration, first its expression pattern was compared with the expression of *snail2* and *twist* that are expressed in the NC (Figure 6.4a,a'). *c3* is strongly expressed in NC cells before and during their migration (Figure 6.4b,b'). Western blots of embryo protein extracts revealed that C3 protein is present at the stages of NC migration (Figure 6.4c). Importantly, the cleaved form of C3, C3a, could be also detected (Figure 6.4c'). To ensure that the presence of C3 protein was enhanced in the NC, immunohistochemistry was performed in whole mount embryos and in NC cultures. As shown in Figure 6.4d, C3 protein is mainly localised in the NC region. In addition, C3/C3a was detected in migrating NC *in vitro* (Figure 6.4e,e').

Having shown that C3/C3a are in the NC, it is important to investigate its role in NC migration. As a first approach, C3 translation was knocked down using a morpholino (C3 MO). This morpholino efficiently diminishes the levels of C3 protein (Figure 6.5a). When injected in one side of the embryo, C3 MO inhibits NC specification, as shown by the absence or diminution of NC genes such as *slug* and *twist* in the injected side (Figure 6.5b). However, some embryos maintained their NC allowing the analysis of the effect of C3 during migration. As shown in Figure 6.5c, NC cells in the injected side accumulate in the dorsal region without migrating properly.

To analyse the specific role of C3a, and overcome the effect of other domains of C3 in NC development, a more targeted treatment is required (see a schematic representation of C3 and C3a in Figure 6.5d). To do this, a blocking C3a antibody was designed (antiC3a). This antibody targets the C-terminal region of C3a that is essential to interact with its receptor. Then, affi-gel beads were soaked in antiC3a or in a control antibody and then grafted onto embryos in the vicinity of the NC. After a few hours of treatment, embryos

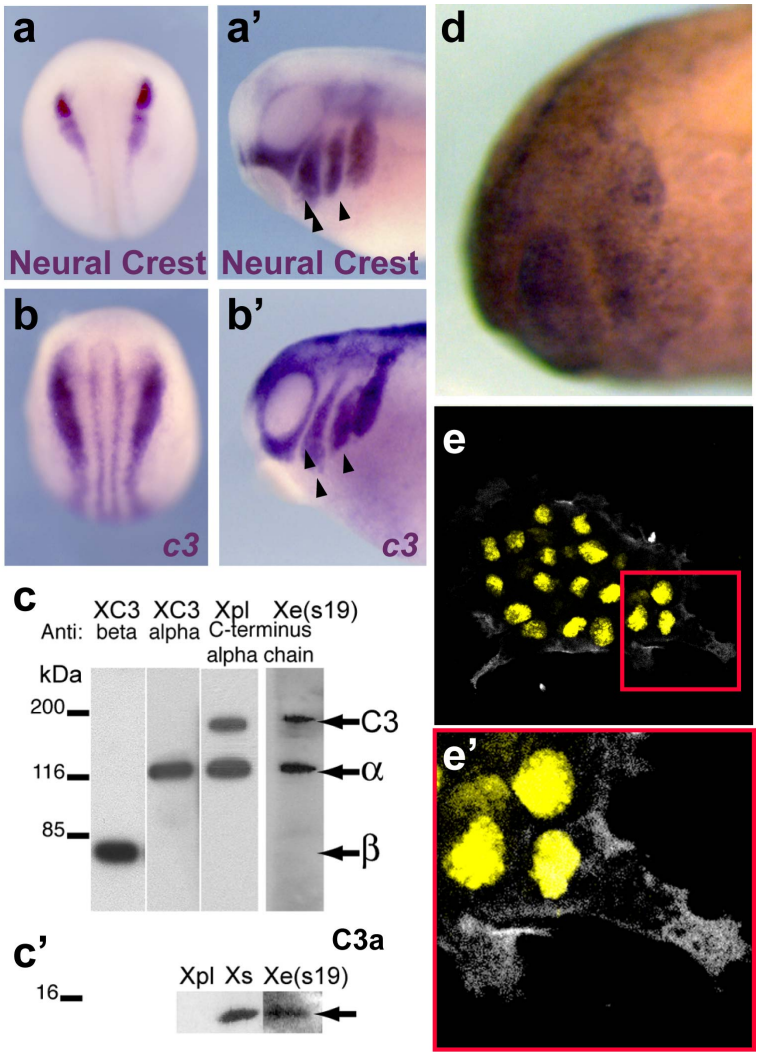

Figure 6.4: **C3 is expressed in NC cells and is cleaved in C3a, a possible co-chemoattractant.** a. Premigratory NC labelled by the expression of *slug* and *twist*. a'. Migratory NC labelled by the expression of the same genes. b. *c3* expression in premigratory NC cells. b'. *c3* expression in migratory NC cells. c. C3 protein is present in *Xenopus* embryos during NC migration as revealed by Western Blot analysis. Importantly, C3a is also present (c'). C3 protein is localised in migratory NC cells as revealed by whole mount IHC (d.) and in *in vitro* cultures (e.). e'. Magnification of the region highlighted in e. C3 in white, yellow: DAPI.

were fixed and their NC were analysed via *in situ* hybridisation. As shown in Figure 6.5f, antiC3a does not affect NC specification. In contrast, NC migration was dramatically affected by this treatment (Figure 6.5g). This effect was specific as control beads did not affect NC migration (Figure 6.5h). A summary of the effect of antiC3a is shown in Figure 6.5e. Altogether, these results show that C3 is expressed and required for NC development

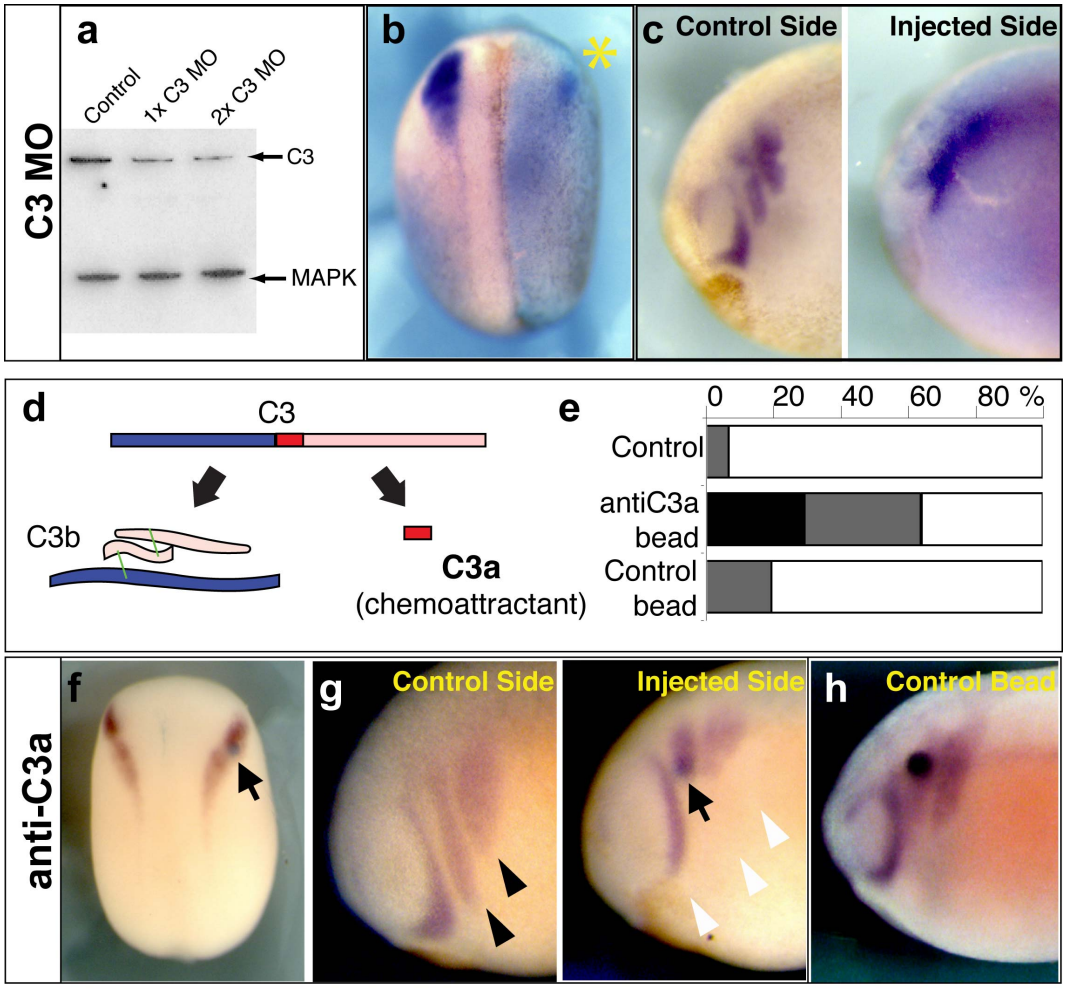

Figure 6.5: **C3 is required for NC specification and migration but C3a is specifically required for NC migration.** a. Western Blot to show the efficiency of C3 MO. 1x: 20ng, 2x: 40ng. MAPK: loading control. b. Dorsal view of an embryo, prior NC migration, injected unilaterally with C3 MO. *: injected side. Note the loss of NC denoted by the absence of *slug* and *twist* expression. c. Lateral view of an embryo injected unilaterally with C3 MO at NC migration stages. Control side shows normal NC migration whereas the injected side shows a strong inhibition in NC migration. d. Schematic representation of C3 and its cleavage by-products. C3a is a putative chemoattractant whose function can by downregulated with a specific antibody (antiC3a). e. Quantification of the effect of beads with antiC3a or control antibodies. f. antiC3a does not affect NC specification. g. antiC3a inhibits NC migration. h. The effect of antiC3a is specific, as control beads do not affect NC migration.

in general. In addition, they show that C3a is also present in NC cells and that it has a specific role in their migration. Therefore, C3a is a good candidate to be the attractant required for coattraction.

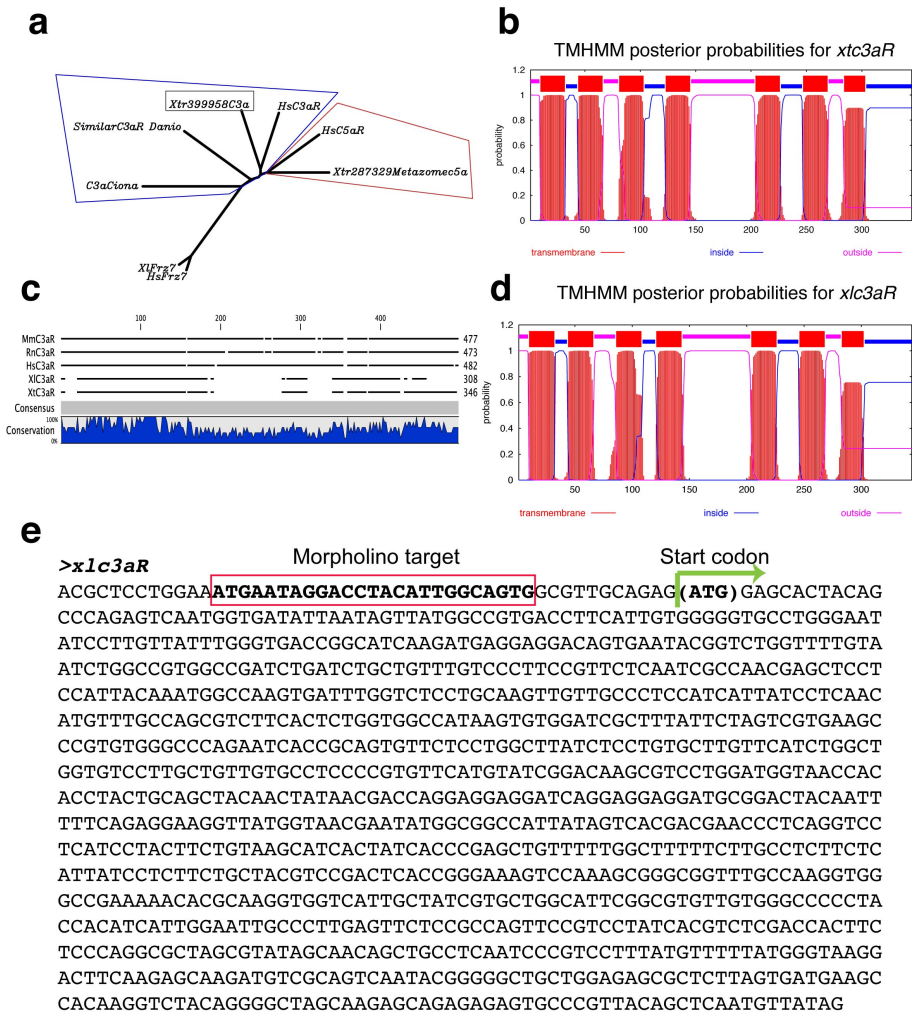

Figure 6.6: **Identification and cloning of C3aR in *Xenopus laevis*.** a,b. A putative C3aR sequence was identified in the genomic sequence of *Xenopus tropicalis* (Xtr899958 or xtC3aR). a. This sequence clusters with other animal C3aR and not with closely related C5aR. b. The amino acid sequence coded by this gene shows the seven transmembrane regions and the large second extracellular loop typical of C3aR. c. Using xtC3aR, degenerate primers where designed and together with RACE, a gene was cloned in *Xenopus laevis*. This gene (called *xlc3aR*) shows a high degree of conservation with other C3aR (c.) and the correct membrane profile (d.). e. *xlc3aR* sequence. The start codon and the morpholino target region are highlighted. Note that the target region is upstream of the start codon. This region was omitted from the synthetic *xlc3aR* mRNA to allow rescuing the morpholino effect.

The proposed mechanism for coattraction (Figure 6.3e) requires that the receptor for the putative chemoattractant is also expressed in the NC. C3a has a specific receptor, C3aR that is well described in other species but not in *Xenopus laevis*. To overcome this, first

DNA sequence that could encode for C3aR homologous gene was identified in the genome of *Xenopus tropicalis*, closely related species. After homology analysis, the identified sequence (xtC3aR) clustered with C3aR, but not with the closely related C5aR, of other species (Figure 6.6a). C3aR is a seven transmembrane receptor with a characteristic long and variable second extracellular loop. A hydrophobicity analysis revealed that xtC3aR also has these characteristics, supporting its identification as a C3aR paralogous (Figure 6.6b). Then, C3aR in *Xenopus laevis* was cloned using xtC3aR as a template to design primers (see Methods 2.2.11). The cloned sequence (xlC3aR) showed very high homology with xtC3aR (Figure 6.6c) and the same hydrophobicity map (Figure 6.6d). In addition, a small portion of the 5'-UTR region of the gene was sequenced allowing the design of a specific morpholino (C3aR MO, Figure 6.6e).

After cloning *Xenopus laevis* C3aR, its expression in NC development was studied. *c3aR* is poorly expressed before NC migration showing a diffuse and unspecific pattern (Figure 6.7a). On the contrary, this gene was strongly expressed in migratory NC cells (Figure 6.7a'). Importantly, C3aR protein was present at this embryological stage as revealed by Western Blot analysis (Figure 6.7b, first lane).

The designed C3aR MO (Figure 6.6e), was used to study the function of this gene. As shown in Figure 6.7b, C3aR MO efficiently inhibits the translation of C3aR protein. Unilateral injection of C3aR does not have any effect in NC specification (Figure 6.7c). However, the same treatment completely inhibited NC migration (Figure 6.7d). Importantly, the effect of C3aR MO is specific as it can be rescued when co-injected with *c3aR* mRNA (Figure 6.7e). This mRNA lacks the region targeted by the morpholino (Figure 6.6e). This expression and functional analysis show that C3aR is required for NC migration.

An interesting observation is that not only *c3* and *c3aR* are expressed in the NC but many other members of the complement (Figure 6.8). The specific function of each of these components, or the role of the complement cascade in NC development, is out of the scope of this thesis. However, this finding opens many questions and is a lead worth following. One interesting aspect of this is that virtually all the complement components upstream C3 are in the NC (Figure 6.8a,d). Importantly, the components of the classical

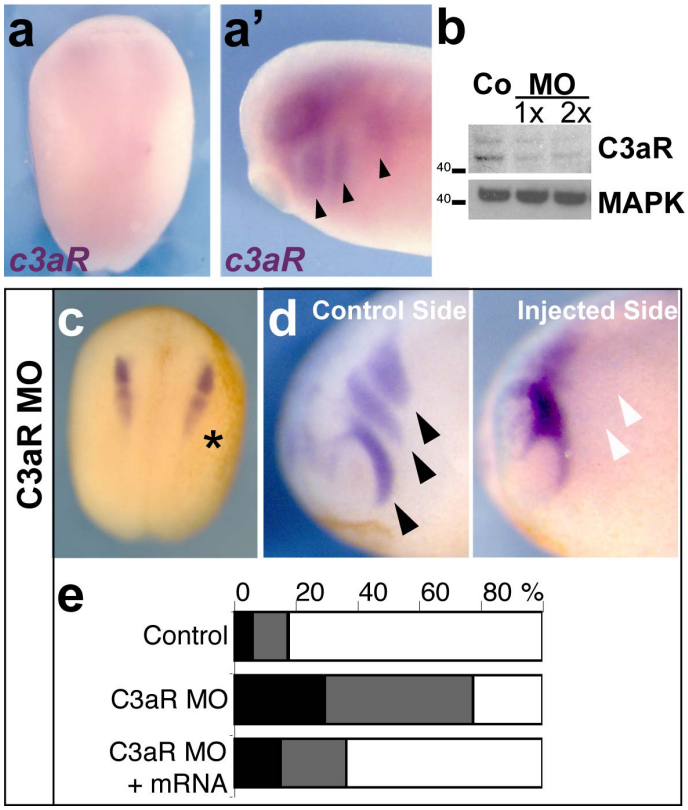

Figure 6.7: **Expression and loss-of-function of C3aR.** a. *c3aR* expression is neither strong nor clearly localised before NC migration. b. *c3aR* expression is strongly localised in migratory NC cells. Black arrowheads: NC streams. Western blot showing C3aR protein in *Xenopus* embryos (Co) and its reduction by C3aR MO. 1x: 15ng, 2x: 30ng of C3aR MO. MAPK: loading control. c. Dorsal view of an embryo, prior NC migration, injected unilaterally with C3aR MO showing no effect in NC specification *: injected side. d. Lateral view of an embryo injected unilaterally with C3aR MO at NC migration stages. Control side shows normal NC migration whereas the injected side shows a strong inhibition in NC migration. e. Quantification of the effect of C3aR MO in NC migration. Note that its effect can be rescued with *c3aR* mRNA showing that the effect of the MO is specific.

(C3 and C4) and alternative (Factor B and C3) C3-cleavase, are present. This suggest that the cleavage required to produce C3a from C3 may be regulated by the same factors that in the immune system.

To test if C3a and C3aR are functional, a *Xenopus*-specific C3a peptide and two control peptides were made (C3a-desArg, an inactive form of C3a that does not bind to the receptor; and scramC3a, a control peptide with a scrambled sequence of C3a). NC explants cultured in a medium with C3a seemed to disperse quicker than explants cultured with

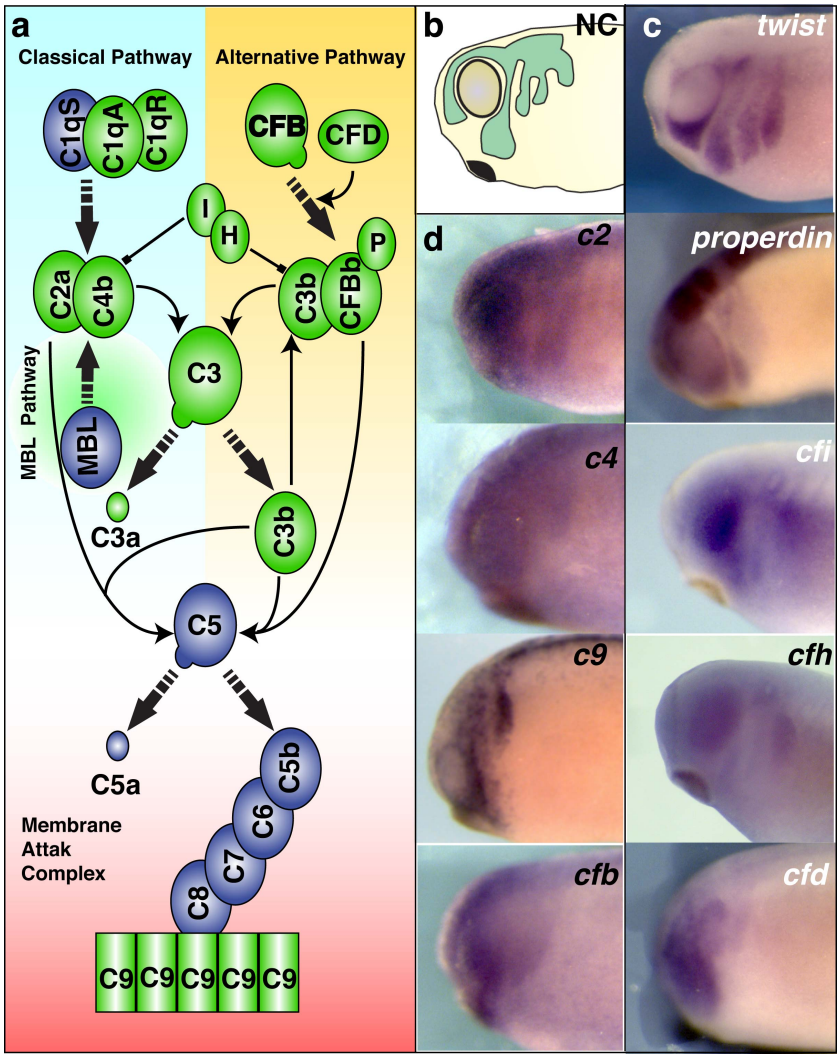

Figure 6.8: **A significant portion of the complement cascade is present in the NC and may be regulating C3a production.** a. Schematic representation of the complement cascade. Components in green are members so far known to be expressed in or around migratory NC. b. Schematic representation of migratory NC cells. c. Typical expression of a gene (*twist*) expressed in migratory NC cells. d. Expression pattern of several complement members.

control peptides. To quantify cell dispersion independently of cell number or density variation, the closest neighbours of each cell was determined using a Delaunay triangulation algorithm. Then the areas of these triangles were measured and colour-coded accordingly (see Section 3.4.6). NC explants cultured with C3a-desArg showed normal moderate dispersion (Figure 6.9a). In contrast, NC cells treated with C3a showed enhanced dispersion as the areas between neighbours increased dramatically (Figure 6.9b). In addition, cells

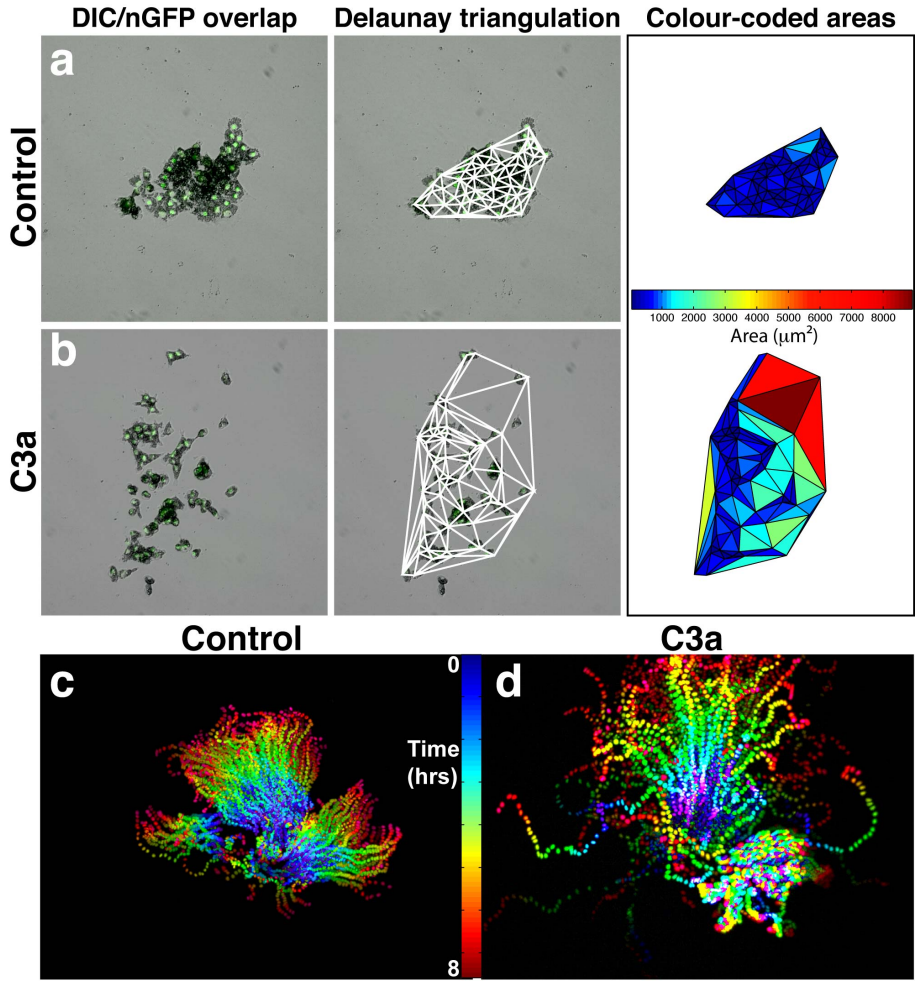

Figure 6.9: **NC cells respond to C3a.** a. Snapshot of NC cultured in 0.7μM of C3a-desArg (control) for 3 hours. Central panel shows Delaunay triangulation of cells at the left panel. These triangles were colour-coded according their area as shown in the right panel. b. Similar to a. but for NC cultured in 0.7μM of C3a. Note the increase in cell dispersion. c. Temporal projection of migratory NC cultured in 0.7μM of C3a-desArg (control) for 8 hours. d. Similar to c but for NC cultured in 0.7μM of C3a. Note the increased dispersion and disorganisation of migratory paths.

under control conditions exhibited relatively coherent paths of migration, as shown by their temporal projection (Figure 6.9c), whereas NC cells exposed to C3a moved in a much more disorganized fashion (Figure 6.9d). Together, these results show that NC cells respond to C3a, probably via C3aR.

6.4 C3a is a chemoattractant and mediates Coattraction via C3aR.

So far it has been shown that a possible chemoattractant, C3a, and its receptor are expressed in migratory NC cells. Furthermore, their function is required for normal NC migration and NC cells respond to C3a by changing their migratory behaviour. This makes the C3a/C3aR pair, an excellent candidate to mediate coattraction. However, an essential condition is missing. If coattraction is mediated by these molecules, NC should migrate towards a C3a source and this response should be mediated by C3aR. In other words, C3a should be a NC chemoattractant and its effect should require normal C3aR activity. Although C3a acts as a chemoattractant in the immune system (Sahu and Lambris, 2001; Schraufstatter et al., 2009), there is no evidence for such a role in embryonic development.

The effect of C3a in NC explants is suggestive of chemoattraction as cells migrate and disperse faster when exposed to a homogeneous distribution of a chemoattractant (Wilkinson, 1998). However, an assay to directly test the attractive potential of C3a is required. For this aim, heparin beads were soaked in C3a, C3a-desArg or scramC3a solutions. Then NC explants were cultured at close proximity to these beads. As expected, neither scramC3a nor C3a-desArg seemed to change the behaviour of NC cells as they tend to disperse radially with no directional bias (Figure 6.10a,b; Movie 6.4). On the contrary, NC cells migrated with high directionally towards a localized source of C3a (Figure 6.10c; Movie 6.4). To test if the response to C3a depends on C3aR, the same assay was repeated for NC treated with C3aR MO. These cells do not respond to C3a (Figure 6.10d). These results show that C3a functions as a NC chemoattractant via C3aR.

Before testing if C3a and C3aR are involved in coattraction, its potential role in other mechanism was controlled. To do this, C3aR MO was used because it allows a cell autonomous effect in NC migration. From this analysis it was possible to conclude that neither cell-cell or cell-substrate adhesion, nor NC motility were significantly affected by these treatments (Figure 6.11a-e). Importantly, treated cells still exhibit normal CIL (Figure

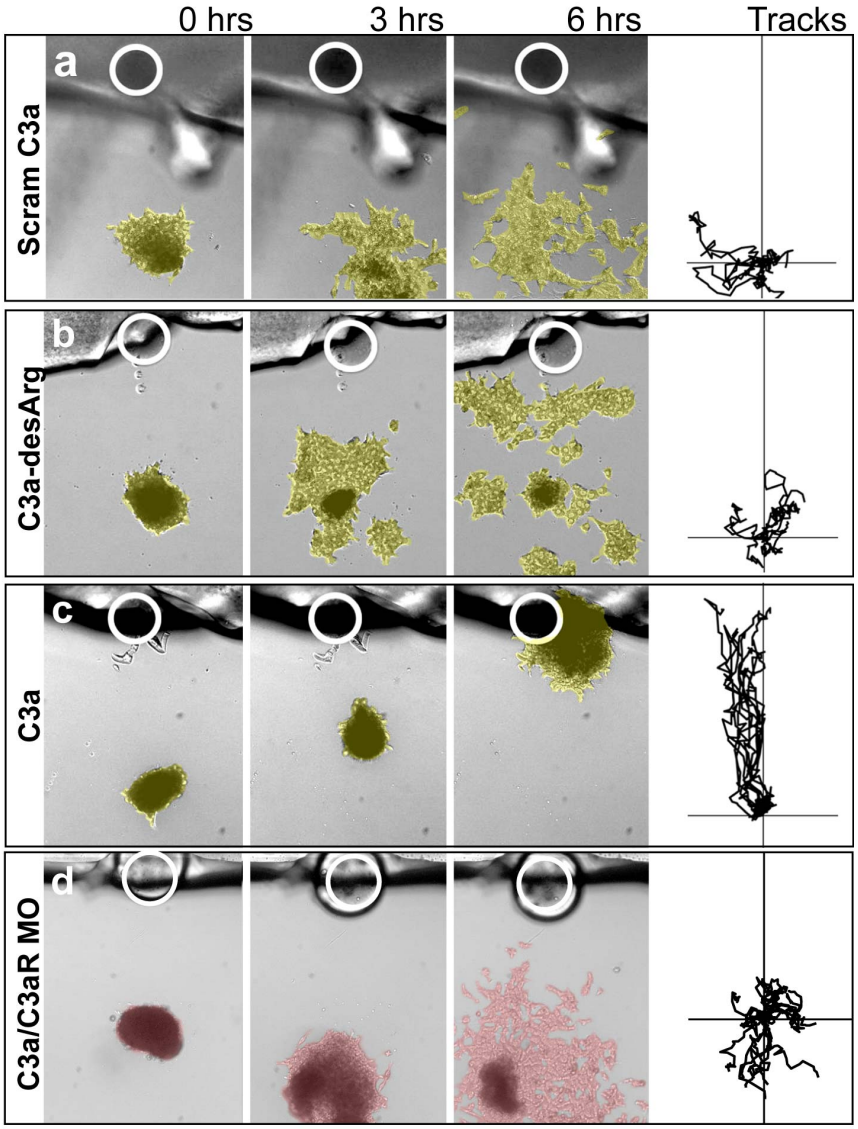

Figure 6.10: **C3a is a NC chemoattractant and is sensed by C3aR.** a. Snapshots and tracks of migration of a NC explant confronted to a bead soaked in a control peptide (White circle, scramC3a). b. Similar to a. but NC confronted to a bead soaked in C3a-desArg. Both treatments did not show significant chemoattraction (C.I.<0.4, $p>0.05$). c. NC confronted to C3a show clear chemoattraction (C.I.: 0.987, $p<0.001$). d. NC chemotactic response to C3a is lost when the receptor, C3aR, is downregulated (C.I.: 0.211, $p>0.05$).

6.11f,g). Nonetheless, C3a or C3aR downregulation dramatically enhanced NC dispersion (Figure 6.12a). These results support the idea that C3a and C3aR may have a specific role in maintaining the unity of the cell cluster. Possibly, counterbalancing the dispersive

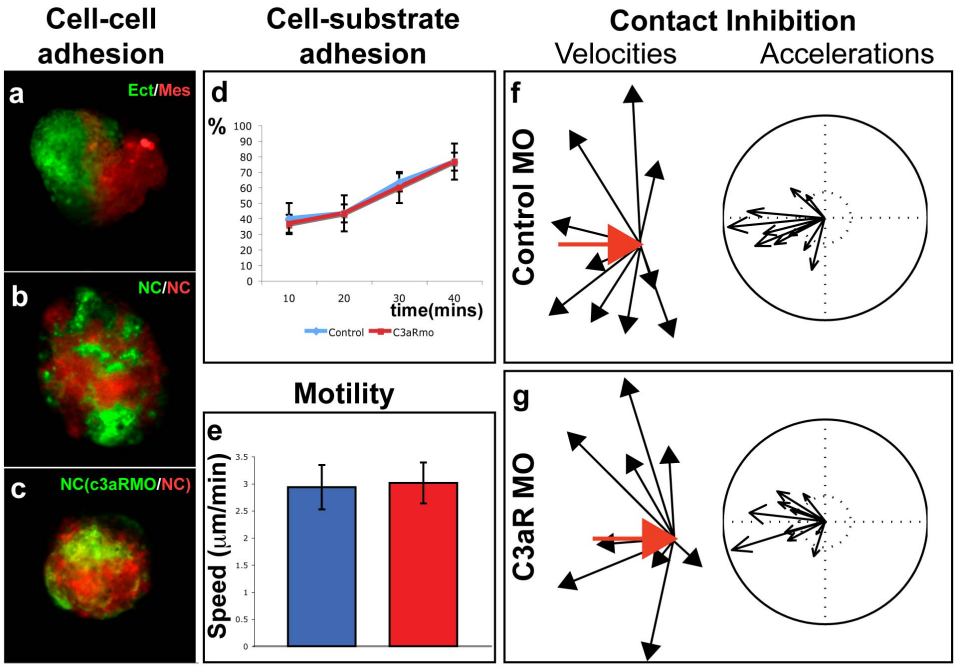

Figure 6.11: **Control NC and C3aR morphant cells do not show significant differences in cell-cell adhesion, cell-substrate adhesion, motility or contact inhibition.** a-c. Cell sorting assay to estimate differential cell-cell adhesive properties. Cells with different adhesive properties will segregate from each other whereas equally adhesive cells will sort homogenously. Dissociated cells were re-aggregated and cultured for 24hrs before analysis. a. Ectoderm (Ect, green) and mesoderm (Mes, red) are known to have different adhesive properties. As expected they segregate from each other. b. Also as expected, NC cells labelled with two different colours mix with each other because they show equal adhesive properties. c. C3aR MO does not affect the cell sorting of NC cells as morphant cells (green) mix perfectly with control NC cells (red). d. Quantification of the adhesion to substrate assay. Control (blue) or C3aR MO (red) NC explants were cultured on fibronectin and the culture dish was flipped over at the indicated times. The percentage of adhered explants was then quantified. Standard deviation obtained from three independent experiments ($p>0.05$). e. Cell motility is not affected by C3aR MO as single control (blue bar) and C3aR MO (red bar) cells show the same speed of migration. f,g. Control and C3aR MO cells have normal CIL. Red arrow: velocity vector before collision; black arrow: velocity vector after collision. Cluster of acceleration vectors is not changed by C3aR MO, indicating that CIL is not affected.

effect of CIL. Given that C3a/C3aR conform a chemotactic pair, this counterbalancing effect is likely to be what has been defined here as coattraction.

To test whether C3a/C3aR are required for attraction, the confrontation assay was used. As shown in Figure 6.12b, neither the control antibody nor the control morpholino affected the consistent mutual attraction between NC explants. On the contrary, this highly signif-

icant directional bias was completely lost when either molecule was downregulated (Figure 6.12b; Movie 6.5 and 6.6). In other words, treated NC lost coattraction as they dispersed randomly and were unaffected by the presence of other explants in their surroundings. The same assay was repeated with other inhibitory molecules of the C3a/C3aR axis and similar effects were obtained. This demonstrated that the lose of coattraction was independent from the method used to disrupt this pathway (Figure 6.12c). These methods included the addition of a C3aR antagonist (SB290157), a blocking C3aR antibody or of a homogenous excess of C3a in the culture media. The bars plot in Figure 6.12d summarise the results obtained with all these treatments.

In summary, the data presented in this chapter shows that NC migrate collectively not only when *in* the embryo but also when cultured *in vitro* where external cues are absent. This shows that NC cells can self-organise to generate a collective migratory pattern. Using a simple computer model it was proposed that, in addition to the repulsive CIL behaviour described in the previous chapters, an attractive interaction in between NC cells could lead to the emergence of collective migration (Figure 6.1). Then, it was shown that this attractive interaction, or coattraction, does take please in NC cells (Figures 6.2 and 6.3). Moreover, the molecular bases of this interaction were unveiled. C3a and its receptor C3aR were found to act as a chemotactic pair (Figure 6.9 and 6.10). Moreover, they are expressed in the NC and they are essential for their migration (Figures 6.4, 6.5, 6.6 and 6.7). Importantly if their function was blocked, coattraction was specifically inhibited (Figures 6.11 and 6.12). Hence, NC cells exhibit coattraction, which is achieved by producing and sensing C3a, a chemoattractant.

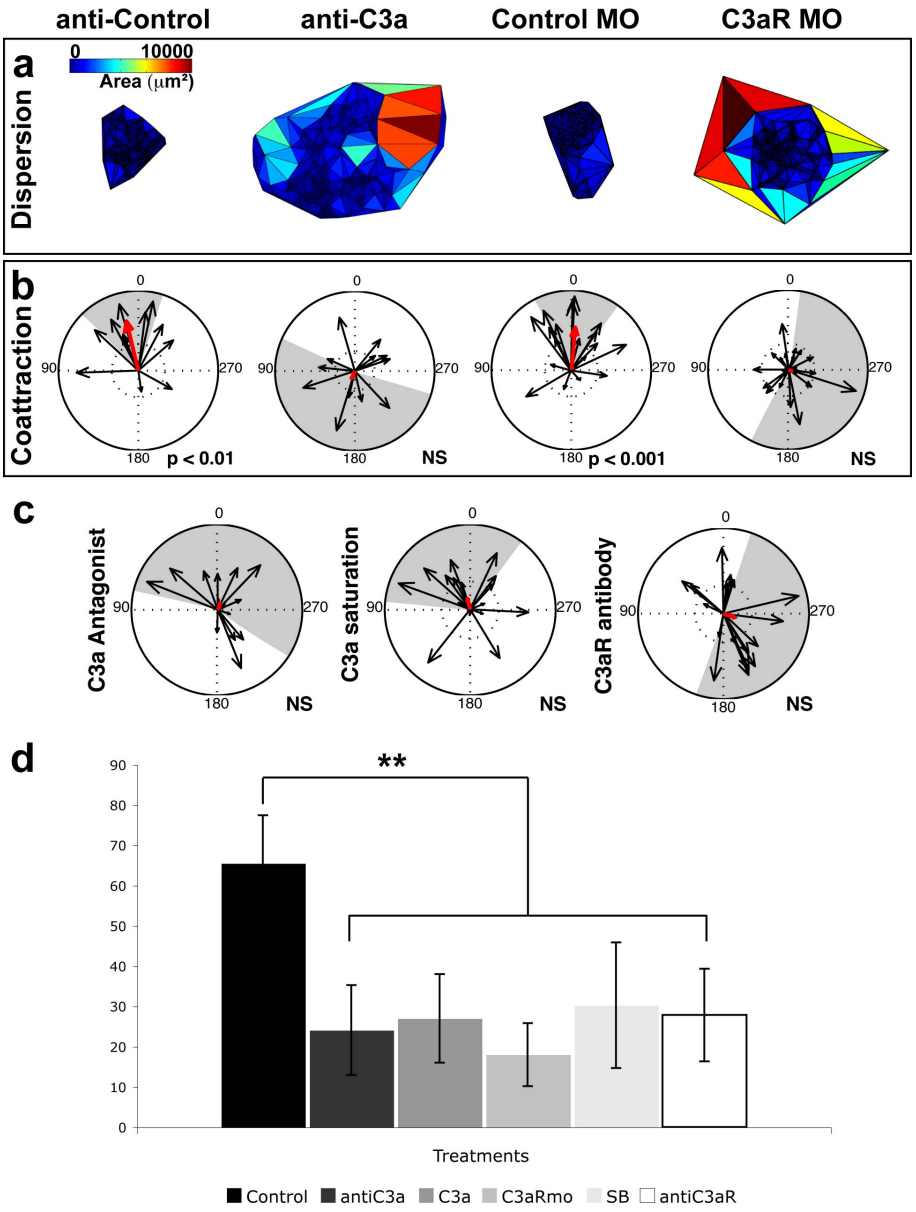

Figure 6.12: **C3a and C3aR are required for NC coattraction.** a. Delaunay triangulation of individual NC explants treated as shown. NC cells disperse quickly when either C3a or C3aR are downregulated. b. Migration vectors of confronted NC pairs calculated as in Figure 6.3b. Note that while control pairs show significant CoA ($p < 0.01$); C3a or C3aR loss-of-function resulted in the absence of CoA as NC explants disperse randomly. c. Further methods to inhibit C3a and C3aR confirm that these factors are required for CoA. d. Summary of the effects of all treatments shown here. Bars indicate the percentage of explants exhibiting coattraction for each treatment ($p < 0.01$, n 20 for each experiment). The control bar includes measurements of control peptide (to control the effect of C3a), Rabbit-IgG (to control C3a and C3aR antibodies), control morpholino (to control C3aR MO) and DMSO (to control SB290157). No significant difference was found between different control treatments. Standard deviation obtained from three independent experiments. $^{**}p < 0.01$

Chapter 7

Collective ensembles require harmonic movements

7.1 Collective migration and NC self-organisation require coattraction.

In the previous chapter it was shown that NC cells exhibit coattraction, a mutual cell-cell attraction force. Moreover, the molecular bases of this interaction were outlined as the attractant, C3a and its receptor C3aR, were found to mediate NC coattraction. These molecules were shown to be required for NC migration. However, the role of coattraction at the single-cell level in collective migration was not studied in detail.

To analyze the role of coattraction in collective migration, *in vivo* nuclear-labelled NC cells were grafted onto unlabelled host embryos and migration was analysed using time-lapse. Grafted cells and host embryos were previously treated with control MO or with C3aR MO. Control NC cells showed directional migration and low dispersion (Figure 7.1a and Movie 7.1). Note how labelled cells remain together almost as cluster along the whole migratory path. This is evident in the Delaunay triangulation as it shows uniformly small areas in between neighbours (Figure 7.1b) and in the tracks shown in Figure 7.1c. In

contrast, C3aR morphant NC cells showed high dispersion and poor directionality (Figure 7.1d and Movie 7.1). The increase in dispersion is shown in the triangulation in Figure 7.1e. These cells lost collective migration as cells seem to adopt individual directions (Figure 7.1f). The distribution of angles of migration and persistence also revealed a profound loss of collective directionality after inhibition of C3aR (Figure 7.1g,h). Thus, coattraction is required for NC collective migration *in vivo*.

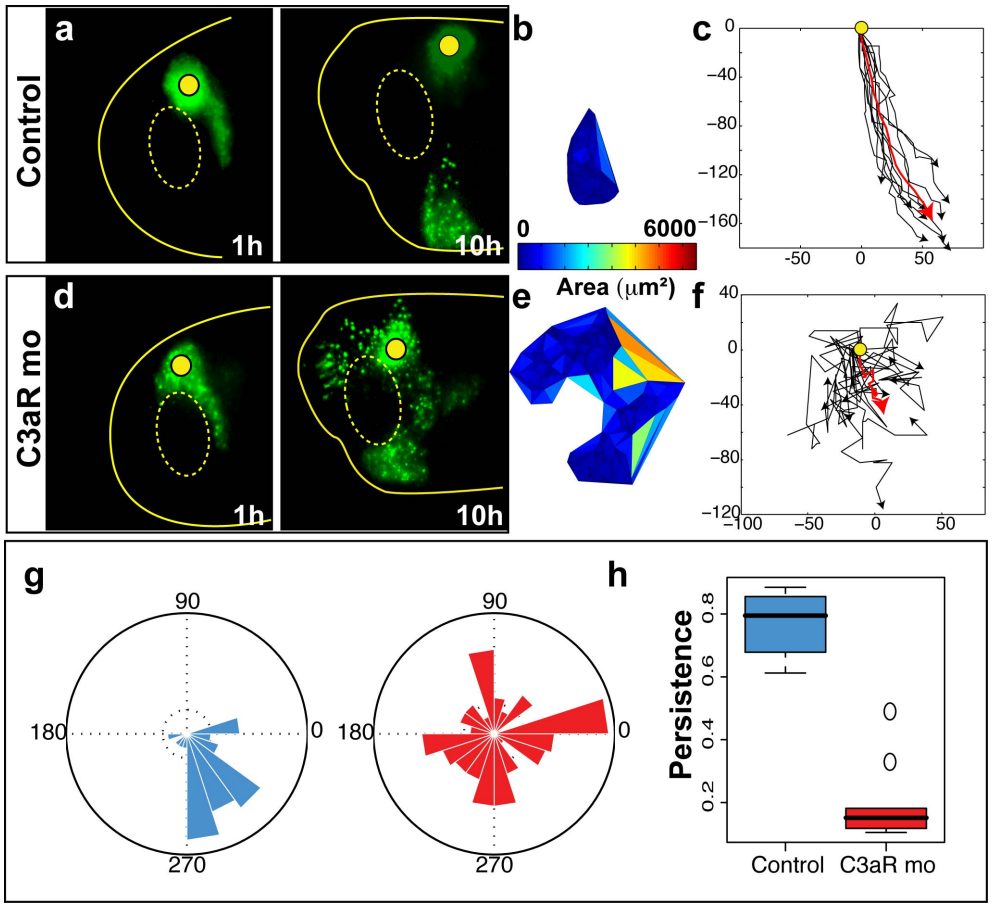

Figure 7.1: **Coattraction is required to maintain NC collective migration *in vivo*.** Labelled NC cells were grafted onto unlabelled embryos and their migration was analysed. a. Selected frames of control NC cells migrating *in vivo*. Yellow line: outline of the embryo. Dotted line: eye. Yellow circle: approximate site of transplantation. b. Delaunay triangulation of a. c. Tracks of cells in a. Red track: average track. d. Selected frames of NC treated with C3aR MO migrating *in vivo*. e. Delaunay triangulation of the morphant cells. f. Tracks of cells in d. g. Rose plot showing the distribution of angles of migration for control (blue) and morphant (red) explants. Only angles from control cells have a distribution significantly different from random ($p < 0.01$). h. Box plot showing the persistence of control (blue) and morphant (red) cells (t-test, $p < 0.01$).

Cultured NC cells can self-organise to generate collective migration in the absence of external cues, and the computer model predicted that coattraction was essential for this (Figure 6.1). Thus, a similar analysis to the one shown in Figure 7.1 was performed *in vitro*. Control NC explants cultured on stripes of concentrated fibronectin (flanked by lower-concentration stripes) migrate as clusters. These cells acquire collective directionality and rarely leave the fibronectin-rich stripes they are cultured on (Figure 7.2a and Movie 7.2). As *in vivo*, these cells showed little dispersion (Figure 7.2b) and coherent tracks (Figure 7.2c). Coattraction was found to be essential in this process as C3aR inhibition depleted NC collective migration. NC cells injected with C3aR MO migrate as individuals and they even go to regions with low levels of fibronectin (Figure 7.2d and Movie 7.2). This resulted in increased dispersion (Figure 7.2e) and tracks without a clear directional trend or collective organisation (Figure 7.2d).

The results shown in Figure 6.11 suggested that the effect of C3a/C3aR inhibition lead to a specific effect on coattraction as other mechanisms such adhesion, motility and CIL were not affected. Nonetheless, a better control would be a functional rescue of coattraction. NC cells are known to respond to CXCL12, a chemokine also known as Sdf1, via its specific receptor CXCR4 (Kucia et al., 2004). Whereas CXCR4 is expressed in migratory NC cells, Sdf1 is not. It was hypothesised that if Sdf1 is artificially expressed in NC cells, it should work as a *"co-chemoattractant"* as its receptor is endogenously present in these cells. To test this, the collective migration of NC cells *in vitro* was analysed in three conditions. The first two are the same as the ones studied in Figure 7.2. The third one is aimed as a functional rescue of coattraction. For this, NC cells were co-injected with C3aR MO and Sdf1 mRNA. As expected, control NC cells showed collective motion and low dispersion whereas C3aR MO cells migrated individually and showed a great degree of dispersion (Figure 7.3). Surprisingly, Sdf1 co-injection reverted the effect of C3aR MO almost to the levels of the control situation (Figure 7.3, bottom row). These results indicate that collective migration requires coattraction regardless the nature of the attractant is.

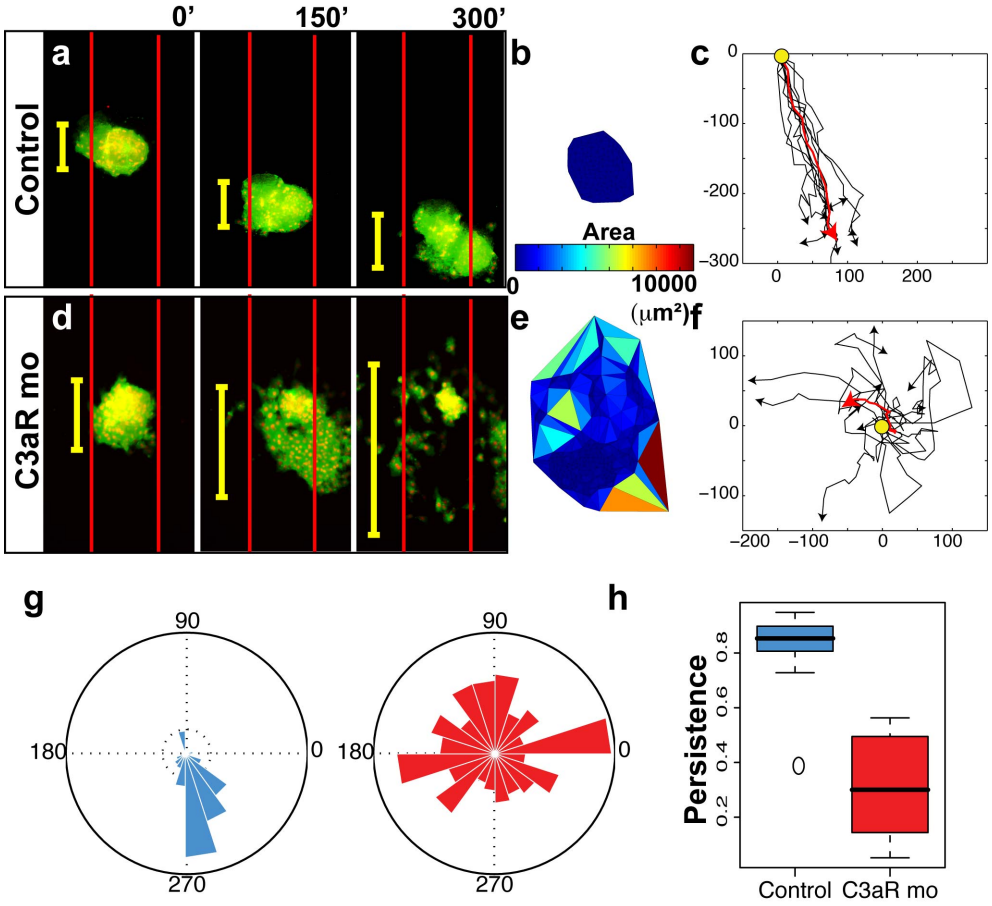

Figure 7.2: **Coattraction is required for the self-organisation of NC in culture.** a. Selected frames of a NC explant treated with a control morpholino. Red lines: limits of region with high levels of fibronectin. Yellow lines: group dispersion. b. Delaunay triangulation of a. c. Tracks of cells in a. Red track: average track. d. Selected frames of a NC explant treated with C3aR MO. e. Delaunay triangulation of the morphant explant. f. Tracks of cells in d. g. Rose plot showing the distribution of angles of migration for control (blue) and morphant (red) explants. Only angles from control cells have a distribution significantly different from random ($p < 0.01$). h. Box plot showing the persistence of control (blue) and morphant (red) cells (t-test, $p < 0.01$).

7.2 Coordinated group response to external cues requires coattraction.

One of the striking features of NC collective migration *in vitro*, is the uniform response to external cues such as chemoattractants. This coordinated response to signals is also observed in other types of collective motion (Rørth, 2009, see for example cases reviewed in). Coattraction seems to be a good candidate to be the mechanism that mediates this

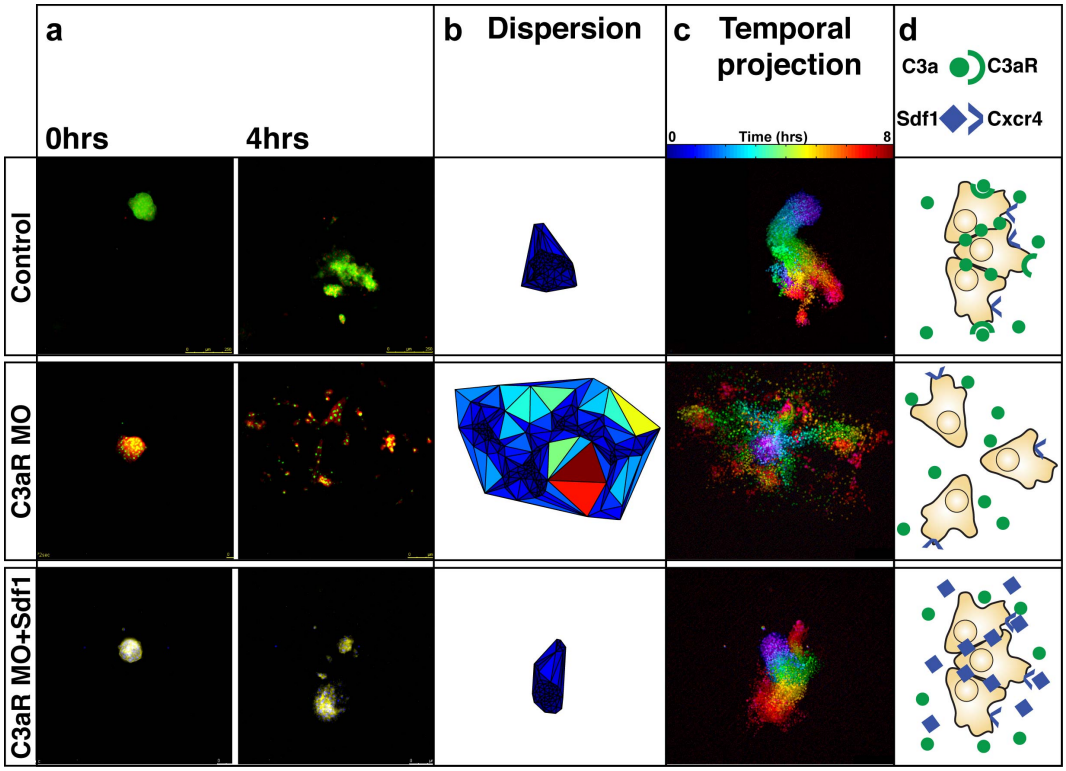

Figure 7.3: **A functional coattraction rescue in C3aR morphant cells.** SDF1 is a NC chemoattractant that is not normally expressed by NC cells, but NC expresses its receptor. a. Frames of time-lapse for the indicated treatments. b. Dispersion, measured by triangulation for the indicated treatments. c. Collective motion depicted via a colour-coded temporal projection of migratory cell nuclei. Note that C3aR MO cells do not show any organization whereas the co-injection of Sdf1 seems to recover the control phenotype. d. Cartoon explaining the results. Upper panel: control cells remain together due production and sensing of the chemoattractant C3a (green circles). Middle panel: in the absence of C3aR (green semi-circumference), C3a cannot be sensed and the collective motion is lost. Bottom panel: this phenotype can be rescued by the co-injection of the chemoattractant Sdf1 (blue squares) because NC cells express its receptor (blue V). This experiment strongly suggests that C3a acts as a co-attractant during NC migration.

collective coordination.

To study this, NC cells were exposed to an external source of Sdf1. NC are known to migrate collectively to such a source (Figure 7.4a, previously described in Theveneau et al., 2010). It is interesting to notice that the degree of attraction is virtually the same for all cells. For example, the ones at the front behave the same as the ones at the back of the explant (tracks in Figure 7.4a and Movie 7.3). This is also reflected in the chemotaxis index and persistence values, which were high for all control cells (Figure 7.4c). In contrast,

C3aR MO cells showed a heterogeneous response to Sdf1. In this case, cells at the front and thus, closer to the Sdf1 source, showed directional attraction to it (Figure 7.4b,c and Movie 7.3). However, cells at the back responded poorly to the attractant producing the disruption of the cluster (Figure 7.4b and Movie 7.3). The heterogeneity of the response is evident when the tracks of front *versus* rear cells are compared (Figure 7.4b) and in the highly variable chemotaxis index (Figure 7.4c). These results indicate that coattraction is required for the homogeneous cell behaviour observed in collective chemotaxis.

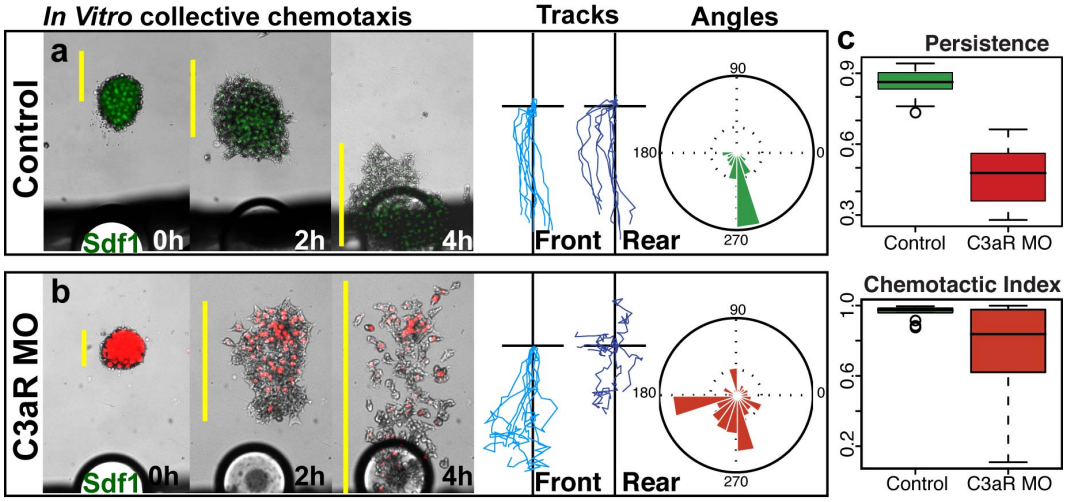

Figure 7.4: **Coordinated group response to external cues requires coattraction.** a. Selected frames, tracks and angles of migration for chemotaxis towards Sdf1 for in control NC cells. Time in hours at the lower right corner. Light blue tracks: Tracks of frontal cells. Dark blue tracks: Tracks of cells at the back. b. Similar to a. but for cells injected with C3aR MO. Note the difference between front and rear tracks. c. Persistence and chemotaxis index for control (green) and morphant cells (red).

7.3 Collective ensembles require harmonic movements.

These results show a clear effect of coattraction on directional cell migration, but do not take into account interactions with neighbouring cells or the collective coherence of the group. To quantify the coherence of the group, the cell alignment and speed at each time point was measured and compared with similar measurements in neighbouring cells. Cell alignment was estimated as the angular deviation from the average path for each cell at

each time point (Figure 7.5a). The average path was obtained by averaging the positions of all cells at any given time point. Morphant cells *in vitro* and *in vivo* showed a higher deviation from the average path than control cells (Figure 7.5b,d). Moreover, control cells showed a smaller range of speed values than morphant cells (Figure 7.5c,e). These two measurements show that control cells move more "harmoniously" than morphant cells, as velocities are similar among neighbours. This congruent movement may help to explain the emergence of collective migration and the homogenous behaviour during collective chemotaxis.

To illustrate this harmony, an analogy between cell movements and musical melodies was made (see Methods and Figure 7.6a-c). Briefly, NC cells were cultured on lanes of fibronectin and then tracked. After that, an arbitrary musical note was assigned to each time step of the average path, in this case the C major scale. Then, all cells were set to play the same melody (C-major) but their pitches were shifted in proportion to their deviation from the average track. At the same time, this was represented this visually using a "harmony map", where a *cell track x time x harmony* matrix was constructed. The third axis, the harmony, was calculated as mentioned above and colour-coded using a heat map. In this representation, similar colours along horizontal stripes represent coherent movements. As expected, the C-major scale was clearly recognizable in control cells (Audio 7.1) and the harmony map shows clear colour stripes (Figure 7.6d). In contrast, the C-major scale was barely recognizable when played by morphant cells (Audio 7.1) and the horizontal stripes in the harmony map became blurred (Figure 7.6d). A similar analysis was also done *in vivo*. Likewise, tracks of control cells resulted in harmonious melodies and striped harmony maps whereas in C3aR MO cells, the melody and the horizontal stripes in the harmony map were more difficult to distinguish (Figure 7.6e, Audio 7.2).

In summary, coattraction is not only required for NC migration but has a specific role in generating collective migration. It coordinates the intrinsic movement of the group and it allows collective chemotaxis. Thus, coattraction and CIL, are two crucial cell interactions for collective migration. Although here they have been studied separately, they are occurring and operating at the same time. CIL allows and stabilise cell polarisation while coattraction counterbalances the dispersion that CIL would lead if on its own.

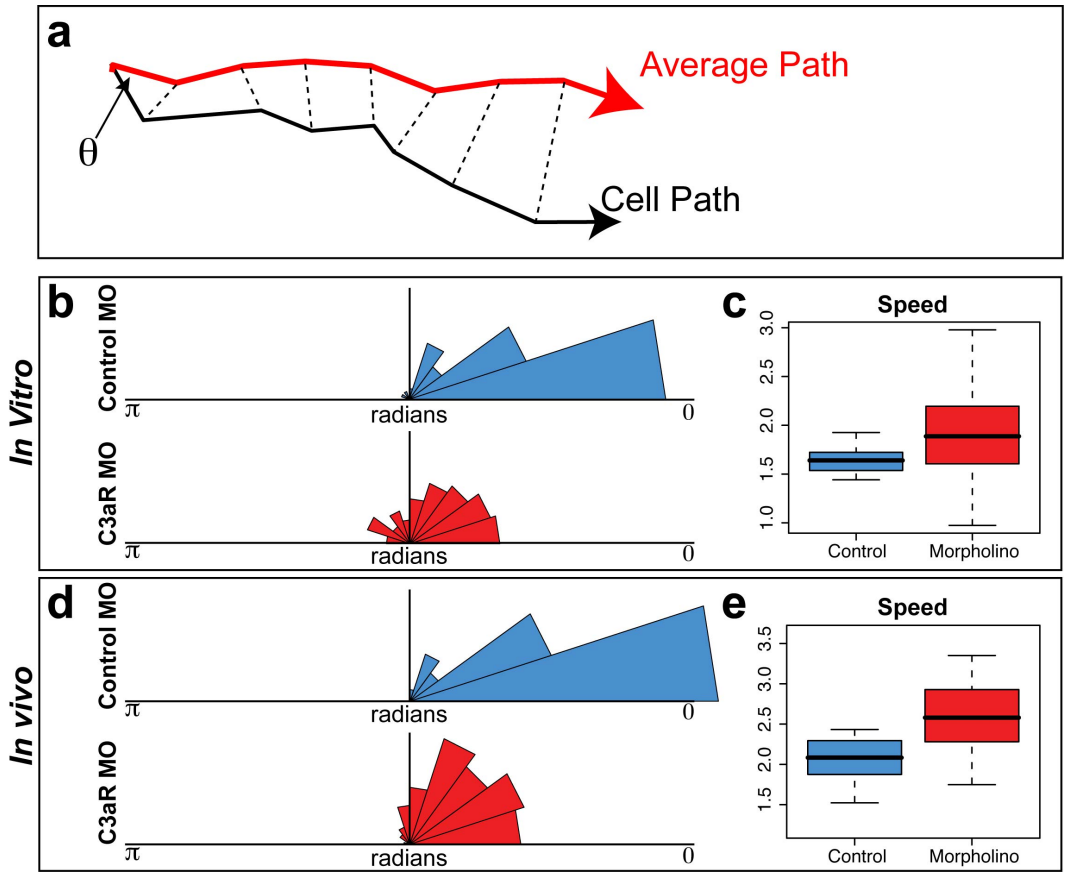

Figure 7.5: **C3aR MO reduces the harmony of migratory paths shown by NC cells *in vitro* and *in vivo*.** a. From all the tracks obtained (only one shown, black) an average track is calculated (red). The alignment θ is defined as the angle in between each migratory path and the average path at all time points (here shown only for the first time). θ ranges from zero to π radians. b. Rose histograms showing the distribution of θ in cells treated with a control morpholino (blue) or a C3aR morpholino (red) *in vitro*. Note that control cells show a higher frequency of small angles reflecting cell alignment. C. Box plots showing speed of control (blue) and C3aR morpholino (red) cells showing that their variance is significantly different ($p < 0.001$, f-test). d,e. Similar to b,c but the analysis was performed *in vivo*.

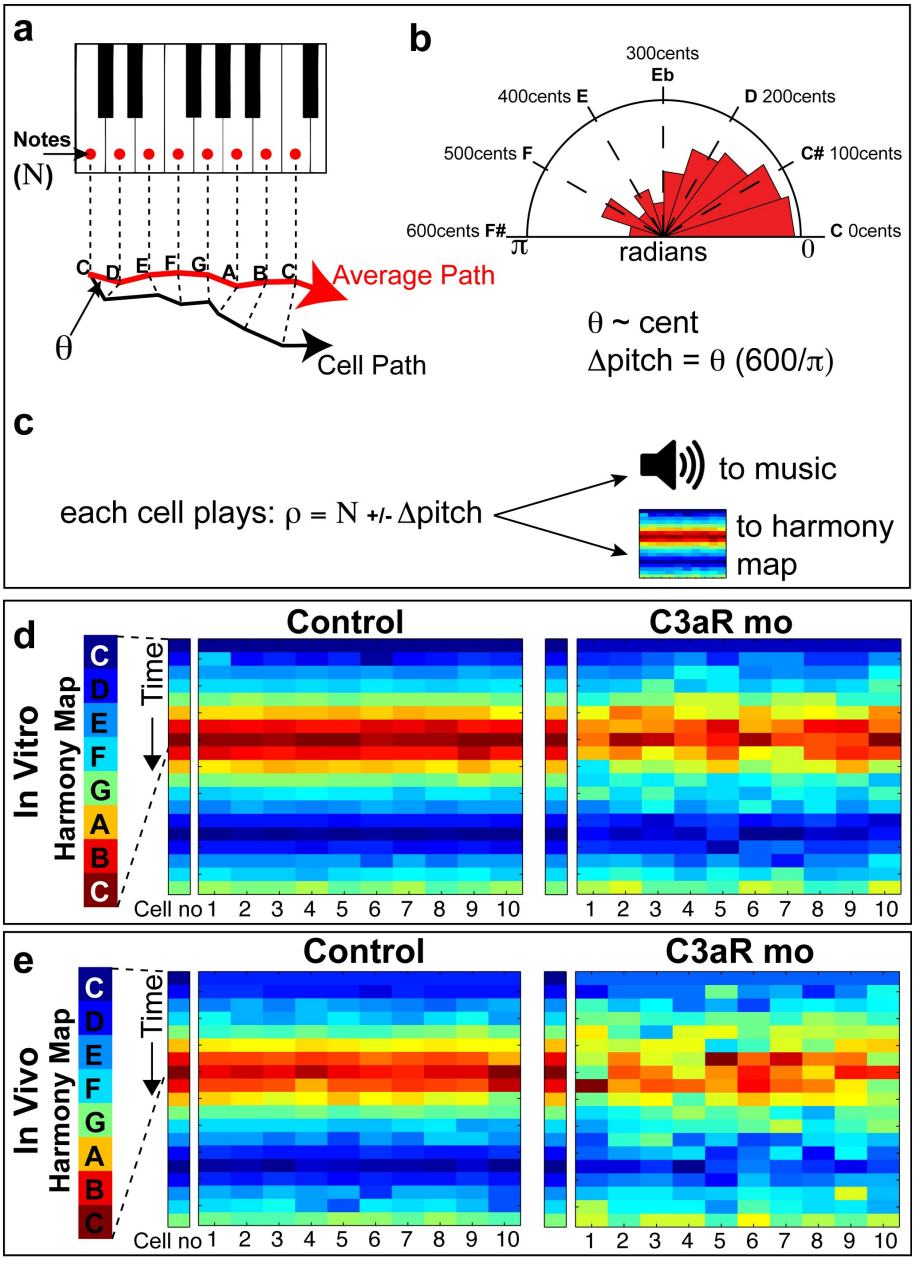

Figure 7.6: **Harmonic cell movements can be visually and acoustically represented.** a. An arbitrary musical note was assigned to each time step of the average path, in this case the C major scale. Then, the alignment θ was calculated for each cell at each time step. b. The alignment angle was linearly transformed to cents to get Δpitch (one cent is a hundredth of a semitone). The maximum deviation, *i.e.* when cells go in the opposite direction to the average ($\theta = \pi$) was assigned 600 cents as this corresponds to the *tritone* (the least harmonic note combination). c. From this, a melody was constructed for each cell where they play the notes assigned to the average path (N) but shifted according Δpitch to obtain a value called ρ. Then, all these melodies were played together. Similarly, a *time x cells* matrix, with the ρ values colour-coded, was constructed. We called it harmony map. If cells are aligned, Δpitch will be small leading to an easy recognition of the melody and to clear horizontal colour stripes in the harmony map. d. Harmony maps for control (left) and C3aR morphant (right) cells migrating *in vitro*. e. Similar to d. but for cells migrating *in vivo*.

Part IV

Conclusions

Chapter 8

Conclusions

8.1 Summary

The aim of this thesis was to determinate to which extend local cell interactions are important for collective NC migration. The main reason to focus in these interactions is that NC cells can self-organise to generate collective migration. This indicates that a core component of collective migration must reside within NC cells and/or their interactions. In this thesis, two cell interactions with major impact in NC migration *in vitro* and *in vivo* were identified and their molecular mechanisms were outlined.

The first mechanism is Contact Inhibition of Locomotion (CIL), a repulsive interaction that occurs after cell-cell contact. This contact produces the collapse of cell protrusions and a concomitant repolarization and redirection of the cell towards a cell-free area. The proposed molecular bases for this mechanism are as follows. A polarised NC cells have a large frontal lamellipodia with high levels of Rac1. In contrast, high levels of RhoA are typically found at the back of these cells. The cell contact, localise members of the PCP pathway to the region of the membrane that is interacting with the other cell producing a local PCP activation that is transduced into RhoA activation. RhoA is known to antagonise Rac1 and to inhibit the formation and maintenance of large lamellipodia. Thus, via RhoA activation and Rac1 inhibition, the cell-cell contact leads to the collapse of cell

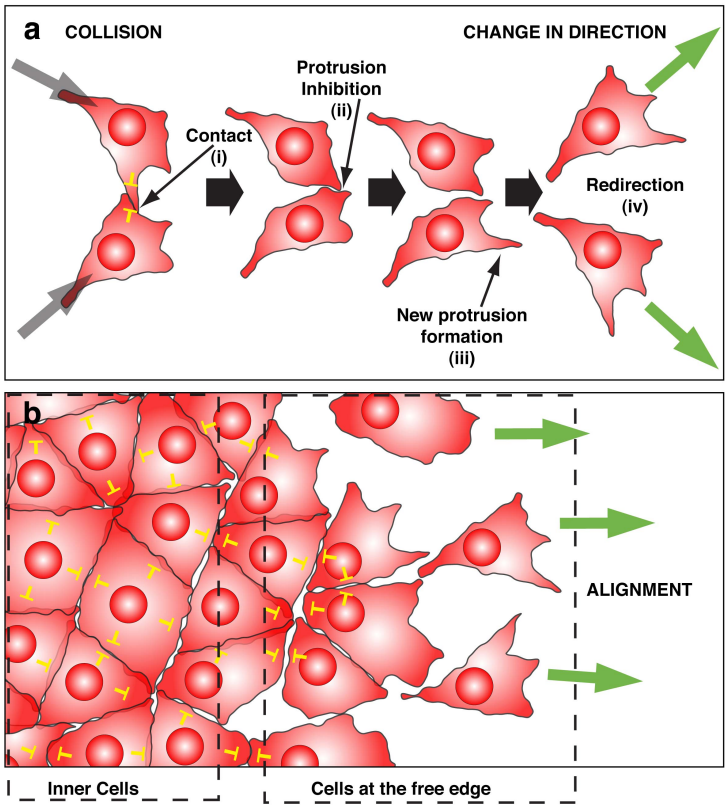

Figure 8.1: **CIL in single and groups of cells.** Contact Inhibition of Locomotion (CIL) in isolated cells (a) or in group of cells (b). CIL is represented by yellow inhibitory arrows. a. Collision between single cells leads to collapse of cell protrusion and a change in the direction of migration (green arrows). The four steps of CIL are shown with roman numerals (see main text for details). b. CIL in a group of cells. CIL between inner cells leads to inhibition of protrusions, while CIL between the leader cells, at the free edge, can lead to cell polarization of the leaders (green arrows) and directional migration. Reprinted from Mayor and Carmona-Fontaine 2010, with permission from Elsevier.

protrusions. This simple mechanism of inhibition of protrusion allows the alignment of colliding individual cells (Figure 8.1a). At the same time, it regulates the global polarity in NC streams and clusters. In these cases, internal cells are known to have little polarisation and they do not form large protrusions. This is accomplished because CIL is operating all around their periphery. On the other hand, cells at the edge are exposed to the substrate and thus free from the inhibition of other cells. Then, these cells will produce cell protrusions only to the front where the lack of cell contact allows high Rac1 and low RhoA levels. This drives to coherent directional migration as front cells can only move towards

the NC-free zone *i.e.* forward. This opens enough space to allow the following row of cells to polarise and move. Then the next row of cells is free to become polarised, and so on (Figure 8.1b). CIL in cells *in vitro* was well described in the literature. However, this is the first demonstration of CIL *in vivo* and one of the first attempts to understand its molecular bases (for a review see Mayor and Carmona-Fontaine, 2010).

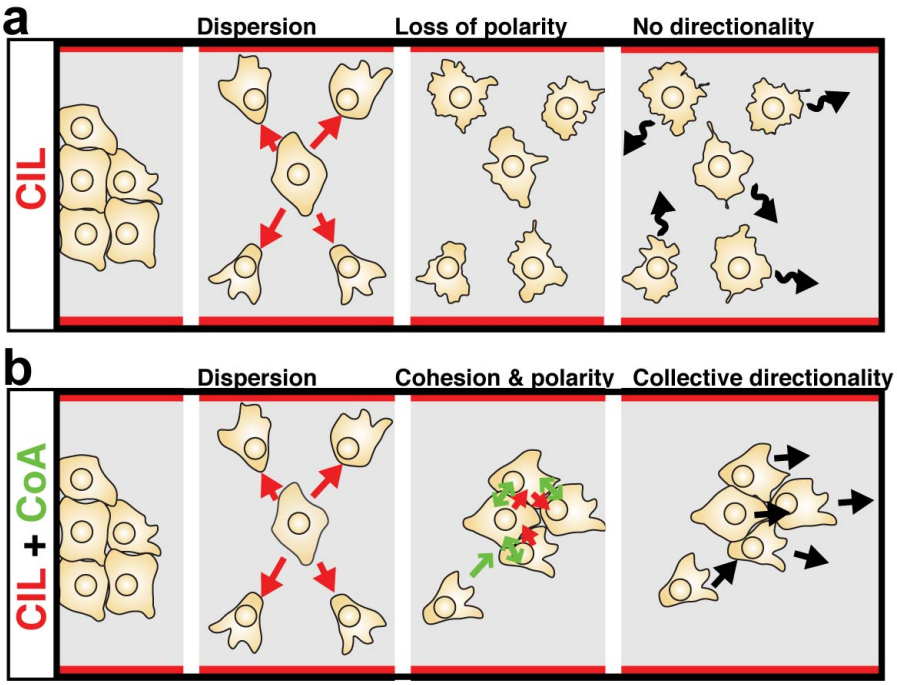

Figure 8.2: **NC collective migration: an interplay between CIL and coattraction.** a. CIL leads to cell dispersion that is counterbalanced by coattraction, allowing cell polarity and directional migration. b. CIL alone leads to cell dispersion, loss of polarity and absence of directional migration.

The second is a mechanism in which migratory NC cells mutually attract each other. This process was called coattraction (CoA). In contrast to the cohesive and coherent collective migration of NC clusters and streams, CIL on its own leads to cell dispersion. This was shown first *in silico*, but then *in vitro* and *in vivo*. The dispersion produced by CIL produce a scattered set of individual cells that are unlikely to interact and thus, to have CIL. The lack of CIL, which is essential to establish and to maintain the polarity of the group, leads to a dramatic decrease in the persistence of these cells (Figure 8.2a). Thus, a cohesive force must compensate this CIL-dependent dispersion. Here is where the role of CoA is

better understood. First, it was shown that NC cells attract each other. So far, this is the first description of mutual attraction among metazoan cells. A schematic representation of the role of CoA is shown in Figure 8.2b. This attraction does not affect CIL, so initially cells could disperse. However, NC cells refrain from this tendency to disperse as, at the same time, they are mutually attracted. Thus, the NC is stable for a longer period of time than a cluster with CIL only. This kind of clusters may be considered as dynamically stable structures maintained by a balance between the dispersive force given by CIL and the attractive force exerted by CoA.

The molecular bases of this attraction were also explored in this thesis. In *Xenopus* NC cells, coattraction is mediated by the secretion and perception of C3a. Surprisingly, C3a is part of the complement, a complex cascade of extracellular reactions essential for innate immunity. The role of the complement in NC migration represents a new function for this cascade. The perception of C3a is possible because NC cells do not only secret it, but they also express its specific receptor, C3aR. The identification of these players, allowed the specific inhibition of CoA that resulted in loss of collective migration. However, this effect can be rescued when another ligand/receptor chemotactic pair is present (such as Sdf1/CXCR4). Thus, coattraction does not depend on the nature of C3a but on its function as an attractant *per se*.

All these experimental observations, with the support of a simple computer model, show that a combination of CIL and coattraction are the minimal conditions that suffice the emergence of collective migration. These are probably the main interactions that occur during NC migration *in vitro*, where external cues are absent. *In vivo*, these mechanisms are likely to be integrated and combined with many others such as external chemoattractants and repulsive cues that delimit the migratory space. This agrees with the experiments *in vitro* where NC cells with coattraction and CIL responded better to inhibitory (such as lack of fibronectin) and attractive (Sdf1 attraction) cues than NC with CIL only. Therefore, it is proposed that the autonomous organisation of NC cells is essential for the collective response to other signals and mechanisms.

8.2 Discussions

8.2.1 Deepening our understanding of the molecular bases of CIL

Although this thesis contributes to our understanding of CIL, there are still some important points that remain unresolved. It is possible to dissect CIL into two core cellular mechanisms requiring two different types of molecular machineries. First, cells need to sense the contact with other cells. This mechanism has to be mediated by molecules located at the cell surface of colliding cells. These molecules are involved in the perception and recognition of the adjacent cell. The second mechanism is a process of cell repolarisation. Upon contact, cells require a mechanism that regulates the withdrawal of protrusions at the contact region followed by the formation of a new protrusion elsewhere. Moreover, these two mechanisms have to be linked and concatenated, thus the molecules mediating the contact are also required to be able to transduce the signal for resetting the polarity of the cell.

Some molecules involved in the two mechanisms described above have been described and shown to be required for proper CIL. However, the linking mechanism has been usually missing. Relevant literature available is briefly reviewed here to propose a possible molecular link between cell perception and repolarisation.

Cell surface and adhesion molecules in CIL

Different pieces of information suggest that molecules, usually linked with cell-cell adhesion, are likely to mediate CIL. Although at a first sight there may be an apparent contradiction between CIL and adhesion, there is actually a long-standing link between these two mechanism (Abercrombie and Ambrose, 1962; Abercrombie and Dunn, 1975). Although CIL implies cell repulsion and dispersion, it also requires adhesion to strengthen the contact and to allow the cell-cell signalling to occur. In fact, the establishment of transient adhesion points between colliding cells has been observed *in vitro* before their lamellipodia are retracted due CIL (Abercrombie, 1970). Moreover, it is quite clear that

classical adhesion molecules, such as cadherins and integrins, do not only provide mechanical adhesion but they also work as ligand/receptor playing an important role in cell signalling (Yap and Kovacs, 2003; Shattil et al., 2010).

Cadherins are a multi-gene family of cell surface glycoproteins that mediate Ca^{2+}-dependent homophilic cell-cell adhesion by their extracellular domains. Cadherins were among the first molecules that were directly implicated in CIL. E-cadherin has been shown to be required for CIL, and interestingly not for Contact Inhibition of Proliferation, in migratory cells and in confluent epithelial cells (Bracke et al., 1997; Huttenlocher et al., 1998; Chen and Obrink, 1991; Ayollo et al., 2009). Likewise, U-cadherin in *Xenopus* (similar to the mammalian P-cadherin) is required for the contact-dependent coordination in collective migration of head mesoderm (Winklbauer et al., 1992). Interestingly, a recent similar study in fish embryos has shown the requirement of E-cadherin for collective migration of mesoderm *in vivo* (Arboleda-Estudillo et al., 2010). Although the authors mostly attribute its role to cell-cell adhesion, they also suggest a possible role for CIL in mesoderm migration. An appealing hypothesis would be that both adhesion and CIL converge at the level of E-cadherin to control collective migration. This is supported by the role of E-cadherin in CIL and the link between CIL and adhesion. Altogether, these data indicate that cadherins are excellent candidates to mediate the cell-cell recognition system required for CIL. At the same time, they highlight that different tissues or cell types may use different cadherins or even other adhesion molecules during CIL (Figure 8.3).

Molecular bases of cell polarity CIL dependent: role of RhoA

A key step in CIL is the inhibition of cell protrusions and the re-setting of the intracellular polarity. Cell protrusions are dynamic and complex structures that are formed largely by actin filaments and are regulated by intricate molecular networks (Pollard and Borisy, 2003). Thus, the inhibition of cell protrusions is not a passive mechanism but, instead, requires the activation of a complex regulatory machinery (Lauffenburger and Horwitz, 1996; Ridley et al., 2003). RhoA is known to control protrusion retraction through the protein kinase ROCK (Xu et al., 2003; Riento and Ridley, 2003). Therefore, RhoA/ROCK

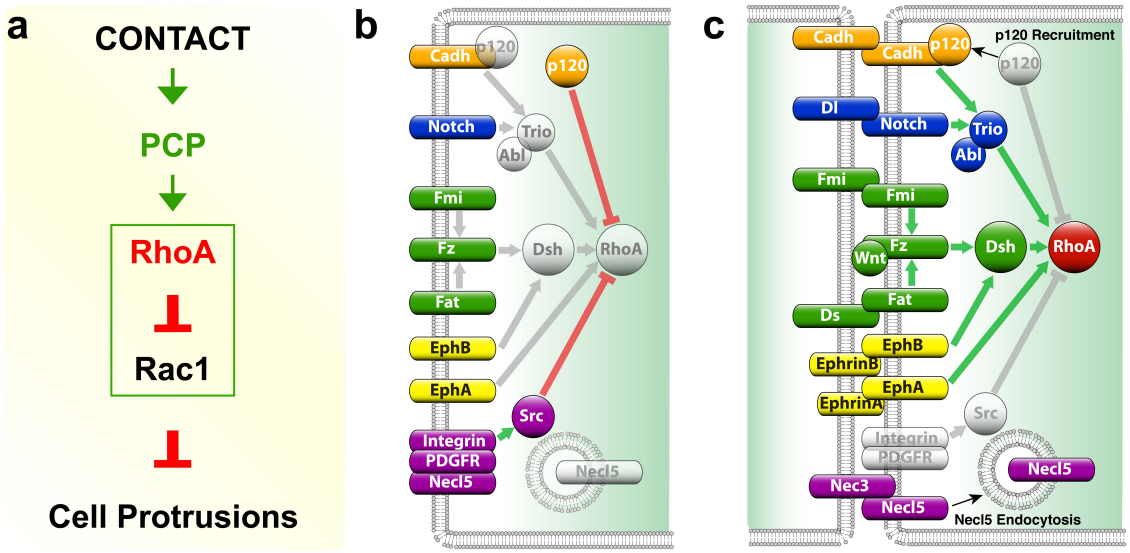

Figure 8.3: **Linking cell-surface molecules with RhoA in CIL.** a. Molecular pathway described for CIL in neural crest cells (Carmona-Fontaine et al., 2008a). b-c. Candidate cell-surface proteins known to up-regulate RhoA activity upon cell contact. b. Molecular state before the cell contact. c. Molecular state after the cell contact.

are good candidates for a protrusion inhibitory mechanism. The spatial and temporal control of RhoA activity is crucial for appropriate inhibition of cell protrusions. This control can be exerted by a variety of molecules, among which, there are cell adhesion molecules and members of the PCP signalling pathway.

As shown in this thesis, RhoA is involved in CIL via the PCP pathway. This pathway is activated at cell-cell contacts, which in turn locally activate RhoA. Activated RhoA would then antagonise Rac1 and inhibit cell protrusions (Matthews et al., 2008b; Carmona-Fontaine et al., 2008b). Interestingly, a similar mechanism has been described for the inhibition of cell protrusions by cell-cell contact during vasculogenesis (Abraham et al., 2009). The regulation of the spatial and temporal activation of Rho-GTPases is an appealing mechanism for CIL-dependent cell repolarisation. However, a complete model of CIL should provide a link between the cell-recognition mechanism, probably mediated by cadherins and other surface molecules, and the activation of RhoA.

Linking cell-surface molecules with RhoA

There is extensive literature showing that cadherin signalling can regulate Rho-GTPases. However, activation of different Rho-GTPases appears to be cell-type and cadherin-type dependent. It is well established that cadherin engagement leads to activation of Rac1 and Cdc42 and inhibition of RhoA at the cell contact region of many cells (Erez et al., 2005). However, activation of RhoA as a result of cell-cell adhesion has been reported in keratinocytes (Calautti et al., 2002) and in N-cadherin dependent cell-cell adhesion of C2C12 myoblasts (Charrasse et al., 2002). It has also been shown that association of N-cadherin with p120 (a catenin that binds to the intracellular domain of cadherins) in cholesterol-rich microdomains leads to activation of RhoA during myogenesis (Taulet et al., 2009). In addition, it has been shown that inhibition of sprouting during vasculogenesis requires VE-cadherin, which in turn activates RhoA and inhibits Rac1 at cell junctions, in a process reminiscent of CIL (Nelson et al., 2004; Abraham et al., 2009).

It is likely that different cells use different cadherins to interact with their neighbours, giving more versatility to CIL. This greater flexibility could explain why the same cell can exhibit CIL with one particular kind of cell but not with others. Moreover, other molecules such as Ephrins/Eph and Notch/Delta and PCP proteins are also possible mediators of CIL as they are localised at the cell membrane and can regulate RhoA. Figure 8.3 illustrate a selection of cell surface molecules and how they are known to activate RhoA (see Mayor and Carmona-Fontaine, 2010, for detail).

8.2.2 CIL in other cell types

One of Abercrombie's unfulfilled aims was to show that CIL occurs *in vivo* (Bellairs, 2000). In this thesis it was shown that, CIL occurs *in vivo* and, because of its critical role in migration, is probably widely spread among other cell types.

There are numerous examples from recent literature of other colliding migratory cells types *in vivo* that appear to display CIL such as zebrafish endodermal cells (Pezeron et al., 2008), anterior visceral endoderm cells in mice (Srinivas et al., 2004), and myeloid

cells of *Xenopus* embryos (Costa et al., 2008), among others.

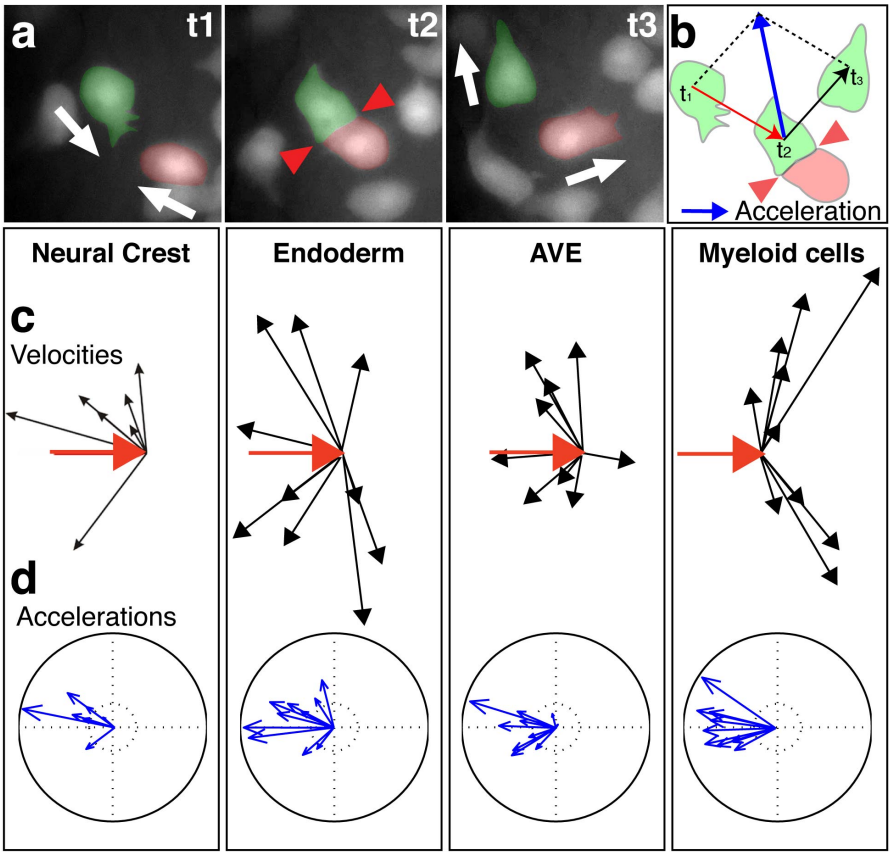

Figure 8.4: a. Example of endodermal cells showing typical CIL behaviour. At $t1$ two cells are approaching, they collide and collapse their protrusions at $t2$ and they change their polarity and direction of migration at $t3$. (Δt, 3.5 min, frames taken from ref. Pezeron et al., 2008). b. Analysis of CIL. The velocity of migration was measured before collision (red arrow) and after collision (black arrow). The difference between these velocities (acceleration, blue arrow) was calculated for each pair of colliding cells. c, d. Examples of CIL for the *in vivo* migration of neural crest from zebrafish embryos (see results section), zebrafish endodermal cells (Pezeron et al., 2008), mouse anterior visceral endoderm (Srinivas et al., 2004), *Xenopus* myeloid cells (Costa et al., 2008). c. Velocity vectors for different pair of cells aligned with respect to the velocity before collision (red arrow); black arrow: velocity after collision. Note the change in the direction of migration after collision. d. Acceleration vectors. Acceleration vectors were compared with random migration using Moore's modification to the Rayleigh's test (Moore, 1980). All p values < 0.001, n=10.

It has been proposed that migration of endodermal cells during zebrafish gastrulation occurs via a combination of random walk and chemoattraction towards Cxcl12 (Pezeron et al., 2008; Nair and Schilling, 2008). Interestingly, these cells do not overlap suggesting that CIL may be also having a role in this movement. Similarly, it was shown that

visceral endoderm cells in mouse embryos are initially scattered over the epiblast. It was suggested that the endoderm forms through coordinated visceral endoderm cell dispersal and concomitant epiblast cell intercalation (Kwon et al., 2008). Similarly, myeloid cells in *Xenopus* embryos disperse from a particular region to the rest of the body (Costa et al., 2008). However, the mechanism of dispersion in neither of these processes is understood. Here, it is proposed that these cells exhibit CIL and that it would be the mechanism that prevents cell overlapping and enhance cell dispersion. Surprisingly, all these cells appear to have CIL when published movies were analysed using the same method that the one described in this thesis (Figure 8.4).

Along the same lines, the migration of Cajal-Retzius cells, a transient neuronal population crucial for the development of the brain cortex, is controlled by the apposed meningeal membranes, which produce and secrete the chemokine Cxcl12 (Borrell and Marin, 2006). However, this chemokine appears to be uniformly distributed along the migratory space and what provides the directionality in the dispersion of these cells are "contact-inhibitory interactions" (Borrell and Marin, 2006), which correspond to CIL. Indeed the assay used to characterize the interactions between these cells is the same as the one used when CIL was initially described (Abercrombie and Heaysman, 1953, 1954). Adding up, this literature analysis suggests that CIL is a general migratory mechanism that co-exists with processes such as chemoattraction, random-walk and cell intercalation. Therefore, CIL is likely to be present in many types of cell migration *in vivo*.

8.2.3 CoA in other cell types

As previously mentioned, this is the first description of coattraction as such. Hence, it is difficult to state whether it is present in other cell types or not. In addition, it is difficult to extract form the literature any information that could suggest coattraction as specific assays are required to test mutual cell attraction. Nonetheless, there is a couple of examples in the literature that could suggest that coattraction is not a mechanisms restricted to the migration of NC cells. Moreover, given its essential role in NC collective migration, it is likely that coattraction, or a similar kind of attractive interaction, is present

in other cell collectives. This would be especially important in the collective migration of mesenchymal cell groups as cell-cell adhesion is strongly reduced in this context.

Coattraction between NC cells is highly reminiscent of the behaviour of *Dictyostelium discoideum*, where individual cells release and respond to a chemoattractant to produce a multicellular aggregate (Bonner et al., 1969; Manahan et al., 2004). However, this is the first clear evidence for this type of mechanism in metazoan cells. Interestingly, in the report of the first direct observation (using Dunn chamber assay and time-lapse) of chemotaxis in cancer cells, there are some observations that may suggest coattraction (Zicha and Dunn, 1995). In this work, it was observed that T15 sarcoma cells responded to an experimentally supplied chemoattractant by migrating directly to the source. However, these cells deviated from the ideal path towards the chemoattractant source in a cell density-dependent manner. This lead the authors to propose the existence of a chemoattractant produced by the cancerous cells themselves, which would be integrated with the external one (Zicha and Dunn, 1995). However, this lead was never followed, nor the nature of the factor identified.

Other cells may also exhibit coattraction. In a recent publication, Li et al. indirectly report some kind of mutual attraction between human stem cells. Furthermore, they suggest that this mutual attraction may be important for the emergence of collective migration of these cells (Li et al., 2010). This is an exciting report that reinforces the idea that CoA may be present in other systems. Thus, it seems likely that coattraction will turn out to be a general mechanism for collective migration of different cell types. Finally, it would be interesting to test whether immune cells exhibit coattraction and if also depends on the complement. If so, coattraction could have been co-opted by the immune system as a positive feedback mechanism for efficient recruitment of cells to particular sites.

8.2.4 Social cell interactions in collective migration

> " A tissue culture is often referred to as a colony of cells, thereby implying that a cell can in some circumstances be regarded as a social organism. [...] that is, to take the cell as a unit and to investigate how its behaviour is influenced by other cells."
> (Abercrombie and Heaysman, 1953)

Here it has been shown that directional collective migration is a self-organizing property of NC cells as it does not require, but can better integrate, external signals. The main emphasis of this thesis has been on the importance of local cell-cell interactions. In other words, this is a study of how the behaviour of a cell is influenced by its neighbours; *i.e.* a study of social interactions among NC cells. Following Abercrombie and Heaysman's advice, the collective behaviour of these cells has been analysed as an emergent property derived form simple interactions at the single cell level. It is difficult to speculate about what a cell is able to perceive but it is likely that most of its inputs come from its immediate surrounding and neighbouring cells. Even if cells may be able to perceive external and distal signals such as morphogens, they may need their neighbours to determine their relative position with respect to the morphogen source (Gurdon and Bourillot, 2001). The relative growth of a regenerating limb and the perception of Hedgehog are good examples of this (Gurdon and Bourillot, 2001; Chen and Struhl, 1996). During embryonic development, groups of cells mutually influence each other by interactions that need to occur in specific times and places. Moreover, signals and responses need to be synchronic in the cell group to diminish noise and incoherent behaviours. Hence, a mechanism of cross-talk between neighbouring cells is probably a much more efficient, robust and reliable mean to direct the differentiation, movement or any other action that requires the coordinated response of a group of cells. Thus, the study of social cell interactions should be at the core of embryology.

Interestingly, a similar combination of local interactions that the ones described in this thesis have been found, and modelled, in other types of collective migration (Grégoire et al., 2003; Grégoire and Chaté, 2004; Buhl et al., 2006; Sumpter et al., 2008; Torney et al., 2009). These examples range from bacteria to mammals and thus, the term social appears to be quite accurate. These collective movements are also self-organised as they can emerge in the absence of a leader. Importantly, they acquire spontaneous directional and persistent motion when density reaches a critical threshold (Grégoire et al., 2003; Grégoire and Chaté, 2004; Buhl et al., 2006; Bazazi et al., 2008). For example, locust kept in an annular chamber (so they can move clockwise or counter-clockwise, *i.e.* in one dimension) they will move randomly when in a low density. If the number of locusts

is increased over a certain density level, the population will start moving in only one direction with sudden "switches" to the opposite one. However, if the locust density is further increased, the population will now move in one direction and remain doing so for the duration of the whole experiment (∼10 hours Buhl et al., 2006).

Density also appears to be an essential parameter in NC migration. CIL alone leads to rapid dispersion of the group, leaving individual migratory cells that progress poorly as they no longer interact. Thus, coattraction counterbalances this dispersion by maintaining NC cells at a density that allows interactions. This density level is required for CIL to maintain the directionality of migration of the cell group. In fact, the corridor experiments were performed to restrict NC dispersion in one axis. By doing so, NC cell density was maintained and collective migration emerged with a higher frequency that when the cells dispersed freely. This indicates that the attractive effect of coattraction is not strong enough to always maintain the critical density of the cluster, especially when the possible migratory space is virtually infinitive. Nonetheless, this is not the *in vivo* situation where NC streams are surrounded by restrictive lateral regions (see section 1.4.1). Thus, the *in vitro* corridor situation is much closer to the *in vivo* scenario. Of note, the assay to study the collective migration in locusts can be seen as an infinitive circular corridor indicating that, in order to maintain a high population density, it is important to control the degree of freedom in the movement of individuals.

Another shared property of animal and NC cell collective motion is the increased efficiency in the transference of external information. For example, swarms of animals with attractive and repulsive local interactions, can respond uniformly to threads that only affect a small number of individuals (Couzin et al., 2005; Torney et al., 2009). Similarly, external cues including both repulsive signals (such as those mediated by Semaphorins and ephrines, reviewed in Kuriyama and Mayor, 2008), as well as attractive factors (such as VEGF and Sdf1; McLennan et al., 2010; Svetic et al., 2007; Killian et al., 2009; Theveneau et al., 2010), are most likely, affecting only a small subset of cells in the NC cluster. Nonetheless, NC streams and cluster show a uniform and coordinate response to these signals. Thus, coattraction and CIL organise NC cells by maintaining a critical cell density that allows them to respond more efficiently and uniformly to external cues.

The idea of social interactions among cells is not new (Abercrombie and Heaysman, 1953). However, it is sometimes underestimated as an approach to understand developmental biology. Collective NC migration provides an excellent model to study the importance of these social interactions. Interestingly, although attraction-repulsion models have been used in animals and bacteria, they have not been previously used in the movement of metazoan cells. This thesis shows that this approach can actually help to understand collective migration in animal cells. Similarly, it may be possible that several problems of morphogenesis, pattern formation and development in general, may be better understood when cells are considered as social individuals.

8.2.5 Towards an embryology based on "cellular sociology".

> "a system in which large networks of components with no central control and simple rules of operation give rise to complex collective behaviour, sophisticated information processing, and adaptation via learning or evolution. "
> (Mitchell, 2009, [1])

The emergence of a being from a single fertilised egg is possibly a problem without a final solution. However, if we try to understand how complex patterns and multicellular structures or behaviours emerge from relatively simpler intercellular relations, we may get a better understanding of how development occurs. Here is the importance to take a cellular approach to development, especially when cells are considered as individuals that interact with their peers. As mentioned in the introduction, complexity is a growing field in mathematics often applied to ecology, econometrics and neuroscience. However, developmental biology may also benefit if looked under the prism of complexity.

Embryology is not only complex in the sense of complication but also have some of the main features of the interest of complexity as a field. Is by definition a non-central process, as there is no central control for development. It is true that there are inducing centres and organisers that direct the fate of surrounding tissues. Nonetheless, the emergence of those centres is internally controlled. They are determined probably by some initial asymmetries (initiated by the entry of the sperm, asymmetric division, maternal influence, etc...),

[1] Quoted in Couzin 2010

but once development is triggered inside a bird's egg, for example, the system evolves autonomously.

Another property of a complex system, as highlighted by Mitchell, is the simplicity of the operation rules. Cell activities during development are actually simple, or at least limited. Cells can differentiate, move, change their shape, divide or die. They can signal, modulate signals and respond to them. Besides that, little is left for a cell. Moreover, signalling pathways are limited and different cell processes share many core components. Thus, the rules of interactions are rather simple. However, there is an endless possibility of combination of these rules and is that infinitive space of combinations, what allows the emergence of development as such. It is true that the intracellular regulation of these behaviours may be amazingly complex in itself. There is increasing evidence showing the imbricated regulatory mechanisms of gene transcription and translation, transcriptional noise elimination and intracellular protein trafficking to name just a few (Pearson, 2006; Rao et al., 2002; Lippincott-Schwartz et al., 2000). However, there is no need to consider all that internal complexity when analysing how entire cells interact to generate multicellular behavioural patterns. These are problems at a different scale. Importantly, in development, these relatively simple operation rules *evolve* to generate a complex structure, an embryo, an animal or a plant. The bottom line is that development has all the elements of a complex system: no central control, relatively simple operations and a complex output. Indeed, the quote at the beginning of this section could also be a rather cold and technical, but not wrong, definition of development.

Current genetic and visualisation techniques are allowing us to determine precisely the behaviour of cells over time and their interactions with other cells. At the same time, we are collecting more and more information about the molecules required for these interactions and signals. We are also getting a better idea of the molecular machineries required for the intracellular processing of these signals. Thus, there is no real technical limitation to start seriously applying the knowledge and power of *complexity* to embryology. Again, this requires focusing on cells as individuals that interact in different social manners. When these relations are integrated at a larger scale, collective behaviours, complex shapes and unpredictable patterns; can emerge. The new developmental biology may become a social

science. The study of how cellular societies can generate something as complex as any being.

8.3 Final Remarks

Now, it is possible to conclude that a large proportion of the mechanisms of NC collective migration, reside within these cells and their relations.

A balance between repulsion, given by Contact Inhibition of Locomotion, and mutual attraction, given by a process called coattraction, are key components of the autonomous control of collective migration in NC cells. These interactions are present within fellow NC cells and can be considered social cell interactions.

The autonomous configuration that NC cells can adopt is also a better substrate for external signals. Once NC are organised they are much more efficient in responding uniformly to external cues and signals. They can be seen as a functional module, a field of cells that self-organise and interact with other functional modules to generate an embryo. These proposed functional modules can be thought as the functional counterpart of morphogenetic fields.

The approach to the embryo in this thesis may seem to be more of an abstract cell biology work than a proper embryological thesis focused in the development of the Neural Crest. This is true in one way and not so correct in another. To some extent, the author considers that many of the features of NC biology are not exclusive to this tissue but shared by other embryonic and non-embryonic cell populations. Moreover, the abstraction of the problem allows to find simple features that, although they may not allow to understand the system completely, they allow to predict some of its behaviours. Nonetheless, the inspiration for all this work comes from the observation of embryonic development and from the degree of independence that embryonic cells seem to have when observed *in vivo*. Thus, it is an attempt to dissect the embryo into functional modular units that interact with others to proceed with development. Therefore, this is a work of embryology.

Part V

Appendix

Publications

- Carmona-Fontaine C, Acuña G, Ellwanger K, Niehrs C, Mayor R. *Neural crests are actively precluded from the anterior neural fold by a novel inhibitory mechanism dependent on Dickkopf1 secreted by the prechordal mesoderm.* **Developmental Biology** 2007; 309(2):208-21.

- Matthews HK, Marchant L, Carmona-Fontaine C, Kuriyama S, Larran J, Holt MR, Parsons M, Mayor R. *Directional migration of neural crest cells in vivo is regulated by Syndecan-4/Rac1 and non-canonical Wnt signaling/RhoA.* **Development** 2008; 135(10):1771-80.

- Carmona-Fontaine C, Matthews HK, Mayor R. *Directional cell migration in vivo: Wnt at the crest.* **Cell Adhesion & Migration** 2008; 2(4):240-2.

- Carmona-Fontaine C, Matthews HK, Kuriyama S, Moreno M, Dunn GA, Parsons M, Stern CD, Mayor R. *Contact inhibition of locomotion in vivo controls neural crest directional migration.* **Nature** 2008; 256(7224): 957-61.

- Mayor R and Carmona-Fontaine C, *Keeping in Touch with Contact inhibition of locomotion.* **Trends in Cell Biology** 2010; 20(6):319-328.

Available online at www.sciencedirect.com
ScienceDirect
Developmental Biology 309 (2007) 208–221
DEVELOPMENTAL BIOLOGY
www.elsevier.com/developmentalbiology

Neural crests are actively precluded from the anterior neural fold by a novel inhibitory mechanism dependent on Dickkopf1 secreted by the prechordal mesoderm

Carlos Carmona-Fontaine [a], Gustavo Acuña [b], Kristina Ellwanger [c], Christof Niehrs [c], Roberto Mayor [a,b,*]

[a] *Department of Anatomy and Developmental Biology, University College London, UK*
[b] *Universidad de Chile, Chile*
[c] *German Cancer Research Center, Im Neuenheimer Feld 280, Heidelberg, Germany*

Received for publication 18 April 2007; revised 13 June 2007; accepted 6 July 2007
Available online 12 July 2007

Abstract

It is known the interactions between the neural plate and epidermis generate neural crest (NC), but it is unknown why the NC develops only at the lateral border of the neural plate and not in the anterior fold. Using grafting experiments we show that there is a previously unidentified mechanism that precludes NC from the anterior region. We identify prechordal mesoderm as the tissue that inhibits NC in the anterior territory and show that the Wnt/β-catenin antagonist Dkk1, secreted by this tissue, is sufficient to mimic this NC inhibition. We show that Dkk1 is required for preventing the formation of NC in the anterior neural folds as loss-of-function experiments using a Dkk1 blocking antibody in *Xenopus* as well as the analysis of *Dkk1*-null mouse embryos transform the anterior neural fold into NC. This can be mimicked by Wnt/β-catenin signaling activation without affecting the anterior posterior patterning of the neural plate, or placodal specification. Finally, we show that the NC cells induced at the anterior neural fold are able to migrate and differentiate as normal NC. These results demonstrate that anterior regions of the embryo lack NC because of a mechanism, conserved from fish to mammals, that suppresses Wnt/β-catenin signaling via Dkk1.

Keywords: Neural crest; Neural induction; Dkk1; Wnt; *Snail2*; *Snail1*; Anterior–posterior axis; *Xenopus*; Zebrafish, Mouse

Introduction

The neural crest (NC) is a cell population characteristic of vertebrates that gives rise to a variety of cell types, including neurons and glia in the peripheral nervous system, connective tissues of the craniofacial structures and pigment cells of the skin (LeDouarin and Kalcheim, 1999). From studies in chick, amphibian and zebrafish embryos, some of the signals involved in the induction of the NC have been identified, including BMPs, Wnts, FGF, Notch and RA (Liem et al., 1995; Mayor et al., 1995, 1997; Saint-Jeannet et al., 1997; Marchant et al., 1998; Nguyen et al., 1998; LaBonne and Bronner-Fraser, 1998; Lekven et al., 2001; Deardorff et al., 2001; Villanueva et al., 2002; Garcia-Castro et al., 2002; Tribulo et al., 2003; Endo et al., 2003; Glavic et al., 2004; Lewis et al., 2004; Bastidas et al., 2004, reviewed in Mayor and Aybar, 2001; Knecht and Bronner-Fraser, 2002; Aybar and Mayor, 2002; Basch et al., 2004; Steventon et al., 2005). At early stages of crest induction an intermediate level of BMP may be necessary, neither so high as to specify ventral epidermis nor so low as to specify neural tissue (LaBonne and Bronner-Fraser, 1998; Nguyen et al., 1998; Morgan and Sargent, 1997; Marchant et al., 1998; Barth et al., 1999). In addition, signaling by Wnts, FGF and RA is required for full induction of the NC (Saint-Jeannet et al., 1997; Mayor et al., 1997; LaBonne and Bronner-Fraser, 1998; Lekven et al., 2001; Deardorff et al., 2001; Villanueva et al., 2002).

Despite these important advances in understanding NC induction and the identification of many inductive molecules, we still do not fully understand how NC is patterned within the ectoderm. It has been shown that NC cells originate at the neural

* Corresponding author. Department of Anatomy and Developmental Biology, University College London, UK.
E-mail address: r.mayor@ucl.ac.uk (R. Mayor).

0012-1606/$ - see front matter © 2007 Elsevier Inc. All rights reserved.
doi:10.1016/j.ydbio.2007.07.006

plate border as a consequence of the interactions between the neural plate and the non-neural ectoderm (Moury and Jacobson, 1990; Selleck and Bronner-Fraser, 1995; Mancilla and Mayor, 1996; Mayor et al., 1997). However it is well established that no NC forms in the anterior neural folds, where a neural plate/non-neural ectoderm border also exists. Early work in the amphibian embryo established that the anterior neural ridge (anterior neural fold, ANF) does not produce NC (Hörstadius, 1950). More recent work, using the quail–chick marker system (LeDouarin and Kalcheim, 1999), also supports the conclusion that the ANF does not give rise to NC (Couly and Le Douarin, 1985; Couly et al., 1993). If interactions between neural plate and epidermis are sufficient to induce NC, why is there no NC at the ANF, where the neural plate is also apposed to epidermis?

There are three possible explanations as to why no NC is generated from the ANF. First, NC inductive signals are present only in regions where NC is normally induced, but absent from the ANF or the adjacent epidermis (Fig. 1A). Second, posteriorizing signals cannot reach the anterior region of the embryo and thus the NC is not induced there (Fig. 1B). Recently, it has been shown that signals coming from the posterior region of the embryo, such as Wnts, Fgfs and retinoic acid, are required for NC induction (Villanueva et al., 2002). The activation of NC inductive pathways, such as Wnt or FGF, in the ANF leads to an expansion of NC markers in that region (Villanueva et al., 2002; Monsoro-Burq et al., 2003; Wu et al., 2005; Voigt and Papalopulu, 2006) supporting the notion that the absence of these inductive signals explains the lack of NC at the ANF. Nevertheless, these data have never been discussed in this context before. However, we have observed that anterior neural plate explants conjugated with anterior epidermis can interact and give rise to NC if they are isolated from the embryo (Mancilla and Mayor, 1996). This observation strongly suggests that there is a transient and early induction of NC at the ANF challenging the idea that all the required signals are never present in this region.

Here we propose a third explanation for the absence of NC in the ANF. We show the existence of a NC inhibitory mechanism at the anterior region of the embryo that precludes the NC development there (Fig. 1C). In addition, we identified the tissue that produces this negative signal and the inhibitory molecule secreted by this tissue. This is the first time that an inhibitory signal is described to control neural crest specification.

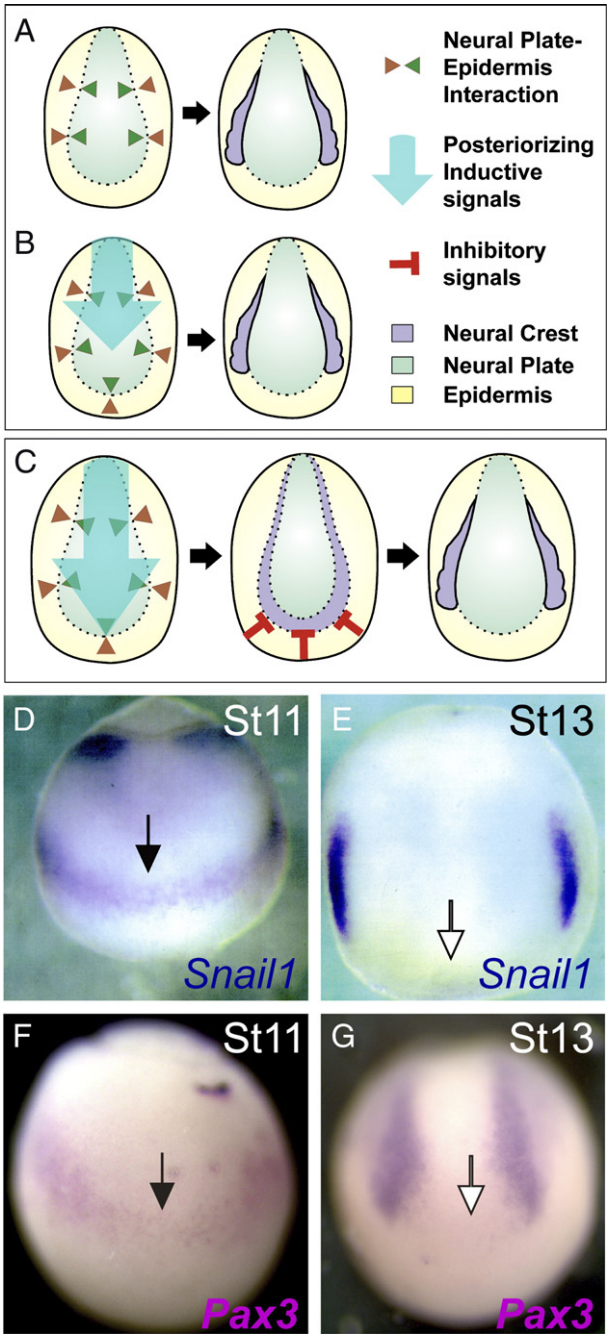

Fig. 1. Alternative models for the absence of NC at the ANF. (A, B) Current models. (A) The NC inductive signals (neural plate/epidermis interaction) are present only where the NC is induced and absent from the ANF. (B) Posteriorizing signals required to induce NC do not reach the ANF. (C) Proposed model: the NC inductive signals are present along the entire border of the neural plate and the NC is induced along the entire neural plate border, but at a later stage a specific NC inhibitory signal is produced at the ANF that restricts NC development to the lateral sides of the neural plate border. (D) Expression of *Snai1* at stage 11, showing expression at the ANF (arrow). (E) Expression of *Snail1* at stage 13, showing absence of expression at the ANF (arrow). (F) Expression of *Pax3* at stage 11, showing expression at the ANF (arrow). (G) Expression of *Pax3* at stage 13, showing absence of expression at the ANF (arrow).

Materials and methods

Micromanipulation, whole-mount in situ hybridization, DiI and cartilage staining

Dissections and grafts were performed as described by Mancilla and Mayor (1996). For in situ hybridization, antisense digoxigenin or fluorescein labeled RNA probes were used. Specimens were prepared, hybridized and stained using the method of (Harland, 1991), and NBT/BCIP or BCIP alone was used as a substrate for the alkaline phosphatase. The genes analyzed were for *Xenopus*: *Snail* (Mayor et al., 1993); *Snail2* (Mayor et al., 1995); *Wnt8* (Christian and Moon, 1993); *Bf1* (Hardcastle and Papalopulu, 2000); *Cpl1* (Richter et al., 1988); *Krox20* (Bradley et al., 1993), and *Otx2* (Pannese et al., 1995); for mouse: *Sox10* (Southard-Smith et al., 1998); for zebrafish: *FoxD3* (Kelsh et al., 2000); *Rx3* (Chuang et al., 1999). Proliferating cells were labeled with BrdU essentially as described by Hardcastle and Papalopulu (2000). To distinguish the injected from the control side of the embryos, we combined the BrdU immunohistochemistry with a second immunostaining against fluorescein used

as a lineage tracer. In these experiments the number of BrdU-positive cells in the injected side was compared with that of the uninjected control side. DiI labeling was performed at the neurula stage as described in Linker et al. (2000) and for cartilage staining an adaptation of the zebrafish protocol previously described was used (Barrallo-Gimeno et al., 2004). NC and ANF in vitro migration assays were performed as described before (De Calisto et al., 2005).

RNA synthesis in vitro, microinjection of mRNAs or morpholino oligonucleotides and dexamethasone activation

All plasmids were linearized and transcribed as described (Harland and Weintraub, 1985), using SP6 or T7 RNA polymerases, and the GTP cap analogue (New England Biolabs). The RNA was co-injected with FLDx (fluorescein dextran; Molecular Probes) or *β-gal* mRNA using 8–12 nl needles into 2- or 8-cell embryos, or at the D1.1 blastomere of 16-cell and A1 of 32-cell embryos as described before (Aybar et al., 2003). The constructs used were: *Dkk1* (Glinka et al., 1998), *β-catenin-GR* (Domingos et al., 2001), *Wnt8* (Christian et al., 1991), *Crescent* (Pera and De Robertis, 2000) and *Cerberus* (Bouwmeester et al., 1996). Treatment with dexamethasone was performed as we described previously (Tribulo et al., 2003). *Tcf3a* morpholino was used as described before (Kim et al., 2000).

Dkk1 protein and antibody treatment

Heparin coated acrylic beads (Sigma) were incubated overnight with 40 μg/ml of Dkk1 protein (Dkk1 human recombinant, Calbiochem) or BSA as controls and grafted into embryos at the appropriate stage. The Dkk1 antibody was injected into the blastocoel cavity as described in Kazanskaya et al. (2000). Treatment of explants with Dkk1 was performed as described in Kazanskaya et al. (2000).

Results

Inhibition of NC at the ANF by the prechordal mesoderm

We hypothesize that the absence of NC from the ANF is due to an inhibitory mechanism that restricts them only to the lateral border of the neural plate. As a first approach to test this idea, we analyzed the expression of the earliest NC-specific genes *Snail1* and *Pax3*. Surprisingly, an undescribed early expression at the ANF was found at the beginning of gastrulation (Figs. 1D, F). This expression was lost by the end of gastrulation (Figs. 1E, G) when these markers were restricted to the lateral border of the neural plate.

To test whether neural crest development is actively inhibited at the ANF or not, we grafted NC from embryos at different neurulation stages into the ANF region of stage 14 host embryos and analyzed them at late neurula stage by in situ hybridization (Fig. 2A). These NC explants were already specified as NC as they maintained the expression of NC-specific genes (such as *Snail2*) when cultured alone (60/60; Fig. 2B). Surprisingly, when these NC explants from early neurula stage embryos were grafted in the ANF of the host, the NC-specific gene expression was completely lost (48/48; Figs. 2C, D). If the same experiment is repeated but with NC taken from later embryos, the ability of the anterior portion of the embryo to inhibit NC was gradually decreased and lost at stage 17 (Fig. 3D, black bar). This inhibitory effect was due the existence of an active mechanism located specifically at the anterior region of the embryo because no NC inhibition was observed on explants of any stage when grafted on other parts of the embryo (10/10; Fig. 2E).

Then we decided to identify the tissue responsible of this NC inhibition. Two main tissues are close to the ANF at the early neurula stage, the prechordal mesoderm (PM) and the anterior ectoderm (AE). Therefore, we decided to graft explants of these tissues laterally to normal crests and analyzed if they were able to inhibit NC (Fig. 2F). When pieces of AE were grafted near the NC, no effect on *Snail2* or other NC-specific genes was observed (24/24; Fig. 2G). On the contrary, a strong inhibition of *Snail2* was observed when pieces of PM were grafted near the crest region, (27/35; Fig. 2H). To confirm this, we conjugated specified NC explants with pieces of AE or PM, both from early neurula embryos. The conjugates were cultured until the equivalent of late neurula stage and then analyzed by in situ hybridization (Fig. 2I). Similarly to the previous experiment, when NC explants were conjugated with pieces of AE, no *Snail2* inhibition was observed (23/23; Fig. 2J); however, when a similar NC explant was co-cultured with PM, a strong inhibition of *Snail2* was observed (30/38; Fig. 2K). These results also show that the PM is sufficient to restrict NC development.

Altogether, these results reveal the existence of a previously unidentified signal of NC inhibition at the anterior region of the embryo. This signal is likely to be produced by the PM as this structure is sufficient to inhibit NC development.

Dkk1 is an inhibitor of NC induction at the ANF

Next we tried to identify the signaling molecule involved in this inhibition. We developed an in vitro assay to test the ability of candidate molecules to inhibit NC development. We screened candidate molecules for the following criteria: to be expressed in the prechordal mesoderm and to be a secreted molecule related to the known signaling pathways in NC induction. mRNA encoding the molecule of interest was injected at the one-cell stage. The embryos were cultured until blastula stage, when animal caps were dissected and conjugated with NC taken from early neurula stage embryos (stage 15). After culture, the expression of the NC marker *Snail2* was analyzed (Fig. 3A). Control caps injected with FLDx alone did not have the ability to inhibit *Snail2* expression in NC explants (67/67; Fig. 3B). Nevertheless, caps injected with the canonical Wnt/β-catenin antagonist Dickkopf1 (Dkk1, Glinka et al., 1998) completely abolished *Snail2* expression in conjugated NC explants (51/51; Fig. 3C). NC conjugates with animal caps expressing other PM molecules showed inconclusive results or no effect (noggin, chordin, BMP4, Cyp26, Raldh2, Sprouty and Spred, data not shown).

As we observed that grafts of late neurula NC were not inhibited as much as early neurula NC, we decided to test if something similar happened with the response of NC to Dkk1. Consequently, we conjugated Dkk1 expressing animal caps with NC coming from embryos at different stages (form stage 13 to 17). *Snail2* expression was analyzed by in situ hybridization. Interestingly, the NC response in the in vivo experiments (Fig. 2A) and in vitro experiments with Dkk1 (Fig. 3A) showed a very similar kinetic, i.e. strong *Snail2* inhibition at early neurula and low or no effect later in development. Fig. 3D summarizes the results of both experiments.

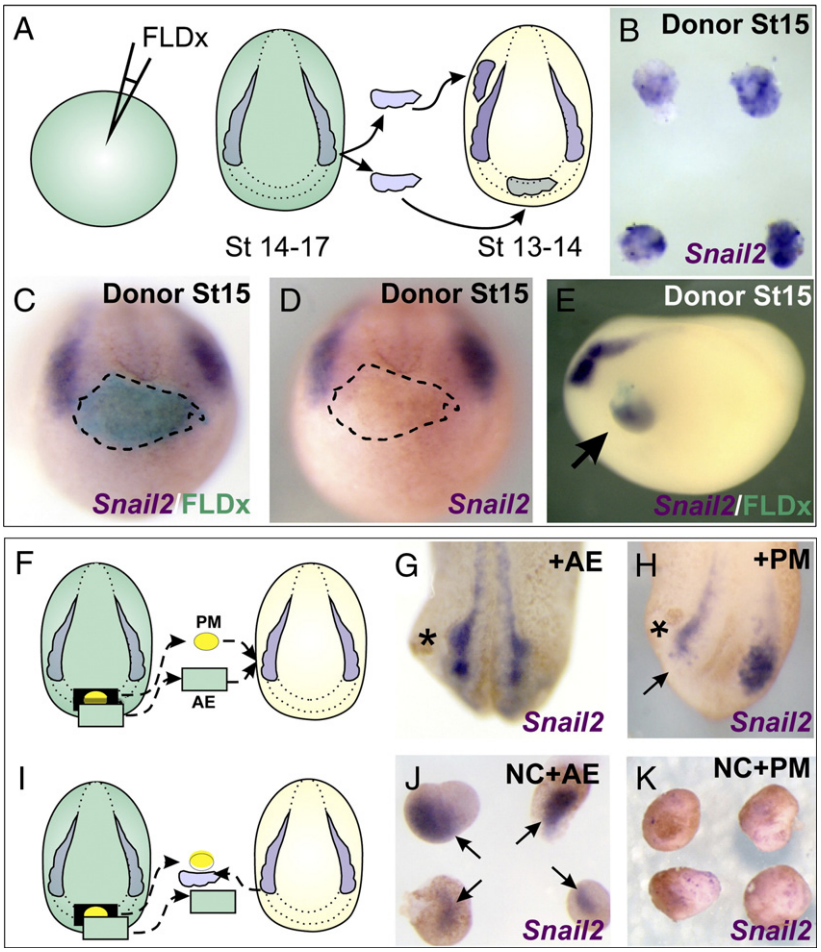

Fig. 2. The NC is inhibited at the ANF by the PM. (A–G) Inhibition of NC induction at the ANF. (A) Embryos were injected at the 1-cell stage with FLDX, at stages 14–18 the NC were dissected and grafted into the ANF, or lateral epidermis of a stage 13/14 control embryos, or cultured in vitro until stage 18/19, when the expression of *Snail2* was analyzed. (B) NC dissected at stage 15 and cultured in vitro until stage 18 showing expression of *Snail2* ($n=60$, 100% of expression). (C) Anterior view of an embryo containing a graft of stage 15 NC as described. Dotted line shows the green color of the FLDx graft. (D) Same embryo as in C, showing the absence of *Snail2* in the graft (dotted line). (E) Lateral view of an embryo in which NC taken from a stage 15 embryo was grafted in lateral epidermis, showing expression of *Snail2* in the graft. Approximately 50 embryos were analyzed for each case. (F–K) PM inhibits NC induction. (F) Anterior ectoderm (AE, green square) or prechordal mesoderm (PM, yellow circle) was dissected from a stage 15 embryo and grafted next to the NC from a control embryo, after culture until stage 18, the expression of *Snail2* was analyzed. (G) No effect on *Snail2* expression was observed with the AE graft. Asterisk: graft, $n=24$, 100% of expression. (H) Inhibition of *Snail2* expression with PM graft. Asterisk: graft, $n=35$; 78% of grafted embryos exhibited inhibition of *Snail2* expression. (I) PM and NC were dissected from stage 15 embryos, conjugated in vitro and the expression of *Snail2* was analyzed at the equivalent of stage 18. (J) NC cultured in vitro showing normal expression of *Snail2* (arrow); $n=23$; 100% of expression. (K) Conjugate of NC and PM showing inhibition of *Snail2* expression; $n=38$, 80% of conjugates with inhibition of *Snail2* expression.

To confirm that Dkk1 can indeed inhibit NC induction in vivo, we soaked heparin beads either in a human Dkk1 recombinant protein solution or in BSA as a control and then grafted them next to the NC of an early neurula embryo (Fig. 3E). As expected, beads soaked in BSA did not affect NC induction (20/20; Fig. 3F), while Dkk1 was a clear inhibitor of *Snail2* (13/14; Fig. 3G).

Dkk1 is expressed in the prechordal (head) mesoderm of other vertebrates such as mouse (Glinka et al., 1998) and zebrafish (Caneparo et al., 2007). If Dkk1 acts as an NC inhibitor, we expected that its expression should be complementary to the expression of NC markers. This was indeed the case when the expression of *Pax3* was compared to the *Dkk1* expression (Figs. 3H–M). Interestingly before *Pax3* expression was precluded from the ANF (stage 11, Fig. 3H), *Dkk1* expression had not yet reached the anterior region (Figs. 3I, J). On the contrary, at stage 13 the expression of *Dkk1* (Fig. 3L) correlated perfectly with the absence of *Pax3* in the ANF (Figs. 3K, M). Taken together, these results show that *Dkk1* is sufficient to inhibit NC induction and its expression pattern makes it a good candidate to be the signal that limits the anterior edge of the NC.

Dkk1 loss of function is sufficient to transform the ANF into NC

Although we have demonstrated that Dkk1 can inhibit NC in vitro and in vivo, we have not shown whether this is the actual mechanism of precluding NC from the ANF. To address this issue, we performed some Dkk1 loss-of-function experiments. First, in *Xenopus* embryos, we injected an antibody against Dkk1, which has been characterized as a specific inhibitor of

Dkk1 activity, into the blastocoel (Kazanskaya et al., 2000). Embryos injected with a control antibody never expressed *Snail2* at the ANF (0/40; Fig. 4A), while embryos injected with Dkk1 antibody showed strong expression of NC-specific genes in the entire ANF (52/82; Fig. 4B, black arrow). In addition, we were able to block the inhibitory activity of Dkk1 in vitro. Stage 15 NC was conjugated with PM that has already been specified (stage 15) and the expression of NC markers analyzed at stage 20, as described in Fig. 2I. As expected, no conjugate cultured in control media expressed *Snail2* (0/7, Fig. 4C). However, when conjugates were cultured in a media containing the Dkk1 antibody, most of them showed a strong *Snail2* expression (6/8, Fig. 4D). This shows that the PM is inhibiting NC via Dkk1.

Finally, the expression of the NC marker *Sox10* was analyzed in *Dkk1* null mutant mouse embryos (Mukhopadhyay et al., 2001). This mutation displays defects in forebrain development but NC markers have not been analyzed. Wild type (*Dkk1*+/+) embryos show the characteristic absence of *Sox10* expression in the ANF (arrow, Fig. 4E), while homozygous mutants (Dkk1−/−) exhibit a strong expression of *Sox10* in the ANF (10/12; Fig. 4F), similar to the phenotype observed in *Xenopus* embryos injected with anti-Dkk antibody (Fig. 4B). These experiments indicate that Dkk1 activity is not only sufficient to inhibit NC but also required to preclude NC from the ANF.

As Dkk1 is known to work as a Wnt inhibitor (Glinka et al., 1998) we tested whether a similar transformation of the ANF into NC could be achieved by activation of the Wnt pathway. In *Xenopus*, we restricted the effect by injecting mRNA coding elements of the Wnt pathway in the A1 blastomere of a 32-cell morula, which is fated to form the ANF (Fig. 5A). Accordingly with our prediction, the injection of Wnt8 mRNA provoked a complete transformation of the ANF into a tissue expressing NC-specific genes like *Snail2* (28/50; Figs. 5C, D). This effect is notoriously similar to the Dkk1 inmunodepletion effect (Fig. 4B). Because Wnt8 is a diffusible molecule the effect was not only restricted to the injected cells but to all the cells at the ANF (Fig. 5D). This is an interesting observation because it shows that only the neural plate border can transform its fate to NC in response to this treatment. Nonetheless, this diffusible feature of Wnt8 opens the possibility to explain this transformation as an indirect phenotype caused by the effect on other regions like the mesoderm. To exclude this possibility we repeated the same experiment but this time injecting mRNA coding β-catenin, an intracellular component of this pathway. As shown in Figs. 5E and F, a similar transformation of the ANF occurs but in this case it is restricted only to the injected cells present at the neural plate border demonstrating that it is a cell autonomous effect (33/49).

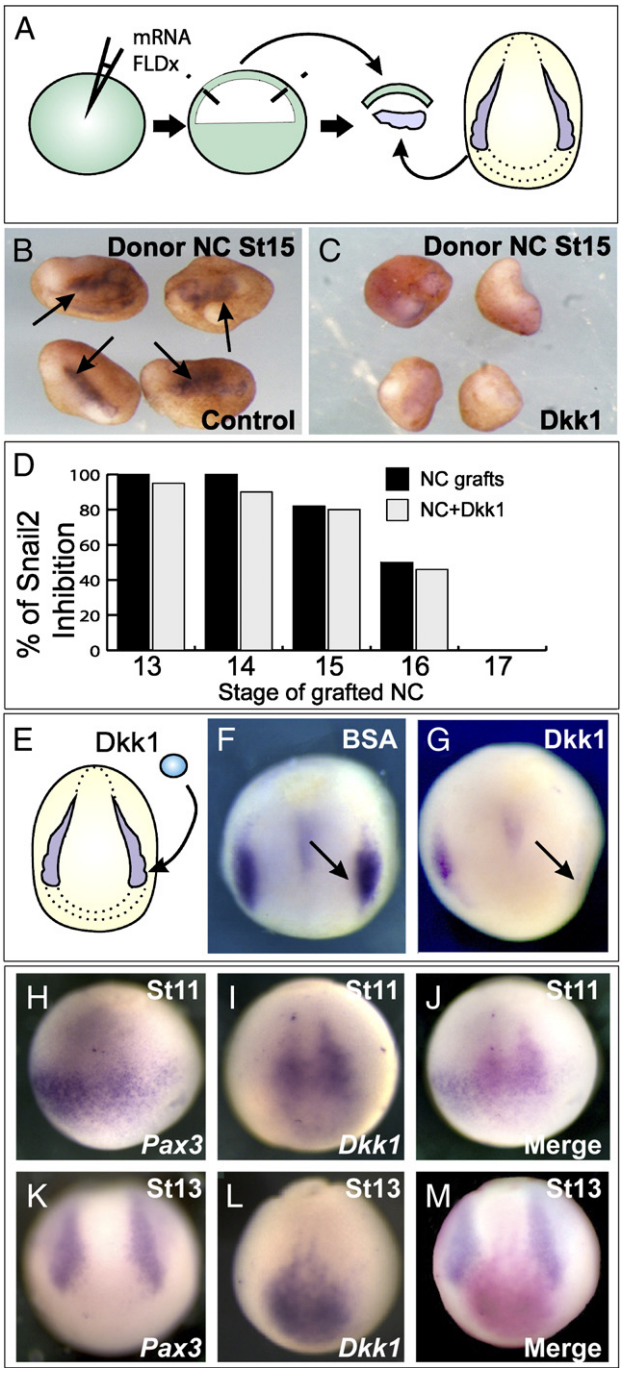

Fig. 3. Assay to identify NC inhibitors in vitro. (A) Embryos were injected at the 1-cell stage with mRNA coding for the tested molecules, at stage 9 animal caps were dissected and conjugated with NC taken from stages 13–17 control embryo; the expression of *Snail2* was analyzed. (B) Stage 15 NC conjugated with control animal caps shows normal *Snail2* expression; $n=67$, 100% of expression. (C) Stage 15 NC conjugated with AC expressing Dkk1 shows absence of *Snail2* expression. (D) Summary of expression of *Snail2* in grafts into the ANF of NC taken from embryos at different stages (as described in Fig. 2A; black bars) and Dkk1 expressing animal caps (as described in panel A; light gray bars). Note a similar trend on NC inhibition in the graft and in the Dkk1 conjugates. Approximately 50 embryos were analyzed for each stage. (E) Beads soaked with BSA or Dkk1 protein were grafted next to the NC of a stage 15 embryo. (F) Control bead soaked with BSA (arrow) shows no effect on *Snail2* expression; $n=20$, 100% of expression. (G) Bead soaked with Dkk1 shows inhibition of *Snail2* expression; $n=14$, 92% of inhibition. (H–M) Analysis of *Pax3* and *Dkk1* expression. (H) Expression of *Pax3* in a stage 11 embryo. (I) Expression of *Dkk1* in stage 11 embryo. (J) Overlapping of pictures shown in panels I and J after artificial color change. (K) Expression of *Pax3* in a stage 13 embryo. (L) Expression of *Dkk1* in stage 13 embryo. (M) Overlapping of pictures shown in panels K and L after artificial color change. Note the correlation between *Dkk1* expression and *Pax3* restriction.

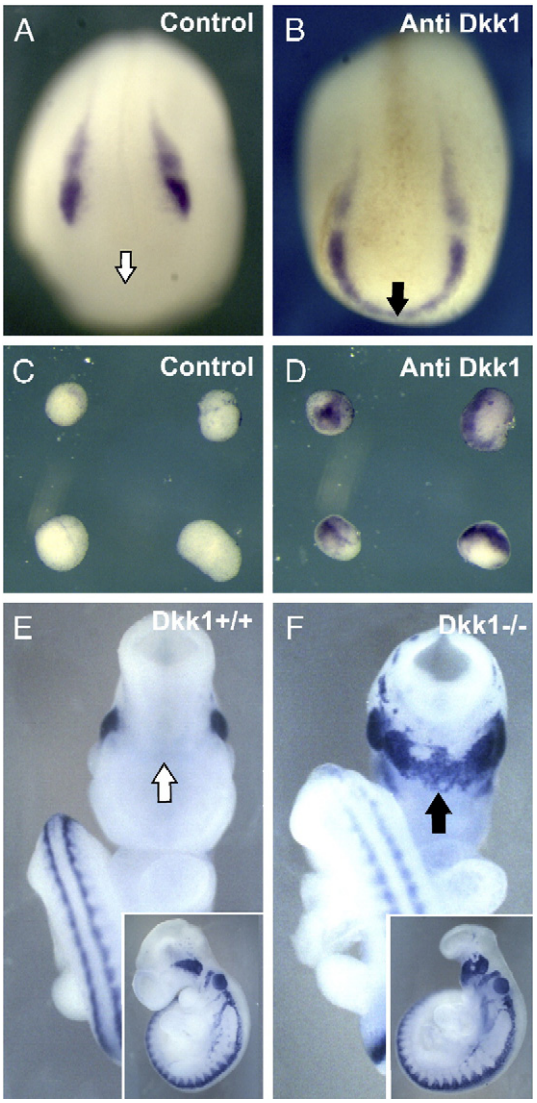

Fig. 4. Dkk1 is essential for NC inhibition at the ANF. (A–D) Effect on *Xenopus*. Embryos are shown in dorso-anterior view. (A) Embryo injected at the blastula stage with an anti-prolactin antibody as control, it shows absence of *Snail2* expression at the ANF (arrow); $n=40$, 0% of expression at the ANF. (B) Embryo injected at the blastula stage with anti-Dkk1 antibody showing *Snail2* expression at the ANF (arrow); $n=86$, 60% of expression. (C) Control NC/PM conjugates (0% of *Snail2* expression, $n=7$). (D) NC/PM conjugates cultured with the anti-Dkk1 antibody (75% *Snail2* of expression, $n=8$). (E, F) Effect on mouse. (E) Anterior view of wild type mouse embryo (E9.5) showing normal expression of *Sox10*, and no expression at the ANF (arrow). Inset: lateral view of the same embryo. (F) Anterior view of Dkk1 mutant mouse embryo (E9.5) showing expression of *Sox10* at the ANF (arrow). Inset: lateral view of the same embryo; $n=12$, 83% of embryos showing expression of *Sox10* at the ANF. Note that the expression of *Sox10* is normal in the midbrain, hindbrain and trunk NC, suggesting more NC rather than a truncation.

We wanted to further corroborate the epistasic relationship between Dkk1 and the canonical Wnt pathway in establishing the limits of the NC. For that, we injected zebrafish embryos with morpholino oligonucleotides that specifically block the translation of *Tcf3a* (*Tcf3aMO*). This treatment has been shown to activate Wnt signaling in the anterior region of the embryo (Kim et al., 2000). As expected, an equivalent transformation of ANF into NC was produced in the injected embryos (Fig. 5H), which is never observed in control embryos (Fig. 5G). Taken together, we have shown that these three different treatments that activate Wnt signaling lead to the same transformation of the ANF into NC, suggesting that Dkk1 works as a Wnt inhibitor in the process precluding NC induction at the ANF.

Temporal analysis of ANF transformation into NC

Is it possible to dissociate the ANF transformation from other processes like the NC expansion observed in other reports where Wnt activity was also increased? (Saint-Jeannet et al., 1997; LaBonne and Bronner-Fraser, 1998). This expansion is different from the Dkk1 loss-of-function effect where the ANF cells were transformed but no border expansion was observed along the medio-lateral axis (Fig. 4B). Although we could phenocopy this effect by increasing Wnt activity (Figs. 5C–H, 6A), we observed some embryos showing a medio-lateral expansion accompanying the transformation (Fig. 6B). Note that in the embryo with the transformation, the NC looks normal lateral to the plate; but in the embryo with the expansion the NC is affected laterally to the neural plate as much as it is frontally to the neural plate (Figs. 6A, B). We thought it might be possible to separate these two effects by modulating either the time or level of β-catenin activity. To manipulate the timing, we used an inducible β-catenin construct in which the time of activation could be controlled (Domingos et al., 2001). Different doses of this construct were injected in A1 blastomere and the embryos were analyzed after activation of β-catenin at different stages (Fig. 6C). Embryos injected with the same dose of β-catenin but activated at different times clearly showed differences on the penetrance of the two phenotypes (Fig. 6D). Embryos in which the β-catenin was activated at stage 9 showed less transformation than the embryos in which the β-catenin construct was activated between stage 10 and 12 (Fig. 6D). On the contrary, the expansion phenotype was favored when β-catenin was activated at the earliest stages and decreased later (Fig. 6D, inset).

Interestingly, when we tried injecting different doses of β-catenin, we found that even when activated at stages where the transformation effect was predominant (stages 10–11, Fig. 6D) it was possible to get a dominance of the expansion phenotype if the dose was increased enough (inset in Fig. 6E). These results show that it is possible to phenocopy the Dkk1 loss-of-function phenotype by locally increasing Wnt activity. In addition, they show that is possible to dissect it from other Wnt-dependent effects like the previously described NC expansion. These results show the importance of the time, space and dose control in order to get a clean transformation, and they suggest that the NC inhibition at the ANF takes place slightly later than the process of NC induction.

Transformation of ANF into NC by Wnt activation is not dependent on anterior–posterior (AP) patterning of the neural plate or inhibition of placodal fates

A possible alternative explanation of this transformation of the ANF into NC is that there is a truncation of the anterior neural plate produced by a general disruption of the anterior–

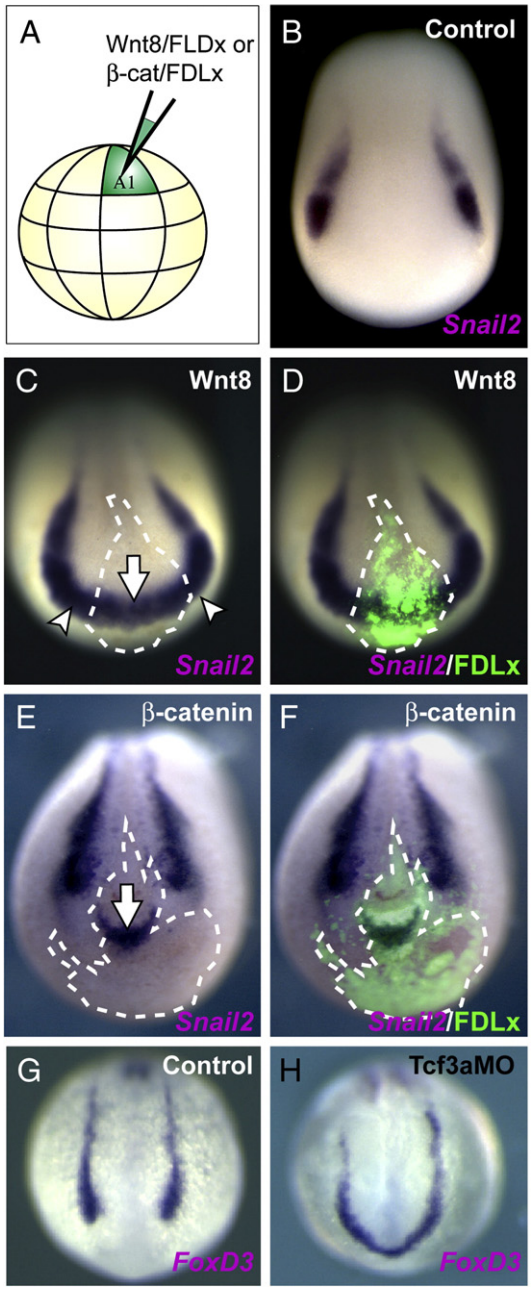

Fig. 5. Activation of Wnt signaling leads to transformation of ANF into NC. (A–F) Effect on *Xenopus*. Embryos are shown in dorso-anterior view. (A) Diagram showing where the injections were performed. (B) Control embryo showing normal *Snail2* expression. (C, D) Embryos injected with 2 ng of Wnt8 mRNA and FLDx into A1 blastomere of a 32-cell stage embryo. Green cells in panel D correspond to the injected cells, which are indicated by the dotted line in panels C and D. Note expression of *Snail2* in all the ANF (arrows and arrowheads); $n=50$, 55% of embryos showing ectopic *Snail2* expression. (E, F) Embryos injected with 130 pg of β-catenin-GR mRNA and FLDx into A1 blastomere of a 32-cell stage embryo, induced at stage 10.5. Green cells in F correspond to the injected cells which are indicated by the dotted line in E. Note expression of *Snail2* at the ANF but this time restricted to the injected cells (arrow); $n=67$, 56% of embryos showing ectopic *Snail2* expression. (G, H) Zebrafish embryos showing expression of *Foxd3*. (G) Control embryo. (H) Embryo injected with 0.01 pmol of *Tcf3a* MO.

posterior (AP) axis. As a result of the absence of anterior structures, the more posterior and lateral regions could be fused, including the two lateral domains of the NC. That would mean that there is an abolition of the ANF rather than a transformation. To address this possibility we analyzed the transformation of the ANF into NC under very controlled conditions of space, time and levels of Wnt signaling. We used the conditions that favored the transformation phenotype (130 pg of β-catenin mRNA and activation at stage 10.5, see Fig. 6) and analyzed the expression of anterior–posterior neural plate and placodal markers. No shift in the expression of the AP markers *Krox20* (2/40) or *Otx2* (10/45) was observed (Figs. 7A, B), suggesting that the general AP pattern of the neural plate was not affected. Nevertheless, this does not rule out the possibility of the anterior truncation as more anterior regions of the neural plate could be absent. Therefore, we analyzed the expression of the most anterior markers *Bf1* and *Cpl1* under the same conditions and found that they are not affected (5/41, 10/42; Figs. 7C, D). Interestingly, when we injected higher concentrations of β-catenin an effect on the AP markers was observed (Fig. S1A) as has been reported elsewhere (Braun et al., 2003; Kiecker and Niehrs, 2001; McGrew et al., 1997; Erter et al., 2001, Itoh and Sokol, 1997; Niehrs, 2001; Nordstrom et al., 2002). Under conditions where the *Tcf3a*MO can produce the transformation of ANF into NC in zebrafish embryos, (Figs. 7E, F), no effect was observed on the expression of the anterior neural plate marker *Rx3* (30/40; Figs. 7G, H). Of note, this effect was achieved by standardizing the concentrations in a similar way to the one described above for *Xenopus* experiments; if higher levels of *Tcf3a*MO are injected, an inhibition of *Rx3* was observed confirming previous observations (Figs. S1C, D; Kim et al., 2000).

Another possible tissue that could be affected by the transformation of the ANF into NC is the preplacode field, as it has been shown that inhibition of Wnt signaling is required for its specification (Brugmann et al., 2004; Litsiou et al., 2005). When the preplacodal-specific gene *Six1* (23/48; Fig. 7I) and the preplacodal domain of *Sox3* (20/45; Figs. 7J, K) were analyzed, a marked anterior–ventral shift was observed (compare the white lines in the control and injected side in Figs. 7I, K); however the level of placodal marker expression was hardly affected. When higher levels of Wnt activity were used preplacodal markers were usually inhibited (Fig. S1B). Taken together, these results show that the transformation of the ANF into NC is not an indirect effect of an anterior truncation of the embryo. In addition, they indicate that this transformation can be at least experimentally dissociated from the general AP patterning of the embryo; however, this does not mean that they work as two different processes in a normal embryo.

Importantly, we are not affecting the development or migration of the prechordal mesoderm as injected embryos show normal Dkk1 expression (36/40; Fig. 7L). This is an important control because, as we have shown here, the prechordal mesoderm contains the inhibitory signals that preclude the expression of NC markers from the ANF. A schematic representation of the effect of these experiments on the ectoderm is displayed in Fig. 7M.

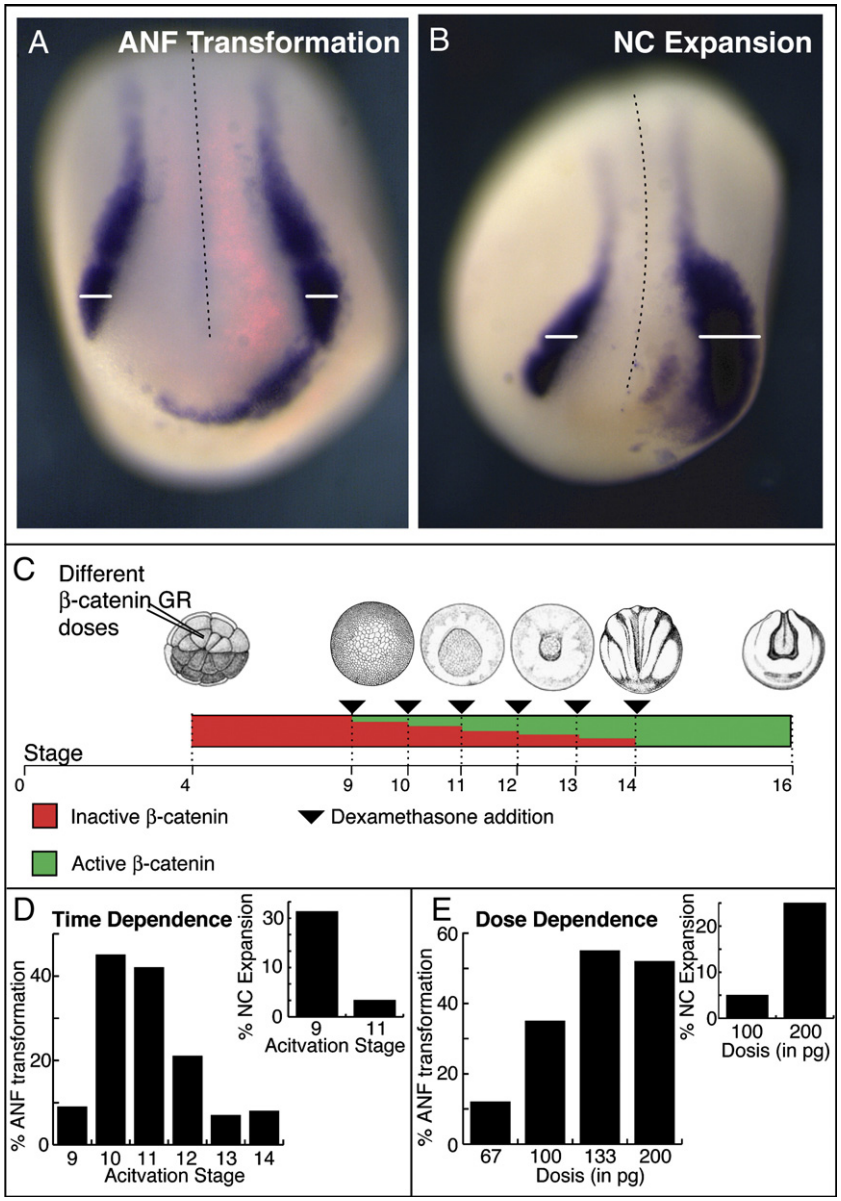

Fig. 6. Temporal analysis of transformation of ANF into NC. (A) Representative embryo showing transformation phenotype monitored by the expression of the NC-specific gene *Snail2*. Note the transformation of the ANF into NC with almost no effect in the medio-lateral axis. (B) Representative embryo showing the expansion phenotype monitored by the expression of *Snail2*. Note that the expansion of the NC is as much in the anterior–posterior axis as it is in the medio-lateral axis. (C) Diagram to show the experimental design used in panels D and E. Embryos were injected with different doses of β-catenin-GR mRNA at the 32-cell stage and treated with dexamethasone at different stages (green bar), the expression of NC markers was analyzed at stage 16. (D) Analysis of the ANF transformation phenotype and NC expansion phenotype (inset) after injection of 100 pg of β-catenin-GR and activation at different stages. Note that the highest ANF transformation is reached with activation at stage 10–11 while the highest NC expansion phenotype is reached with activation at stage 9. (E) Analysis of the ANF transformation phenotype and NC expansion phenotype (inset) after injection of different doses of β-catenin and activation at stage 11. Note that the higher doses of β-catenin can still induce NC expansion at later stages (inset).

According to these results, the ectopic induction of NC is not at expenses of anterior neural tissue or placodes. Because usually the injected embryos have a thicker ectoderm, we hypothesized that this could be due to an increase in cell number. To test this, we analyzed the levels of cell proliferation on β-catenin injected embryo by BrdU staining. A significant increase ($p<0.05$) on the number of BrdU-positive nuclei was observed in injected regions (Figs. 7N, O). This difference was most obvious in the ANF region (Fig. 7N, black arrowhead). These experiments suggest that, in parallel to the ANF transformation, the activation of the Wnt signaling might increase the cell number by promoting proliferation. This can account for the coexistence of NC and other populations on the transformed ANF.

NC cells induced at the ANF are able to migrate and differentiate as normal NC cells

It is possible that some treatments can transiently change the expression profile of a cell population without changing its fate and behavior at later stages. Can NC cells induced at the ANF by

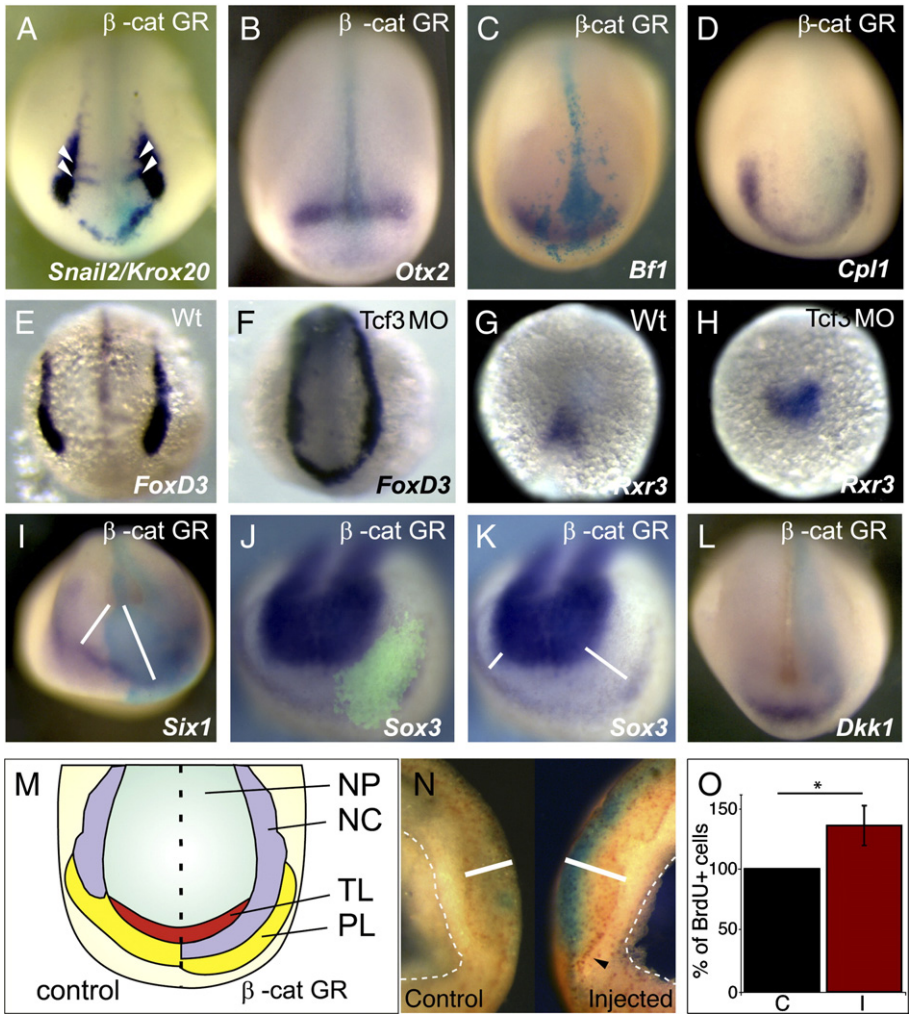

Fig. 7. Analysis of neural plate and placodal markers in embryos with NC at the ANF. (A–D, I–L) *Xenopus* embryos were injected with 130 pg of β-catenin mRNA in A1 blastomere at 32-cell stage, treated with dexamethasone at stage 10.5, and the expression of different markers was analyzed at stage 16. All embryos are shown in anterior views; injected side is to the right and recognized by FLDx or β-gal staining (blue color). (A) *Snail2*/*Krox20*. Note expression of *Snail2* (52%, $n=50$) at the ANF and normal expression of *Krox20* (white arrowheads, 95%, $n=40$). (B) *Otx2*. Note no effect on *Otx2* in the injected side (23%, $n=45$). (C) *Bf1*. No effect on *Bf1* at the injected side (12%, $n=41$). (D) *Cpl1*. No effect on *Cpl1* at the injected side (17%, $n=42$). (E, F) Zebrafish embryos. (E) Wild type embryos showing expression of *FoxD3*. (F) Embryo injected with 0.01 pmol of Tcf3a MO. Note the expression of *FoxD3* at the ANF (100%, $n=50$). (G, H) Sibling embryos of panels E and F, respectively analyzed for *Rxr3* expression. Note the normal expression of *Rxr3* in wild type and injected embryo (75%, $n=40$). (I–L) Placodal markers. White lines indicate the distance between the neural grove or neural plate and the placodal markers. (I) *Six1* expression. Note the anterior–ventral shift in the expression of *Six1* at the injected side (47%, $n=48$). (J, K) *Sox3* expression. Note the shift in the preplacodal domain of *Sox3* expression (45%, $n=45$), while the neural plate domain is not affected. (L) Dkk1 expression; note similar expression in the injected and uninjected side (99%, $n=40$). (M) Summary of anterior markers. NP: neural plate; NC: neural crest; TL: telencephalon; PL: placodal field. (N) BrdU staining. Left: control side; right: injected side. Bar indicates the thickness of the ectoderm which is higher in the injected side; black arrowhead shows the ANF where there is a particularly higher number of stained nuclei in the injected side. (O) Summary of BrdU staining. BrdU-positive nuclei in the injected ectoderm compared with the ones on the contralateral uninjected region.

inhibition of Dkk1 or activation of Wnt behave like normal NC cells? The most prominent characteristics of NC cells are their abilities to migrate and to differentiate into derivatives such as melanocytes, cartilaginous and bony elements in the head, among others. To test whether the ectopically induced NC cells are able to migrate, β-catenin mRNA was co-injected with nuclear GFP under conditions that induce ectopic expression of NC markers in the ANF. At the neurula stage (stage 16) the ANF was labeled with DiI on both the injected and control side (Fig. 8A). The embryos were cultured and cell migration was analyzed by looking at the DiI fluorescence. Immediately after DiI labeling the fluorescence was similar in the control and β-catenin injected sides (Fig. 8B). In the control side at the late neurula stage the DiI labeling remains in the anterior region of the head (Fig. 8D), while the β-catenin injected cells have moved backwards (Fig. 8C, black arrowhead) and start to migrate, joining the normal streams of NC cells (Fig. 8E). This observation shows not only that the NC cells are able to migrate but also that they are able to follow the NC in their normal migratory pathway. In some few cases the ectopically induced NC cells migrated in the head region and did not join the endogenous, more caudal, NC. A second experiment was performed to show the migratory ability of the induced NC cells. When normal NC cells are cultured on fibronectin they are able

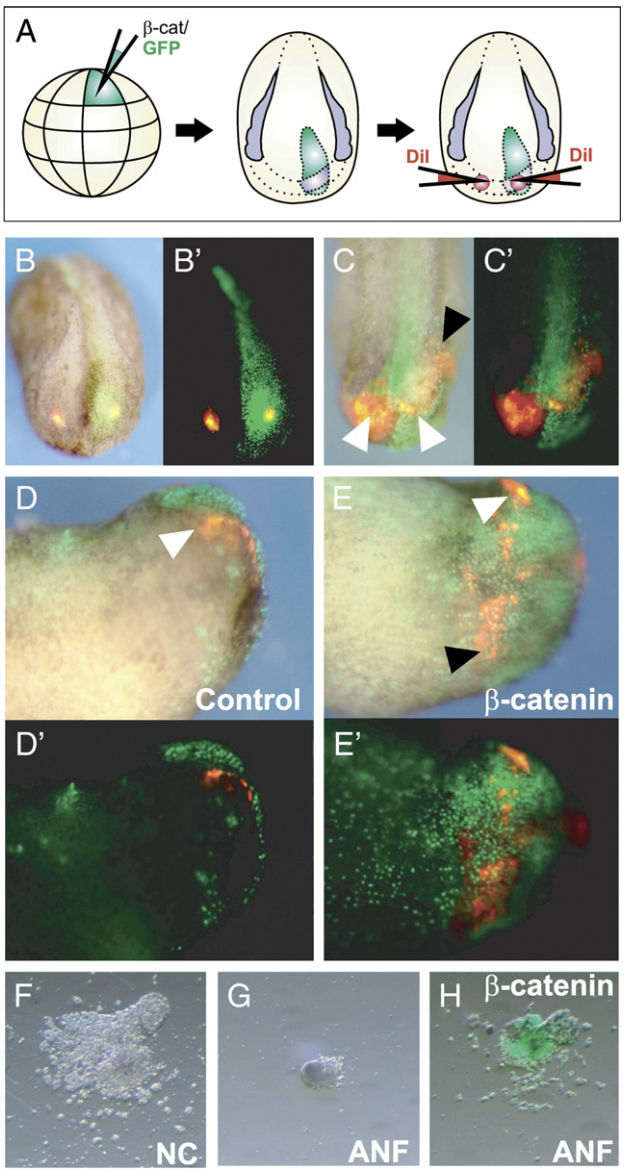

Fig. 8. NC induced at the ANF is able to migrate. (A) Embryos were injected with β-catenin-GR and nuclear GFP in A1 blastomere at 32-cell stage and activated at stage 10.5. At stage 16 symmetrical points at the injected and uninjected ANF were DiI labeled, the embryos were cultured until stage 28, when the migration of the DiI labeled cells was analyzed. (B) Dorso-anterior view of an embryo immediately after the DiI labeling; note the symmetric distribution of both DiI spots and that one overlaps with the GFP. (C) Dorso-anterior view of an embryo at stage 25. Note that both DiI spots have enlarged, but the one that overlaps with GFP has moved backwards and has started to move ventrally (black arrowhead); white arrowhead: initial position of DiI. (D, D′) Control side of a stage 28 embryo, showing a small expansion of the DiI label but no ventral migration; $n=24$, 0% of embryos with migration. (E, E′) Injected side of a stage 28 embryo, showing ventral migration of the DiI labeled cells; $n=24$, 79% of embryo with migration. (F) Control NC was dissected from a stage 15 embryo and cultured on fibronectin for 16 h. Note the migration of NC cells; $n=5$, 100% of migration. (G) ANF dissected from a stage 15 embryo and cultured on fibronectin for 16 h. No migration is observed, $n=5$, 0% migration. (H) ANF dissected from a stage 15 embryo, previously injected with β-catenin into the ANF region. Note the migration of the cells similar to the NC cells; $n=5$, 100% of migration.

to migrate in vitro (Fig. 8F; Alfandari et al., 2003); as expected, cells from the ANF cultured under the same conditions are never able to migrate (Fig. 8G). However, an equivalent ANF taken from an embryo injected with β-catenin under the previous conditions shows migratory activity undistinguishable from normal NC cells, indicating that this is a cell autonomous property (Fig. 8H). In conclusion, the ANF that expresses NC markers is able to migrate in vivo and in vitro as normal NC cells.

A second characteristic of the NC is its ability to differentiate into specific cell types. When embryos injected with β-catenin were left to develop at later stages several NC derivatives were increased or in some case ectopic NC derivatives were observed. Meckel, ceratohyal and ceratobranchial cartilage were expanded in β-catenin injected embryos (Figs. 9A–D); melanocytes were more numerous in the head and sometimes produced a completely black head (Figs. 9E, F). The dorsal fin which in control embryos ends up at the posterior limit of the head (Fig. 9G, arrowhead) was usually extended to the most anterior tip of the head (Fig. 9H, arrow), and sometime ectopic fin-like structures were observed in the head (not shown). Very frequently we observed gill-like structures, which are present only in the branchial arches region of control embryos (Figs. 9I, J), also in the anterior region of the head in the injected embryos (Figs. 9K, L). We should mention that cephalic cartilage and melanocytes are clearly NC derivatives, while dorsal fin and gill are not only NC derived. Taken together, these observations show that the NC induced at the ANF behave as normal cranial NC cells in their migratory and differentiation potential.

Discussion

Fate map studies show that NC originated from the neural plate border except from the most anterior neural fold (Couly and Le Douarin, 1985; Couly et al., 1993). The expression pattern of NC markers (*Snail2*, *Snail*, *FoxD3*, etc.) also supports this conclusion (Essex et al., 1993; Mayor et al., 1995; Sasai et al., 2001; Schlosser and Ahrens, 2004). These studies revealed that the ANF contributes to the forebrain and some placodal cells. However, it was not known by which mechanism the ANF is deprived of NC. Here we present evidence that an active inhibition of NC cells takes place at the ANF. First, grafts of NC into the ANF prevent them from expressing NC markers, which are otherwise expressed when they are cultured in vitro (Fig. 2); second, juxtaposition of NC with prechordal mesoderm (PM) is sufficient to inhibit NC formation (Fig. 2); third, Dkk1, which is produced by the PM, can mimic this NC inhibition (Fig. 3). Finally, loss-of-function experiments of Dkk1, using a functional blocking antibody in *Xenopus* or a *Dkk1* null mouse mutant, transform the ANF into NC (Fig. 4). To our knowledge, this is the first time that an inhibitory signal has been implicated in NC formation.

As shown in transplant experiments (Fig. 2), the highest level of NC inhibition is reached with NC at stage 14 or younger, while hardly any inhibition can be obtained after stage 17. This timing of NC inhibition in vivo is similar to the inhibition seen when using Dkk1 mRNA (Fig. 3D), showing that Dkk1 activity can also mimic the temporal aspects of inhibition of NC formation in vivo.

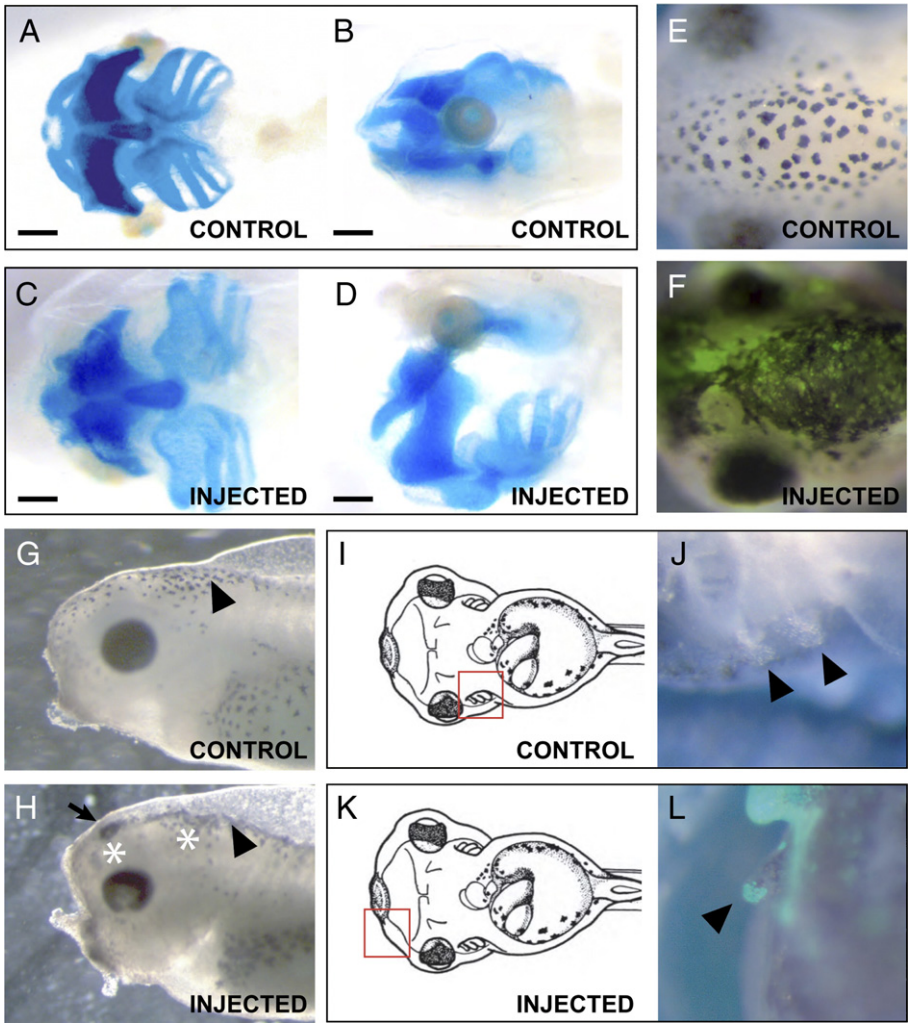

Fig. 9. NC induced at the ANF is able to differentiate. (A–D) Cartilage staining of embryos at stage 40. Scale bar: 150 μm. (A, B) Control embryos. (A) Ventral view; (B) lateral view. (C, D) Embryo injected with β-catenin in the ANF. (C) Ventral view; (D) lateral view. Note the expansion on the cartilages (30–40%). (E) Dorsal view of the head of a stage 40 embryo, showing the normal melanocyte pattern. (F) Dorsal view of the head of an embryo stage 40 injected with β-catenin in the ANF, note the increase in the number of melanocytes (50–60%). (G) Lateral view of the head of a stage 35 embryo; arrowhead indicates the anterior end of the dorsal fin. (H) Lateral view of the head of a stage 35 embryo injected with β-catenin in the ANF; note that the normal position of the anterior limit of the dorsal fin (arrowhead) has moved anteriorly (arrow, 40–50%). Note also a mild increase on the number of dorsal melanocytes (white asterisks). (I–L) Analysis of gill-like structures. (I, J) Gills of a normal embryo, localized in the branchial region (arrowhead). Square in panel I corresponds to the region shown in panel J. (K, L) Ectopic gill-like structures formed in the anterior region of the head in an embryo injected with β-catenin in the ANF (50–60%). Square in panel K corresponds to the region shown in panel L. Approximately 100 embryos were analyzed.

The experiments using the Dkk1 antibody and the *Dkk1* null mutant show the essential role of Dkk1 for the inhibition of NC formation at the ANF. However, it is well established that in the *Dkk1* null mutant there is a dramatic reduction of forebrain development (inset in Fig. 4F and Mukhopadhyay et al., 2001), and the expression of the NC markers at the ANF could be only a morphological consequence of the absence of forebrain tissue which in normal embryos separates the two lateral NC domains. However, more detailed observation of the embryos suggests that this is not the case as the most anterior domain of *Sox10* expression is larger in the mutant than in wild type embryos, indicating an increase in the number of crest cells in the anterior region. This observation is confirmed in *Xenopus* where we can have a better control of Wnt signaling, in space and time, and in which we were able to transform the ANF into NC without affecting forebrain specification. This improved control of Wnt signaling was reached by local expression of inducible β-catenin, a downstream target of Wnt. In addition to forebrain development, Wnt signaling has been implicated in placodal and anterior–posterior patterning (Braun et al., 2003; Kiecker and Niehrs, 2001; McGrew et al., 1997; Erter et al., 2001, Itoh and Sokol, 1997; Niehrs, 2001; Nordstrom et al., 2002; Brugmann et al., 2004; Litsiou et al., 2005). However, as we can control the space, time and level of β-catenin activation we have been able to dissociate the transformation of the ANF into NC from the effect of Wnt signaling on placodal development and AP patterning, in addition to forebrain development. Thus, our embryos show ectopic expression of NC markers in the ANF, and normal levels in the expression of forebrain, placodal and AP markers (Fig. 7M). This observation that no

anterior markers are lost at the expense of NC cells can be explained by the increase in cell number after activation of Wnt signaling. In fact, we observed an increase in cell proliferation in the ANF that was accompanied by the expression of NC markers (Figs. 7N, O).

We show that the ANF transformation into NC is not the result of lack of anterior structures in injected embryos as anterior markers do not disappear. We were able to experimentally dissociate the ANF transformation from AP patterning but we cannot say that ectodermal patterning and NC inhibition at the ANF are actually two completely different processes in the developing embryo. Nonetheless, our results suggest that at least different levels of Wnt activity are required to subdivide the anterior neural plate region, the preplacodal field and the NC, the latter being the most sensitive. If higher levels of Wnt signaling are reached at the ANF, an inhibition of forebrain and placodal markers is observed (Fig. S1), as has been already described for the Dkk1 mouse mutant, the *headless* zebrafish mutant and by activation of Wnt signaling in *Xenopus* and chick embryos (Kim et al., 2000; Mukhopadhyay et al., 2001; Brugmann et al., 2004; Litsiou et al., 2005). An interesting observation is the anterior–ventral shift of the placodal markers produced by the transformation of ANF into NC. This suggests that the induction of NC at the ANF is not at the expense of placodal ectoderm as the ectopically induced NC cells "push" the preplacodal field away.

It has been shown by many laboratories that Wnt activity is required for NC induction (Saint-Jeannet et al., 1997; LaBonne and Bronner-Fraser, 1998; Lekven et al., 2001; Deardorff et al., 2001; Villanueva et al., 2002; Garcia-Castro et al., 2002; Tribulo et al., 2003; Lewis et al., 2004; Bastidas et al., 2004). Therefore, it is possible that the transformation of ANF into NC described here is part of the process of NC induction. However, our results suggest that these are two different processes. Competence of ectoderm to Wnt signaling to expand the NC territory is almost lost after the beginning of gastrulation, while the ability of the same signal to transform the ANF into NC reaches its peak during gastrulation; only treatments producing high levels of β-catenin are able to generate both phenotypes after gastrulation (Fig. 6).

Another interesting observation is that inhibition of Wnt signaling by Dkk1 in cells that are already specified as NC is able to reverse the specification state and blocks the expression of NC markers (Fig. 3); this is something that had not been tested before as all the published experiments blocked Wnt signaling before the stage at which the NC begins to express any of its characteristic markers. The inhibition of NC in vitro by Dkk1 suggests that the NC produces its own secreted Wnt, which can be blocked by Dkk1. We have also observed that Wnt8 is expressed in the NC of early neurula embryos (C. C-F. and R. M. unpublished), which further supports this idea. This observation suggests that NC cells require a continuous source of Wnt signaling and that part of the mechanism of NC specification could be the production of Wnts by the NC itself.

The activation of Wnt signaling in the anterior neural plate leads to a very discrete expression of NC markers only in the ANF. This suggests that additional and earlier factors control the competence of this region to respond to the Wnt signals and produce NC cells. As already discussed, induction of NC appears to be an earlier event as inhibition of NC development at the ANF. These observations suggest that, in an early step of NC specification, several signals (including Wnt and BMPs) specify the entire border of the neural plate as prospective NC, and then Dkk1 inhibits NC development at the ANF as a later step (Fig. 1C).

Here we provide evidence that Dkk1 activity is essential for this inhibition but we cannot rule out the possibility that additional molecules, which may or may not be related to Wnt or other NC inductive signals, could also be involved. It is interesting to note that inhibition of Cullin-1, a protein that targets β-catenin for degradation, leads to a similar transformation of ANF into NC (Voigt and Papalopulu, 2006). We should emphasize that, although the transformation of ANF into NC has been reported before by treatments that activate Wnt, FGF or retinoic acid signaling (Villanueva et al., 2002; Monsoro-Burq et al., 2003; Wu et al., 2005; Voigt and Papalopulu, 2006), this is the first time that an active process of neural crest inhibition has been described (Fig. 2). Thus, the simple observation that activation of a signaling pathway at the ANF leads to the expression of NC markers in that region, as it has been described (Villanueva et al., 2002; Monsoro-Burq et al., 2003; Wu et al., 2005; Voigt and Papalopulu, 2006), does not prove that there is inhibition of those signals at the ANF. Additional experiments will be required to analyze whether a similar inhibitory mechanism acts on other neural crest inducing signals in the ANF.

Our results show that the induced ANF cells are proper NC cells, with the ability to migrate in vitro and in vivo, to follow the normal migratory pathways and to differentiate into many normal cranial NC derivatives, such as cartilage, melanocytes, dorsal fin and gill-like structures (Figs. 8, 9). We have observed that when ectopic NC is induced at the ANF some few cells remain at that position and differentiate to produce ectopic NC derivatives in the anterior region of the head. However, most of the ectopically induced NC cells join the normal migratory pathways and contribute to enlarged NC derivatives. The ability of the NC to join the correct migratory pathways could suggest the existence of repulsive molecules in the ectopic location. The role for negatives cues that repress NC migration, such as ephrins, Slit/Robo and semaphorins, has been very well documented (Krull et al., 1997; Smith et al., 1997; De Bellard et al., 2003; Kawasaki et al., 2002). Alternatively, positive signals from the NC or the NC migratory pathways might also contribute to guide the ectopic NC cells to normal migratory paths.

Finally, we have shown a similar transformation of the ANF into NC in fish, amphibian and mammals, indicating that the inhibition of NC at the ANF has been conserved during evolution.

Acknowledgments

We thank Claudio Stern, Sei Kuriyama, Helen Mathews, Ben Steventon, Eric Theveneau and Lorena Marchant for comments

on the manuscript and G. Gestri, J. Smith, C. Linker, S. Moody, S. Kuriyama, F. Cavodeassi and S. Wilson for reagents and useful advises. This investigation was supported by an International Research Scholar Award from the Howard Hughes Medical Institute to R.M. and by grants from MRC, BBSRC and the Millennium Program. C. C-F. is a recipient of a Boehringer Ingelheim Fonds scholarship.

Appendix A. Supplementary data

Supplementary data associated with this article can be found, in the online version, at doi:doi:10.1016/j.ydbio.2007.07.006.

References

Alfandari, D., Cousin, H., Gaultier, A., Hoffstrom, B.G., DeSimone, D.W., 2003. Integrin [alpha]5[beta]1 supports the migration of *Xenopus* cranial neural crest on fibronectin. Dev. Biol. 260, 449–464.

Aybar, M.J., Mayor, R., 2002. Early induction of neural crest cells: lessons learned from frog, fish and chick. Curr. Opin. Genet. Dev. 12, 452–458.

Aybar, M.J., Nieto, M.A., Mayor, R., 2003. Snail precedes Slug in the genetic cascade required for the specification and migration of the *Xenopus* neural crest. Development 130, 483–494.

Barrallo-Gimeno, A., Holzschuh, J., Driever, W., Knapik, E.W., 2004. Neural crest survival and differentiation in zebrafish depends on mont blanc/tfap2a gene function. Development 131, 1463–1477.

Barth, K.A., Kishimoto, Y., Rohr, K.B., Seydler, C., Schulte-Merker, S., Wilson, S.W., 1999. Bmp activity establishes a gradient of positional information throughout the entire neural plate. Development 126, 4977–4987.

Basch, M.L., Garcìa-Castro, M.I., Bronner-Fraser, M., 2004. Molecular mechanisms of neural crest induction. Birth Defects Res., C Embryo Today 72, 109–123.

Bastidas, F., Calisto, J.D., Mayor, R., 2004. Identification of neural crest competence territory: role of Wnt signaling. Dev. Dyn. 229, 109–117.

Bouwmeester, T., Kim, S.-H., Sasai, Y., Lu, B., Robertis, E.M.D., 1996. Cerberus is a head-inducing secreted factor expressed in the anterior endoderm of Spemann's organizer. Nature 382, 595–601.

Bradley, L.C., Snape, A., Bhatt, S., Wilkinson, D.G., 1993. The structure and expression of the *Xenopus* Krox-20 gene: conserved and divergent patterns of expression in rhombomeres and neural crest. Mech. Dev. 40, 73–84.

Braun, M.M., Etheridge, A., Bernard, A., Robertson, C.P., Roelink, H., 2003. Wnt signaling is required at distinct stages of development for the induction of the posterior forebrain. Development 130, 5579–5587.

Brugmann, S.A., Pandur, P.D., Kenyon, K.L., Pignoni, F., Moody, S.A., 2004. Six1 promotes a placodal fate within the lateral neurogenic ectoderm by functioning as both a transcriptional activator and repressor. Development 131, 5871–5881.

Caneparo, L., Huang, Y.-L., Staudt, N., Tada, M., Ahrendt, R., Kazanskaya, O., Niehrs, C., Houart, C., 2007. Dickkopf-1 regulates gastrulation movements by coordinated modulation of Wnt/betacatenin and Wnt/PCP activities, through interaction with the Dally-like homolog Knypek. Genes Dev. 21, 465–480 (%R 10.1101/gad.406007).

Christian, J.L., Moon, R.T., 1993. Interactions between Xwnt-8 and Spemann organizer signaling pathways generate dorsoventral pattern in the embryonic mesoderm of *Xenopus*. Genes Dev. 7, 13–28.

Christian, J.L., McMahon, J.A., McMahon, A.P., Moon, R.T., 1991. Xwnt-8, a *Xenopus* Wnt-1/int-1-related gene responsive to mesoderm-inducing growth factors, may play a role in ventral mesodermal patterning during embryogenesis. Development 111, 1045–1055.

Chuang, J.C., Mathers, P.H., Raymond, P.A., 1999. Expression of three Rx homeobox genes in embryonic and adult zebrafish. Mech. Dev. 84, 195–198.

Couly, G.F., Le Douarin, N.M., 1985. Mapping of the early neural primordium in quail–chick chimeras: I. Developmental relationships between placodes, facial ectoderm, and prosencephalon. Dev. Biol. 110, 422–439.

Couly, G.F., Coltey, P.M., Le Douarin, N.M., 1993. The triple origin of skull in higher vertebrates: a study in quail–chick chimeras. Development 117, 409–429.

De Bellard, M.E., Rao, Y., Bronner-Fraser, M., 2003. Dual function of Slit2 in repulsion and enhanced migration of trunk, but not vagal, neural crest cells. J. Cell Biol. 162, 269–279.

De Calisto, J., Araya, C., Marchant, L., Riaz, C.F., Mayor, R., 2005. Essential role of non-canonical Wnt signalling in neural crest migration. Development 132, 2587–2597.

Deardorff, M.A., Tan, C., Saint-Jeannet, J.-P., Klein, P.S., 2001. A role for frizzled 3 in neural crest development. Development 128, 3655–3663.

Domingos, P.M., Itasaki, N., Jones, C.M., Mercurio, S., Sargent, M.G., Smith, J.C., Krumlauf, R., 2001. The Wnt/[beta]-catenin pathway posteriorizes neural tissue in *Xenopus* by an indirect mechanism requiring FGF signalling. Dev. Biol. 239, 148–160.

Endo, Y., Osumi, N., Wakamatsu, Y., 2003. Deltex/Dtx mediates NOTCH signaling in regulation of Bmp4 expression in cranial neural crest formation during avian development. Dev. Growth Differ. 45, 241–248.

Erter, C.E., Wilm, T.P., Basler, N., Wright, C.V.E., Solnica-Krezel, L., 2001. Wnt8 is required in lateral mesendodermal precursors for neural posteriorization in vivo. Development 128, 3571–3583.

Essex, L.J., Mayor, R., Sargent, M.G., 1993. Expression of *Xenopus snail* in mesoderm and prospective neural fold ectoderm. Dev. Dyn. 198, 108–122.

Garcia-Castro, M.I., Marcelle, C., Bronner-Fraser, M., 2002. Ectodermal Wnt function as a neural crest inducer. Science 297, 848–851.

Glavic, A., Silva, F., Aybar, M.J., Bastidas, F., Mayor, R., 2004. Interplay between Notch signaling and the homeoprotein Xiro1 is required for neural crest induction in *Xenopus* embryos. Development 131, 347–359.

Glinka, A., Wu, W., Delius, H., Monaghan, A.P., Blumenstock, C., Niehrs, C., 1998. Dickkopf-1 is a member of a new family of secreted proteins and functions in head induction. Nature 391, 357–362.

Hardcastle, Z., Papalopulu, N., 2000. Distinct effects of XBF-1 in regulating the cell cycle inhibitor p27(XIC1) and imparting a neural fate. Development 127, 1303–1314.

Harland, R.M., 1991. In situ hybridization: an improved whole-mount method for *Xenopus* embryos. Methods Cell Biol. 36, 685–695.

Harland, R., Weintraub, H., 1985. Translation of mRNA injected into *Xenopus* oocytes is specifically inhibited by antisense RNA. J. Cell Biol. 101, 1094–1099.

Hörstadius, S., 1950. The Neural Crest: Its Properties and Derivatives in the Light of Experimental Research. Oxford University Press, London.

Itoh, K., Sokol, S.Y., 1997. Graded amounts of *Xenopus* dishevelled specify discrete anteroposterior cell fates in prospective ectoderm. Mech. Dev. 61, 113–125.

Kawasaki, T., Bekku, Y., Suto, F., Kitsukawa, T., Taniguchi, M., Nagatsu, I., Nagatsu, T., Itoh, K., Yagi, T., Fujisawa, H., 2002. Requirement of neuropilin 1-mediated Sema3A signals in patterning of the sympathetic nervous system. Development 129, 671–680.

Kazanskaya, O., Glinka, A., Niehrs, C., 2000. The role of *Xenopus* dickkopf1 in prechordal plate specification and neural patterning. Development 127, 4981–4992.

Kelsh, R.N., Dutton, K., Medlin, J., Eisen, J.S., 2000. Expression of zebrafish fkd6 in neural crest-derived glia. Mech. Dev. 93, 161–164.

Kiecker, C., Niehrs, C., 2001. A morphogen gradient of Wnt/beta-catenin signalling regulates anteroposterior neural patterning in *Xenopus*. Development 128, 4189–4201.

Kim, C.-H., Oda, T., Itoh, M., Jiang, D., Artinger, K.B., Chandrasekharappa, S.C., Driever, W., Chitnis, A.B., 2000. Repressor activity of Headless/Tcf3 is essential for vertebrate head formation. Nature 407, 913–916.

Knecht, A.K., Bronner-Fraser, M., 2002. Induction of the neural crest: a multigene process. Nat. Rev., Genet. 3, 453–461.

Krull, C.E., Lansford, R., Gale, N.W., Collazo, A., Marcelle, C., Yancopoulos, G.D., Fraser, S.E., Bronner-Fraser, M., 1997. Interactions of Eph-related receptors and ligands confer rostrocaudal pattern to trunk neural crest migration. Curr. Biol. 7, 571–580.

LaBonne, C., Bronner-Fraser, M., 1998. Neural crest induction in *Xenopus*: evidence for a two-signal model. Development 125, 2403–2414.

LeDouarin, N.M., Kalcheim, C., 1999. The Neural Crest. Cambridge University Press, Cambridge.
Lekven, A.C., Thorpe, C.J., Waxman, J.S., Moon, R.T., 2001. Zebrafish wnt8 encodes two Wnt8 Proteins on a bicistronic transcript and is required for mesoderm and neurectoderm patterning. Dev. Cell 1, 103–114.
Lewis, J.L., Bonner, J., Modrell, M., Ragland, J.W., Moon, R.T., Dorsky, R.I., Raible, D.W., 2004. Reiterated Wnt signaling during zebrafish neural crest development. Development 131, 1299–1308.
Liem, J.K.F., Tremml, G., Roelink, H., Jessell, T.M., 1995. Dorsal differentiation of neural plate cells induced by BMP-mediated signals from epidermal ectoderm. Cell 82, 969–979.
Linker, C., Bronner-Fraser, M., Mayor, R., 2000. Relationship between gene expression domains of Xsnail, Xslug, and Xtwist and cell movement in the prospective neural crest of *Xenopus*. Dev. Biol. 224, 215–225.
Litsiou, A., Hanson, S., Streit, A., 2005. A balance of FGF, BMP and WNT signalling positions the future placode territory in the head. Development 132, 4051–4062.
Mancilla, A., Mayor, R., 1996. Neural crest formation in *Xenopus laevis*: mechanisms of Xslug induction. Dev. Biol. 177, 580–589.
Marchant, L., Linker, C., Ruiz, P., Guerrero, N., Mayor, R., 1998. The inductive properties of mesoderm suggest that the neural crest cells are specified by a BMP gradient. Dev. Biol. 198, 319–329.
Mayor, R., Aybar, M.J., 2001. Induction and development of neural crest in *Xenopus laevis*. Cell Tissue Res. 305, 203–209.
Mayor, R., Essex, L.J., Bennett, M.F., Sargent, M.G., 1993. Distinct elements of the xsna promoter are required for mesodermal and ectodermal expression. Development 119, 661–671.
Mayor, R., Morgan, R., Sargent, M.G., 1995. Induction of the prospective neural crest of *Xenopus*. Development 121, 767–777.
Mayor, R., Guerrero, N., Martinez, C., 1997. Role of FGF and noggin neural crest induction. Dev. Biol. 189, 1–12.
McGrew, L.L., Hoppler, S., Moon, R.T., 1997. Wnt and FGF pathways cooperatively pattern anteroposterior neural ectoderm in *Xenopus*. Mech. Dev. 69, 105–114.
Monsoro-Burq, A.H., Fletcher, R.B., Harland, R.M., 2003. Neural crest induction by paraxial mesoderm in *Xenopus* embryos requires FGF signals. Development 130, 3111–3124.
Morgan, R., Sargent, M.G., 1997. The role in neural patterning of translation initiation factor eIF4AII; induction of neural fold genes. Development 124, 2751–2760.
Moury, J.D., Jacobson, A.G., 1990. The origins of neural crest cells in the axolotl. Dev. Biol. 141, 243–253.
Mukhopadhyay, M., Shtrom, S., Rodriguez-Esteban, C., Chen, L., Tsukui, T., Gomer, L., Dorward, D.W., Glinka, A., Grinberg, A., Huang, S.-P., 2001. Dickkopf1 is required for embryonic head induction and limb morphogenesis in the mouse. Dev. Cell 1, 423–434.
Nguyen, V.H., Schmid, B., Trout, J., Connors, S.A., Ekker, M., Mullins, M.C., 1998. Ventral and lateral regions of the zebrafish gastrula, including the neural crest progenitors, are established by abmp2b/swirlPathway of genes. Dev. Biol. 199, 93–110.
Niehrs, C., 2001. The Spemann organizer and embryonic head induction. EMBO J. 20, 631–637.
Nordstrom, U., Jessell, T.M., Edlund, T., 2002. Progressive induction of caudal neural character by graded Wnt signaling. Nat. Neurosci. 5, 525–532.
Pannese, M., Polo, C., Andreazzoli, M., Vignali, R., Kablar, B., Barsacchi, G., Boncinelli, E., 1995. The *Xenopus* homologue of Otx2 is a maternal homeobox gene that demarcates and specifies anterior body regions. Development 121, 707–720.
Pera, E.M., De Robertis, E.M., 2000. A direct screen for secreted proteins in *Xenopus* embryos identifies distinct activities for the Wnt antagonists Crescent and Frzb-1. Mech. Dev. 96, 183–195.
Richter, K., Grunz, H., Dawid, I.B., 1988. Gene expression in the embryonic nervous system of *Xenopus laevis*. Proc. Natl. Acad. Sci. U. S. A. 85, 8086–8090.
Saint-Jeannet, J.-P., He, X., Varmus, H.E., Dawid, I.B., 1997. Regulation of dorsal fate in the neuraxis by Wnt-1 and Wnt-3a. PNAS 94, 13713–13718.
Sasai, N., Mizuseki, K., Sasai, Y., 2001. Requirement of FoxD3-class signaling for neural crest determination in *Xenopus*. Development 128, 2525–2536.
Schlosser, G., Ahrens, K., 2004. Molecular anatomy of placode development in *Xenopus laevis*. Dev. Biol. 271, 439–466.
Selleck, M.A., Bronner-Fraser, M., 1995. Origins of the avian neural crest: the role of neural plate–epidermal interactions. Development 121, 525–538.
Smith, A., Robinson, V., Patel, K., Wilkinson, D.G., 1997. The EphA4 and EphB1 receptor tyrosine kinases and ephrin-B2 ligand regulate targeted migration of branchial neural crest cells. Curr. Biol. 7, 561–570.
Southard-Smith, E.M., Kos, L., Pavan, W.J., 1998. *Sox10* mutation disrupts neural crest development in Dom Hirschsprung mouse model. Nat. Genet. 18, 60–64.
Steventon, B., Carmona-Fontaine, C., Mayor, R., 2005. Genetic network during neural crest induction: from cell specification to cell survival. Semin. Cell Dev. Biol. 16, 647–654.
Tribulo, C., Aybar, M.J., Nguyen, V.H., Mullins, M.C., Mayor, R., 2003. Regulation of Msx genes by a Bmp gradient is essential for neural crest specification. Development 130, 6441–6452.
Villanueva, S., Glavic, A., Ruiz, P., Mayor, R., 2002. Posteriorization by FGF, Wnt, and retinoic acid is required for neural crest induction. Dev. Biol. 241, 289–301.
Voigt, J., Papalopulu, N., 2006. A dominant-negative form of the E3 ubiquitin ligase Cullin-1 disrupts the correct allocation of cell fate in the neural crest lineage. Development 133, 559–568.
Wu, J., Yang, J., Klein, P.S., 2005. Neural crest induction by the canonical Wnt pathway can be dissociated from anterior–posterior neural patterning in *Xenopus*. Dev. Biol. 279, 220–232.

Development ePress online publication date 9 April 2008

Development 135, 1771-1780 (2008) doi:10.1242/dev.017350

Directional migration of neural crest cells in vivo is regulated by Syndecan-4/Rac1 and non-canonical Wnt signaling/RhoA

Helen K. Matthews[1], Lorena Marchant[1], Carlos Carmona-Fontaine[1], Sei Kuriyama[1], Juan Larraín[2], Mark R. Holt[3], Maddy Parsons[3] and Roberto Mayor[1,*]

Directed cell migration is crucial for development, but most of our current knowledge is derived from in vitro studies. We analyzed how neural crest (NC) cells migrate in the direction of their target during embryonic development. We show that the proteoglycan Syndecan-4 (Syn4) is expressed in the migrating neural crest of *Xenopus* and zebrafish embryos. Loss-of-function studies using an antisense morpholino against *syn4* show that this molecule is required for NC migration, but not for NC induction. Inhibition of Syn4 does not affect the velocity of cell migration, but significantly reduces the directional migration of NC cells. Furthermore, we show that Syn4 and PCP signaling control the directional migration of NC cells by regulating the direction in which the cell protrusions are generated during migration. Finally, we perform FRET analysis of Cdc42, Rac and RhoA in vitro and in vivo after interfering with Syn4 and PCP signaling. This is the first time that FRET analysis of small GTPases has been performed in vivo. Our results show that Syn4 inhibits Rac activity, whereas PCP signaling promotes RhoA activity. In addition, we show that RhoA inhibits Rac in NC cells. We present a model in which Syn4 and PCP control directional NC migration by, at least in part, regulating membrane protrusions through the regulation of small GTPase activities.

KEY WORDS: Cell migration, Neural crest, Directionality, Persistence, Syndecan-4, Non-canonical Wnt signaling, PCP, RhoA, Rac1

INTRODUCTION

Considerable progress has been made recently in understanding cell migration, which is crucial to the comprehension of normal and disease-related processes, such as morphogenesis and metastasis in cancer. However, most of these studies have been performed in vitro, and some discrepancies have been found between cell behaviour in vivo and in vitro (Even-Ram and Yamada, 2005). Here, we use the migration of an embryonic tissue, the neural crest (NC), as an in vivo model to study cell migration.

The NC has been called 'the explorer of the embryo' because of its inherent migratory abilities. NC cells migrate from the dorsal neural tube, covering extremely long distances and colonizing almost all the tissues of the embryo. Upon reaching their destination, they differentiate into a wide range of cell types, including neurons, glial cells, skeletal and connective tissue, and adrenergic and pigment cells (LeDouarin and Kalcheim, 1999).

The migration of the NC is a highly ordered process; individual NC cells migrate with high persistence towards the direction of their targets (Teddy and Kulesa, 2004), but it is not known how this directionality is controlled. A number of molecules have been identified as being key players in neural crest migration (for a review, see Kuriyama and Mayor, 2008). However most of these molecules function as inhibitory signals, which are required to prevent the migration of NC cells into prohibited areas. Although chemoattraction has been one of the proposed mechanisms to explain this directional migration, no chemoattractant has thus far been found in the NC. This prompted us to look for alternative mechanisms that might generate directional migration. Interestingly, researchers studying cell migration in vitro have observed that cultured cells can migrate with a high directionality even in the absence of external chemoattractants. It is known that in vitro cell migration requires the formation of membrane protrusions at the leading edge of the cell, membrane adhesive interactions with the substrata and the coordinated dynamics of the cytoskeleton (Lauffenburger and Horwitz, 1996; Pollard and Borisy, 2003; Ridley et al., 2003; Sheetz et al., 1999). Small GTPases (Rac, Rho and Cdc42) are well-known modulators of several of these activities (for reviews, see Ridley et al., 2003; Jaffe and Hall, 2005). Moreover, it has been shown that directional migration in vitro in the absence of extrinsic chemoattractants is controlled by the level of Rac activity (Pankov et al., 2005). Rac promotes the formation of peripheral lamella during random migration, while slightly lower levels of Rac suppress peripheral lamella and favour the formation of a polarized cell with lamella just at the leading edge (Pankov et al., 2005).

Syndecan-4 (Syn4) is a proteoglycan that is involved in the migration of cells cultured in vitro, and it has been proposed as a key regulator of RhoA and Rac activities, focal adhesion formation and planar cell polarity (PCP) signaling (for a review, see Alexopoulou et al., 2007). In this study, we examined the role of Syn4 in neural crest migration in *Xenopus* and zebrafish embryos. We show that *syn4* is expressed specifically in the migrating neural crest and that it is essential for its migration. In addition, we show that Syn4 controls directional migration by regulating the polarized formation of cell protrusions, in a manner similar to non-canonical Wnt signaling. In order to understand the molecular mechanism by which Syn4 and planar cell polarity (PCP) signaling control the orientation of cell protrusions, we performed fluorescence resonance energy transfer (FRET) analysis to measure the activity of the small GTPases, Cdc42, RhoA and Rac. This is the first time that this kind of FRET analysis has been carried out in vivo. Our results indicate that whereas Syn4 inhibits Rac activity, PCP signaling activates RhoA. In addition, we show that RhoA, through Rock, is an inhibitor of Rac activity in the neural crest. Thus, the

[1]Department of Anatomy and Development Biology, University College London, Gower Street, London WC1E 6BT, UK. [2]P. Universidad Católica de Chile, Alameda 340, Santiago, Chile. [3]Randall Division of Cell and Molecular Biophysics, King's College London, Guy's Campus, London SE1 1UL, UK.

*Author for correspondence (e-mail: r.mayor@ucl.ac.uk)

Accepted 19 March 2008

convergence of Syn4 and PCP signaling through the regulation of small GTPases contributes to the directional migration of neural crest cells.

MATERIALS AND METHODS

Xenopus and zebrafish embryos, micromanipulation and graft experiments

Xenopus embryos were obtained and dissections carried out as previously described (Mancilla and Mayor, 1996). Embryos were staged according to Nieuwkoop and Faber (Nieuwkoop and Faber, 1967). Zebrafish strains were maintained and bred according to standard procedures (Westerfield, 2000). Transgenic *sox10:egfp* (Carney et al., 2006) embryos were obtained by crossing heterozygous adults. *Xenopus* NC grafts were carried out as described by De Calisto et al. (De Calisto et al., 2005). Zebrafish cell transplants were performed according to Westerfield (Westerfield, 2000); *sox10:egfp* donor embryos were injected at the one- or two-cell stage with a mixture of tetramethylrhodamine dextran (RDX) (1 ng/nl; Molecular Probes) and either control or *syn4* morpholino oligonucleotides (MOs). At the sphere stage, single or small groups of around 10 donor cells were transplanted into the apical region of unlabelled wild-type host embryos using an oil-filled manual injector (Sutter Instrument Company). Embryos were cultured until 12 somites and observed using time-lapse microscopy (Leica DM5500).

Whole-mount in situ hybridization and cartilage staining

In situ hybridization was carried out according to Harland (Harland, 1991) using digoxigenin-labelled antisense RNA probes (Roche Diagnostics). Probes used were: *Xenopus syn4* (Munoz et al., 2006); and zebrafish *syn4*, *snail2* (Mayor et al., 1995), *fli* (Meyer et al., 1995), *foxd3* (Kelsh et al., 2000) and *crestin* (Luo et al., 2001). For cartilage staining, 5-dpf zebrafish were stained according to Barrallo-Gimeno et al. (Barrallo-Gimeno et al., 2004).

RNA synthesis and morpholino microinjection

cDNA was linearized and RNA was synthesized using the mMessage mMachine Kit (Ambion), according to the manufacturer's instructions. mRNA and MOs were co-injected into *Xenopus* embryos with fluorescein dextran (FDX, Molecular Probes) at the eight- or 32-cell stage (Aybar et al., 2003). For zebrafish microinjection, 4 nl was injected at the one- or two-cell stage. The mRNA constructs used were: *Xenopus syn4* (Munoz et al., 2006); and zebrafish *syn4*, DshDEP+ and DshΔN (Tada and Smith, 2000), and mutant *syn4*. Two translation-blocking MOs against zebrafish *syn4* were designed over the 5′UTR region: *syn4* MO1, 5′CGGACAACTTTATTCACTCGGGCTA3′; and *syn4* MO2, 5′GAGAAG(ATG)TTGAAAGTTTACCTCA3′. As both MOs produced the same phenotype, we used mainly *syn4* MO1 (called *syn4* MO), except in some experiments where *syn4* MO2 or a mixture of both MOs was used, as indicated in the text and figure legends. A standard control MO was used: 5′CCTCTTACCTCAGTTACAATTTATA3′. Injection of this control MO into wild-type zebrafish embryos caused no defective phenotype. Two translation-blocking MOs against *Xenopus syn4* were used: *syn4* MO1, 5′GCACAAACAGCAGGGTCGGACTCAT3′; and *syn4* MO2, 5′CTAAAAGCAGCAGGAGGCGATTCAT3′ (Munoz et al., 2006). Throughout this work, a 1:1 mixture of both MOs called *syn4* MO was used. A 5-base mismatched MO against *Xenopus syn4* was used as a control (5′GCAGAAAGATCAGCGTCCGACTGAT3′). The other MO used was directed against *wnt5a* (Lele et al., 2001). Unless stated otherwise, 6 ng of MO was used for zebrafish and 8 ng for *Xenopus*.

For the mutation in the PKCα-binding site of Syn4 (called Syn4*), a mutation was introduced in the PIP2-binding site that enables interaction with PKCα. Amino acid residues Y^{185}KK were changed to LQQ using PCR with mutated primers. According to Horowitz et al., this mutation reduces the affinity of PIP2 binding to Syn4 (Horowitz et al., 1999). We observed that this mutant has the same activity as wild-type Syn4 in a neural plate induction assay (our unpublished results).

Time-lapse microscopy

sox10:egfp was used to analyze NC migration in vivo (Carney et al., 2006). Embryos were processed as described by Westerfield (Westerfield, 2000). Each embryo was staged according to the number of somites and only embryos with equal numbers of somites were compared. The embryos were dechorionated, inserted into a drop of 0.20% agarose in embryo medium (Westerfield, 2000) and mounted in a custom-built chamber. Control and experimental embryos were mounted side-by-side in the same chamber. A compound (Leica DM5500) or a confocal (Leica SP2-DMRE) microscope was used for time-lapse imaging. Digital images were typically collected at 30 to 90 second intervals for a period of between 1 and 14 hours. We performed *z*-stack in preliminary experiments to establish how deep the NC migrates in the embryo. After 6- to 8-hour time-lapse imaging of 20-somite embryos, we found that cephalic NC cells migrate between 500 and 800 μm in the anteroposterior axis, between 40 and 60 μm in the dorsoventral axis, and between 7 and 9 μm in the periphery-center axis. Consequently, for tracking analysis, we can assume that most of the cell migration is performed in two dimensions; the third dimension (in the *z*-axis when the embryo has a lateral orientation) can be neglected.

Sequences of images were quantitatively analyzed using the public domain program NIH ImageJ (developed at the US National Institutes of Health) and Matlab (MathWorks). Tracking of individual cells was used to calculate velocity (total distance traveled divided by time), persistence (defined as the ratio between the linear distance from the initial to the final point and the total length of the migratory path) and the angle of migration (with respect to its previous position).

The shape of individual cells was analyzed using NIH ImageJ. Thresholds were fixed at the same value for control and *syn4* MO-injected cells. The outline/analyze particles function was used to draw the contour of each cell at different time points, which were overlapped maintaining the original XY positions. Two independent methods were used to analyze cell protrusions. For the first method, we defined Cell extension (CE) as the new positive area between two consecutives frames (separated by the shortest time of 1 minute in the time-lapse analysis). During the course of one minute, the body (and centroid) of the cell does not move a significant distance and most of the new area generated corresponds to lamellipodia extension. Note, fillopodia were not considered in this analysis as they move faster and the intensity of fluorescence is weaker. Using ImageJ, we subtracted two consecutives frames, in a manner that the new growing area was shown in red and the unchanged area in white (Fig. 6C,H,M). The centroid (defined as the average of the *x* and *y* coordinates of all the cell pixels) was calculated and a vector between the centroid (x) and the center of the red area was drawn (arrow in Fig. 6N). These vectorial data were used to analyze the distribution of CE orientation under different conditions. As a second method to estimate cell protrusion, we measured the Cell Smoothness (CS), defined as the ratio between the perimeter of an ideal ellipse-shaped cell and the actual perimeter of the cell. The ellipse was the best-fit ellipse and we used the standard built-in ImageJ function. This value gives us an unbiased measure of how folded a cell is (i.e. how many protrusions a cell has). *P*-values were obtained using a one-way analysis of variance (ANOVA). All statistical analyses and their graphical illustrations were performed on Matlab, using both built-in functions and customized scripts (available from the authors on request).

Fluorescence (Förster) resonance energy transfer (FRET)

Plasmid DNA encoding FRET probes [Raichu-Rac, Raichu-Cdc42 (Itoh et al., 2002) and RhoA biosensor (Pertz et al., 2006)] was injected directly into *Xenopus* embryos at the eight-cell stage and NCs were dissected at stage 15. For in vitro analysis, NC cells were cultured on fibronectin, as described by Alfandari et al. (Alfandari et al., 2003), and fixed with 4% PFA after 5-7 hours migration. For the in vivo analysis, injected neural crests were grafted into wild-type hosts. Embryos were fixed in MEMFA at stage 26, and 12 μm cryostat sections were taken.

Samples for FRET analysis were imaged using a Zeiss lSM 510 META laser scanning confocal microscope and a 63× Plan Apochromat NA 1.4 Ph3 oil objective. The CFP and YFP channels were excited using the 405-nm blue diode laser and the 514-nm argon line, respectively. The two emission channels were split using a 545-nm dichroic mirror, which was followed by a 475-525 nm bandpass filter for CFP and a 530 nm longpass filter for YFP. Pinholes were opened to give a depth of focus of 3 mm for each channel. Scanning was performed on a line-by-line basis with the zoom level set to two. The gain for each channel was set to approximately 75% of dynamic range (12-bit, 4096 gray levels) and offsets set such that

backgrounds were zero. The time-lapse mode was used to collect one pre-bleach image for each channel before bleaching with 50 scans of the 514 nm argon laser line at maximum power (to bleach YFP). A second post-bleach image was then collected for each channel. Pre- and post-bleach CFP and YFP images were imported into Mathematica 5.2 for processing. Briefly, images were smoothed using a 3×3 box mean filter, background subtracted and post-bleach images fade compensated. A FRET efficiency ratio map over the whole cell was calculated using the following formula: $(CFP_{postbleach}–CFP_{prebleach})/CFP_{postbleach}$. Ratio values were then extracted from pixels falling inside the bleach region, as well as an equal-sized region outside of the bleach region, and the mean ratio was determined for each region and plotted on a histogram. The non-bleach ratio was then subtracted from the bleach region ratio to give a final value for the FRET efficiency ratio. Data from images were used only if YFP bleaching efficiency was greater than 70%.

RESULTS

Syn4 is expressed in the NC and is required for NC development

The expression of zebrafish and *Xenopus syn4* was compared with that of specific neural crest markers. In both species, *syn4* is expressed in the NC as soon as the cells start to migrate (Fig. 1A,G). In zebrafish, the migrating NC can be recognized at 20 hpf as disperse cells in the head and as streams of cells migrating through the somites in the trunk (Fig. 1B,C). This pattern of expression is indistinguishable from that of the NC marker *crestin* (Fig. 1E,F). Visualization of trunk NC is more difficult in *Xenopus*, but a similar pattern of expression of *syn4* was observed in the migrating cephalic NC (Fig. 1G-I), where NC cells were identified with the migratory NC markers *twist* and *fli* (Fig. 1J-L). The early expression of *syn4* in *Xenopus* does not delineate the NC as precisely as do the NC markers (Fig. 1G,J), which suggests that *syn4* is also expressed in cells adjacent to the migrating NC.

This highly localized expression of *syn4* prompted us to analyze its function in NC development. Two morpholino antisense oligonucleotides (MO1, MO2) were developed to inhibit zebrafish *syn4*. We tested the efficiency of MO1 by analyzing its ability to reduce the fluorescence of a Syn4-GFP fusion protein (Fig. 2A-C).

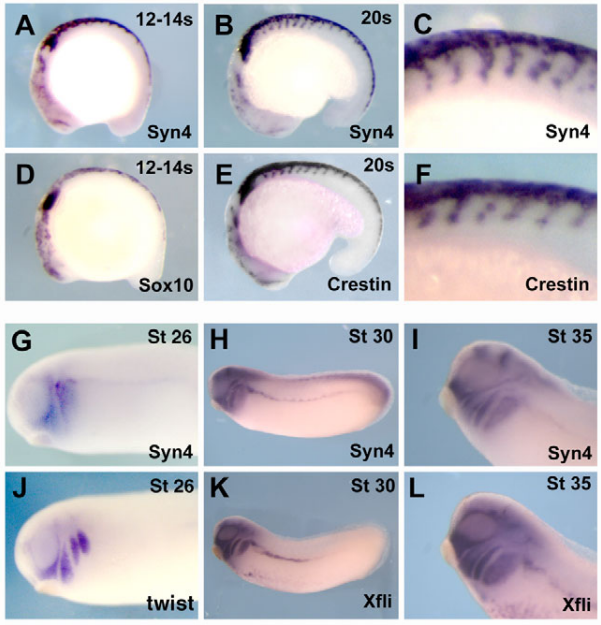

Fig. 1. *syn4* is expressed in the migrating NC. (**A-L**) Lateral views of zebrafish (A-F) and *Xenopus* (G-L) embryos. Anterior is to the left. (A,D) 12- to 14-somite embryo. (B,E) 20-somite embryo; (C,F) higher magnification of the trunk region in B,E. (A-C) *syn4* expression; (D) *sox10* expression; (E,F) *crestin* expression. Note that the expression of *syn4* in the migrating NC cannot be distinguished from the expression of the NC markers. (G,J) Stage 26 embryo. (H,K) Stage 30 embryo. (I,L) Cephalic region of a stage 35 embryo. (G-I) *syn4* expression. (J) *twist* expression. (K,L) *fli* expression. Note the expression of *syn4* in the migrating cephalic NC.

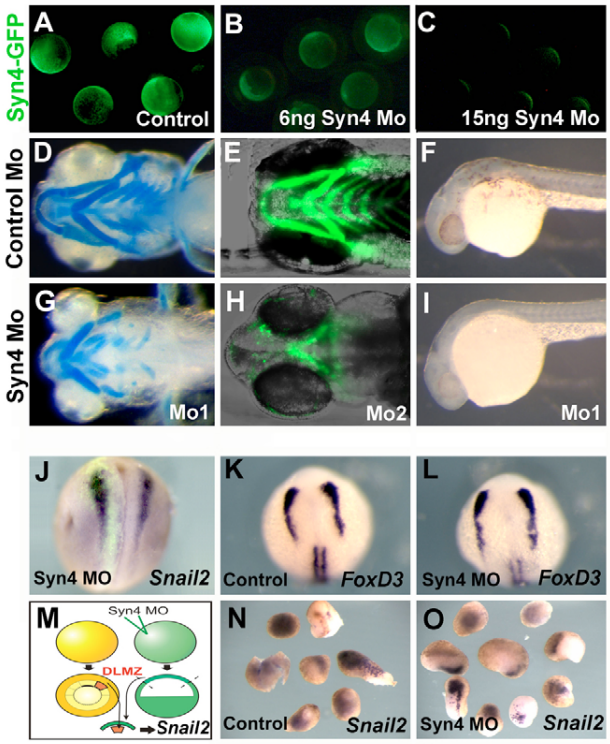

Fig. 2. Syn4 is required for NC development but not for NC induction. (**A-C**) Efficiency of the *syn4* MO. Zebrafish embryos were injected with 250 pg of *syn4-egfp* mRNA containing the MO-binding site (A). Fluorescence was significantly decreased by co-injection of 6 ng *syn4* MO (B) and was totally abolished with 15 ng MO (C), demonstrating that the MO is able to efficiently inhibit Syn4. (**D**,**E**,**G**,**H**) Ventral view of zebrafish embryos showing cartilage development, analyzed by Alcian Blue staining (D,G) or cartilage fluorescence in the *sox10:egfp* line (E,H). (D,E) Control MO; (G) 6 ng of *syn4* MO1; (H) 6 ng of *syn4* MO2. (**F**,**I**) Lateral view of zebrafish embryos showing melanocytes. (F) Control MO; (I) *syn4* MO. (**J-O**) Syn4 is not required for NC induction. (J) *syn4* MO was co-injected with FDX into one blastomere of a two-cell stage *Xenopus* embryo and the expression of *snail2* was analyzed at stage 18, before NC migration. No effect on the expression of *snail2* was observed (96%, *n*=42). (K,L) Zebrafish embryos were injected with control MO (K) or *syn4* MO (L), and the expression of the premigratory NC marker *foxd3* was analyzed. No effect on the expression of *foxd3* was produced by injection of *syn4* MO. (M) *syn4* MO was injected into one-cell stage *Xenopus* embryos, and at the blastula stage animal caps were dissected and conjugated with dorsolateral marginal zone (DLMZ), which is know to induce NC. The expression of *snail2* was analyzed at the equivalent of stage 18. (N) Conjugates of DLMZ with control animal caps show a strong induction of *snail2* (100%, *n*=15). (O) Conjugates of DLMZ with *syn4*-MO injected animal caps also show a strong induction of *snail2* (100%, *n*=10).

Injection of *syn4* MO1 or *syn4* MO2 into zebrafish produces a dramatic reduction of neural crest derivatives, including cartilage (Fig. 2D,E,G,H; see also Fig. S1 in the supplementary material) and melanocytes (Fig. 2F,I; Fig. S1 in the supplementary material). We ruled out a possible role for Syn4 in NC specification by analyzing the expression of early NC markers. No effect on the expression of NC markers was seen in *Xenopus* (Fig. 2J) or zebrafish (Fig. 2K,L) embryos injected with *syn4* MOs. In addition, when either control ectoderm, or ectoderm injected with *syn4* MO, was combined with dorsolateral mesoderm to test for induction of the NC, no difference was observed (Fig. 2M-O).

Syn4 is required for NC migration

Next, we analyzed whether Syn4 is involved in NC migration. Migration of cephalic neural crest can be recognized in *Xenopus* as three streams of cells (Fig. 3A), whereas the migrating trunk NC can be visualized in zebrafish as streams of cells in the somites (Fig. 3F). Injection of *syn4* MO or mRNA leads to a strong inhibition of cephalic and trunk NC migration (Fig. 3B,C,G,H). Co-injection of *syn4* mRNA, which does not contain the MO-binding site, together with the MO can rescue NC migration, demonstrating that the MO specifically targets *syn4* (Fig. 3D,E,I,J). Importantly, however, overexpression of *syn4* carrying a mutation in the PKCα-binding site does not rescue NC migration in *syn4*-MO-injected embryos (Fig. 3E, two last columns), which is different to what has been reported for the effect of this mutation in cells cultured in vitro (Bass et al., 2007).

Our results show that *syn4* MO affects NC migration; however, it is also possible that the MO interferes with NC migration in a non-cell-autonomous manner, as it is known, for example, that *syn4* MO affects convergent extension of mesoderm (Munoz et al., 2006) (L.M. and R.M., unpublished). Two experiments were performed to analyze this possibility. First, we injected zebrafish embryos with a MO against *has2*, the synthesizing enzyme of Hyaluronan, which has been described to perturb convergent extension (Bakkers et al., 2004). Injection of the *has2* MO produced a strong phenotype in convergent extension, as previously described, but no difference in the migration of NC between control and *has2* MO-injected embryos was observed (see Fig. S2A,B in the supplementary material). A second set of experiments were performed to show that *syn4* MO inhibits cell migration in a cell-autonomous manner. Grafts of fluorescein dextran (FDX)- or *syn4* 5-base mismatched MO (*syn4* 5mm MO)-injected *Xenopus* NC into control embryos (Fig. 4A) show normal migration (Fig. 4B,C; uninjected, 87% grafts migrated, n=15; *syn4* 5mm MO, 75% grafts migrated, n=12); however, grafts of NC injected with *syn4* MO exhibit a complete inhibition of migration (Fig. 4D; 0% grafts migrated, n=15). This result suggests that Syn4 is required in a cell-autonomous manner for NC migration. However, the NC graft contains a large number of cells that could affect each other in a non-cell-autonomous manner; therefore, true cell-autonomy can only be examined by grafting single cells. As it is technically difficult to do this in *Xenopus*, we used zebrafish embryos for this experiment, using a transgenic line that expresses GFP only in NC cells (*sox10:egfp*) (Carney et al., 2006). We grafted either NC cells injected with the *syn4* MO into wild-type embryos (Fig. 4E) or wild-type NC cells into embryos injected with the MO (Fig. 4F). Fig. 4G-N shows the GFP-positive cells after 4 hours of migration. The average distance traveled in 4 hours by several grafts is shown in Fig. 4O,P. The control MO did not inhibit NC migration (Fig. 4O,P; compare position at time 0, indicated by the black arrow in Fig. 4G-J with the position 4 hours later, white arrow in Fig. 4H,J). However, *syn4* MO had a significant effect on NC migration,

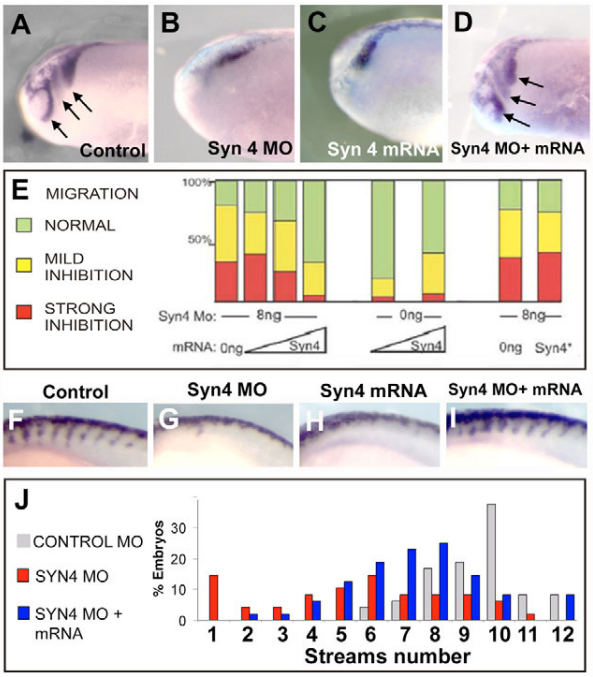

Fig. 3. Syn4 is required for NC migration. (**A-D**) Lateral view of *Xenopus* cephalic NC at stage 24, analyzed by the expression of *snail2*. Arrows indicate streams of migrating NC. (A) 8 ng control MO; (B) 8 ng *syn4* MO; (C) 100 pg *syn4* mRNA; (D) 8 ng *syn4* MO and 100 pg *syn4* mRNA. (**E**) *Xenopus* embryos were injected with 8 ng of *syn4* MO together with 0, 25, 50 or 100 pg of *syn4* mRNA (1st to 4th bar), 50 or 100 pg of *syn4* mRNA only (5th and 6th bar), or 8 ng *syn4* MO with 0 or 150 pg of *syn4* mRNA mutated in the PKCα-binding site (Syn4*, 7th and 8th bar). NC migration was analyzed by the expression of *snail2* at stage 24, as shown in A. Embryos were scored as a normal migration, mild or strong inhibition. Co-injection of *syn4* mRNA rescues the inhibition of NC migration produced by the *syn4* MO (1st to 4th bar), but no rescue is observed with Syn4 mutated in the PKCα-binding site (Syn4*, 7th and 8th bar). (**F-I**) Lateral view of zebrafish at 20 somites. Trunk NC migration was analyzed by the expression of *crestin*. Dorsal to the top; anterior to the left. (F) Control MO (6 ng); (G) *syn4* MO (6 ng); (H) *syn4* mRNA (250 pg); (I) *syn4* MO and *syn4* mRNA. (**J**) NC migration was analyzed by the expression of *crestin* when the embryo had 20 somites. The number of streams of NC migrating through the somites was counted. Co-injection of *syn4* mRNA rescues the reduction in the number of streams of NC produced by *syn4 MO*.

whether present in the grafted NC or in the host (Fig. 4K-P). These results suggest that Syn4 is required autonomously in the NC to control its migration, but that an interaction with other NC cells expressing *syn4* is also required.

Syn4 controls the directionality of NC migration and the orientation of cell protrusions

As the migration of NC cells is a complex process involving an early delamination step followed by active cell migration, we explored which step is affected by *syn4* MO. We used the *sox10:egfp* zebrafish transgenic line to visualize migrating NC cells (Carney et al., 2006).

The movement of individual cephalic NC cells was followed (Fig. 5A-D; similar results were seen with trunk NC, data not shown) and their migration path was tracked (Fig. 5E). A strong inhibition of the migration of NC cells in the *syn4* MO-injected embryos was

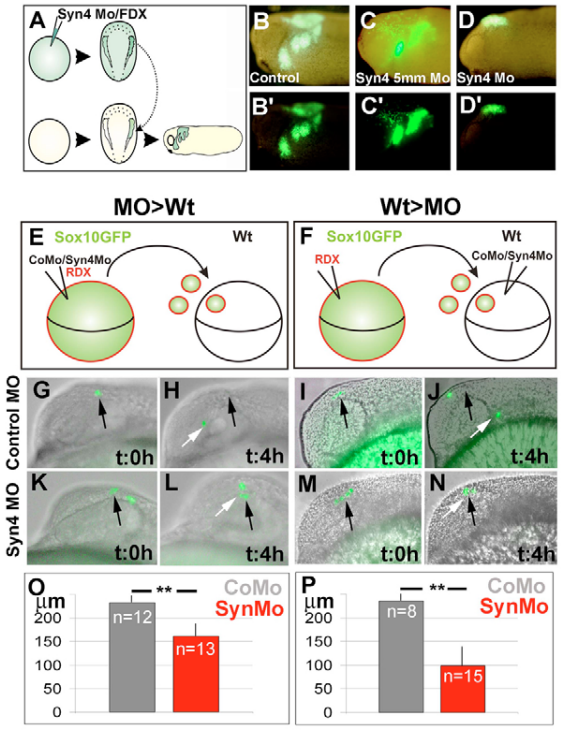

Fig. 4. Syn4 is required for NC migration in a cell- and non-cell-autonomous manner. (**A-D'**) *Xenopus* NC grafts. (A) Embryos were injected at the one-cell stage with 8 ng of *syn4* MO and FDX; at stage 16, the NC were dissected, grafted into a normal host and NC migration was analyzed by looking at the fluorescence. (B,B') Control showing normal NC migration (87% of migration, *n*=15). (C,C') *syn4* 5-base mismatch morpholino *(syn4* 5mm MO)-injected embryo, showing normal NC migration (75% of migration, *n*=12). (D,D') *syn4* MO-injected embryo showing inhibition of NC migration (0% of migration, *n*=15). (**E-P**) Zebrafish graft embryos. (E) *sox10:egfp* embryos were co-injected with RDX and control or *syn4* MO; cells taken from these embryos were grafted into wild-type embryos and NC migration was analyzed. (F) *sox10:egfp* embryos were injected with RDX; cells taken from these embryos were grafted into wild-type embryos previously injected with control or *syn4* MO and NC migration was analyzed. (G-N) GFP-expressing cells were overlapped on DIC image. Black arrow indicates the initial position of the NC; white arrow indicates the position of the NC after 4 hours. (G-J) Control MO; (K-N). *syn4* MO. (O) Average distance traveled for the grafted cells in 4 hours in experiment shown in E. (P) Average distance traveled for the grafted cells in 4 hours in experiment shown in F. ***P*<0.005.

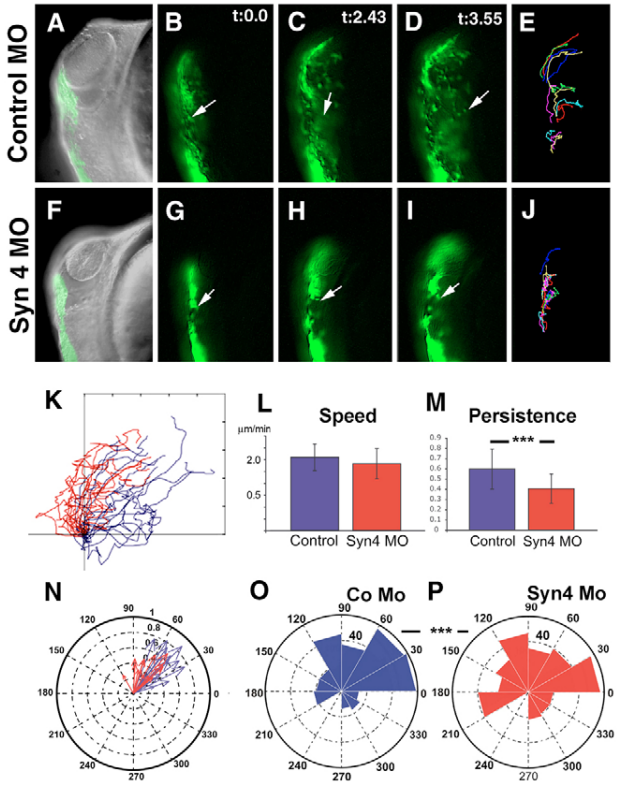

Fig. 5. Syn4 controls the persistence of NC migration. A *sox10:egfp* zebrafish transgenic line was used to analyze NC migration in vivo. (**A-D**,**F-I**) Time lapse of embryos at 16 hpf carried out for 4 hours, three frames (*t*=0.0 min, *t*=2.43 min and *t*=3.55 min) are shown; first frame is also overlapped with a DIC image. Dorsal to the left; anterior to the top. Arrow indicates an individual cell as an example. (**E**,**J**) Trajectories of 4 hours of migration. (A-E) Control MO; (F-J) *syn4* MO. (**K**) Trajectories of cells from different experiments. Blue, control MO; red, *syn4* MO. (**L**) Velocity of migration. (**M**) Persistence of migration. (**N**) Angle of migration for each individual cell. Blue, control MO; red, *syn4* MO. (**O**,**P**) Rose plot showing the distribution of angles of each time point during the 4 hours of migration. The area of each bin represents the number of cells moving in that direction. (O) Control MO; (P) *syn4* MO. ***P*<0.005.

observed (Fig. 5F-I; see also Fig. S3 in the supplementary material); the cells were motile, but their overall migration was reduced, as shown by the cell tracks (Fig. 4J). We confirmed that these effects were not due to a delay in cell migration by analyzing embryos at later stages of development (see Movie 1 in the supplementary material). Moreover, these data suggest that delamination and cell motility are not inhibited, as cells can migrate as individuals. Tracks of individual cells (Fig. 5K) showed no significant difference in the velocity of migration between control and *syn4* MO cells (Fig. 5L; *P*=0.2276, *n*=15). However, the directionality of migration [measured as persistence (the linear displacement of the cell divided by the total distance traveled)] was significantly affected by the *syn*4 MO (Fig. 5M; *P*=0.0049, *n*=15). The distribution of angles of migration for each individual cell at each time point also demonstrated a significant difference between control MO (Fig. 5N,O) and *syn4* MO (Fig. 5N,P; *P*=0.0044, *n*=665) cells. Taken together, these results indicate that the *syn4* MO affects NC migration by interfering with the directionality of migration. As far as we know, this is the first time that a specific effect on the directional migration of NC cells has been described during development.

As persistence of migration usually depends on the orientation of cell protrusions (Ridley et al., 2003), we analyzed whether cell protrusions are affected by the *syn4* MO. In Fig. 6A,B, the NC cells migrating around the optic vesicle (mandibular stream) are shown at two time points. Strikingly, the cell morphologies observed in control MO- (Fig. 6A,B,D; Movie S2 in the supplementary material) and *syn4* MO- (Fig. 6F,G,I; Movie S3 in the supplementary material) injected cells are very different; control cells are elongated along the axis of migration, whereas *syn4* MO-injected cells are more rounded. In order to quantify these differences, we measured two different parameters. First, we measured cell smoothness (CS; defined as the ratio between the perimeter of an ideal ellipse-shaped

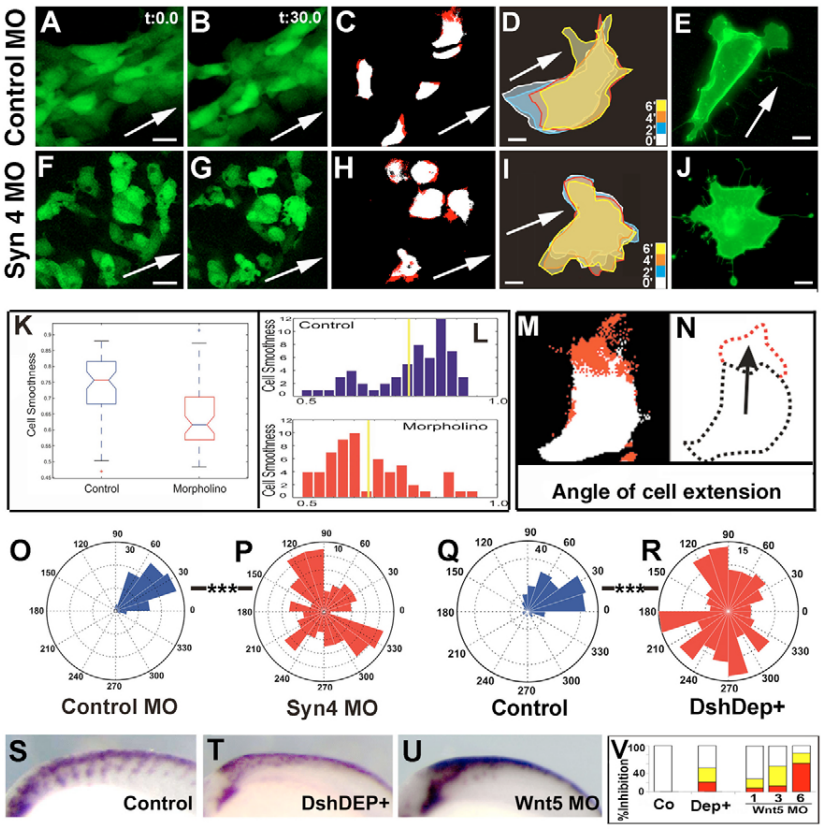

Fig. 6. Syn4 and PCP signaling control the orientation of cell protrusions. (**A**,**B**,**F**,**G**) Time-lapse analysis of the mandibular NC stream of a *sox10:egfp* embryo at 18 hpf for 30 minutes. The initial and final frames are shown. Arrow indicates the expected direction of migration based on the orientation of the embryo. Cell extensions are shown in **C** and **H** in red. (**D**,**I**) Outline of individual cells at different times (minutes). (**E**,**J**) NC cells cultured in vitro, expressing membrane GFP. (A-E) Control MO; (F-J) *syn4* MO. Scale bars: 25 μm in A,F; 10 μm in D,E,I,J. (**K**,**L**) Quantification of cell smoothness (CS) of NC cells. (K) Box-plot showing the distribution of CS values for control and *syn4* MO-injected cells. A significant difference was observed ($P<0.005$). (L) Histogram of CS for control and *syn4*-MO injected cells. (**M**,**N**) Analysis of CE. (M) Two consecutives frames were subtracted, in a manner that the new growing area is shown in red and the unchanged area in white. A vector between the centroid of the cell and the centroid of the red area was drawn (arrow in N). (**O-R**) Rose plots showing the orientation of CE. (O) Control MO; (P) *syn4* MO; (Q) control embryo; (R) embryo injected with DshDep+. Note the difference in scale. Scale bar: 20 μm; ***$P<0.005$. (**S-V**) Non-canonical Wnt signaling is required for zebrafish neural crest migration. Lateral views of dorsal neural tubes of 20-somite zebrafish embryos are shown after *crestin* staining by in situ hybridization. Dorsal to the top; anterior to the left. (S) Control; (T) 200 pg of DshDep+ mRNA; (U) 3 ng of *wnt5* MO. (V) Percentage of inhibition in trunk NC migration. White, no inhibition; yellow, mild inhibition; red, strong inhibition.

cell and the actual perimeter of the cell, which gives us an unbiased measure of how folded a cell is, i.e. how many protrusions a cell has). A significant difference in CS was observed between the control and *syn4* MO (Fig. 6K,L; $P<0.0005$, $n=59$). A second parameter related to cell protrusions that we call cell extension (CE) was also measured (Fig. 6M). We define CE as the new positive area between two consecutives frames (separated by 1 minute). During the course of a minute, the body (and centroid) of the cell does not move a significant distance and careful comparison of the morphology of the cell between consecutive frames strongly suggests that CE corresponds to cell protrusions, such as lamellipodia (Fig. 6C,M). However, fillopodia cannot be observed, as they move faster and the intensity of fluorescence is weaker. Comparison with control and *syn4* MO-injected NC cells cultured in vitro, where the lamellipodia can be easily identified, strongly suggest that our CE corresponds to lamellipodia (Fig. 6C-E). Most CEs are formed at the anterior edge of control cells (Fig. 6C), whereas equivalent CEs are found all over the cell in embryos injected with the *syn4* MO (Fig. 6H). We measured the orientation of CE by calculating the direction of a vector drawn from the centroid of the cell to the centroid of the CE (Fig. 6N). A significant difference in the orientation of the CE was found between control and *syn4* MO cells (Fig. 6O,P; $P<0.005$, $n=180$). In conclusion, *syn4* MO is required for the polarized formation of CEs.

Interestingly, we have previously shown that the inhibition of PCP signaling in vitro in *Xenopus* NC cells leads to the formation of long cell protrusions all over the cells (De Calisto et al., 2005), reminiscent of the phenotype observed here for *syn4* MO. In order to confirm this finding in vivo, we carried out a similar analysis of CE in zebrafish. First, we had to test that non-canonical Wnt signaling is also required for NC migration in zebrafish embryos, as this has only been shown in *Xenopus*. Three different treatments that specifically affect PCP signaling were used and migration of trunk neural crest was analyzed (Fig. 6S). Embryos injected with a dominant-negative form of Dishevelled (Dsh) specific for the PCP pathway (DshDep+), or with a MO that has been shown to specifically inhibit *wnt5* (Kilian et al., 2003; Lele et al., 2001) (Fig. 6S-V), and the PCP mutant *tri* (*trilobite*, also known as *strabismus*;

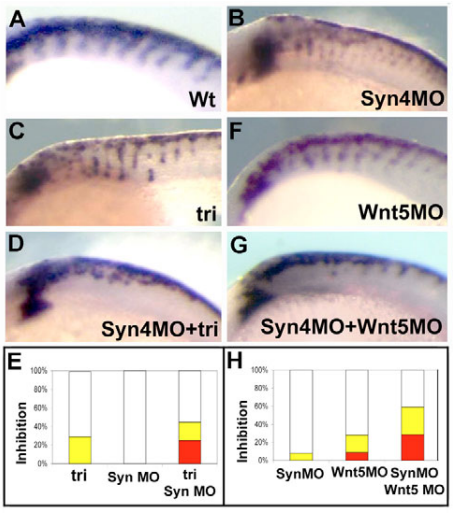

Fig. 7. Interaction between Syn4 and PCP signaling. Zebrafish genetic interaction experiment. Lateral views of dorsal neural tubes of 20-somite zebrafish embryos are shown after *crestin* staining by in situ hybridization. Dorsal to the top; anterior to the left. (**A**) Wild-type embryo. (**B**) Wild-type embryo injected with 1 ng of *syn4* MO. (**C**) *tri* mutant. (**D**) *tri* mutant injected with 1 ng of *syn4* MO. (**E**) Percentage of inhibition of NC migration. White, no inhibition; yellow, mild inhibition; red, strong inhibition. (**F**) Wild-type embryo injected with 1 ng of *wnt5* MO. (**G**) Wild-type embryo co-injected with 1 ng of *wnt5* MO and 1 ng of *syn4* MO. (**H**) Percentage of inhibition of trunk NC migration.

Fig. 7C) showed defects in NC migration, although the *tri* mutant exhibited a milder NC phenotype than those caused by the other two treatments. These results show that in zebrafish, as in *Xenopus* (De Calisto et al., 2005), PCP signaling is required for NC migration. Next, we used the *sox10:egfp* transgenic line to analyze the orientation of CE after Dsh inhibition by injection of DshDep+. A significant difference in the orientation of CE was observed compared with control NC cells (Fig. 6Q,R; $P<0.0005$, $n=101$). Taken together, our results show that both the activity of Syn4 and PCP signaling are required to restrict the formation of CEs to the anterior edge of the cell in vivo.

As the inhibition of Syn4 and PCP signaling produce a similar NC phenotype, we investigated whether there was an interaction between these two signals by performing a genetic interaction study in zebrafish embryos. *syn4* MO was co-injected with a MO specific for *wnt5* (Kilian et al., 2003; Lele et al., 2001). When 1 ng of *syn4* or *wnt5* MO was injected into wild-type embryos only a mild inhibition of NC migration was observed (Fig. 7B,F); however, co-injection of both MOs together produced a much stronger NC phenotype (Fig. 7G,H). An equivalent experiment, with similar results, was performed with the *tri* mutant (Fig. 7A,C,D). These results indicate that Syn4 interacts genetically with the PCP signaling pathway. This genetic interaction could be compatible with either a hierarchical relationship between Syn4 and Dsh, or an interaction between two parallel pathways.

Syn4 and PCP signaling control the localized activity of Rac and RhoA

It has been observed in many in vitro studies of cell migration that cell polarity and the formation of cell protrusions are dependent on the activity of members of the small Rho GTPase family (Jaffe and Hall, 2005). To analyze the activity of GTPases in the NC in vitro and in vivo, we used fluorescence resonance energy transfer (FRET) biosensors for Cdc42, Rac and RhoA (Itoh et al., 2002; Pertz et al., 2006). The inhibition of Syn4 leads to a fivefold increase in Rac activity (Fig. 8A-C). No significant effect on the activity or localization of Cdc42 or RhoA was seen between control and *syn4* MO-injected cells (Fig. 8A). Therefore, Syn4 inhibits Rac activity in the NC cell migrating in vitro.

Next, we investigated whether Dsh could also play a role in GTPase signaling. The activation of Cdc42, Rac and RhoA was compared among control NC cells and cells from embryos injected with DshΔn or DshDep+ (Fig. 8D-F). The activation or inhibition of

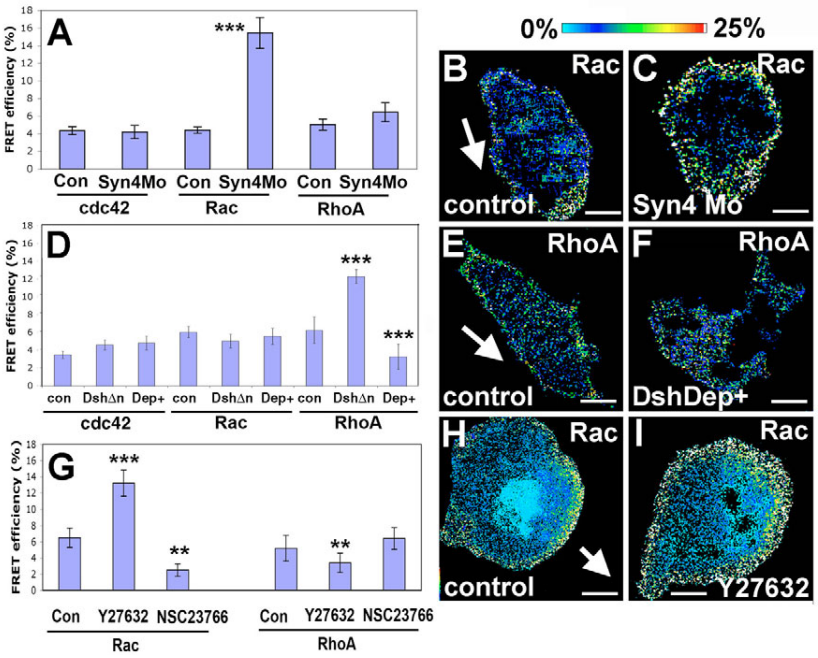

Fig. 8. FRET analysis of Cdc42, Rac and RhoA activity in NC migrating in vitro after modification of Syn4 and PCP signaling. Embryos were injected with the probes for Cdc42, Rac and RhoA. Neural crest was dissected, cultured in vitro and FRET analysis performed. (**A**) FRET efficiency for Cdc42, Rac and RhoA in control or *syn4* MO-injected NC cells. (**B**) Rac FRET efficiency for control NC. Arrow indicates the direction of migration, determined by time-lapse analysis of cell behavior immediately before fixation. (**C**) Rac FRET efficiency for *syn4* MO NC. (**D**) FRET efficiency for Cdc42, Rac and RhoA in control or cells injected with 1 ng DshΔn or 1 ng DshDep+ (Dep+). (**E**) RhoA FRET efficiency for control NC. Arrow indicates the direction of migration. (**F**) RhoA FRET efficiency for DshDep+-injected NC. (**G**) FRET analysis for RhoA and Rac was performed after treatment with the RhoA inhibitor Y27632 or the Rac inhibitor NSC23766. (**H**) Rac FRET efficiency for control NC. Arrow indicates the direction of migration. (**I**) Rac FRET efficiency for the cell treated with Y27632. ***$P<0.005$; **$P<0.01$. Scale bar: 10 μm.

Dsh had no significant effect on the activity of Cdc42 or Rac (Fig. 8D). However, the activation of Dsh led to a significant increase in RhoA activity, whereas the inhibition of Dsh produced a significant decrease in RhoA activity (Fig. 8D-F). Thus, Dsh-PCP promotes RhoA activity in NC migration in vitro.

Crosstalk between Rac and RhoA has been described in a number of different cell types. We wished to discover whether a similar feedback loop was present in the NC cells. Cells were treated with Y27632 to specifically inhibit the RhoA effector Rock (Uehata et al., 1997), or with NSC23766 to inhibit Rac activity (Gao et al., 2004), and the activity of Rac and RhoA was analyzed by FRET. The inhibition of Rock led to a significant increase in Rac activation (Fig. 8G-I), suggesting that RhoA (Rock) can act as an inhibitor of Rac activity in the NC cells. In addition, the inhibition of Rock produced an increase in cell protrusions in different directions, whereas the inhibition of Rac reduced the number of cell protrusions (not shown).

These measurements of small Rho GTPase activity were performed in NC cells cultured on fibronectin in vitro. A growing number of reports suggest that there are important differences in the migration of cells cultured in two-dimensional (2D) versus 3D matrices (Even-Ram and Yamada, 2005), and that those differences could be even bigger when cell migration is analyzed in vivo, so we decided to perform FRET analysis of NC cells migrating in the embryo. To our knowledge, this is the first time that small GTPase activity has been observed in vivo using FRET. DNA coding the FRET probes for RhoA and Rac was injected in blastomeres fated to become NC cells. At the early neurula stages, the NCs were dissected from the injected *Xenopus* embryos and grafted into control hosts. NC cells could be identified by the fluorescence of membrane-RFP, which was co-injected with each probe. During migration the embryos were fixed and sectioned, and FRET analysis was performed. Fig. 9A-D shows the migrating NC, and in Fig. 9A′-D′ cells expressing the biosensors can be seen. Examples of FRET efficiency for individual cells migrating in vivo are shown in Fig. 9E-H. A clear increase in Rac activity is observed in *syn4* MO cells (Fig. 9I), whereas an inhibition of RhoA is observed after Dsh inhibition (Fig. 9J). This confirms our in vitro observations, indicating that, in terms of Rho GTPase regulation, there is no apparent difference between the 2D in vitro and in vivo migration of NC cells. Taken together, our results indicate that Syn4 acts as an inhibitor of Rac and that the Dsh-PCP pathway promotes the activity of RhoA. In addition, activation of RhoA by PCP signaling may also result in Rac inhibition via the inhibitory activity of Rock upon Rac. These data all support a model whereby the Syn4 and PCP activities converge to polarize the formation of cell protrusions, restricting them to the front of the cell. More specifically, they control the levels of Rac, by both a Rac-Syn4 and a RhoA-PCP dependent pathway.

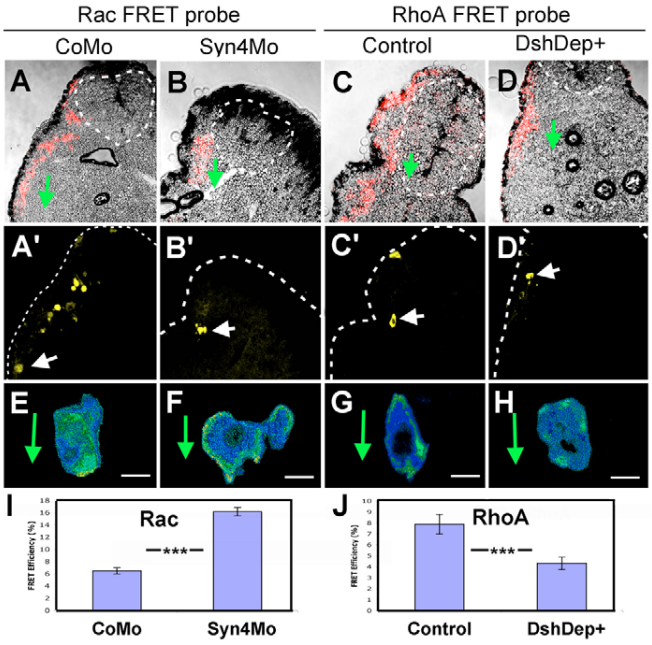

Fig. 9. FRET analysis in vivo for Rac and RhoA after modification of Syn4 and PCP signaling. Embryos were injected with the FRET probes for Rac and RhoA and membrane-RFP. Before migration, the NCs were grafted into wild-type host embryos. NC migration was observed in vivo and then the embryos were fixed, sectioned and processed for FRET analysis. (**A-D**) Overlay of membrane-RFP and bright-field images. Dotted circle indicates the neural tube; arrow, direction of migration. (**A′-D′**) Fluorescence from the FRET probes. Arrow indicates the selected cells shown in E-H. (**E-H**) Examples of FRET efficiency. Arrow indicates the direction of migration. (A,A′,E) Rac probe in cells injected with control MO. (B,B′,F) Rac probe in cells injected with *syn4* MO. (C,C′,G) RhoA probe in cells injected with control MO. (D,D′,H) RhoA probe in cells injected with DshDep+. (**I**) FRET efficiency for Rac. (**J**) FRET efficiency for RhoA. ***P<0.005. Scale bar: 10 μm.

DISCUSSION

Here, we reveal a crucial role for Syn4 in the migration of NC cells in vivo during embryo development, and its interaction with PCP signaling. Our main conclusions are that: (1) *syn4* is expressed almost exclusively in the NC; (2) Syn4 and PCP signaling control the directional migration of NC cells by regulating the polarized formation of cell protrusions; and (3) Syn4 inhibits Rac, whereas Dsh promotes RhoA activity in the NC cell. Thus, Syn4 and PCP signaling work in a coordinated manner to control the directionality of NC migration both in vitro and in vivo, by regulating cell polarity and the cytoskeletal machinery that controls the formation of cell protrusions.

Cdc42 has been shown to be active at the front of migrating cells and it has been suggested that this may be required for cell polarity (Etienne-Manneville and Hall, 2002). However, more recent studies show no significant effects of loss of Cdc42 upon cell polarity [either by genetic ablation or siRNA targeting (Czuchra et al., 2005; Pankov et al., 2005)]. Our data demonstrate that the inhibition of Syn4 or PCP has no effect on the activation status of Cdc42, despite having a profound effect upon cell polarity and directed migration. This would suggest that in NC migration, Cdc42 is not the primary GTPase regulating polarization and protrusion formation.

Rac activation at the front of a cell has also been shown to be a key event for directional migration (Grande-Garcia et al., 2005; Nishiya et al., 2005). Several factors control the localized activity of Rac, such as specific guanine nucleotide-exchange factors (GEFs) that are delivered to the front of the cell in a PI3K-dependent manner (Welch et al., 2003), and the formation of lipid rafts (del Pozo et al., 2004). Once Rac is active, numerous feedback loops help to maintain directional protrusions (Ridley et al., 2003). We have shown here that Syn4 contributes to the inhibition of Rac, as an antisense MO against *syn4* increases the levels of Rac in the entire cell, leading to loss of cell polarity similar to that seen in other cells types in vitro (Bass et al., 2007; Saoncella et al., 2004). Bass and colleagues showed that the regulation of Rac levels by Syn4 contributes to a persistent migration in vitro, with Syn4-null fibroblasts showing an activation of Rac around the cell periphery

(Bass et al., 2007), similar to what we have observed in the NC. However, there are some notable differences between their results and those shown here, primarily that they demonstrate that Syn4 stimulates a wave of Rac activation upon initial cell spreading, whereas we only observed a negative regulation of Rac by Syn4. Additionally, Bass et al. showed that Syn4 containing a mutation in the PKCα-binding site was able to rescue persistent migration in vitro, whereas we were unable to rescue the embryonic phenotype of the *syn4* MO with this same mutant. Thus, our results support the previous notion that the PKCα-binding site is essential for Syn4 function (Alexopoulou et al., 2007). The differences between our results and those of Bass et al. (Bass et al., 2007) could be due to the added complexity of migration in an in vivo environment, or to an intrinsic difference between NC cells and fibroblasts.

Differences in cell migration in vivo and in vitro have been widely documented. A number of research groups have now begun to switch to 3D models, which provide a better representation of the microenvironment of living tissues (Even-Ram and Yamada, 2005). There are some key differences between cell migration in two and three dimensions. For example, $\alpha_v\beta_3$ integrin is not detected in 3D-matrix adhesion, and focal adhesion kinase (FAK) is less phosphorylated at residue Y397 in fibroblasts in a 3D matrix than it is in those on a 2D substrate (Cukierman et al., 2001). It has been suggested that Syn4 plays no role in migration in vivo, as, despite its role in vitro, the disruption of Syn4 in mice causes only a relatively minor and specific defect in wound healing (Echtermeyer et al., 2001). However, here, we have demonstrated a clear role for Syn4 in controlling cell migration in vivo. The minor phenotype in mice could be due to redundancy between syndecans, with Syn1 possibly being able to compensate for the lack of Syn4 activity. Interestingly, Syn1 has not been found in zebrafish (R.M., unpublished). A double Syn4/Syn1 mouse knock-out would be able to clarify this point.

Unlike with Syn4, no significant effect on Rac activity was observed after modifying PCP signaling in our study, consistent with the role of Rock on convergent extension (Marlow et al., 2002). This is paradoxical, because we show that PCP signaling promotes RhoA activation and that RhoA, via Rock, inhibits the activity of Rac in NC cells. One possible explanation is that a residual amount of RhoA remaining after Dsh inhibition is sufficient to maintain the normal Rac level.

It has been demonstrated that RhoA, Rac1 and Cdc42 all act downstream of PCP signaling (Choi and Han, 2002; Habas et al., 2003; Penzo-Mendez et al., 2003). Convergent extension in *Xenopus* and zebrafish are dependent on RhoA/Rac activity, controlled by PCP signaling (Habas et al., 2003; Habas et al., 2001; Tahinci and Symes, 2003). Our results show that RhoA, but not Rac, is dependent on PCP signaling. Interestingly, a triple deletion of the three Rac genes in *Drosophila*, *Rac1*, *Rac2* and *Mtl*, fails to cause PCP defects (Adler, 2002; Hakeda-Suzuki et al., 2002), suggesting that Rac signaling is not essential for the PCP pathway.

One open question is: how exactly does Syn4 interact with PCP signaling to control NC migration? Our results clearly indicate that Syn4 and PCP activate two parallel pathways that lead to the inhibition of Rac activity and the activation of RhoA, respectively (Fig. 10). However, we also show that RhoA inhibits Rac activity in the NC. Thus, both pathways ultimately have the same effect of decreasing the overall levels of Rac, either directly or indirectly, which is necessary for the polarized formation of cell protrusions and for maintaining persistent migration (Pankov et al., 2005). The requirement for precise levels of Rac signaling for persistent migration may explain why both inhibition and overexpression of

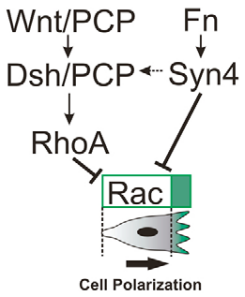

Fig. 10. Model of NC polarization by Wnt/PCP and Syn4. Non-canonical Wnt signaling (Wnt/Dsh/PCP) activates RhoA, which in turn inhibits Rac activity, whereas Syn4 (activated by Fibronectin, Fn) inhibits Rac activity directly. The concerted activation of these parallel pathways leads to the inhibition of Rac (green) at the back of the cell, with the consequent formation of cell protrusions at the front of the cell and directional migration (thick arrow). There is also evidence of an interaction between Syn4 and Dsh (broken arrow).

Syn4 produce an inhibition of migration, as has been previously shown for the PCP signaling pathway (De Calisto et al., 2005; Wallingford et al., 2000). It has recently been shown that Syn4 interacts with PCP signaling during convergent extension of the mesoderm (Munoz et al., 2006). They propose a direct interaction of Syn4 with Dsh and Frz7. Thus, it is possible that, in addition to this interaction between Syn4 and the Wnt receptor, each of these molecules could lead to the activation of parallel pathways that control the activity of small GTPases, as we have shown here.

Chemotaxis has been suggested as one of the mechanisms to explain the directional migration of NC cells; however, there is no sound evidence for this proposal. Moreover, persistent directional migration occurs in vitro in the absence of chemoattractants. Instead, interactions between the extracellular matrix, integrins, and the levels of Rac and Syn4 can control persistent migration (Bass et al., 2007; Choma et al., 2004; Pankov et al., 2005; White et al., 2007). Here, we provide evidence that a similar mechanism regulates the migration of NC cells in vivo. Syn4 and PCP signaling in the NC act on RhoA and Rac to maintain the balance of Rac required for the formation of directional cell protrusions, which results in a persistent, directional migration.

We thank M. Tada for useful comments and reagents during the course of this work. We also thank C. Stern for comments on the manuscript, R. Kelsh for the *sox10:egfp* transgenic line, M. Matsuda for the Cdc42 and Rac FRET probes, and K. Hahn for the RhoA FRET probe. This investigation was supported by grants from the MRC and BBSRC. H.K.M. and C.C.-F. are MRC and Boehringer Ingelheim Fonds PhD scholarship holders, respectively.

Supplementary material

Supplementary material for this article is available at
http://dev.biologists.org/cgi/content/full/135/10/1771/DC1

References

Adler, P. N. (2002). Planar signaling and morphogenesis in Drosophila. *Dev. Cell.* **2**, 525-535.

Alexopoulou, A. N., Multhaupt, H. A. and Couchman, J. R. (2007). Syndecans in wound healing, inflammation and vascular biology. *Int. J. Biochem. Cell Biol.* **39**, 505-528.

Alfandari, D., Cousin, H., Gaultier, A., Hoffstrom, B. G. and DeSimone, D. W. (2003). Integrin α5β1 supports the migration of Xenopus cranial neural crest on fibronectin. *Dev. Biol.* **260**, 449-464.

Aybar, M. J., Nieto, M. A. and Mayor, R. (2003). Snail precedes slug in the genetic cascade required for the specification and migration of the Xenopus neural crest. *Development* **130**, 483-494.

Bakkers, J., Kramer, C., Pothof, J., Quaedvlieg, N. E., Spaink, H. P. and Hammerschmidt, M. (2004). Has2 is required upstream of Rac1 to govern dorsal migration of lateral cells during zebrafish gastrulation. *Development* **131**, 525-537.
Barrallo-Gimeno, A., Holzschuh, J., Driever, W. and Knapik, E. W. (2004). Neural crest survival and differentiation in zebrafish depends on mont blanc/tfap2a gene function. *Development* **131**, 1463-1477.
Bass, M. D., Roach, K. A., Morgan, M. R., Mostafavi-Pour, Z., Schoen, T., Muramatsu, T., Mayer, U., Ballestrem, C., Spatz, J. P. and Humphries, M. J. (2007). Syndecan-4-dependent Rac1 regulation determines directional migration in response to the extracellular matrix. *J. Cell Biol.* **177**, 527-538.
Carney, T. J., Dutton, K. A., Greenhill, E., Delfino-Machin, M., Dufourcq, P., Blader, P. and Kelsh, R. N. (2006). A direct role for Sox10 in specification of neural crest-derived sensory neurons. *Development* **133**, 4619-4630.
Choi, S. C. and Han, J. K. (2002). Xenopus Cdc42 regulates convergent extension movements during gastrulation through Wnt/Ca^{2+} signaling pathway. *Dev. Biol.* **244**, 342-357.
Choma, D. P., Pumiglia, K. and DiPersio, C. M. (2004). Integrin α3β1 directs the stabilization of a polarized lamellipodium in epithelial cells through activation of Rac1. *J. Cell Sci.* **117**, 3947-3959.
Cukierman, E., Pankov, R., Stevens, D. R. and Yamada, K. M. (2001). Taking cell-matrix adhesions to the third dimension. *Science* **294**, 1708-1712.
Czuchra, A., Wu, X., Meyer, H., van Hengel, J., Schroeder, T., Geffers, R., Rottner, K. and Brakebusch, C. (2005). Cdc42 is not essential for filopodium formation, directed migration, cell polarization, and mitosis in fibroblastoid cells. *Mol. Biol. Cell* **16**, 4473-4484.
De Calisto, J., Araya, C., Marchant, L., Riaz, C. F. and Mayor, R. (2005). Essential role of non-canonical Wnt signalling in neural crest migration. *Development* **132**, 2587-2597.
del Pozo, M. A., Alderson, N. B., Kiosses, W. B., Chiang, H. H., Anderson, R. G. and Schwartz, M. A. (2004). Integrins regulate Rac targeting by internalization of membrane domains. *Science* **303**, 839-842.
Echtermeyer, F., Streit, M., Wilcox-Adelman, S., Saoncella, S., Denhez, F., Detmar, M. and Goetinck, P. (2001). Delayed wound repair and impaired angiogenesis in mice lacking syndecan-4. *J. Clin. Invest.* **107**, R9-R14.
Etienne-Manneville, S. and Hall, A. (2002). Rho GTPases in cell biology. *Nature* **420**, 629-635.
Even-Ram, S. and Yamada, K. M. (2005). Cell migration in 3D matrix. *Curr. Opin. Cell Biol.* **17**, 524-532.
Gao, Y., Dickerson, J. B., Guo, F., Zheng, J. and Zheng, Y. (2004). Rational design and characterization of a Rac GTPase-specific small molecule inhibitor. *Proc. Natl. Acad. Sci. USA* **101**, 7618-7623.
Grande-Garcia, A., Echarri, A. and Del Pozo, M. A. (2005). Integrin regulation of membrane domain trafficking and Rac targeting. *Biochem. Soc. Trans.* **33**, 609-613.
Habas, R., Dawid, I. B. and He, X. (2003). Coactivation of Rac and Rho by Wnt/Frizzled signaling is required for vertebrate gastrulation. *Genes Dev.* **17**, 295-309.
Habas, R., Kato, Y. and He, X. (2001). Wnt/Frizzled activation of Rho regulates vertebrate gastrulation and requires a novel Formin homology protein Daam1. *Cell* **107**, 843-854.
Hakeda-Suzuki, S., Ng, J., Tzu, J., Dietzl, G., Sun, Y., Harms, M., Nardine, T., Luo, L. and Dickson, B. J. (2002). Rac function and regulation during Drosophila development. Nature **416**, 438-442.
Harland, R. M. (1991). In situ hybridization: an improved whole-mount method for Xenopus embryos. *Methods Cell Biol.* **36**, 685-695.
Itoh, R. E., Kurokawa, K., Ohba, Y., Yoshizaki, H., Mochizuki, N. and Matsuda, M. (2002). Activation of Rac and Cdc42 video imaged by fluorescent resonance energy transfer-based single-molecule probes in the membrane of living cells. *Mol. Cell. Biol.* **22**, 6582-6591.
Jaffe, A. B. and Hall, A. (2005). Rho GTPases: biochemistry and biology. *Annu. Rev. Cell Dev. Biol.* **21**, 247-269.
Kelsh, R. N., Dutton, K., Medlin, J. and Eisen, J. S. (2000). Expression of zebrafish fkd6 in neural crest-derived glia. *Mech. Dev.* **93**, 161-164.
Kilian, B., Mansukoski, H., Barbosa, F. C., Ulrich, F., Tada, M. and Heisenberg, C. P. (2003). The role of Ppt/Wnt5 in regulating cell shape and movement during zebrafish gastrulation. *Mech. Dev.* **120**, 467-476.
Kuriyama, S. and Mayor, R. (2008). Molecular analysis of neural crest migration. *Philos. Trans. R. Soc. Lond. B Biol. Sci.* **363**, 1349-1362.
Lauffenburger, D. A. and Horwitz, A. F. (1996). Cell migration: a physically integrated molecular process. *Cell* **84**, 359-369.
LeDouarin, N. M. and Kalcheim, C. (1999). *The Neural Crest*, 2nd edn. Cambridge: Cambridge University Press.
Lele, Z., Bakkers, J. and Hammerschmidt, M. (2001). Morpholino phenocopies of the swirl, snailhouse, somitabun, minifin, silberblick, and pipetail mutations. *Genesis* **30**, 190-194.
Luo, R., An, M., Arduini, B. L. and Henion, P. D. (2001). Specific pan-neural crest expression of zebrafish Crestin throughout embryonic development. *Dev. Dyn.* **220**, 169-174.
Mancilla, A. and Mayor, R. (1996). Neural crest formation in Xenopus laevis: mechanisms of Xslug induction. *Dev. Biol.* **177**, 580-589.
Marlow, F., Topczewski, J., Sepich, D. and Solnica-Krezel, L. (2002). Zebrafish Rho kinase 2 acts downstream of Wnt11 to mediate cell polarity and effective convergence and extension movements. *Curr. Biol.* **12**, 876-884.
Mayor, R., Morgan, R. and Sargent, M. G. (1995). Induction of the prospective neural crest of Xenopus. *Development* **121**, 767-777.
Meyer, D., Stiegler, P., Hindelang, C., Mager, A. M. and Remy, P. (1995). Whole-mount in situ hybridization reveals the expression of the Xl-Fli gene in several lineages of migrating cells in Xenopus embryos. *Int. J. Dev. Biol.* **39**, 909-919.
Munoz, R., Moreno, M., Oliva, C., Orbenes, C. and Larrain, J. (2006). Syndecan-4 regulates non-canonical Wnt signalling and is essential for convergent and extension movements in Xenopus embryos. *Nat. Cell Biol.* **8**, 492-500.
Nieuwkoop, P. D. and Faber, J. (1967). *Normal Table of* Xenopus laevis *(Doudin)*. Amsterdam: Elsevier-North Holland Publishing.
Nishiya, N., Kiosses, W. B., Han, J. and Ginsberg, M. H. (2005). An alpha4 integrin-paxillin-Arf-GAP complex restricts Rac activation to the leading edge of migrating cells. *Nat. Cell. Biol.* **7**, 343-352.
Pankov, R., Endo, Y., Even-Ram, S., Araki, M., Clark, K., Cukierman, E., Matsumoto, K. and Yamada, K. M. (2005). A Rac switch regulates random versus directionally persistent cell migration. *J. Cell Biol.* **170**, 793-802.
Penzo-Mendez, A., Umbhauer, M., Djiane, A., Boucaut, J. C. and Riou, J. F. (2003). Activation of Gβγ signaling downstream of Wnt-11/Xfz7 regulates Cdc42 activity during Xenopus gastrulation. *Dev. Biol.* **257**, 302-314.
Pertz, O., Hodgson, L., Klemke, R. L. and Hahn, K. M. (2006). Spatiotemporal dynamics of RhoA activity in migrating cells. *Nature* **440**, 1069-1072.
Pollard, T. D. and Borisy, G. G. (2003). Cellular motility driven by assembly and disassembly of actin filaments. *Cell* **112**, 453-465.
Ridley, A. J., Schwartz, M. A., Burridge, K., Firtel, R. A., Ginsberg, M. H., Borisy, G., Parsons, J. T. and Horwitz, A. R. (2003). Cell migration: integrating signals from front to back. *Science* **302**, 1704-1709.
Saoncella, S., Calautti, E., Neveu, W. and Goetinck, P. F. (2004). Syndecan-4 regulates ATF-2 transcriptional activity in a Rac1-dependent manner. *J. Biol. Chem.* **279**, 47172-47176.
Sheetz, M. P., Felsenfeld, D., Galbraith, C. G. and Choquet, D. (1999). Cell migration as a five-step cycle. *Biochem. Soc. Symp.* **65**, 233-243.
Tada, M. and Smith, J. C. (2000). Xwnt11 is a target of Xenopus Brachyury: regulation of gastrulation movements via Dishevelled, but not through the canonical Wnt pathway. *Development* **127**, 2227-2238.
Tahinci, E. and Symes, K. (2003). Distinct functions of Rho and Rac are required for convergent extension during Xenopus gastrulation. *Dev. Biol.* **259**, 318-335.
Teddy, J. M. and Kulesa, P. M. (2004). In vivo evidence for short- and long-range cell communication in cranial neural crest cells. *Development* **131**, 6141-6151.
Uehata, M., Ishizaki, T., Satoh, H., Ono, T., Kawahara, T., Morishita, T., Tamakawa, H., Yamagami, K., Inui, J., Maekawa, M. and Narumiya, S. (1997). Calcium sensitization of smooth muscle mediated by a Rho-associated protein kinase in hypertension. *Nature* **389**, 990-994.
Wallingford, J. B., Rowning, B. A., Vogeli, K. M., Rothbacher, U., Fraser, S. E. and Harland, R. M. (2000). Dishevelled controls cell polarity during Xenopus gastrulation. *Nature* **405**, 81-85.
Welch, H. C., Coadwell, W. J., Stephens, L. R. and Hawkins, P. T. (2003). Phosphoinositide 3-kinase-dependent activation of Rac. *FEBS Lett.* **546**, 93-97.
Westerfield, M. (2000). *The Zebrafish Book. A guide for the laboratory use of zebrafish* (Danio rerio). 4th edn. Eugene, OR: University of Oregon Press.
White, D. P., Caswell, P. T. and Norman, J. C. (2007). αvβ3 and α5β1 integrin recycling pathways dictate downstream Rho kinase signaling to regulate persistent cell migration. *J. Cell Biol.* **177**, 515-525.

[Cell Adhesion & Migration 2:4, 240-242; October/November/December 2008]; ©2008 Landes Bioscience

Commentary & View

Directional cell migration in vivo

Wnt at the crest

Carlos Carmona-Fontaine, Helen Matthews and Roberto Mayor*

Department of Cell and Developmental Biology; University College London; London, UK

Key words: directional migration, cell migration, syndecan-4, PCP, non-canonical Wnt, neural crest, RhoA, Rac

Directional cell migration is essential for almost all organisms during embryonic development, in adult life and contributes to pathological conditions. This is particularly critical during embryogenesis where it is essential that cells end up in their correct, precise locations in order to build a normal embryo. Many cells have solved this problem by following a gradient of a chemoattractant usually secreted by their target tissues. Our recent research has found an alternative, complimentary, mechanism where intracellular signals are able to generate cell polarity and directional migration in absence of any external chemoattactant. We used neural crest cells to study cell migration in vivo, by performing live imagining of the neural crest cell migrating during embryo development. We show that the Planar Cell Polarity (PCP) or non-canonical Wnt signaling pathway interacts with the proteoglycan syndecan-4 to control the direction in which cell protrusions are generated, and in consequence, the direction of migration. By analyzing the activity of the small GTPases using in vivo FRET imaging we showed that PCP signaling activates RhoA, while syndecan-4 inhibits Rac, both at the back of the neural crest cell. Here we discuss a model where these signals are integrated to generate directional migration in vivo.

The ability of cells to move in a directed manner is a fundamental requirement for life. In multi-cellular organisms, this requirement begins in the embryo, where morphogenetic processes are dependent on the correct movement of large numbers of cells. In the adult too, cell migration plays a vital role in many systems including the immune system and wound healing. Cell migration defects can contribute to the pathology of many diseases including vascular diseases such as atherosclerosis, and chronic inflammatory diseases like asthma and multiple sclerosis. Likewise, metastasis in cancer is characterized by mis-regulation of the normal cell migration machinery and results in cells that are normally static becoming aggressively motile and invasive.

Cell migration requires cell polarization and the formation of protrusions at one end of the cell. Polarization results in a different molecular ensemble at the front of the cell compared to that at the back. Cell protrusion formation at the front of the cell requires reorganization of the actin and microtubule cytoskeleton to produce a protrusion either in the form of a broad sheet-like lamellipodium or spiky filopodium. Small GTPases are well known modulators of these processes (reviewed in ref. 1).

Several mechanism has been proposed as involved in directional migration during embryo development, such as chemotaxis (migration toward an soluble chemoattractant),[2] haptotaxis (migration toward a substrate-bound chemoattractant),[3] population pressure (migration from a region of high towards a region of low cell density)[4] and contact inhibition of locomotion (change in the direction of migration as a consequence of cell-cell contact),[5] being chemotaxis the most widely accepted and studied.

The correct orientation of the cell and its protrusion is the keystone of directional migration and, in the case of chemotaxis, it is supposed to be controlled by the action of external chemical cues (chemoattractants) that are produced by or near to the target tissue.[6] One of the best examples for chemoattraction in vivo is the migration of the progenitor germ cells, which are attracted by the chemokine SDF-1.[2] It has been shown in vitro and in vivo, that upon receiving a chemotactic signal, the cell becomes polarized in the direction of migration. Nevertheless, it is known that cells cultured in vitro can became polarized and exhibit directional migration in absence of extrinsic chemoattractants.[7] Pankov et al. showed that persistent directional migration in vitro can be achieved solely by modulating the activity of the small GTPase, Rac: high levels of Rac promotes the formation of peripheral lamella during random migration, while slightly lower levels of Rac suppress peripheral lamella and favour the formation of a polarized cell with lamella just at the leading edge.[7] Is it possible that a similar mechanism of directional migration could occur in vivo?

The migration of Neural Crest (NC) cells has been used as a model to study directional cell migration in vivo.[8-10] The neural crest is an embryonic population of cells that are specified at the border between the neural plate and the epidermis.[11] Upon induction neural crest cells undergo an epithelial to mesenchymal transition,[12] detach from the neural tube and migrate following defined pathways that eventually allow them to colonize almost the entire embryo.[13] Finally, after reaching their destination NC cells differentiate to form many different cell types including neurons, glia, cartilage, skeleton and pigment cells.[14] The migration of the NC cells is critical for the

*Correspondence to: Roberto Mayor; Department of Cell and Developmental Biology; University College London; Gower Street; London, WC1E 6BT UK; Email: r.mayor@ucl.ac.uk

Submitted: 04/28/08; Accepted: 08/05/08

Previously published online as a *Cell Adhesion & Migration* E-publication: http://www.landesbioscience.com/journals/celladhesion/article/6747

proper differentiation of their derivatives and there are several human syndromes associated with failures in this process.

The migration of NC cells is a highly ordered process; individual NC cells migrate with high persistence towards the direction of their targets,[8] but until now it was not known how this directionality is controlled. A number of molecules have been identified as key players in neural crest migration, such as Ephrins, Semaphorins, Slit/Robo, etc. (reviewed in ref. 13). However most of these molecules work as inhibitory signals, which are required to restrict the migration of NC cells from prohibited areas. Although chemoattraction has been one of the proposed mechanisms to explain this directional migration, no chemoattractant has thus far been found in the NC.

It has been known for many years that NC cells can migrate in vitro with a high directionality even in the absence of external signals.[15] Therefore, our work has been focused on understanding how NC directionality is controlled. Recently, we have unveiled some of the molecules that control this directional migration in vitro. More importantly, we have been able to show that the same molecular machinery controls directional migration in vivo.[9,10]

One of the key factors that controls directional migration of NC cells is the Planar Cell Polarity (PCP) or non-canonical Wnt signaling pathway.[9,10,16] PCP signaling was first described in Drosophila, where a number of mutations were identified that disrupt the formation of bristles and hairs on the adult cuticle.[17] In the Drosophila wing, epithelial cells are highly polarized, with a single hair outgrowth forming at the distal end of each cell. Mutations in PCP genes cause loss in cell polarity in this tissue with hairs forming in a disorganized pattern.[18] In vertebrates, PCP signaling also regulates cell polarity during a number of different developmental processes including neural tube closure, cochlear hair orientation and ciliogenesis.[19]

We have shown that the PCP pathway is essential for correct neural crest migration in Xenopus. Injection of dominant negative forms of the intracellular PCP component Dishevelled (Dsh), which inhibit the PCP pathway but not canonical Wnt signaling, block the migration of cranial neural crest cells in vivo.[9] Recently this role has also been extended to zebrafish where directional migration of neural crest is severely disrupted in the PCP mutant *trilobite* (*strabismus*) and in embryos injected with a dominant negative form of Dsh or a morpholino against *wnt5a*,[10] with no effect in neural crest cell motility.[9,10] Two factors, *pescadillo* and *syndecan-4* that have recently been proposed as modulators of the PCP signaling,[20,21] are also required for NC migration.[10,21] Taken together, these data point to an essential role for PCP signaling in neural crest migration.

What is the cellular and molecular mechanism by which PCP signaling controls migration of NC cells? In order to investigate this question we analyzed the direction of neural crest migration and cell polarity in vitro and in vivo after interfering with two elements of the PCP signaling pathway: *syndecan-4* and Dsh. One of the key finding of our work was that the inhibition of NC migration through *syndecan-4* depletion does not affect the velocity of cell migration, but significantly reduces the directional migration of the cells in vivo (Fig. 1A and B). Consequently, when the orientation of cell protrusions was analyzed we found that *syndecan-4* depletion does not affect the formation of cell protrusions, but the direction in which the cell protrusions are generated during migration. More precisely, normal cells extend their lamellipodia at the front of the cell (Fig. 1D), while cells where *syndecan-4* is inhibited generate protrusion in all directions

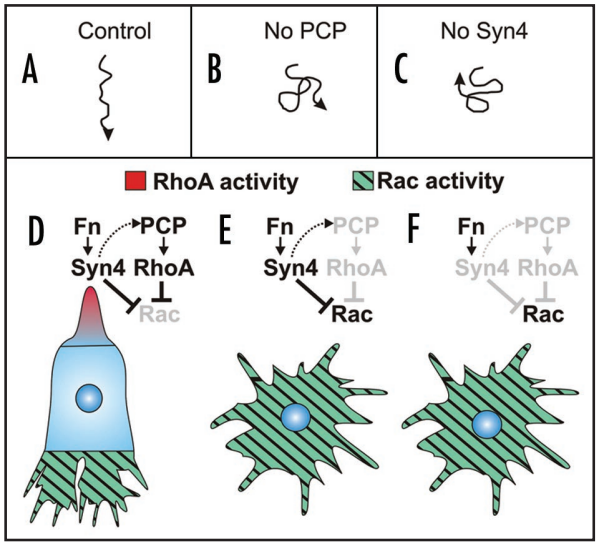

Figure 1. Directional migration of neural crest cells. (A and B) Example of track of a single cell migrating in vivo. (A) Control cell showing persistent directional migration. (B) Cell in which the PCP signaling has been inhibited, showing absence of directional migration. (C) Cell in which syndecan-4 has been inhibited, showing no persistent migration. (D–F) Analysis of cell polarity and model of directional migration. Fn: fibronectin; Syn4: syndecan-4. (D) Control cell. Activation of Fn/Syn4 and PCP/RhoA lead to inhibition of Rac at the back of the cell, with the consequence polarization and directional migration. (E) Inhibition of PCP signaling leads to absence of RhoA activity, and in consequence an increase of Rac activity at the back of the cell. It seems that the inhibition of Rac activity by Syn4 is not sufficient to keep low levels of Rac at the back of the cells. High levels of Rac at the back produce a loss in cell polarity and in directional migration. (F) Inhibition of Syn4 generates high levels of Rac activity by a double mechanism: absence of direct inhibition of Rac and absence of RhoA which is dependent on PCP signaling. High levels of Rac at the back produce a loss of cell polarity and directional migration.

(Fig. 1E). A similar analysis was performed for embryos expressing a mutated form of Dsh that works as a dominant negative of PCP signaling and an equivalent effect on directional migration and the orientations of cell protrusions was observed (Fig. 1C and F).

As cell protrusions are known to be controlled by small GTPases and as PCP and *syndecan-4* signaling regulates the activities of small GTPases,[18,22] we analyzed the activity of cdc42, RhoA and Rac after interfering with Dsh and *syndecan-4*. We choose to perform FRET analysis of these molecules as it is a technique that allows the visualization of their localized activity. More interestingly we succeeded in performing FRET analysis in cells migrating in vivo for the first time. Our results show that *syndecan-4* inhibits Rac activity, while Dsh signaling promotes RhoA activity. In addition, we show that RhoA inhibits Rac in neural crest cells.[10] The regulation of Rac by *syndecan-4* is similar to that seen in other cells types in vitro.[23,24]

The model that emerges from these results to explain directional migration of NC cells in vivo is as follows (Fig. 1D). After delamination NC cells come into contact with fibronectin in the extracellular matrix, which is known to provide the main substrate for neural crest cells during their migration.[25,26] The interaction of fibronectin with *syndecan-4* leads to two major changes in the cell: activation of PCP signaling and inhibition of Rac activity. The activated PCP signaling becomes localized at the back of the cell. From here, PCP contributes

to the inhibition of Rac at the back of the cell, through the activation of RhoA. The coordinated activities of *syndecan-4* and PCP signaling lead to polarised Rac activity across the cell, with Rac enriched at the leading edge, where it promotes the polymerization of actin and formation of lamellipodia, resulting in directional migration (Fig. 1D). Inhibition of PCP signaling produces high levels of Rac all over the cell as Rac, an inhibitor of RhoA in many cell types including neural crest cells, is absent (Fig. 1E). This generates cell protrusions in all directions with the consequent loss of cell polarity. If *syndecan-4* is absent, the levels of Rac activity are also high all over the cell as the inhibition of Rac by *syndecan-4* is absent (Fig. 1F), which also leads to a loss of cell polarity.

Although detailed study of the localized activity of small GTPases has not been performed for other migratory cells in vivo, it is likely that the machinery will be similar to the one described here for NC cells. For example, it is well established in Xenopus, zebrafish and chick embryos that the migration of mesodermal cells during gastrulation requires PCP signaling.[27-29] It has also been shown that gastrulation in Xenopus[20] and in zebrafish (unpublished observations) requires the activity of *syndecan-4*. Thus, it is expected that cell polarity established during the migration of mesodermal cells will be dependent on small GTPases controlled by non-canonical Wnt signaling and *syndecan-4.*

This novel integrated view of PCP, syndecan-4 and small GTPase activity during directional cell migration in vivo is an important advance in our knowledge of cell migration. Nevertheless, how the PCP signaling becomes activated only at the back of the cell, is a key question that needs to be answered. Future studies will be necessary to solve this and other crucial problems.

Acknowledgements

The work in R.M. laboratory is supported by grants from MRC and BBSRC. H.M. and C.C.-F. are MRC and Boehringer Ingelheim Fonds Ph.D. scholarship holders respectively.

References

1. Jaffe AB, Hall A. Rho GTPases: biochemistry and biology. Annu Rev Cell Dev Biol 2005; 21:247-69.
2. Raz E. Germ cells: sex and repression in mice. Curr Biol 2005; 15:600-3.
3. Cattaruzza S, Perris R. Proteoglycan control of cell movement during wound healing and cancer spreading. Matrix Biology 2005; 24:400-17.
4. Barlow AJ, Wallace AS, Thapar N, Burns AJ. Critical numbers of neural crest cells are required in the pathways from the neural tube to the foregut to ensure complete enteric nervous system formation. Development 2008; 135:1681-91.
5. Erickson CA. Control of neural crest cell dispersion in the trunk of the avian embryo. Dev Biol 1985; 111:138-57.
6. Van Haastert PJ, Devreotes PN. Chemotaxis: signalling the way forward. Nat Rev Mol Cell Biol 2004; 5:626-34.
7. Pankov R, Endo Y, Even-Ram S, Araki M, Clark K, Cukierman E, Matsumoto K, Yamada KM. A Rac switch regulates random versus directionally persistent cell migration. J Cell Biol 2005; 170:793-802.
8. Teddy JM, Kulesa PM. In vivo evidence for short- and long-range cell communication in cranial neural crest cells. Development 2004; 131:6141-51.
9. De Calisto J, Araya C, Marchant L, Riaz CF, Mayor R. Essential role of non-canonical Wnt signalling in neural crest migration. Development 2005; 132:2587-97.
10. Matthews HK, Marchant L, Carmona-Fontaine C, Kuriyama S, Larrain J, Holt MR, et al. Directional migration of neural crest cells in vivo is regulated by Syndecan-4/Rac1 and non-canonical Wnt signaling/RhoA. Development 2008; 135:1771-80.
11. Steventon B, Carmona-Fontaine C, Mayor R. Genetic network during neural crest induction: from cell specification to cell survival. Semin Cell Dev Biol 2005; 16:647-54.
12. Thiery JP, Sleeman JP. Complex networks orchestrate epithelial-mesenchymal transitions. Nat Rev Mol Cell Biol 2006; 7:131-42.
13. Kuriyama S, Mayor R. Molecular analysis of neural crest migration. Philos Trans R Soc Lond, Ser B: Biol Sci 2008; 363:1349-62.
14. Le Douarin N, Kalcheim C. The Neural Crest. Cambridge University Press 1999.
15. Davis EM, Trinkaus JP. Significance of cell-to cell contacts for the directional movement of neural crest cells within a hydrated collagen lattice. J Embryol Exp Morphol 1981; 63:29-51.
16. Garriock RJ, Krieg PA. Wnt11-R signaling regulates a calcium sensitive EMT event essential for dorsal fin development of Xenopus. Dev Biol 2007; 304:127-40.
17. Gubb D, Garcia-Bellido A. A genetic analysis of the determination of cuticular polarity during development in *Drosophila melanogaster*. J Embryol Exp Morphol 1982; 68:37-57.
18. Veeman MT, Axelrod JD, Moon RT. A second canon. Functions and mechanisms of beta-catenin-independent Wnt signaling. Dev Cell 2003; 5:367-77.
19. Wang Y, Nathans J. Tissue/planar cell polarity in vertebrates: new insights and new questions. Development 2007; 134:647-58.
20. Munoz R, Moreno M, Oliva C, Orbenes C, Larrain J. Syndecan-4 regulates non-canonical Wnt signalling and is essential for convergent and extension movements in Xenopus embryos. Nat Cell Biol 2006; 8:492-500.
21. Gessert S, Maurus D, Rossner A, Kuhl M. Pescadillo is required for *Xenopus laevis* eye development and neural crest migration. Dev Biol 2007; 310:99-112.
22. Couchman JR. Syndecans: proteoglycan regulators of cell-surface microdomains? Nat Rev Mol Cell Biol 2003; 4:926-37.
23. Bass MD, Roach KA, Morgan MR, Mostafavi-Pour Z, Schoen T, Muramatsu T, et al. Syndecan-4-dependent Rac1 regulation determines directional migration in response to the extracellular matrix. J Cell Biol 2007; 177:527-38.
24. Saoncella S, Calautti E, Neveu W, Goetinck PF. Syndecan-4 regulates ATF-2 transcriptional activity in a Rac1-dependent manner. J Biol Chem 2004; 279:47172-6.
25. Alfandari D, Cousin H, Gaultier A, Hoffstrom BG, DeSimone DW. Integrin alpha5beta1 supports the migration of Xenopus cranial neural crest on fibronectin. Dev Biol 2003; 260:449-64.
26. Newgreen D, Thiery JP. Fibronectin in early avian embryos: synthesis and distribution along the migration pathways of neural crest cells. Cell Tissue Res 1980; 211:269-91.
27. Wallingford JB, Habas R. The developmental biology of Dishevelled: an enigmatic protein governing cell fate and cell polarity. Development 2005; 132:4421-36.
28. Montero JA, Heisenberg CP. Gastrulation dynamics: cells move into focus. Trends Cell Biol 2004; 14:620-7.
29. Hardy KM, Garriock RJ, Yatskievych TA, D'Agostino SL, Antin PB, Krieg PA. Non-canonical Wnt signaling through Wnt5a/b and a novel Wnt11 gene, Wnt11b, regulates cell migration during avian gastrulation. Dev Biol; 2008 320:391-401.

LETTERS

Contact inhibition of locomotion *in vivo* controls neural crest directional migration

Carlos Carmona-Fontaine[1], Helen K. Matthews[1], Sei Kuriyama[1], Mauricio Moreno[1], Graham A. Dunn[2], Maddy Parsons[2], Claudio D. Stern[1] & Roberto Mayor[1]

Contact inhibition of locomotion was discovered by Abercrombie more than 50 years ago and describes the behaviour of fibroblast cells confronting each other *in vitro*, where they retract their protrusions and change direction on contact[1,2]. Its failure was suggested to contribute to malignant invasion[3–6]. However, the molecular basis of contact inhibition of locomotion and whether it also occurs *in vivo* are still unknown. Here we show that neural crest cells, a highly migratory and multipotent embryonic cell population, whose behaviour has been likened to malignant invasion[6–8], demonstrate contact inhibition of locomotion both *in vivo* and *in vitro*, and that this accounts for their directional migration. When two migrating neural crest cells meet, they stop, collapse their protrusions and change direction. In contrast, when a neural crest cell meets another cell type, it fails to display contact inhibition of locomotion; instead, it invades the other tissue, in the same manner as metastatic cancer cells[3,5,9]. We show that inhibition of non-canonical Wnt signalling abolishes both contact inhibition of locomotion and the directionality of neural crest migration. Wnt-signalling members localize at the site of cell contact, leading to activation of RhoA in this region. These results provide the first example of contact inhibition of locomotion *in vivo*, provide an explanation for coherent directional migration of groups of cells and establish a previously unknown role for non-canonical Wnt signalling.

Neural crest (NC) cells cultured *in vitro* move away from each other, dispersing quickly[10]. *Xenopus* NC explants revealed that only the leading-edge cells were polarized, having large lamellipodia at the front as shown by scanning electron microscopy (arrowheads in Fig. 1a–c) or in a live NC explant expressing membrane-localized green fluorescent protein (GFP) (Fig. 1d). Time-lapse analysis revealed that edge cells had a higher persistence in the direction of migration than cells in the interior of the explant (Fig. 1d′). To establish whether these differences in polarity and migration correspond to two different cell populations or whether they are due to cell–cell contact, we dissociated NC explants into single cells and then re-aggregated them into small or large clusters. Peripheral cells in small or large clusters rapidly became polarized and migrate away from each other (Fig. 1e), whereas internal cells moved randomly (Supplementary Fig. 2 and Supplementary Movie 1), similarly to those in non-dissociated explants. In addition, the randomly migrating internal cells of these explants became polarized when made to have a free edge by wounding or removal of their neighbours (Supplementary Fig. 3). These results suggest that the differential behaviour of leading versus internal cells in explants is due not to intrinsic cell differences but to interactions between neighbouring cells. Furthermore, the average persistence of the leading cells (defined by their position at the border of an explant) in a

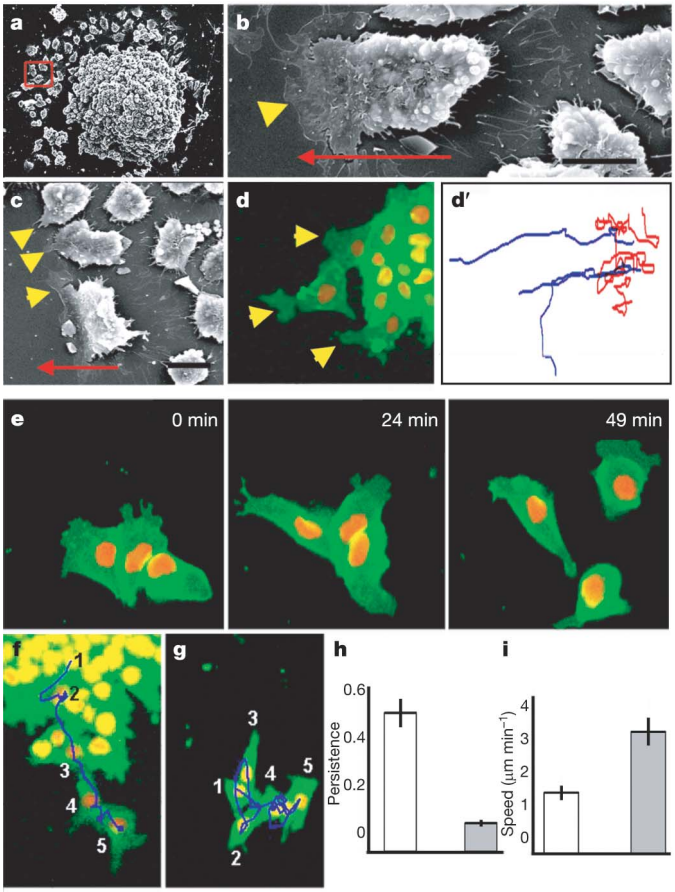

Figure 1 | Cell–cell contacts polarize migrating NC cells *in vitro*. **a**–**g**, NCs were cultured *in vitro* and analysed by scanning electron microscopy (**a**–**c**) or time-lapse microscopy of cells expressing membrane-GFP and nuclear-RFP (**d**–**g**). The red square in **a** indicates leading cells (defined by its position at the edge of migration; higher magnifications of other leading cells are shown in **b** and **c**). Arrowheads indicate lamellipodia (note their presence only in the leading cells, either by scanning electron microscopy (**c**); or fluorescence (**d**)); the arrow indicates the direction of migration. Scale bars in **b**, **c**, 50 μm. **d′**, Tracks of leading (blue) and trailing (red) cells shown in **d**. **e**, Three frames of a time-lapse movie for dissociated and re-aggregated NC cells. **f**, **g**, Temporal projection to compare the migration of a group of NC cells (**f**) with that of individual cells (**g**). Numbers indicate the position of the same cell at different time frames 10 min apart. The track is shown as a blue line. **h**, **i**, Persistence (**h**) and speed of migration (**i**) for the migration as a group (white bars) or as an individual cell (grey bars) ($P < 0.005$, $n = 60$). Error bars show s.d.

[1]Department of Anatomy and Developmental Biology, University College London, London WC1E 6BT, UK. [2]Randall Division of Cell and Molecular Biophysics, King's College London, London SE1 1UL, UK.

non-dissociated cluster was much higher than that of individual cells; the latter often made little progress and moved in circles, although their overall speed of migration was greater (Fig. 1f–i and Supplementary Movie 2). A similar phenomenon has been reported for cell types showing contact inhibition of locomotion[1]. Taken together, these results indicate that the directional migration of cultured NC cells is dependent on cell–cell contact, which is likely to inhibit the formation of cell protrusions, leading to cell polarization.

To study the behaviour of NC cells when confronted with other cells, we developed an explant-confrontation assay[1,11]. Two NC explants were cultured in close proximity such that their leading cells would encounter cells from the other explant migrating in the opposite direction (Fig. 2A). We found that cells from NC explants aggressively invaded mesodermal (Fig. 2E) and ectodermal (not shown) explants, but never invaded other NC explants (Fig. 2C, Supplementary Fig. 4a–c and Supplementary Movie 3). Confocal microscopic analyses showed that whereas NC cells stopped migrating when confronted with other NC cells, they engulfed the mesoderm explant, with some cells penetrating deep layers of this tissue (Fig. 2D, F and Supplementary Fig. 4d–i). These observations suggest that contact inhibition of locomotion occurs between NC cells (homotypic) but not between NC cells and other cell types (heterotypic), in the same way as with some malignant cells[4,5,9].

It is tempting to speculate that such homotypic contact inhibition of locomotion could function in guiding the migration of NC cells in normal development. To determine whether this is true we developed a confrontation assay *in vivo* and found that NC cells can invade the tissue of an adjacent *Xenopus* embryo lacking NC (Fig. 2O) but this invasion is blocked when the host NC is present (Fig. 2N). This result is compatible with contact inhibition of locomotion having this function, but it does not directly demonstrate that NC cells show contact inhibition of locomotion. We therefore performed time-lapse analysis in the explant-confrontation assay, focusing on individual cells. When a NC cell came into contact with a cell from the opposite group, its lamellipodium collapsed and the direction of its migration changed (Fig. 2G and Supplementary Movie 4). This is described precisely by Abercrombie's original definition of contact inhibition of locomotion as "the phenomenon of a cell ceasing to continue moving in the same direction after contact with another cell"[5]. So far, contact inhibition of locomotion has been

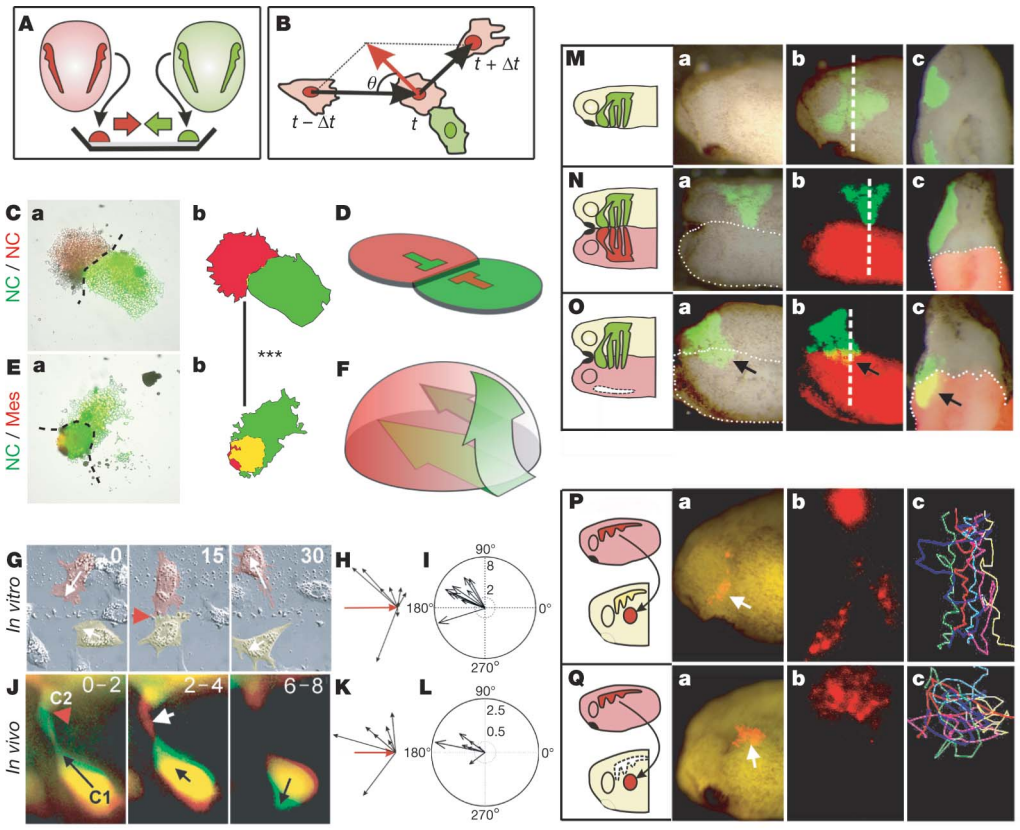

Figure 2 | Contact inhibition of locomotion in NC cells *in vitro* and *in vivo*. **A**, Experimental design. **B**, Analysis of contact inhibition of locomotion. Mean velocities were measured Δt minutes before and after the collision. Acceleration (red) was calculated for each cell. The angle of collision, θ, was calculated after initial trajectory alignment. **C–F**, Invasion of confronted explants *in vitro*. **C**, There is no invasion in NC/NC confrontations (**a**), outlines in (**b**), overlapping area in yellow; shown schematically in **D**. **E**, NC explants completely invade and cover mesodermal (mes) explants (**a**), outlines in (**b**), overlapping area in yellow; shown schematically in **F**. Green arrows in **F** indicate the NC path of invasion (see Supplementary Fig. 3 for supporting confocal images). Three asterisks in **b** show a significant difference in the overlapping area (yellow), $P < 0.005$ ($n = 5$ for each condition). **G–L**, Contact inhibition of locomotion. **G**, Collision between two pseudocoloured NC cells *in vitro*. Time is shown in minutes. White arrows indicate the direction of migration; the red arrowhead indicates collision. **H**, Velocity vectors for NC *in vitro*; the red arrow indicates the initial velocity vector. **I**, Acceleration vectors for NC collisions *in vitro*. They are clustered after the collision ($P < 0.005$, $n = 10$). **J**, Collision of two NC cells (C1 and C2) *in vivo* shown as the difference between two consecutive 2-min frames. Green, new area; red, collapsing area; black arrow, direction of migration; red arrowhead, cell contact; white arrow, collapsing protrusion. **K**, *In vivo* velocity vectors. **L**, *In vivo* acceleration. They are clustered after the collision ($P < 0.01$, $n = 10$). **M–O**, NC invasion *in vivo*. **a**, **b**, lateral view; **c**, transverse section along the dashed line shown in **b**. **M**, Labelled and transplanted NC cells in control embryos migrate normally. **N**, **O**, NC cells are not able to invade an adjacent embryo that has NC (**N**; 0% of invasion, $n = 15$), but they can invade an embryo without NC (**O**; arrow, 80% of invasion, $n = 10$). **P**, **Q**, Cell directionality *in vivo*. A small group of nuclear-RFP-labelled NC cells were grafted into a normal embryo (**P**) or into an embryo from which the NC had previously been removed (**Q**). Note that grafted cells migrated directionally in the intact embryo (persistence 0.6 ± 0.04 (mean ± s.d), $n = 30$), but not when the host NCs were removed (persistence 0.2 ± 0.02 (mean ± s.d.), $n = 20$).

described only *in vitro*. To address whether it also occurs *in vivo*, we used two Sox10–GFP transgenic zebrafish lines, one expressing GFP in the cytoplasm[12] and the other in the membrane of NC cells, and analysed their migration using live-imaging techniques. Similarly to the observations *in vitro*, whenever two NC cells made contact, they changed their direction of migration and their protrusions collapsed (Fig. 2J, Supplementary Fig. 5 and Supplementary Movies 5–7). Contact inhibition of locomotion can be measured by the change in velocity after cell–cell contact[4,11]. Large changes in the direction of cell migration were seen after each cell collision (Fig. 2B and Supplementary Methods) both *in vitro* and *in vivo* (velocity is shown in Fig. 2H, K, acceleration in Fig. 2I, L). The changes were not stochastic but were strongly biased in the opposite direction to the collision ($P < 0.005$), as predicted by Abercrombie[5,11]. Similarly, in *Xenopus*, grafted NC cells integrated into the endogenous migratory pathway and migrated directionally (Fig. 2P). However, grafted NC lost their directional migratory behaviour when the host NC was removed (Fig. 2Q), suggesting that the directionality of NC migration depends on interactions with other NC cells and supporting our conclusion that contact inhibition of locomotion is required for normal NC migration *in vivo*.

We next explored the molecular mechanisms underlying contact inhibition of locomotion in NC cells. Previous studies have shown that the Wnt planar cell polarity (PCP, or non-canonical) pathway is required for NC migration in *Xenopus* and zebrafish embryos, whereas canonical Wnt signalling is not[13,14]. To determine whether PCP signalling is involved in contact inhibition of locomotion, we analysed cells expressing a dominant-negative form of *dishevelled* (*DshDep*$^+$), which specifically inhibits the PCP pathway[15]. In control explants, only the leading cells were highly polarized, extending cell protrusions at the front, whereas trailing cells were not (Fig. 1a–c). In contrast, *DshDep*$^+$ cells were not polarized but extended large protrusions in all directions (Fig. 3a–c). Live imaging showed that cells expressing *DshDep*$^+$ crawled on top of one another, extending protrusions between the neighbour cells, a characteristic of some metastatic cancer cells[3,5,9] (Fig. 3d, e, and Supplementary Movie 8). All *DshDep*$^+$ (leading and trailing) cells behaved similarly to trailing control cells on the basis of their low persistence of migration and the angles at which they changed direction (Fig. 3f–i). No difference in persistence and speed of migration was observed between dissociated control and *DshDep*$^+$ cells: both behaved like trailing cells (Fig. 3j–m and Supplementary Movie 9). This indicates that the effect of PCP signalling on NC migration requires cell–cell contact.

To test whether contact inhibition of locomotion is dependent on PCP signalling *in vivo*, we measured the speed of cell migration before and after cell collision in control embryos and in embryos in which PCP signalling had been disrupted (either by expressing *DshDep*$^+$, by a dominant-negative form of the PCP ligand Wnt11 or by antisense morpholinos against the PCP pathway members *strabismus* (*Stb*; ref. 16) or *prickle1* (*Pk1*; ref. 17)). The lamellipodia of PCP-inhibited cells failed to collapse when they collide with each other *in vivo*, even after 1 h of contact (control, Supplementary Fig. 6a; PCP disrupted, Supplementary Fig. 6b, c; Supplementary Movie 10). In contrast to control cells (Fig. 4a, g), these cells did not significantly change their direction of migration (Fig. 4b–d), and as shown by the small acceleration vectors, cell velocity was hardly affected by cell–cell contact ($P \gg 0.05$; Fig. 4h–j). Rather, PCP-inhibited cells migrated on top of one another, remaining in close contact (Supplementary Movie 10). Similar observations were made *in vitro* after inhibition of PCP signalling by the expression of *DshDep*$^+$, by a dominant-negative form of Wnt11 (*dnWnt11*)[15], by a morpholino against a protein closely related to mammalian Wnt11 (*Wnt11R*)[18,19] or by a mixture of *dnWnt11* and *Wnt11R* (Fig. 4e, f, k, l, and Supplementary Fig. 7e, f), where PCP inhibited cells did not collapse their protrusions after the collision (Supplementary Fig. 7a–c). Moreover, when control cells and *DshDep*$^+$-expressing cells were confronted, only control cells collapsed their lamellipodia and moved away from the *DshDep*$^+$ cells (Supplementary Fig. 7d and Supplementary Movie 11), indicating that PCP/Dsh signalling is required only in the responding cell.

Activation of the PCP pathway is typically accompanied by membrane localization of Dishevelled (Dsh)[20]. We therefore analysed the subcellular localization of Dsh during NC migration *in vitro* and *in vivo*. In both premigratory NC cells and NC cells cultured on poly-(L-lysine, a non-permissive substrate for NC migration[21], Dsh was seen in cytoplasmic dots (Supplementary Fig. 8a, b). In contrast, clear membrane localization of Dsh was observed at cell–cell contacts of NC cells grown on a permissive fibronectin substrate (Fig. 4o). For the leading cell, the region of cell–cell contact, and therefore the region of Dsh accumulation, was at the trailing end of the cell *in vitro* (Supplementary Fig. 8c). When two leading cells collided, Dsh became relocalized at the point of cell–cell contact, with a subsequent change in the direction of migration (Fig. 4p and Supplementary Movie 12). Similar observations on Dsh localization at cell–cell contacts between NC cells and at the trailing end of a leading cell were made *in vivo* (Supplementary Fig. 8e, f). A lack of PCP signalling led to a loss of Dsh accumulation in the cell contact (Supplementary Fig. 9). This membrane-localized Dsh is reminiscent of the foci described after activation of Dsh in mesodermal cells[22]. We also observed a redistribution of Wnt11 and the receptor Fz7 at cell–cell contacts *in vitro* (Fig. 4m, n) and *in vivo* (Supplementary Fig. 8g, and not

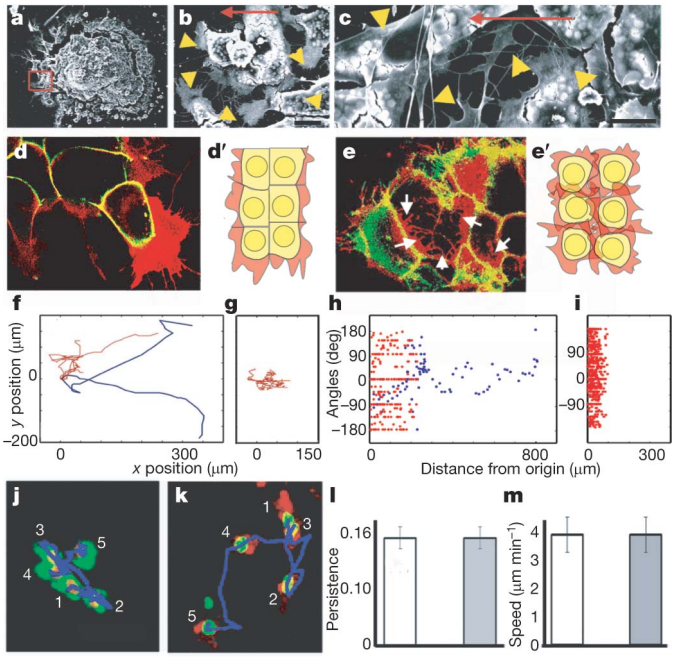

Figure 3 | Effect of PCP signalling on cell contacts. **a**–**c**, Scanning electron microscopy of *Xenopus* cultured NC expressing *DshDep*$^+$. The red square indicates leading cells. Higher magnifications of other leading cells are shown in **b** and **c**. Arrowheads indicate cell protrusions; the arrow indicates the direction of migration. Scale bars, 25 μm (**b**), 50 μm (**c**). **d**, **e**, Two-plane confocal image to show cell protrusions (red) and cell shape (green). Cell protrusions are produced only at the border of the control explant (**d**), whereas they are observed between the *DshDep*$^+$ cells (arrows in **e**). **d′**, **e′**, Schematic representations of **d** and **e**, respectively. **f**–**i**, Analysis of tracks of migrating NC cells. Blue, leading cells; red, trailing cells. **f**, **g**, Tracks of control (**f**) and *DshDep*$^+$ (**g**) cells. **h**, **i**, Plots of distribution of angles of migration for leading (blue) and trailing (red) control (**h**) and *DshDep*$^+$ (**i**) cells against the distance from the origin. **j**–**m**, Analysis of migration of dissociated NC cells. **j**, **k**, Five frames taken every 10 min were overlapped for a control cell (**j**) and a *DshDep*$^+$ cell (**k**). Numbers indicate consecutive positions of the cell. The blue lines shows the tracks. **l**, **m**, Persistence (**l**) and speed of migration (**m**) were calculated for control (white bars) and *DshDep*$^+$ (grey bars) cells ($P < 0.05$; $n = 62$). Error bars show s.d.

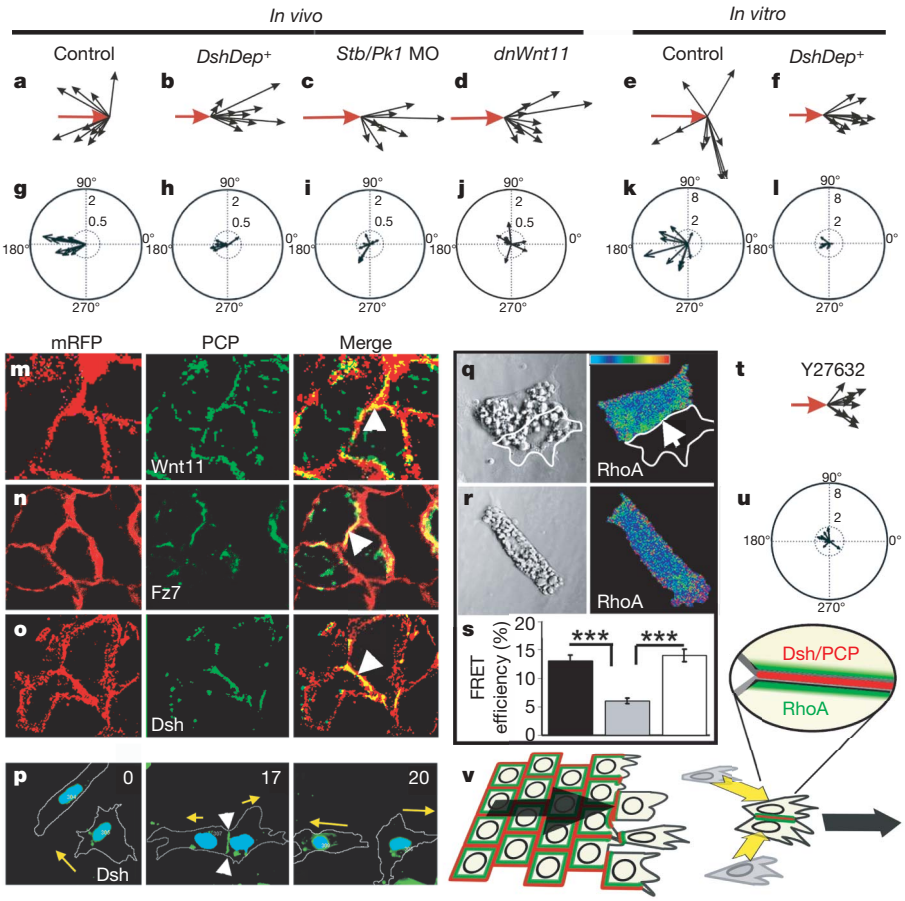

Figure 4 | Contact inhibition of locomotion: requirement of PCP and RhoA activities. **a–l**, Cell collisions were analysed *in vivo* (**a–d**, **g–j**) and *in vitro* (**e**, **f**, **k**, **l**). Velocities (**a–f**) and accelerations (**g–l**) were measured after the indicated treatments. MO, morpholino. The scales are the same for all panels. The change of velocity was significantly clustered in the controls ($P < 0.005$, $n = 10$). No significant change was observed in any of the PCP treatments ($P \gg 0.05$, $n = 10$ for all cases). **m–p**, Different PCP components are localized at the cell–cell contact (arrowheads). mRFP, membrane-RFP. **m**, Wnt11–YFP (yellow fluorescent protein). **n**, Fz7–YFP. **o**, Dsh–GFP. **p**, Cells expressing Dsh–GFP were analysed during a cell collision. The outline of the cell is taken from the differential interference contrast images. Time is shown in minutes. The arrow indicates the direction of migration; the arrowhead indicates cell contact showing Dsh localization. **q–u**, Role of RhoA. **q–s**, FRET analysis of RhoA activity. **q**, Two NC cells in contact showing RhoA activity localized at the cell contact (arrow). **r**, Single NC cell. **s**, RhoA FRET efficiency. Black bar, cells in contact; grey bar, single cell; white bar, single cell in which PCP has been activated by the expression of DshΔN. Three asterisks, $P < 0.005$ ($n = 12$ for each condition). Error bars show s.d. **t**, **u**, Cell collisions were analysed in the presence of the Rock inhibitor Y27632. **t**, Velocity vectors; **u**, acceleration vectors. No significant change in velocity was observed ($P \gg 0.05$, $n = 10$). **v**, Contact inhibition of locomotion is controlled by localization of PCP elements (red) and RhoA activity (green) at the cell contact, leading to directional migration (arrows).

shown); both became co-localized at the trailing end of the leading cell (Supplementary Fig. 8d). Our results suggest that cell–cell contacts polarize the cell by regulating the accumulation of ligands, receptors and intracellular element of the PCP signalling pathways.

It is well established that small GTPases are important in cell polarity and cell migration. One of them, RhoA, is a known downstream effector of PCP/Dsh during NC migration[14]. To examine a possible role for RhoA in contact inhibition of locomotion, we analysed the levels of RhoA activity in isolated and colliding cells by fluorescence resonance energy transfer (FRET). A significant increase in RhoA activity was detected during cell collision, with the highest activity in regions of cell–cell contact (Fig. 4q–s). When PCP signalling was activated in individual cells by expressing DshΔN[13,15] a similar increase in RhoA activity was observed (Fig. 4s and Supplementary Fig. 10a–c). Finally, inhibition of Rock, a downstream target of RhoA, led to a complete loss of contact inhibition of locomotion (Fig. 4t, u, Supplementary Fig. 10d and Supplementary Movie 13). These results implicate RhoA as downstream effector of the PCP in contact inhibition of locomotion.

Although contact inhibition of locomotion was described for cultured cells more than 50 years ago[1,2], we present the first evidence that it occurs *in vivo* and has a key function in the directional migration of NC cells. We show that the PCP (non-canonical) Wnt pathway is involved in the process. The data are consistent with a model (Fig. 4v) in which cell–cell contact leads to the localized activation of the PCP signalling in the region of cell contact, which is required for the activation of RhoA. The localization of RhoA at the cell contact directs the collapse of cell protrusions and the change in cell polarity. It is commonly believed that directional cell migration during embryogenesis involves the localized production of molecules that attract migrating cells (chemotaxis)[23–25]. Although we do not rule out chemoattraction, we suggest that contact inhibition of locomotion could be sufficient for NC directional migration. This mechanism could also direct the coherent migration of groups of cells (for example mesoderm[26] or lateral line primordium[27]) and the efficient occupation by one cell population of another's territory during metastasis or development (including NC, angioblasts and neurons[28,29]). Most cells migrating *in vivo* maintain close proximity and move in groups. Accordingly, the inhibition of cell protrusions between these clustered cells is equivalent to the process of contact inhibition of locomotion. Their typical coherent directional migration is accomplished through a 'tip-toe' movement in which front cells can move only towards the NC-free zone; that is, forwards. This opens a little space where trailing cells move, and so on (Supplementary Fig. 1).

NC cells behave similarly to some cancer cells in that they display contact inhibition of locomotion towards like, but not towards unlike, cell types[3,5–9]. We propose that homotypic contact inhibition of locomotion confers cells with directionality during migration and that the lack of heterotypic contact inhibition allows them to invade other tissues.

METHODS SUMMARY

Xenopus NC was labelled with nuclear-red fluorescent protein (RFP)/membrane-GFP or membrane-RFP/nuclear-GFP. *In vitro* analysis of NC migration was performed with *Xenopus* NCs cultured on fibronectin-coated plates. For *in vivo* studies we used *Xenopus* embryos grafted with labelled NC or zebrafish transgenic-line embryos expressing cytoplasm or membrane-GFP under the NC promoter *sox10*. Time-lapse photography was performed with differential interference contrast or fluorescent/confocal microscopy. FRET analysis was performed as described in ref. 14. Full methods are given in Supplementary Methods.

Received 17 July; accepted 19 September 2008.
Published online 10 December 2008.

1. Abercrombie, M. & Heaysman, J. E. M. Observations on the social behaviour of cells in tissue culture. I. Speed of movement of chick heart fibroblasts in relation to their mutual contacts. *Exp. Cell Res.* **5,** 111–131 (1953).
2. Abercrombie, M. & Heaysman, J. E. M. Observations on the social behaviour of cells in tissue culture: II. 'Monolayering' of fibroblasts. *Exp. Cell Res.* **6,** 293–306 (1954).
3. Abercrombie, M. & Heaysman, J. E. Invasiveness of sarcoma cells. *Nature* **174,** 697–698 (1954).
4. Paddock, S. W. & Dunn, G. A. Analysing collisions between fibroblasts and fibrosarcoma cells: fibrosarcoma cells show an active invasionary response. *J. Cell Sci.* **81,** 163–187 (1986).
5. Abercrombie, M. Contact inhibition and malignancy. *Nature* **281,** 259–262 (1979).
6. Hendrix, M. J. *et al.* Reprogramming metastatic tumour cells with embryonic microenvironments. *Nature Rev. Cancer* **7,** 246–255 (2007).
7. Kulesa, P. M. *et al.* Reprogramming metastatic melanoma cells to assume a neural crest cell-like phenotype in an embryonic microenvironment. *Proc. Natl Acad. Sci. USA* **103,** 3752–3757 (2006).
8. Kuriyama, S. & Mayor, R. Molecular analysis of neural crest migration. *Phil. Trans. R. Soc. B* **363,** 1349–1362 (2008).
9. Heaysman, J. E. Non-reciprocal contact inhibition. *Experientia* **26,** 1344–1345 (1970).
10. Davis, E. M. & Trinkaus, J. P. Significance of cell-to-cell contacts for the directional movement of neural crest cells within a hydrated collagen lattice. *J. Embryol. Exp. Morphol.* **63,** 29–51 (1981).
11. Dunn, G. A. & Paddock, S. W. Analysing the motile behaviour of cells: a general approach with special reference to pairs of cells in collision. *Phil. Trans. R. Soc. Lond. B* **299,** 147–157 (1982).
12. Carney, T. J. *et al.* A direct role for Sox10 in specification of neural crest-derived sensory neurons. *Development* **133,** 4619–4630 (2006).
13. De Calisto, J. *et al.* Essential role of non-canonical Wnt signalling in neural crest migration. *Development* **132,** 2587–2597 (2005).
14. Matthews, H. *et al.* Directional migration of neural crest cells in vivo is regulated by Syndecan-4/Rac1 and non-canonical Wnt signaling/RhoA. *Development* **135,** 1771–1780 (2008).
15. Tada, M. & Smith, J. C. *Xwnt11* is a target of *Xenopus* Brachyury: regulation of gastrulation movements via Dishevelled, but not through the canonical Wnt pathway. *Development* **127,** 2227–2238 (2000).
16. Park, M. & Moon, R. T. The planar cell-polarity gene *stbm* regulates cell behaviour and cell fate in vertebrate embryos. *Nature Cell Biol.* **4,** 20–25 (2002).
17. Carreira-Barbosa, F. *et al.* Prickle 1 regulates cell movements during gastrulation and neuronal migration in zebrafish. *Development* **130,** 4037–4046 (2003).
18. Garriock, R. J., D'Agostino, S. L., Pilcher, K. C. & Krieg, P. A. Wnt11-R, a protein closely related to mammalian Wnt11, is required for heart morphogenesis in *Xenopus*. *Dev. Biol.* **279,** 179–192 (2005).
19. Matthews, H., Broders-Bondon, F., Thiery, J. P. & Mayor, R. *Wnt11r* is required for cranial neural crest migration. *Dev. Dyn.* **237,** 3404–3409 (2008).
20. Axelrod, J. D. *et al.* Differential recruitment of Dishevelled provides signaling specificity in the planar cell polarity and Wingless signaling pathways. *Genes Dev.* **12,** 2610–2622 (1998).
21. Alfandari, D. *et al.* Integrin α5β1 supports the migration of *Xenopus* cranial neural crest on fibronectin. *Dev. Biol.* **260,** 449–464 (2003).
22. Witzel, S. *et al.* Wnt11 controls cell contact persistence by local accumulation of Frizzled 7 at the plasma membrane. *J. Cell Biol.* **175,** 791–802 (2006).
23. Condeelis, J., Singer, R. H. & Segall, J. E. The great escape: When cancer cells hijack the genes for chemotaxis and motility. *Annu. Rev. Cell Dev. Biol.* **21,** 695–718 (2005).
24. Devreotes, P. N. & Zigmond, S. H. Chemotaxis in eukaryotic cells—a focus on leukocytes and *Dictyostelium*. *Annu. Rev. Cell Biol.* **4,** 649–686 (1988).
25. Raz, E. Primordial germ-cell development: The zebrafish perspective. *Nature Rev. Genet.* **4,** 690–700 (2003).
26. Keller, R. Cell migration during gastrulation. *Curr. Opin. Cell Biol.* **17,** 533–541 (2005).
27. Lecaudey, V. & Gilmour, D. Organizing moving groups during morphogenesis. *Curr. Opin. Cell Biol.* **18,** 102–107 (2006).
28. Risau, W. & Flamme, I. Vasculogenesis. *Annu. Rev. Cell Dev. Biol.* **11,** 73–91 (1995).
29. Ayala, R., Shu, T. & Tsai, L. H. Trekking across the brain: the journey of neuronal migration. *Cell* **128,** 29–43 (2007).

Supplementary Information is linked to the online version of the paper at www.nature.com/nature.

Acknowledgements We thank M. Tada, M. Tawk, J. Clarke, C.-P. Heisenberg, R. Kelsh, L. Dale and S. Fraser for reagents, constructs and fish lines; C. F. Riaz for scanning electron microscopy images; and M. Bronner-Fraser, M. Raff, J. Green and A. Ridley for comments on the manuscript. This study was supported by grants to R.M. from the Medical Research Council (MRC) and the Biotechnology and Biological Sciences Research Council. H.K.M. and C.C.-F. are MRC and Boehringer Ingelheim Fonds PhD scholarship holders, respectively, and M.M. is an EMBO postdoctoral fellow.

Author Contributions C.C.-F. and R.M. designed the experiments. C.C.-F., H.K.M. and R.M. performed most of the experiments. C.C.-F. and R.M. did the movie analysis. C.C.-F., G.A.D. and R.M. planned and performed the statistical analysis. M.P., S.K., C.C.-F., H.K.M. and R.M. conducted the FRET analysis. M.M. made some of the constructs and the zebrafish transgenic. M.M., C.C.-F., H.K.M. and R.M. performed the PCP localization experiments. C.C.-F., C.S. and R.M. wrote the paper.

Author Information Reprints and permissions information is available at www.nature.com/reprints. Correspondence and requests for materials should be addressed to R.M. (r.mayor@ucl.ac.uk).

Review

Cell PRESS

Keeping in touch with contact inhibition of locomotion

Roberto Mayor and Carlos Carmona-Fontaine

Department of Cell and Developmental Biology, University College London, Gower Street, London WC1E 6BT, UK

Contact inhibition of locomotion (CIL) is the process by which cells *in vitro* change their direction of migration upon contact with another cell. Here, we revisit the concept that CIL plays a central role in the migration of single cells and in collective migration, during both health and disease. Importantly, malignant cells exhibit a diminished CIL behaviour which allows them to invade healthy tissues. Accumulating evidence indicates that CIL occurs *in vivo* and that regulation of small Rho GTPases is important in the collapse of cell protrusions upon cell contact, the first step of CIL. Finally, we propose possible cell surface proteins that could be involved in the initial contact that regulates Rho GTPases during CIL.

Social behaviour of migratory cells

In multicellular organisms, cell migration is essential for normal development and is required throughout life for numerous processes, including wound healing and responses to infections. Disregulation in the control of cell migration can lead to, or exacerbate, human diseases such as cancer, atherosclerosis and chronic inflammatory pathologies. More than a century of research in this area has generated a detailed morphological description of moving cells and this has allowed researchers to deepen their understanding of the molecular mechanisms that control cell polarity and cell protrusions during migration. An important concept to emerge is the idea that most cells do not move as isolated entities *in vivo* but rather interact with their neighbours during migration. Even cells of the immune system that can migrate singly have to interact with other non-motile cells along their migratory paths. Thus, cells must have their locomotory machinery adapted to these constant interactions. This has prompted scientists for decades to try to investigate the 'social behaviour of cells' [1]. However, how cells interact during migration is still not fully understood.

More than five decades ago, Abercrombie and Heaysman found that the direction of migration of fibroblasts cultured *in vitro* was affected by their interaction with other cells [1]. They called this process 'contact inhibition of locomotion' (CIL, see Refs. [2,3], Box 1) and it was proposed as an explanation for wound healing of epithelia, as this inhibition of cell contact dependent cell migration was released during wound healing, allowing the migration of the cells at the border of the wound [3,4]. The potential importance of this idea became immediately apparent when they observed that malignant mesenchymal cells showed a reduced CIL response, being able to invade fibroblast cultures in what was compared to invasive metastasis (see Refs [3–5]). Nonetheless, several factors led to a gradual loss of interest in the basis of this phenomenon. The molecular mechanism that orchestrates CIL has remained elusive for decades with only few recent advances [6–9]. This is partly owing to the fact that evidence for CIL occurring *in vivo* has been sparse [9–11]. Moreover, a different process, involving cell division rather than locomotion, was also named contact inhibition, leading to some confusion in the literature (see Glossary). Finally, there are also some common misconceptions, for example that CIL only happens when cells collide, or that its sole function is to inhibit migration.

In this article, we revisit the data that indicate CIL is a crucial mechanism for cell migration *in vivo*. Recent advances support a view of CIL as a general mechanism of local inhibition of cell protrusions in migratory cells. This leads to directional migration via the redirection of colliding single cells. Also, it is possible that CIL leads to directional movement in collective cell migration via promotion of coherence among cells. Thus, we propose that CIL could play an important role in coordinating the migration of this recognized mode of migration in embryonic and cancer cells [12,13]. Ongoing improvements in live imaging allow us to analyze CIL *in vivo* to test its importance in this context. We will review the few molecules reported to be involved in CIL. Moreover, recent advances

Glossary

Contact inhibition of locomotion (CIL): the phenomenon of a cell ceasing to continue moving in the same direction after contact with another cell.
Contact inhibition of proliferation (CIP): the phenomenon of a cell ceasing to proliferate after contact with other cells.
Heterotypic contact inhibition of locomotion: CIL present between cells of different types. It is usually lost in cancer cells when confronted with normal cells.
Homotypic contact inhibition of locomotion: CIL present between cells of the same type. It is exhibited by many normal and cancer cells.
Neural crest: A stem cell-like, migratory population of embryonic cells that forms laterally to the prospective central nervous system. It is essential for vertebrate development because of the wide range of derivatives to which it gives rise.
Endodermal cells: cells composing the inner-most embryonic germinal layer, that is the endoderm. These cells will differentiate mostly into the respiratory and digestive tracts of the adult body.
Myeloid cells: Blood cell precursors. In vertebrates there are two waves of haematopoiesis (the generation of blood cells). The first one, and the one relevant for the movements described in this article, is an embryonic (primitive) haematopoiesis in which blood cell precursors disperse from specific regions of the embryo to populate the entire body.
Cajal-Retzius cells: Transient neuronal population crucial for the development of the brain cortex.

Corresponding author: Mayor, R. (r.mayor@ucl.ac.uk).

0962-8924/$ – see front matter doi:10.1016/j.tcb.2010.03.005 Available online xxxxxx

Box 1. The discovery of CIL

The concept of CIL gradually emerged from the work of Abercrombie and Heaysman starting in 1953. They wanted to study how the behaviour of a cell is influenced by other cells, i.e. their '*social behaviour*'.

Heaysman and Abercrombie observed what happened when two embryonic chicken heart explants were placed in close proximity. Collisions occur between fibroblasts migrating from opposing explants. At the time they started their experiments, they could not perform detailed microscopic observations. Instead, they did careful macroscopic measurements obtaining statistical parameters to describe cell behaviour. Nonetheless, they made at least two crucial observations. First, they observed that fibroblasts will lower their speed in proportion to the number of cells they encounter. Thus, contact with or the proximity to other cells will reduce cell motility [1]. Moreover, they observed that at the region where the two explants encountered each other, the fibroblasts would never clump on top of each other. Instead, they will halt their migration or disperse elsewhere [2]. They concluded that a cell would preferentially adhere to the substrate rather than to its neighbouring cell. They called this restriction CIL and proposed that the tendency of alignment between neighbouring cells and the monolayering of explants were outcomes of CIL [2].

Later on, with improved observation tools, they added important cellular details to the process such as the retraction of the cell protrusion after contact and that the ruffling activity of the membrane will be restarted elsewhere in the cell perimeter [64]. Thus, CIL will more often lead to the redirection of colliding fibroblasts than to stop their movement [4,38]. All these observations integrated a more complete definition of CIL: '*the phenomenon of a cell ceasing to continue moving in the same direction after contact with another cell*' [3].

During the following years, different degrees of CIL were found in a large number of healthy and cancerous cell types (reviewed in Ref. [3]). Efforts were exerted to try to observe CIL *in vivo* with only limited success [10,11]. At the same time the implications of CIL in migration and morphogenesis were disputed [65–67]. By contrast, important advances in the field of cell migration were made with the identification of several molecular components that allowed the generation of models of cell polarization and chemotaxis [45,68–70]. These important new discoveries on directional cell migration were unmatched by a sufficiently detailed molecular understanding of CIL and the initial excitement on CIL faded away.

in our understanding of the molecular bases of cell migration will allow us to propose more candidate molecules that mediate CIL and a molecular link among them.

What is CIL?

The concept of CIL describes the observed behaviour of a cell to change the direction of its movement after contact with another cell (Box 1). The typical sequence of cell activities implicated in CIL are: (i) cell–cell contact, (ii) inhibition of cell protrusive activities at the site of contact, (iii) generation of a new protrusion away from the site of cell contact and (iv) migration in the direction of the new protrusion (Figure 1a). However, this sequence can be modified by different factors. For example, one of the cells might not be responsive to the other and thus, only one of the cells will be redirected. The number of surrounding cells can also alter the outcome of CIL. This four-step sequence is usually observed when individual cells, such as two fibroblasts, collide. However, in a sheet of cells only the cells at the free edge will produce lamellipodia whereas cells in contact with others at the centre of the cluster will generate smaller and more transient protrusions, if any. In this case, CIL will lead to the inhibition of cell protrusions of the inner cells in a cluster (Figure 1b). If a cluster of packed cells has a free edge, only the cells at the leading edge will produce protrusions. This can lead to directional migration of the whole cluster (Figure 1b), [2,4]. As a consequence of this behaviour, cells exhibiting CIL do not crawl over their neighbours leading to monolayer formation in groups and to scattering in single cells.

The lamellipodium has been described as the typical locomotory apparatus used to sense the adjacent cells during CIL; however, it is possible that other cell protrusions are also involved in this phenomenon (Box 2). For example, it has been recently proposed that filopodia could be the actual sensory structure in CIL [14]. This could mediate a type of CIL that would operate at longer distances than the cell body size and would probably involve collapse of protrusions but not necessarily a contact between the cell bodies. In fact, analysis of neural crest (NC) migration *in vivo* shows that these cells establish filopodia-like contacts with neighbouring cells and that this contact is sufficient to promote CIL [9,15].

CIL can control cell polarity

Spatial cues such as chemoattractants are usually considered to explain the persistent orientation of cell polarity that leads to directional migration [16]. CIL can also contribute to cell polarization because the cells form their protrusions away from the cell–cell contact. Molecules localized to the cell–cell contact will be absent from the leading edge and therefore contribute to polarity [17–19]. Thus, CIL does not only halt migration of cells but also allow cells to re-polarize and migrate in a new direction, serving as another type of spatial cue [20]. This is crucial during the migration of cells that disperse from an original common location, which is a frequent feature found in embryo development. For example, endodermal cells from mouse and zebrafish embryos are initially localized in a specific region of the forming body from where they disperse to colonize their final destinations (respiratory and digestive tracts) [21,22], or the myeloid cells, formed in the ventral region of the *Xenopus* embryo that need to scatter along the entire epidermis [23]. When migration of all these kinds of cells is carefully analysed, a clear suggestion of CIL behaviour is observed (refer to the supplementary videos in the aforementioned references). Cell collisions lead to a change in the direction of migration, upon which cells move away from each other. In addition, these cells rarely overlap and when protrusions are visible, they seem to retract upon contact. These features suggest that these migratory cells, and probably many others, exhibit CIL *in vivo*. The observation that cells are constantly contacting each other argues against the role of a chemorepellent as a mechanism of dispersion; although it is probable that a combination of different mechanisms drives cell migration in this and other processes during development.

Several mechanisms are known to operate during cell migration *in vivo* such as random walk, chemoattraction and cell intercalation [21,24]. However, time lapse analysis of these migrating cells is consistent with CIL being an additional mechanism that contributes to cell migration. For example, the migration of Cajal-Retzius cells, a transient neuronal population crucial for the development of

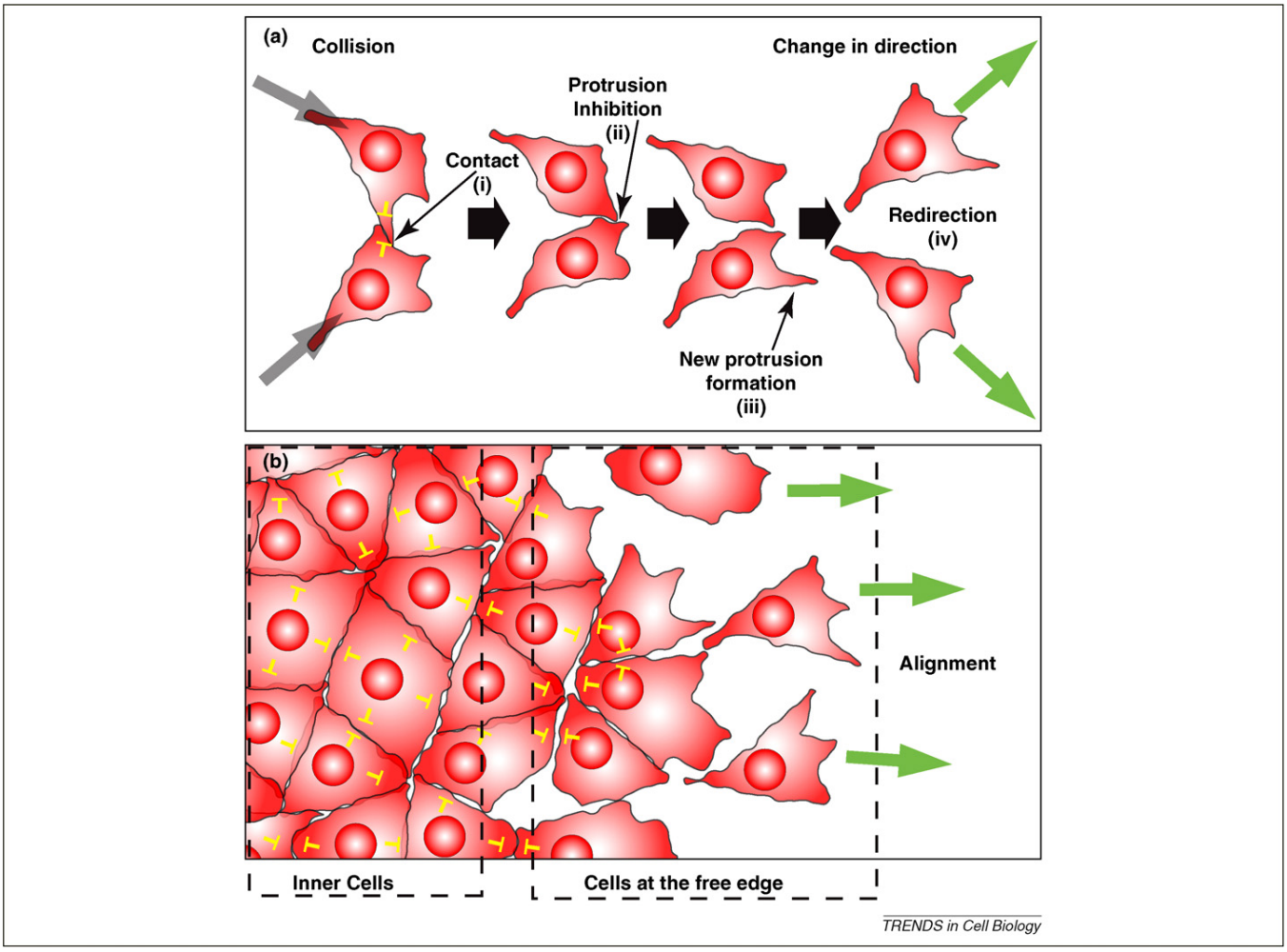

Figure 1. CIL in isolated cells **(a)** or in a group of cells **(b)**. CIL is represented by yellow inhibitory arrows. **(a)** Collision between single cells leads to collapse of cell protrusion and a change in the direction of migration (green arrows). The four steps of CIL are shown with roman numerals (see main text for details). **(b)** CIL in a group of cells. CIL between inner cells leads to inhibition of protrusions, whereas CIL between the leader cells, at the free edge, can lead to cell polarization of the leaders (green arrows) and directional migration.

the brain cortex, is controlled by the apposed meningeal membranes, which produce and secrete the chemokine Cxcl12 [25]. However, this chemokine seems to be uniformly distributed along the migratory space and what provides the directionality in the dispersion of these cells are 'contact-inhibitory interactions' [25], which correspond to CIL. Indeed the assay used to characterize the interactions between these cells is the same as the one used by Abercrombie and Heaysman when CIL was initially described [2]. These observations suggest that CIL could be a general migratory mechanism that co-exists with processes such as chemoattraction, random-walk and cell intercalation to re-set the polarity of migratory cells.

Collective cell migration: migratory ensembles require harmonic movements

In multicellular organisms, cells often move in groups rather than as singular cells. Cell migration in loosely or closely associated groups has been called collective cell migration (reviewed in Refs [12,13,26]). Collective cell migration is now a widely recognized mode of migration during embryogenesis and cancer. Both collective cell migrations and CIL are defined by the ability of cells to interact with their neighbours during migration and it is probable that these two processes are linked. There is a wide variety of collective cell migration, from sheets of migrating cells found in carcinomas and in head mesoderm of amphibian embryos (Figure 2a, [6,27,28]), to closely associated clusters of cells such as the migration of the lateral line in zebrafish, border cells in *Drosophila* embryos or melanomas (Figure 2b, [29,30]). Other cells are organized in chains such as *Drosophila* myoblasts or squamous cell carcinoma (Figure 2c, [31,32]). Another example of this is the migration of endothelial cells during sprouting in angiogenesis, in which inhibition of cell protrusion between the cells and presence of large lamellipodia and filopodia in the leader cells has been compared to CIL [33]. Another mode of collective cell migration has been called streaming (Figure 2d), and has been found in the migration of neural crest cells, mammalian endoderm and possibly in some breast carcinomas [9,15,34,35]. In this type of migration, the cells move as a loose cluster in which individual cells can be identified but are constantly interacting with each other. Interestingly, it has been shown

Box 2. Rho GTPases and cell polarity

Directional cell migration is dependent on cell polarity which influences the formation of the leading and trailing cell edges. A typical polarized migrating cell exhibits cell protrusions, such as filopodia and lamellipodia, at the front and large focal adhesion complex at the back (Figure I). Directional cell migration is achieved by the polarized formation of cell protrusions at the front and the contraction of stress fibres at the trailing edge. The typical Rho GTPases – RhoA, Rac1 and Cdc42 – play a crucial role in controlling cell polarity. These three Rho GTPases regulate different aspects of cytoskeleton dynamics. Cdc42 has been shown to be involved in controlling the actin cytoskeleton present in protrusions known as filopodia [71]. Rac1 promotes the formation of lamellipodia – large, flattened and ruffling protrusions – by regulating actin polymerization [72]. The three Rho isoforms – RhoA, RhoB and RhoC – can induce stress fibre formation [73]. The general view is that in polarized cells Rac1 and Cdc42 are active at the front where they promote the formation of cell protrusions, whereas RhoA is active at the back where it controls cell contraction. In addition a clear mutual inhibition between Rac1 and RhoA has been established [74]. However, recent studies have shown that all three GTPases can be activated at the front of migrating cells, where RhoA has a role in the initial events of protrusion, whereas Rac1 and Cdc42 are involved in reinforcement and stabilization of newly expanded protrusions [75,76].

In addition to their role in actin dynamics, the Rho GTPases also control polarized adhesion to the substratum during directional migration. Small focal complex structures are localized in the lamellipodia of most migrating cells, and are important for the attachment of the extending lamellipodium to the extracellular matrix [68]. It has been shown that Rac is required for focal complex assembly [74,77]. Focal complexes can be disassembled as the cell lamella moves over them or can mature into focal adhesions induced by RhoA [74].

For many cells the final step of the cell migration cycle is the retraction of the back to move forward. This cell body contraction is dependent on actomyosin contractility and can be regulated by RhoA via ROCKs (also known as Rho-kinases) to affect myosin light chain (MLC) phosphorylation, both by inhibiting MLC phosphatase and by phosphorylating MLC [78].

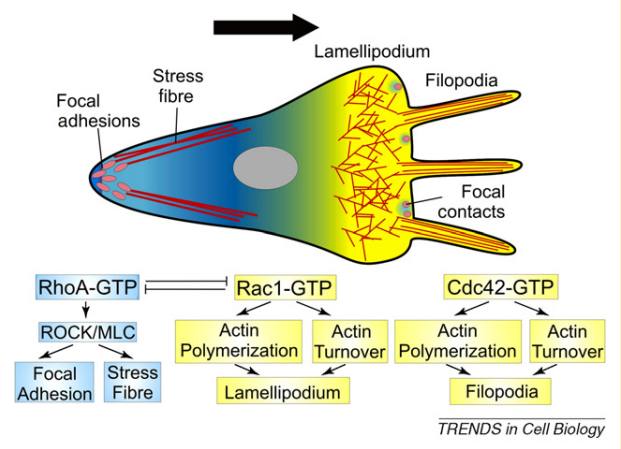

Figure I. Rho GTPases and cell protrusion control.

that during neural crest migration, an example of cell streaming, cells make local and transient contacts which are required for CIL [9,15].

Despite the diversity of types of collective migration, there is a common theme for all of them: they all have major protrusions at the leading edge and show a high degree of organization and coordination during migration, which are features of CIL [6,9]. Although the degree of inhibition of cell protrusions between cells is variable and in some cases cryptic protrusions are observed between cells [36,37], it is tempting to speculate that the inhibition of protrusions in cell clusters during collective cell migration is based on CIL. If so, the two types of CIL – in single cell migration (Figure 1a) and in collective movements (Figure 1b) – would represent two aspects of the same process. It has been shown that CIL plays a role in collective migration of mesenchymal cells, such as neural crest [9,15], but there is no evidence that it could have a similar role in migration of more epithelial cells. Further knowledge of the molecular basis of CIL is required to compare it with the molecular mechanism that inhibits cell protrusions during collective cell migration.

Predictions for the molecular bases of CIL

The molecular mechanisms that regulate CIL are still unknown, which is largely owing to the lack of investigation and debate on this topic. Despite the sparse data available, it is still possible to dissect CIL into two core cellular mechanisms requiring two different types of molecular machineries. First, cells need to sense the contact with other cells. This mechanism needs to be mediated by molecules located at the cell surface and to have a cognate ligand/receptor pair on the surface of the contacting cell. Moreover, molecules mediating the contact are also required to be able to transduce the signal from the juxtaposed cell into the responding cell. This response is the second mechanism. Upon contact, cells require a mechanism that regulates the withdrawal of protrusions at the contact region followed by the formation of a new protrusion elsewhere. Thus, the second mechanism is basically a repolarization mechanism. Importantly, molecules involved in these two mechanisms have been described as required for proper CIL. However, these two mechanisms have not been directly linked to each other. In this section we will review this evidence and propose a possible molecular link between these findings. Also we propose other surface molecules that could be mediating CIL (Box 3).

Cell surface molecules potentially involved in CIL

Different pieces of information suggest that molecules, usually linked with cell–cell adhesion, are likely to mediate CIL. Although at a first sight there might be an apparent contradiction between CIL and adhesion, there is actually a long-standing link between these two mechanisms [4]. Although CIL implies cell repulsion and dispersion, it also requires adhesion to strengthen the contact and to allow cell–cell signalling to occur. In fact, the establishment of transient adhesion points between colliding cells has been observed *in vitro* before their lamellipodia are retracted owing to CIL [38]. Moreover, it is clear that adhesion molecules do not only provide mechanical adhesion but they also work as ligand/receptor pairs playing an important role in cell signalling.

One of these molecule families is cadherins. Cadherins are a multigene family of cell surface glycoproteins that

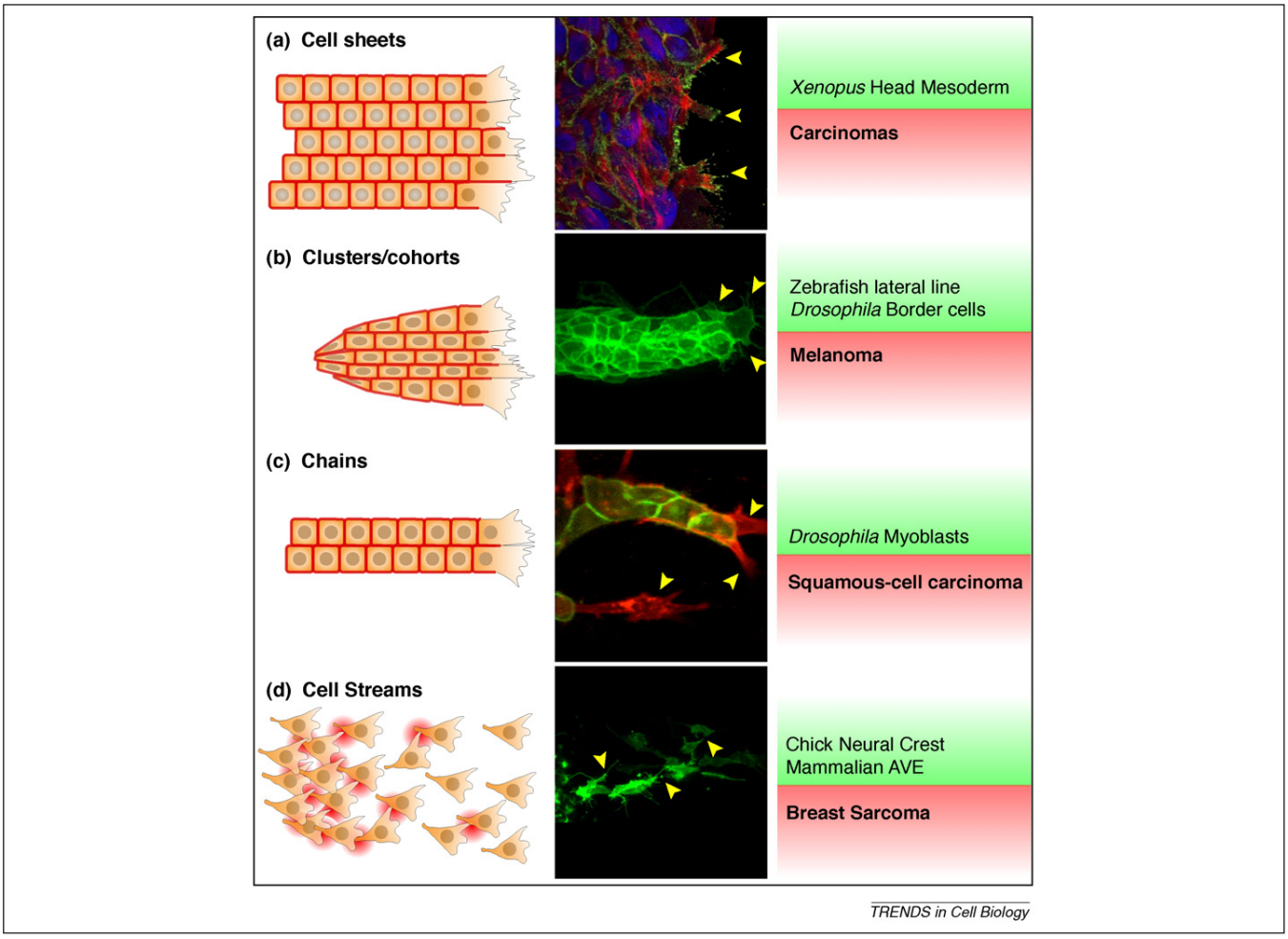

Figure 2. Examples of collective cell migration. First column: schematic representation of different migratory types. The regions where cells are interacting are depicted as a red border. Second column: examples. **(a)** Intestinal epithelial cells. From Ref. [94], used with permission. **(b)** Zebrafish lateral line. Reprinted from: Haas *et al.* (2006) Chemokine signaling mediates self-organizing tissue migration in the zebrafish lateral line, *Developmental Cell* 10, 673–680, with permission from Elsevier. **(c)** Fibroblast-leaded squamous cell carcinoma invasion. Adapted by permission from Macmillan Publishers Ltd: *Nature Cell Biology* [32]. **(d)** Avian neural crest. Reprinted from: Rupp *et al.* (2007) A role for RhoA in the two-phase migratory pattern of post-otic neural crest cells, *Developmental Biology* 311, 159–171, with permission from Elsevier. Yellow arrowheads show localised protrusion formation. Third column: examples of these different types of migration in health (green background) and disease (red background). AVE: anterior visceral endoderm.

mediate Ca^{2+}-dependent homophilic cell–cell adhesion by their extracellular domains. Moreover, they can activate intracellular signals involved in cell polarity and in cytoskeleton control such as RhoA and Ena/VASP [39]. Cadherins were among the first molecules that were directly implicated in CIL. E-cadherin has been shown to be required for CIL, and interestingly not for contact inhibition of proliferation (CIP), in migratory cells and in confluent epithelial cells [7,8,40,41]. Likewise, the XB/U-cadherin in *Xenopus* (similar to the mammalian P-cadherin) is required for the contact-dependent coordination in collective migration of head mesoderm [6]. Interestingly, a recent similar study in fish embryos has shown the requirement of E-cadherin for collective migration of mesoderm *in vivo* [42]. Although the authors mostly attribute its role to cell–cell adhesion, they also suggest a possible role for CIL in mesoderm migration. An appealing hypothesis would be that both adhesion and CIL converge at the level of E-cadherin to control collective migration. This is supported by the role of E-cadherin in CIL and the link between CIL and adhesion. Altogether, these data indicate that cadherins are essential for CIL. At the same time they highlight that different tissues or cell types could use different cadherins or even other adhesion molecules during CIL (Box 3).

Molecular bases of CIL-dependent cell polarity

A key step in CIL is the inhibition of cell protrusions and the re-setting of the intracellular polarity. Cell protrusions are dynamic and complex structures that are formed largely by actin filaments and are regulated by intricate molecular networks (see Box 2, Ref. [43]). Thus, the inhibition of cell protrusions is not a passive mechanism but, instead, requires the activation of a complex regulatory machinery [44,45]. Members of the family of small Rho GTPases are essential in the control of both cell polarity and protrusions [46] (Box 2). RhoA is known to control myosin II-dependent contraction of the trailing end of a cell through the protein kinase ROCK [47,48]. Therefore, RhoA can be a negative regulator of protrusion formation and,

Box 3. Possible surface molecules that control CIL

Candidates for cell–cell recognition required in CIL should be transmembrane molecules involved in contact-mediated cell signalling. They also should control cell protrusion formation/retraction, probably via the regulation of the cytoskeleton dynamics. Cadherins accomplish these criteria (see main text) but other molecules could also have a potential role in CIL.

Another group of CIL candidate molecules are the **atypical cadherins** Dachsous (Ds), Fat and Flamingo (Fmi), which are involved in planar cell polarity (PCP) or non-canonical Wnt signalling. Because Ds, Fat and Fmi play crucial roles in the localization of the typical PCP receptor Frizzled (Fz), [39] it is possible that cell collision during CIL engages these atypical cadherins, which in turn activate Fz and Dsh in the region of cell contact. Interestingly, it has been shown that Fmi plays a crucial role in cell movements and migration during zebrafish gastrulation [79]. However, the role of these atypical cadherins in CIL needs to be directly tested.

The ***Notch-Delta*** signalling pathway is usually known by its transcriptional regulation that occurs after Delta, a transmembrane protein binds its receptor Notch in an adjacent cell. This leads to the cleavage of Notch whose intracellular domain is translocated to the cell nucleus [80,81]. However, there are recent data in *Drosophila* for non-transcriptional branches of the Notch signalling [82,83]. This non-transcriptional function is based on the interaction of Notch with the intracellular tyrosine kinase Abl and its cofactors, crucial for the motility and guidance of motor axons (Refs [84–86]). Interestingly, one of the molecules that interacts with Notch and Abl is Trio, a guanine nucleotide exchange factor (GEF) protein that can activate RhoA [87,88].

Ephrins comprise a family of transmembrane proteins that bind to their cognate receptor tyrosine kinase Eph. Both ephrins and Eph receptors can transduce signals and they are crucial regulators of cell–cell communication in processes like cell adhesion and repulsion [89]. The repulsive activity of Eph/ephrin signals has been well characterized in axonal guidance. It is possible that this repulsive activity could be similar in molecular terms to the collapse of protrusions in CIL.

There are two classes, A and B, of Ephrins, which usually interact with EphA and EphB receptors, respectively. They can activate Rho GTPases, such as RhoA (preferentially via ephrinA/EphA binding) and Rac1 and Cdc42 (preferentially via ephrinB/EphB binding, Ref. [90]). Nonetheless, ephrinB/EphB can also activate RhoA via Dsh/PCP signalling [91–93].

Nectins have various roles in cell polarization, differentiation, movement, proliferation and survival and they have been directly implicated in contact inhibition [61]. They are known to inhibit RhoA, in an Src dependent manner, by a ternary complex formed by Necl5, integrin $\alpha v\beta 3$ and PDGFR. It has been proposed that cell–cell contact allows the interaction between Nectin3 and Nectin-like 5 (Necl5) which leads to endocytosis of Necl5, so releasing RhoA inhibition [61]. However, it has not been properly clarified if this mechanism leads to the inhibition of proliferation or to proper CIL.

thus, a good candidate for a protrusion inhibitory mechanism. The spatial and temporal control of RhoA activity is crucial for appropriate inhibition of cell protrusions. This control can be exerted by a variety of molecules, among which, we find cell adhesion molecules and members of the non-canonical Wnt or planar cell polarity (PCP) signalling pathway.

Recent evidence in neural crest cells shows that RhoA is involved in CIL via the PCP pathway [9]. Here it was shown that CIL members of the PCP signalling would be activated at cell–cell contacts, which in turn locally activate RhoA. Activated RhoA would then antagonise Rac1 and inhibit cell protrusions [9,34]. Interestingly, a similar mechanism has been described for the inhibition of cell protrusions by cell–cell contact during vasculogenesis [33]. Although this is an interesting mechanism, it does not fully account for how the presence of an adjacent cell is transduced into this intracellular mechanism. However, with the literature available it is possible to propose a molecular link between cadherins and RhoGTPases.

Linking cadherins with Rho

Activation of different Rho GTPases appears to be cell type and cadherin-type dependent. It is well established that cadherin engagement leads to activation of Rac1 and Cdc42 and inhibition of RhoA at the cell contact region of many cells [49]. However, activation of RhoA as a result of cell–cell adhesion has been reported in keratinocytes [50] and in N-cadherin dependent cell–cell adhesion of C2C12 myoblasts [51]. It has also been shown that association of N-cadherin with p120 (a catenin that binds to the intracellular domain of cadherins) in cholesterol-rich microdomains leads to activation of RhoA during myogenesis [52]. Whether a similar mechanism occurs in migratory cells remains unknown. It is known that one of the functions of p120ctn is the regulation of Rho GTPases, which has led to suggest that the inhibitory activity of p120ctn on RhoA is dependent on the cytoplasm localisation of p120ctn. Expression of different cadherins sequestrates p120ctn to the membrane and blocks the inhibition of RhoA by p120ctn, suggesting that formation of cadherin-based cell–cell adhesion established during CIL sequesters p120ctn to the membrane and away from cytoplasmic pools therefore relieving the inhibition of RhoA activity (Refs [53–56]). In addition, it has been shown that inhibition of sprouting during vasculogenesis requires VE-cadherin, which in turn activates RhoA and inhibits Rac1 at cell junctions, in a process reminiscent of CIL [33,57].

It is probable that different cells use different molecules to interact with their neighbours, giving more versatility to CIL. This greater flexibility could explain why the same cell can exhibit CIL with one particular kind of cell but not with others. Other molecules such as Ephrins/Eph and Notch/Delta and PCP proteins are also possible mediators of CIL (Box 3).

CIL in disease

The first crucial contribution of CIL to cancer research was the idea that cell locomotion is a normal activity of somatic cells that needs to be restricted for the cells to remain at the right place within an organism. This restriction comes from neighbouring cells, which when absent, will allow the migration of cells liberated from this repression. Malignancy, thus, is not necessarily the acquisition of motility by cancerous cells but the absence or lessening of the response to the inhibition of migration exerted by neighbours [3,4]. This intrinsic but inhibited tendency to migrate of at least some somatic cells has been proposed as important for normal physiological processes such as wound healing of epithelia. In addition to CIL the activity of growth factors also plays a role to stimulate re-epithelization and to produce significant changes in adhesion and cell morphology during wound healing [58,59].

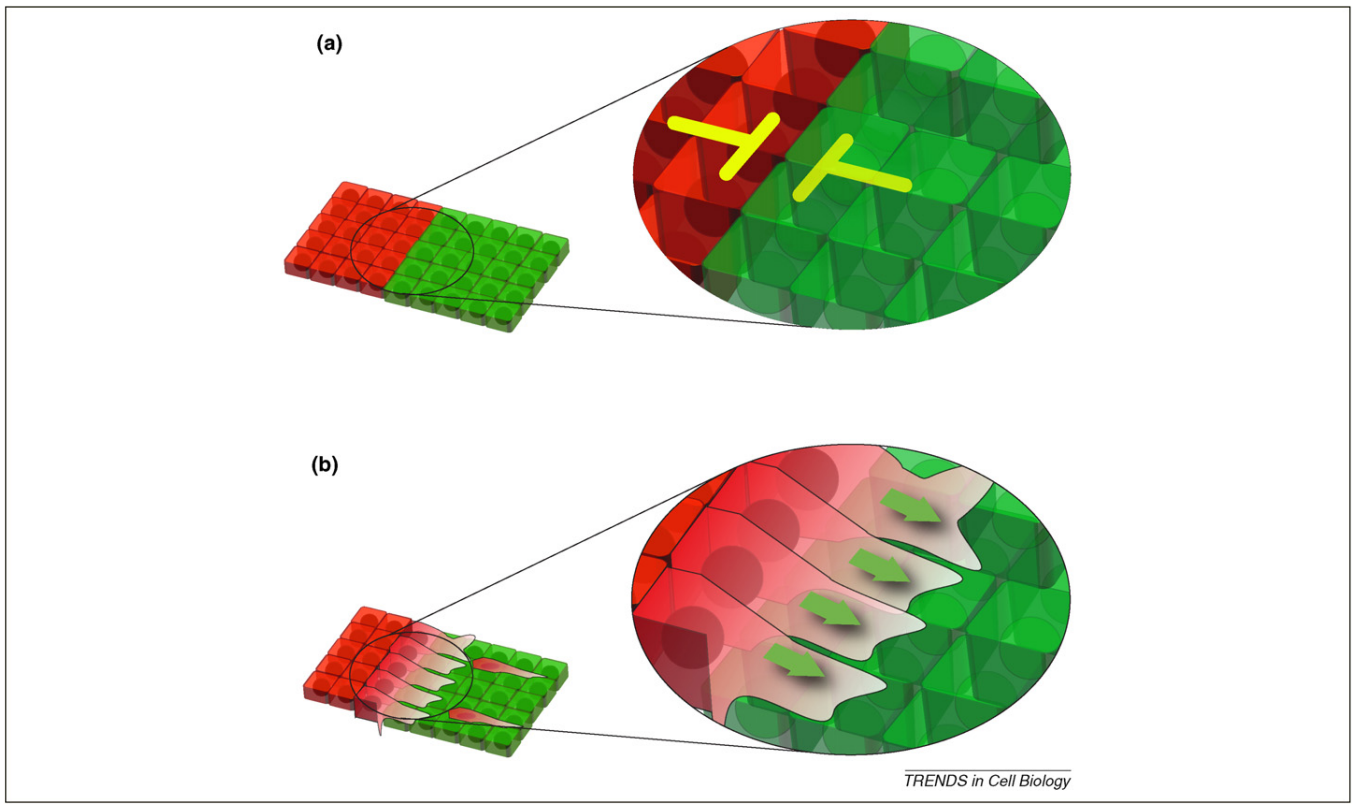

Figure 3. CIL in normal and cancer cells. **(a)** Two cell populations (indicated by two different colours) exhibit mutual CIL (yellow inhibitory arrows). This prevents the mixing of cells from these two populations. This kind of behaviour can be found in normal tissues. **(b)** Two cell populations are confronted and one of them (red cells) has lost CIL with the other (green cells). As a consequence the first group invades the second one. This invasive behaviour can be found in many cancer cells and has been proposed as the basis for metastasis.

To better understand the effect of CIL in normal and cancerous cells, it is necessary to keep in mind that there are two types of CIL. When two cells (or groups of cells) of the same type encounter each other they can exhibit CIL or not. If they do, it is said that they have **homotypic CIL** (see Glossary). This has been extensively documented in chick heart fibroblast [2], among other cell types. Similarly, two different cell types can encounter each other and also display CIL, which would then correspond to **heterotypic CIL** (see Glossary; Figure 3a). Chick heart fibroblasts, for example, exhibit this behaviour when confronted with normal mouse muscle fibroblasts [3].

By contrast, several sarcoma and melanoma cell lines have diminished or absent CIL: they will invade territories populated by other cells, such as normal fibroblasts (Figure 3b). This led to the conclusion that absence of CIL between tumour and normal cells was at the basis of invasive metastasis [3]. A common misunderstanding of these observations is to believe that malignant cells have lost CIL between themselves. It has been shown that malignant cells have lost heterotypic CIL when confronted with normal fibroblasts but they usually do not lose homotypic CIL (Ref. [4], P. Friedl, personal communication). This is similar to what happens to neural crest cells that have homotypic CIL (among neural crest cells) but can invade mesoderm and other tissues during their migration [9]. An appealing hypothesis would be that the invasive behaviour of tumours is facilitated by the absence of heterotypic CIL with normal cells, whereas homotypic CIL between cancer cells helps collective migration and/or dispersion of the tumour. Also, it should be noted that CIL in malignant cells is not always lost but sometimes diminished. For example, the invasion of S180 sarcoma cells is almost completely unobstructed by chick heart fibroblasts, whereas that of mouse melanomas or BAS56 sarcoma cells is partially blocked [3]. The implications of CIL in the invasive properties of tumours *in vivo* remain to be studied. A recent study showed that the activation of the cytoplasmic form of the human oncogene *MET* in mouse liver progenitor cells (MLP29) produced loss of contact inhibition [60]. Interestingly, when these cells are transplanted into the spleen of immunodeficient mice they become highly invasive carcinomas.

The usual misconception that cancer cells have lost contact inhibition only holds true for CIP (see Glossary) and not for CIL between cancer cells. It has been proposed that CIP and CIL are molecularly similar [61], but the evidence for this is scarce, and the simple observation that many tumours do not have CIP but retain CIL with other cancer cells, strongly suggests that these are two different processes. The molecular basis of CIL in cancer is a fascinating, but poorly developed, area of research that could have important practical implications. Understanding the molecular mechanism by which cancer cells have lost CIL with neighbouring cells could lead to new diagnostic and therapeutic tools.

Concluding remarks and future directions

Collective migration is now a well-recognized mechanism of migration both in morphogenesis and in cancer

Box 4. Outstanding questions

- What are the signals that mediate cell–cell recognition during CIL?
- How are homotypic and heterotypic CIL controlled?
- How is the change in cell polarity controlled during CIL?
- How is CIL related with other cellular processes such as axon guidance/repulsion?
- Is the inhibition of cell protrusions observed in collective cell migration dependent on CIL?
- How does CIL modulate the contribution of other mechanisms in migration, such as adhesion, taxis and invasion?
- How is CIL involved in cancer metastasis?

Finally, a better understanding of CIL will contribute to our understanding of wound healing and contribute towards strategies to control cancer cell invasion.

progression [12,13,62]. Thus, the cellular and molecular understanding of the cell–cell interactions in this type of migration is crucial. CIL is a cellular interaction likely to be crucial for collective migration. However, a better description of its molecular basis *in vivo* is needed, as well as an understanding as to whether CIL is actually linked to collective cell migration (see Box 4 for outstanding questions about CIL).

At the same time development of fluorescent transgenic animals and improvements in microscopy techniques, such as confocal microscopy and time lapse imaging, will help to accelerate our molecular description of CIL *in vivo*. These techniques provide non-invasive imaging tools that allow us to investigate cell migration *in vivo* in genetically modifiable organisms where the role of different molecules can be tested.

These are early days in understanding the molecular basis of CIL. However, we have dissected it into two sequential mechanisms with different molecular players. They involve a cell adhesion molecule-dependent first step in which the colliding cells sense each other. This mechanism is followed by a repolarization of the cell. We provide evidence favouring a role for cadherins in the first process, followed by a RhoGTPases-dependent repolarization during the second. Also, we have proposed a link between these two processes. However, other molecules could also be mediating CIL and further investigation is needed to establish a detailed molecular explanation of CIL and to elucidate its cell-type specificity. This is a crucial step because it would allow us to investigate the problem of why most cancerous cell can reduce the heterotypic CIL while maintaining homotypic CIL among them.

The role of CIL in collective migration also raises an interesting problem of how large groups of cells can self-organize from local cell–cell interactions. Self-organization of migratory groups of cells have been described in several morphogenetic movements such as the lateral line [29] and the migration of tumour cohorts [12]. Thus, CIL together with other local interactions such as cell–cell adhesion could organise tissues at a much larger scale. In fact, recent mathematical models have successfully reproduced the behaviour of migratory sheets by only considering local interactions at the single cell level, especially CIL [63]. These cell–cell interactions can complement other mechanisms, such as taxis and physical forces, in promoting migration of groups and clusters of cells. The molecular characterization of CIL is just starting to be unravelled but the increasing evidence of its importance will promote a better understanding of this process in normal and pathological cell migration.

Acknowledgements

We thank Marianne Bronner-Fraser, Martin Raff, Carl-Phillip Heisenberg, Graham Dunn, Nicolas B. David, Mae Woods, Jubin Kashef, Claudio Stern, Rachel Moore, Mae Wood and Roger Singleton for comments on the manuscript; Paul Kulesa, Ann M. Hopkins, Darren Gilmour and Erik Sahai for allowing use of the pictures depicted in Figure 2. RM was supported by the Medical Research Council, Biotechnology and Biological Sciences Research Council and Wellcome Trust, and CC-F by an Overseas Research Scholarships and a Boehringer Ingelheim Fellowship.

References

1 Abercrombie, M. and Heaysman, J.E.M. (1953) Observations on the social behaviour of cells in tissue culture: I. Speed of movement of chick heart fibroblasts in relation to their mutual contacts. *Exp. Cell Res.* 5, 111–131
2 Abercrombie, M. and Heaysman, J.E.M. (1954) Observations on the social behaviour of cells in tissue culture: II. 'Monolayering' of fibroblasts. *Exp. Cell Res.* 6, 293–306
3 Abercrombie, M. (1979) Contact inhibition and malignancy. *Nature* 281, 259–262
4 Abercrombie, M. and Ambrose, E.J. (1962) The surface properties of cancer cells: a review. *Cancer Res.* 22, 525–548
5 Abercrombie, M. and Heaysman, J.E. (1954) Invasiveness of sarcoma cells. *Nature* 174, 697–698
6 Winklbauer, R. *et al.* (1992) Cell interaction and its role in mesoderm cell migration during *Xenopus* gastrulation. *Dev. Dyn.* 195, 290–302
7 Huttenlocher, A. *et al.* (1998) Integrin and cadherin synergy regulates contact inhibition of migration and motile activity. *J. Cell Biol.* 141, 515–526
8 Bracke, M.E. *et al.* (1997) Functional downregulation of the E-cadherin/catenin complex leads to loss of contact inhibition of motility and of mitochondrial activity, but not of growth in confluent epithelial cell cultures. *Eur. J. Cell Biol.* 74, 342–349
9 Carmona-Fontaine, C. *et al.* (2008) Contact inhibition of locomotion in vivo controls neural crest directional migration. *Nature* 456, 957–961
10 Bard, J.B. and Hay, E.D. (1975) The behavior of fibroblasts from the developing avian cornea. Morphology and movement in situ and in vitro. *J. Cell Biol.* 67, 400–418
11 Bard, J.B. *et al.* (1975) Formation of the endothelium of the avian cornea: a study of cell movement in vivo. *Dev. Biol.* 42, 334–361
12 Friedl, P. and Wolf, K. (2003) Tumour-cell invasion and migration: diversity and escape mechanisms. *Nat. Rev. Cancer* 3, 362–374
13 Rørth, P. (2009) Collective cell migration. *Annu. Rev. Cell Dev. Biol.* 25, 407–429
14 Heckman, C.A. (2009) Contact inhibition revisited. *J. Cell. Physiol.* 220, 574–575
15 Teddy, J.M. and Kulesa, P.M. (2004) In vivo evidence for short- and long-range cell communication in cranial neural crest cells. *Development* 131, 6141–6151
16 Petrie, R.J. *et al.* (2009) Random versus directionally persistent cell migration. *Nat. Rev. Mol. Cell Biol.* 10, 538–549
17 Perez-Moreno, M. *et al.* (2003) Sticky business: orchestrating cellular signals at adherens junctions. *Cell* 112, 535–548
18 Ebnet, K. *et al.* (2004) Junctional adhesion molecules (JAMs): more molecules with dual functions? *J. Cell Sci.* 117, 19–29
19 Mellman, I. and Nelson, W.J. (2008) Coordinated protein sorting, targeting and distribution in polarized cells. *Nat. Rev. Mol. Cell Biol.* 9, 833–845
20 Cheng, G. *et al.* (2006) Cell population dynamics modulate the rates of tissue growth processes. *Biophys. J.* 90, 713–724
21 Pezeron, G. *et al.* (2008) Live analysis of endodermal layer formation identifies random walk as a novel gastrulation movement. *Curr. Biol.* 18, 276–281
22 Srinivas, S. *et al.* (2004) Active cell migration drives the unilateral movements of the anterior visceral endoderm. *Development* 131, 1157–1164

23 Costa, R.M. *et al.* (2008) spib is required for primitive myeloid development in *Xenopus*. *Blood* 112, 2287–2296
24 Nair, S. and Schilling, T.F. (2008) Chemokine signaling controls endodermal migration during zebrafish gastrulation. *Science* 322, 89–92
25 Borrell, V. and Marin, O. (2006) Meninges control tangential migration of hem-derived Cajal-Retzius cells via CXCL12/CXCR4 signaling. *Nat. Neurosci.* 9, 1284–1293
26 Montell, D.J. (2008) Morphogenetic cell movements: diversity from modular mechanical properties. *Science* 322, 1502–1505
27 Bell, C.D. and Waizbard, E. (1986) Variability of cell size in primary and metastatic human breast carcinoma. *Invasion Metastasis* 6, 11–20
28 Nabeshima, K. *et al.* (1998) Hepatocyte growth factor/scatter factor induces not only scattering but also cohort migration of human colorectal-adenocarcinoma cells. *Int. J. Cancer* 78, 750–759
29 Haas, P. and Gilmour, D. (2006) Chemokine signaling mediates self-organizing tissue migration in the zebrafish lateral line. *Dev. Cell* 10, 673–680
30 Day, C.L., Jr *et al.* (1981) Malignant melanoma. Prognostic significance of 'microscopic satellites' in the reticular dermis and subcutaneous fat. *Ann. Surg.* 194, 108–112
31 Richardson, B.E. *et al.* (2007) SCAR/WAVE and Arp2/3 are crucial for cytoskeletal remodeling at the site of myoblast fusion. *Development* 134, 4357–4367
32 Gaggioli, C. *et al.* (2007) Fibroblast-led collective invasion of carcinoma cells with differing roles for RhoGTPases in leading and following cells. *Nat. Cell Biol.* 9, 1392–1400
33 Abraham, S. *et al.* (2009) VE-Cadherin-mediated cell-cell interaction suppresses sprouting via signaling to MLC2 phosphorylation. *Curr. Biol.* 19, 668–674
34 Matthews, H. *et al.* (2008) Directional migration of neural crest cells in vivo is regulated by Syndecan-4-dependent Rac1 and non-canonical Wnt signalling-dependent RhoA. *Development* 135, 1771–1780
35 Hegerfeldt, Y. *et al.* (2002) Collective cell movement in primary melanoma explants: plasticity of cell-cell interaction, beta1-integrin function, and migration strategies. *Cancer Res.* 62, 2125–2130
36 Farooqui, R. and Fenteany, G. (2005) Multiple rows of cells behind an epithelial wound edge extend cryptic lamellipodia to collectively drive cell-sheet movement. *J. Cell Sci.* 118, 51–63
37 Vasilyev, A. *et al.* (2009) Collective cell migration drives morphogenesis of the kidney nephron. *PLoS Biol.* 7, e9
38 Abercrombie, M. (1970) Contact inhibition in tissue culture. *In Vitro* 6, 128–142
39 Halbleib, J.M. and Nelson, W.J. (2006) Cadherins in development: cell adhesion, sorting, and tissue morphogenesis. *Genes Dev.* 20, 3199–3214
40 Chen, W.C. and Obrink, B. (1991) Cell-cell contacts mediated by E-cadherin (uvomorulin) restrict invasive behavior of L-cells. *J. Cell Biol.* 114, 319–327
41 Ayollo, D.V. *et al.* (2009) Rearrangements of the actin cytoskeleton and E-cadherin-based adherens junctions caused by neoplasic transformation change cell-cell interactions. *PLoS ONE* 4, e8027
42 Arboleda-Estudillo, Y. *et al.* (2010) Movement directionality in collective migration of germ layer progenitors. *Curr. Biol.* 20, 161–169
43 Pollard, T.D. and Borisy, G.G. (2003) Cellular motility driven by assembly and disassembly of actin filaments. *Cell* 112, 453–465
44 Lauffenburger, D.A. and Horwitz, A.F. (1996) Cell migration: a physically integrated molecular process. *Cell* 84, 359–369
45 Ridley, A.J. *et al.* (2003) Cell migration: integrating signals from front to back. *Science* 302, 1704–1709
46 Ladwein, M. and Rottner, K. (2008) On the Rho'd: the regulation of membrane protrusions by Rho-GTPases. *FEBS Lett.* 582, 2066–2074
47 Xu, J. *et al.* (2003) Divergent signals and cytoskeletal assemblies regulate self-organizing polarity in neutrophils. *Cell* 114, 201–214
48 Riento, K. and Ridley, A.J. (2003) Rocks: multifunctional kinases in cell behaviour. *Nat. Rev. Mol. Cell Biol.* 4, 446–456
49 Erez, N. *et al.* (2005) Signaling from adherens-type junctions. *Eur. J. Cell Biol.* 84, 235–244
50 Calautti, E. *et al.* (2002) Fyn tyrosine kinase is a downstream mediator of Rho/PRK2 function in keratinocyte cell-cell adhesion. *J. Cell Biol.* 156, 137–148
51 Charrasse, S. *et al.* (2002) N-cadherin-dependent cell-cell contact regulates Rho GTPases and {beta}-catenin localization in mouse C2C12 myoblasts. *J. Cell Biol.* 158, 953–965
52 Taulet, N. *et al.* (2009) N-cadherin/p120 catenin association at cell-cell contacts occurs in cholesterol-rich membrane domains and is required for RhoA activation and myogenesis. *J. Biol. Chem.* 284, 23137–23145
53 Anastasiadis, P.Z. *et al.* (2000) Inhibition of RhoA by p120 catenin. *Nat. Cell Biol.* 2, 637–644
54 Grosheva, I. *et al.* (2001) p120 catenin affects cell motility via modulation of activity of Rho-family GTPases: a link between cell-cell contact formation and regulation of cell locomotion. *J. Cell Sci.* 114, 695–707
55 Cozzolino, M. *et al.* (2003) p120 catenin is required for growth factor-dependent cell motility and scattering in epithelial cells. *Mol. Biol. Cell* 14, 1964–1977
56 Anastasiadis, P.Z. (2007) p120-ctn: a nexus for contextual signaling via Rho GTPases. *Biochim. Biophys. Acta* 1773, 34–46
57 Nelson, C.M. *et al.* (2004) Vascular endothelial-cadherin regulates cytoskeletal tension, cell spreading, and focal adhesions by stimulating RhoA. *Mol. Biol. Cell* 15, 2943–2953
58 Singer, A.J. and Clark, R.A.F. (1999) Cutaneous wound healing. *N. Engl. J. Med.* 341, 738–746
59 Gurtner, G.C. *et al.* (2008) Wound repair and regeneration. *Nature* 453, 314–321
60 Boccaccio, C. *et al.* (2005) The MET oncogene drives a genetic programme linking cancer to haemostasis. *Nature* 434, 396–400
61 Takai, Y. *et al.* (2008) Nectins and nectin-like molecules: roles in contact inhibition of cell movement and proliferation. *Nat. Rev. Mol. Cell Biol.* 9, 603–615
62 Friedl, P. and Gilmour, D. (2009) Collective cell migration in morphogenesis, regeneration and cancer. *Nat. Rev. Mol. Cell Biol.* 10, 445–457
63 Bindschadler, M. and McGrath, J.L. (2007) Sheet migration by wounded monolayers as an emergent property of single-cell dynamics. *J. Cell Sci.* 120, 876–884
64 Abercrombie, M. and Ambrose, E. (1958) Interference microscope studies of cell contacts in tissue culture. *Exp. Cell Res.* 15, 332–345
65 Davis, E.M. and Trinkaus, J.P. (1981) Significance of cell-to-cell contacts for the directional movement of neural crest cells within a hydrated collagen lattice. *J. Embryol. Exp. Morphol.* 63, 29–51
66 Erickson, C. and Olivier, K. (1983) Negative chemotaxis does not control quail neural crest cell dispersion. *Dev. Biol.* 96, 542–551
67 Trinkaus, J.P. (1985) Further thoughts on directional cell movement during morphogenesis. *J. Neurosci. Res.* 13, 1–19
68 Lauffenburger, D.A. and Horwitz, A.F. (1996) Cell migration: a physically integrated molecular process. *Cell* 84, 359–369
69 Kay, R. *et al.* (2008) Changing directions in the study of chemotaxis. *Nat. Rev. Mol. Cell Biol.* 9, 445–463
70 King, J.S. and Insall, R.H. (2009) Chemotaxis: finding the way forward with Dictyostelium. *Trends Cell Biol.* 19, 523–530
71 Gupton, S.L. and Gertler, F.B. (2007) Filopodia: the fingers that do the walking. *Sci. Stke.* 400, re5 Erratum. Sci STKE. 2007;401:er4
72 Jaffe, A.B. and Hall, A. (2005) Rho GTPases: biochemistry and biology. *Annu. Rev. Cell Dev. Biol.* 21, 247–269
73 Wheeler, A.P. and Ridley, A.J. (2004) Why three Rho proteins? RhoA, RhoB, RhoC, and cell motility. *Exp. Cell Res.* 301, 43–49
74 Rottner, K. *et al.* (1999) Interplay between Rac and Rho in the control of substrate contact dynamics. *Curr. Biol.* 9, 640–648
75 Pertz, O. *et al.* (2006) Spatiotemporal dynamics of RhoA activity in migrating cells. *Nature* 440, 1069–1072
76 Machacek, M. *et al.* (2009) Coordination of Rho GTPase activities during cell protrusion. *Nature* 461, 99–103
77 Nobes, C.D. and Hall, A. (1995) Rho, rac, and cdc42 GTPases regulate the assembly of multimolecular focal complexes associated with actin stress fibers, lamellipodia, and filopodia. *Cell* 81, 53–62
78 Kaibuchi, K. *et al.* (1999) Regulation of the cytoskeleton and cell adhesion by the Rho family GTPases in mammalian cells. *Annu. Rev. Biochem.* 68, 459–486
79 Carreira-Barbosa, F. *et al.* (2009) Flamingo regulates epiboly and convergence/extension movements through cell cohesive and signalling functions during zebrafish gastrulation. *Development* 136, 383–392
80 Artavanis-Tsakonas, S. *et al.* (1999) Notch signaling: cell fate control and signal integration in development. *Science* 284, 770–776
81 Fortini, M.E. (2009) Notch signaling: the core pathway and its posttranslational regulation. *Dev. Cell* 16, 633–647

82 Zecchini, V. *et al.* (1999) An activity of Notch regulates JNK signalling and affects dorsal closure in Drosophila. *Curr. Biol.* 9, 460–469
83 Hodkinson, P.S. *et al.* (2007) Mammalian NOTCH-1 Activates β1 integrins via the small GTPase R-Ras. *J. Biol. Chem.* 282, 28991–29001
84 Giniger, E. (1998) A role for Abl in Notch signaling. *Neuron* 20, 667–681
85 Crowner, D. *et al.* (2003) Notch steers Drosophila ISNb motor axons by regulating the Abl signaling pathway. *Curr. Biol.* 13, 967–972
86 Le Gall, M. *et al.* (2008) Molecular separation of two signaling pathways for the receptor. *Notch. Dev. Biol.* 313, 556–567
87 Debant, A. *et al.* (1996) The multidomain protein Trio binds the LAR transmembrane tyrosine phosphatase, contains a protein kinase domain, and has separate rac-specific and rho-specific guanine nucleotide exchange factor domains. *Proc. Natl. Acad. Sci. U. S. A.* 93, 5466–5471
88 Kashef, J. *et al.* (2009) Cadherin-11 regulates protrusive activity in *Xenopus* cranial neural crest cells upstream of Trio and the small GTPases. *Genes Dev.* 23, 1393–1398
89 Klein, R. (2009) Bidirectional modulation of synaptic functions by Eph/ephrin signaling. *Nat. Neurosci.* 12, 15–20
90 Noren, N.K. and Pasquale, E.B. (2004) Eph receptor-ephrin bidirectional signals that target Ras and Rho proteins. *Cell. Signal.* 16, 655–666
91 Tanaka, M. *et al.* (2003) Association of Dishevelled with Eph tyrosine kinase receptor and ephrin mediates cell repulsion. *EMBO J.* 22, 847–858
92 Lee, H.S. *et al.* (2006) Dishevelled mediates ephrinB1 signalling in the eye field through the planar cell polarity pathway. *Nat. Cell Biol.* 8, 55–63
93 Ogawa, K. *et al.* (2006) EphB2 and ephrin-B1 expressed in the adult kidney regulate the cytoarchitecture of medullary tubule cells through Rho family GTPases. *J. Cell Sci.* 119, 559–570
94 Hopkins, A.M. *et al.* (2007) Organized migration of epithelial cells requires control of adhesion and protrusion through Rho kinase effectors. *Am. J. Physiol. Gastrointest. Liver Physiol.* 292, G806–G817

Bibliography

Abercrombie, M. (1970). Contact inhibition in tissue culture. *In Vitro*, 6(2):128–142.

Abercrombie, M. (1979). Contact inhibition and malignancy. *Nature*, 281:259 – 262.

Abercrombie, M. and Ambrose, E. (1958). Interference microscope studies of cell contacts in tissue culture. *Experimental Cell Research*, 15(2):332–345.

Abercrombie, M. and Ambrose, E. J. (1962). The surface properties of cancer cells: a review. *Cancer Research*, 22:525–48.

Abercrombie, M. and Dunn, G. (1975). Adhesions of fibroblasts to substratum during contact inhibition observed by interference reflection microscopy. *Exp Cell Res*, 92(1):57–62.

Abercrombie, M. and Heaysman, J. (1954). Observations on the social behaviour of cells in tissue culture. II. Monolayering of fibroblasts. *Experimental Cell Research*, 6(2):293–306.

Abercrombie, M. and Heaysman, J. E. (1953). Observations on the social behaviour of cells in tissue culture. I. Speed of movement of chick heart fibroblasts in relation to their mutual contacts. *Experimental Cell Research*, 5(1):111–31.

Abraham, S., Yeo, M., Montero-Balaguer, M., Paterson, H., Dejana, E., Marshall, C. J., and Mavria, G. (2009). Ve-cadherin-mediated cell-cell interaction suppresses sprouting via signaling to mlc2 phosphorylation. *Current Biology*, 19(8):668–74.

Alfandari, D., Cousin, H., Gaultier, A., Hoffstrom, B. G., and DeSimone, D. W. (2003). Integrin alpha5beta1 supports the migration of Xenopus cranial neural crest on fibronectin. *Developmental Biology*, 260(2):449–64.

Alon, U., Surette, M., Barkai, N., and Leibler, S. (1999). Robustness in bacterial chemotaxis. *Nature*, 397:168–171.

Altschuler, S. J., Angenent, S. B., Wang, Y., and Wu, L. F. (2008). On the spontaneous emergence of cell polarity. *Nature*, 454(7206):886–9.

Anderson, P. W. (1972). More Is Different. *Science*, 177(4047):393–396.

Arboleda-Estudillo, Y., Krieg, M., Sthmer, J., Licata, N. A., Muller, D. J., and Heisenberg, C.-P. (2010). Movement directionality in collective migration of germ layer progenitors. *Current Biology*, 20(2):161–169.

Atherton, E. and Sheppard, R. C. (1989). *Solid phase peptide synthesis: a practical approach*, volume 53 of *Practical approach series*. IRL Press.

Aybar, M. J. and Mayor, R. (2002). Early induction of neural crest cells: lessons learned from frog, fish and chick. *Current Opinion in Genetics & Development*, 12(4):452 – 458.

Ayollo, D. V., Zhitnyak, I. Y., Vasiliev, J. M., and Gloushankova, N. A. (2009). Rearrangements of the actin cytoskeleton and e-cadherin-based adherens junctions caused by neoplasic transformation change cell-cell interactions. *PLoS ONE*, 4(11):e8027.

Babloyantz, A., Salazar, J., and Nicolis, C. (1985). Evidence of chaotic dynamics of brain activity during the sleep cycle. *Physics Letters A*, 111(3):152 – 156.

Bakshy, E. and Wilensky, U. (2007). Netlogo-mathematica link.

Barber, C., Dobkin, D., and Huhdanpaa, H. (1996). The quickhull algorithm for convex hulls. *ACM Trans. on Mathematical Software*, 22(4):469–483.

Bard, J. B. and Hay, E. D. (1975). The behavior of fibroblasts from the developing avian cornea. morphology and movement in situ and in vitro. *Journal of Cell Biology*, 67(2PT.1):400–18.

Bard, J. B., Hay, E. D., and Meller, S. M. (1975). Formation of the endothelium of the avian cornea: a study of cell movement in vivo. *Developmental Biology*, 42(2):334–61.

Barkai, N. and Leibler, S. (1997). Robustness in simple biochemical networks. *Nature*, 387(6636):913–7.

Barlow, A. J., Wallace, A. S., Thapar, N., and Burns, A. J. (2008). Critical numbers of neural crest cells are required in the pathways from the neural tube to the foregut to ensure complete enteric nervous system formation. *Development*, 135(9):1681–1691.

Barrallo-Gimeno, A. and Nieto, M. A. (2005). The Snail genes as inducers of cell movement and survival: implications in development and cancer. *Development*, 132(14):3151–3161.

Bazazi, S., Buhl, J., Hale, J. J., Anstey, M. L., Sword, G. A., Simpson, S. J., and Couzin, I. D. (2008). Collective motion and cannibalism in locust migratory bands. *Current biology*, 18(10):735–9.

Bell, C. D. and Waizbard, E. (1986). Variability of cell size in primary and metastatic human breast carcinoma. *Invasion & Metastasis*, 6(1):11–20.

Bellairs, R. (2000). Michael abercrombie (1912-1979). *International Journal of Developmental Biology*, 44:23–28.

Belmadani, A., Tran, P. B., Ren, D., Assimacopoulos, S., Grove, E. A., and Miller, R. J. (2005). The Chemokine Stromal Cell-Derived Factor-1 Regulates the Migration of Sensory Neuron Progenitors. *Journal of Neuroscience.*, 25(16):3995–4003.

Beloussov, L. V. and Gordon, R. (2006). Preface to developmental morphodynamics (special issue). *Int J Dev Biol*, 50(2-3):79–80.

Bolos, V., Peinado, H., Perez-Moreno, M. A., Fraga, M. F., Esteller, M., and Cano, A. (2003). The transcription factor Slug represses E-cadherin expression and induces epithelial to mesenchymal transitions: a comparison with Snail and E47 repressors. *J Cell Sci*, 116(3):499–511.

Bonano, M., Trbulo, C., Calisto, J. D., Marchant, L., Snchez, S. S., Mayor, R., and Aybar, M. J. (2008). A new role for the endothelin-1/endothelin-a receptor signaling during early neural crest specification. *Developmental Biology*, 323(1):114 – 129.

Bonner, J. T., Barkley, D. S., Hall, E. M., Konijn, T. M., Mason, J. W., O'Keefe, G., and Wolfe, P. B. (1969). Acrasin, acrasinase, and the sensitivity to acrasin in dictyostelium discoideum. *Developmental Biology*, 20(1):72–87.

Borrell, V. and Marin, O. (2006). Meninges control tangential migration of hem-derived cajal-retzius cells via cxcl12/cxcr4 signaling. *Nature Neuroscience*, 9(10):1284–93.

Bracke, M. E., Depypere, H., Labit, C., Van Marck, V., Vennekens, K., Vermeulen, S. J., Maelfait, I., Philippe, J., Serreyn, R., and Mareel, M. M. (1997). Functional downregulation of the e-cadherin/catenin complex leads to loss of contact inhibition of motility and of mitochondrial activity, but not of growth in confluent epithelial cell cultures. *European Journal of Cell Biology*, 74(4):342–9.

Buhl, J., Sumpter, D. J. T., Couzin, I. D., Hale, J. J., Despland, E., Miller, E. R., and Simpson, S. J. (2006). From disorder to order in marching locusts. *Science*, 312(5778):1402–6.

Calautti, E., Grossi, M., Mammucari, C., Aoyama, Y., Pirro, M., Ono, Y., Li, J., and Dotto, G. P. (2002). Fyn tyrosine kinase is a downstream mediator of rho/prk2 function in keratinocyte cell-cell adhesion. *The Journal of Cell Biology*, 156(1):137–148.

Camazine, S., Deneubourg, J.-L., Franks, N. R., Sneyd, J., Theraula, G., and Bonabeau, E. (2001). *Self-Organization in Biological Systems*. Princeton University Press.

Cano, A., Perez-Moreno, M. A., Rodrigo, I., Locascio, A., Blanco, M. J., del Barrio, M. G., Portillo, F., and Nieto, M. A. (2000). The transcription factor snail controls epithelial-mesenchymal transitions by repressing e-cadherin expression. *Nature Cell Biology*, 2(2):76–83.

Carmona-Fontaine, C., Acuña, G., Ellwanger, K., Niehrs, C., and Mayor, R. (2007). Neural crests are actively precluded from the anterior neural fold by a novel inhibitory mechanism dependent on Dickkopf1 secreted by the prechordal mesoderm. *Developmental Biology*, 309(2):208–21.

Carmona-Fontaine, C., Matthews, H., and Mayor, R. (2008a). Directional cell migration in vivo: Wnt at the crest. *Cell Adhesion & Migration*, 2(4):240–2.

Carmona-Fontaine, C., Matthews, H. K., Kuriyama, S., Moreno, M., Dunn, G. A.,

Parsons, M., Stern, C. D., and Mayor, R. (2008b). Contact inhibition of locomotion in vivo controls neural crest directional migration. *Nature*, 456(7224):957–961.

Carney, T. J., Dutton, K. A., Greenhill, E., Delfino-Machín, M., Dufourcq, P., Blader, P., and Kelsh, R. N. (2006). A direct role for Sox10 in specification of neural crest-derived sensory neurons. *Development*, 133(23):4619–30.

Carreira-Barbosa, F., Kajita, M., Morel, V., Wada, H., Okamoto, H., Martinez Arias, A., Fujita, Y., Wilson, S. W., and Tada, M. (2009). Flamingo regulates epiboly and convergence/extension movements through cell cohesive and signalling functions during zebrafish gastrulation. *Development*, 136(3):383–392.

Charrasse, S., Meriane, M., Comunale, F., Blangy, A., and Gauthier-Rouviere, C. (2002). N-cadherin-dependent cell-cell contact regulates rho gtpases and beta-catenin localization in mouse c2c12 myoblasts. *The Journal of Cell Biology*, 158(5):953–965.

Chen, W. C. and Obrink, B. (1991). Cell-cell contacts mediated by e-cadherin (uvomorulin) restrict invasive behavior of l-cells. *The Journal of Cell Biology*, 114(2):319–327.

Chen, W.-S., Antic, D., Matis, M., Logan, C. Y., Povelones, M., Anderson, G. A., Nusse, R., and Axelrod, J. D. (2008). Asymmetric homotypic interactions of the atypical cadherin flamingo mediate intercellular polarity signaling. *Cell*, 133(6):1093 – 1105.

Chen, Y. and Struhl, G. (1996). Dual roles for patched in sequestering and transducing hedgehog. *Cell*, 87(3):553 – 563.

Cohen, J. E. (2004). Mathematics is biology's next microscope, only better; biology is mathematics' next physics, only better. *Plos Biol*, 2(12):e439.

Costa, R. M., Soto, X., Chen, Y., Zorn, A. M., and Amaya, E. (2008). spib is required for primitive myeloid development in xenopus. *Blood*, 112(6):2287–96.

Couzin, I. D. (2010). An Informative Itinerary. *Science*, 328(5977):430–.

Couzin, I. D., Krause, J., Franks, N. R., and Levin, S. A. (2005). Effective leadership and decision-making in animal groups on the move. *Nature*, 433(7025):513.

Curtis, A. S. G. (1964). The Mechanism of Adhesion of Cells to Glass. *The Journal of Cell Biology*, 20(2):199–215.

Davis, E. M. and Trinkaus, J. P. (1981). Significance of cell-to-cell contacts for the directional movement of neural crest cells within a hydrated collagen lattice. *J Embryol Exp Morphol*, 63(1):29–51.

Day, C. L., J., Harrist, T. J., Gorstein, F., Sober, A. J., Lew, R. A., Friedman, R. J., Pasternack, B. S., Kopf, A. W., Fitzpatrick, T. B., and Mihm, M. C., J. (1981). Malignant melanoma. prognostic significance of "microscopic satellites" in the reticular dermis and subcutaneous fat. *Annals of Surgery*, 194(1):108–12.

De Calisto, J., Araya, C., Marchant, L., Riaz, C. F., and Mayor, R. (2005). Essential role of non-canonical Wnt signalling in neural crest migration. *Development*, 132(11):2587–97.

DeLuca, S. M., Gerhart, J., Cochran, E., Simak, E., Blitz, J., Mattiacci-Paessler, M., Knudsen, K., and George-Weinstein, M. (1999). Hepatocyte growth factor/scatter factor promotes a switch from e- to n-cadherin in chick embryo epiblast cells. *Experimental Cell Research*, 251(1):3 – 15.

Drescher, U. (1997). The eph family in the patterning of neural development. *Current Biology*, 7(12):799 – 807.

Dunn, G. A. and Paddock, S. W. (1982). Analysing the motile behaviour of cells: a general approach with special reference to pairs of cells in collision. *Philosophical Transactions of the Royal Society of London. Series B, Biological Sciences*, 299(1095):147–57.

Durham, W. M., Kessler, J. O., and Stocker, R. (2009). Disruption of Vertical Motility by Shear Triggers Formation of Thin Phytoplankton Layers. *Science*, 323(5917):1067–1070.

Erez, N., Bershadsky, A., and Geiger, B. (2005). Signaling from adherens-type junctions. *European Journal of Cell Biology*, 84(2-3):235–244.

Erickson, C. and Olivier, K. (1983). Negative chemotaxis does not control quail neural crest cell dispersion. *Developmental Biology*, 96(2):542–551.

Erickson, C. A. (1985). Control of neural crest cell dispersion in the trunk of the avian embryo. *Developmental Biology*, 111(1):138–57.

Farooqui, R. and Fenteany, G. (2005). Multiple rows of cells behind an epithelial wound edge extend cryptic lamellipodia to collectively drive cell-sheet movement. *Journal of Cell Science*, 118(1):51–63.

Friedl, P. and Gilmour, D. (2009). Collective cell migration in morphogenesis, regeneration and cancer. *Nat Rev Mol Cell Biol*, 10(7):445–457.

Friedl, P. and Wolf, K. (2003). Tumour-cell invasion and migration: diversity and escape mechanisms. *Nature Reviews Cancer*, 3(5):362–74.

Gaggioli, C., Hooper, S., Hidalgo-Carcedo, C., Grosse, R., Marshall, J. F., Harrington, K., and Sahai, E. (2007). Fibroblast-led collective invasion of carcinoma cells with differing roles for RhoGTPases in leading and following cells. *Nature Cell Biology*, 9(12):1392–400.

Garcia Morente, M. (1939). *Lecciones Preliminares De Filosofia/ Preliminary Lessons Of Philosophy*. Losada; 1st. edition (2004).

Gessert, S., Maurus, D., Rssner, A., and Khl, M. (2007). Pescadillo is required for xenopus laevis eye development and neural crest migration. *Developmental Biology*, 310(1):99 – 112.

Gould, S. J. (1977). *Ontogeny and Phylogeny*. Harvard University Press.

Grégoire, G. and Chaté, H. (2004). Onset of collective and cohesive motion. *Phys Rev Lett*, 92(2).

Grégoire, G., Chaté, H., and Tu, Y. (2003). Moving and staying together without a leader. *Physica D*, 181(2):157–170.

Grossberger, D., Marcuz, A., Du Pasquier, L., and Lambris, J. D. (1989). Conservation of structural and functional domains in complement component c3 of xenopus and mammals. *Proceedings of the National Academy of Sciences of the United States of America*, 86(4):1323–7.

Groves, J. T. and Kuriyan, J. (2010). Molecular mechanisms in signal transduction at the membrane. *Nature Publishing Group*, 17(6):659–665.

Gubb, D. and García-Bellido, A. (1982). A genetic analysis of the determination of cuticular polarity during development in Drosophila melanogaster. *Journal of embryology and experimental morphology*, 68:37–57.

Gupton, S. L. and Gertler, F. B. (2007). Filopodia: the fingers that do the walking. *Science's Stke*, 2007(400):re5.

Gurdon, J. B. and Bourillot, P. Y. (2001). Morphogen gradient interpretation. *Nature*, 413(6858):797–803.

Haas, P. and Gilmour, D. (2006). Chemokine signaling mediates self-organizing tissue migration in the zebrafish lateral line. *Developmental Cell*, 10(5):673–80.

Hadeball, B., Borchers, A., and Wedlich, D. (1998). Xenopus cadherin-11 (xcadherin-11) expression requires the wg/wnt signal. *Mechanisms of Development*, 72(1-2):101 – 113.

Harland, R. M. (1991). In situ hybridization: An improved whole-mount method for xenopus embryos. In Kay, B. K. and Peng, H. B., editors, *Xenopus laevis: Practical Uses in Cell and Molecular Biology*, volume 36 of *Methods in Cell Biology*, pages 685 – 695. Academic Press.

Harris, A. (1973). Location of cellular adhesions to solid substrata. *Developmental Biology*, 35(1):97–114.

Heanue, T. A. and Pachnis, V. (2007). Enteric nervous system development and hirschsprung's disease: advances in genetic and stem cell studies. *Nature Reviews Neuroscience*, 8(6):466–479.

Heasman, S. J. and Ridley, A. J. (2008). Mammalian rho gtpases: new insights into their functions from in vivo studies. *Nat Rev Mol Cell Biol*, 9(9):690–701.

Hegerfeldt, Y., Tusch, M., Bröcker, E.-B., and Friedl, P. (2002). Collective cell movement in primary melanoma explants: plasticity of cell-cell interaction, beta1-integrin function, and migration strategies. *Cancer Research*, 62(7):2125–30.

Higgins, D. G. and Sharp, P. M. (1988). Clustal: a package for performing multiple sequence alignment on a microcomputer. *Gene*, 73(1):237 – 244.

Holland, J. H. (1998). *Emergence. From Chaos to Order*. Oxford University Press.

Holtfreter, J. (1943). Properties and functions of the surface coat in amphibian embryos. *Journal of Experimental Zoology*, 93(2):251–323.

Hugli, T. E. (1990). Structure and function of c3a anaphylatoxin. *Current Topics in Microbiology & Immunology*, 153:181–208.

Huttenlocher, A., Lakonishok, M., Kinder, M., Wu, S., Truong, T., Knudsen, K. A., and Horwitz, A. F. (1998). Integrin and cadherin synergy regulates contact inhibition of migration and motile activity. *Journal of Cell Biology*, 141(2):515–26.

Ikegaya, Y., Aaron, G., Cossart, R., Aronov, D., Lampl, I., Ferster, D., and Yuste, R. (2004). Synfire Chains and Cortical Songs: Temporal Modules of Cortical Activity. *Science*, 304(5670):559–564.

Itoh, R. E., Kurokawa, K., Ohba, Y., Yoshizaki, H., Mochizuki, N., and Matsuda, M. (2002). Activation of Rac and Cdc42 Video Imaged by Fluorescent Resonance Energy Transfer-Based Single-Molecule Probes in the Membrane of Living Cells. *Mol. Cell. Biol.*, 22(18):6582–6591.

Izzard, C. and Lochner, L. (1976). Cell-to-substrate contacts in living fibroblasts: an interference reflexion study with an evaluation of the technique. *J Cell Sci*, 21(1):129–159.

Jaffe, A. B. and Hall, A. (2005). Rho gtpases: biochemistry and biology. *Annual Review of Cell & Developmental Biology*, 21:247–69.

Janeway, C. A., Travers, P., Walport, M., and Shlomchik, M. J. (2001). *Immunobiology*. New York: Garland Science, 5 edition.

Jiang, Y., tsai Liu, M., and Gershon, M. D. (2003). Netrins and dcc in the guidance of migrating neural crest-derived cells in the developing bowel and pancreas. *Developmental Biology*, 258(2):364 – 384.

Kaibuchi, K., Kuroda, S., and Amano, M. (1999). Regulation of the cytoskeleton and cell adhesion by the rho family gtpases in mammalian cells. *Annual Review of Biochemistry*, 68:459–86.

Kant, I. (1790). *Critique of Judgement*. Oxford University Press, USA (2007).

Karsenti, E. (2008). Self-organization in cell biology: a brief history. *Nature Review in Molecular & Cell Biology*, 9(3):255–62.

Karsenti, E., Newport, J., Hubble, R., and Kirschner, M. (1984). Interconversion of metaphase and interphase microtubule arrays, as studied by the injection of centrosomes and nuclei into Xenopus eggs. *The Journal of Cell Biology*, 98(5):1730–1745.

Kashef, J., Köhler, A., Kuriyama, S., Alfandari, D., Mayor, R., and Wedlich, D. (2009). Cadherin-11 regulates protrusive activity in xenopus cranial neural crest cells upstream of trio and the small gtpases. *Genes & Development*, 23(12):1393–1398.

Kay, R. R., Langridge, P., Traynor, D., and Hoeller, O. (2008). Changing directions in the study of chemotaxis. *Nature Review in Molecular & Cell Biology*, 9(6):455–463.

Keller, E. F. (June 2007). Contenders for life at the dawn of the twenty-first century: approaches from physics, biology and engineering. *Interdisciplinary Science Reviews*, 32:113–122(10).

Keller, R. (2002). Shaping the Vertebrate Body Plan by Polarized Embryonic Cell Movements. *Science*, 298(5600):1950–1954.

Kelsh, R. N., Dutton, K., Medlin, J., and Eisen, J. S. (2000). Expression of zebrafish fkd6 in neural crest-derived glia. *Mechanisms of Development*, 93(1-2):161 – 164.

Killian, E. C. O., Birkholz, D. A., and Artinger, K. B. (2009). A role for chemokine signaling in neural crest cell migration and craniofacial development. *Developmental Biology*, 333(1):161 – 172.

Kimmel, C. B., Ballard, W. W., Kimmel, S. R., Ullmann, B., and Schilling, T. F. (1995). Stages of embryonic development of the zebrafish. *American Journal of Anatomy*, 203(3):253–310.

King, J. S. and Insall, R. H. (2009). Chemotaxis: finding the way forward with dictyostelium. *Trends In Cell Biology*, 19(10):523–530.

Kirby, M. and Waldo, K. (1990). Role of neural crest in congenital heart disease. *Circulation*, 82(2):332–340.

Kitagawa, T. and Aikawa, T. (1976). Enzyme coupled immunoassay of insulin using a novel coupling reagent. *Journal of Biochemistry*, 79(1):233–6.

Knecht, A. K. and Bronner-Fraser, M. (2002). Induction of the neural crest: a multigene process. *Nature Reviews Genetics*, 3(6):453–461.

Kontges, G. and Lumsden, A. (1996). Rhombencephalic neural crest segmentation is preserved throughout craniofacial ontogeny. *Development*, 122(10):3229–3242.

Krogh, A., Larsson, B., von Heijne, G., and Sonnhammer, E. L. (2001). Predicting transmembrane protein topology with a hidden markov model: application to complete genomes. *Journal of Molecular Biology*, 305(3):567 – 580.

Kucia, M., Jankowski, K., Reca, R., Wysoczynski, M., Bandura, L., Allendorf, D., Zhang, J., Ratajczak, J., and Ratajczak, M. (2004). Cxcr4sdf-1 signalling, locomotion, chemotaxis and adhesion. *Journal of Molecular Histology*, 35:233–245. 10.1023/B:HIJO.0000032355.66152.b8.

Kuriyama, S. and Mayor, R. (2008). Molecular analysis of neural crest migration. *Philosophical Transactions of the Royal Society of London. Series B, Biological Sciences*, 363(1495):1349–62.

Kwon, G. S., Viotti, M., and Hadjantonakis, A. K. (2008). The endoderm of the mouse embryo arises by dynamic widespread intercalation of embryonic and extraembryonic lineages. *Developmental Cell*, 15(4):509–20.

LaBonne, C. and Bronner-Fraser, M. (1998). Neural crest induction in Xenopus: evidence for a two-signal model. *Development*, 125(13):2403–14.

Lartillot, O., Toiviainen, P., and Eerola, T. (2008). A matlab toolbox for music information retrieval. In Christine Preisach, H. B. and Schmidt-thieme, L., editors, *Data analysis, machine learning and applications, studies in classification, data analysis, and knowledge organization*. Reinbek bei Hamburg: Springer-Verlag.

Lauffenburger, D. A. and Horwitz, A. F. (1996). Cell migration: A physically integrated molecular process. *Cell*, 84(3):359–369.

Lawrence, P. A., Struhl, G., and Casal, J. (2007). Planar cell polarity: one or two pathways? *Nature Reviews Genetics*, 8(7):555–563.

LeDouarin, N. and Kalcheim, C. (1999). *The Neural Crest*. Cambridge University Press.

Li, L., Wang, B. H., Wang, S., Moalim-Nour, L., Mohib, K., Lohnes, D., and Wang, L. (2010). Individual cell movement, asymmetric colony expansion, rho-associated kinase, and e-cadherin impact the clonogenicity of human embryonic stem cells. *Biophysical Journal*, 98(11):2442 – 2451.

Lippincott-Schwartz, J., Roberts, T. H., and Hirschberg, K. (2000). Secretory protein trafficking and organelle dynamics in living cells. *Annual Review of Cell and Developmental Biology*, 16(1):557–589.

Litsiou, A., Hanson, S., and Streit, A. (2005). A balance of FGF, BMP and WNT signalling positions the future placode territory in the head. *Development*, 132(18):4051–4062.

Lo, C. W., Cohen, M. F., Huang, G. Y., Lazatin, B. O., Patel, N., Sullivan, R., Pauken, C., and Park, S. (1997). Cx43 gap junction gene expression and gap junctional communication in mouse neural crest cells. *Developmental Genetics*, 20(2):119–132.

Macara, I. G. (2004). Parsing the Polarity Code. *Nature Review in Molecular & Cell Biology*, 5(3):220–231.

Machacek, M., Hodgson, L., Welch, C., Elliott, H., Pertz, O., Nalbant, P., Abell, A., Johnson, G. L., Hahn, K. M., and Danuser, G. (2009). Coordination of rho gtpase activities during cell protrusion. *Nature*, 461(7260):99–103.

Manahan, C. L., Iglesias, P. A., Long, Y., and Devreotes, P. N. (2004). Chemoattractant signaling in dictyostelium discoideum. *Annual Review of Cell and Developmental Biology*, 20(1):223–253.

Marchant, L., Linker, C., Ruiz, P., Guerrero, N., and Mayor, R. (1998). The inductive properties of mesoderm suggest that the neural crest cells are specified by a bmp gradient. *Developmental Biology*, 198(2):319 – 329.

Mardia, K. V. and Jupp, P. E. (2000). *Directional Statistics*. Wiley.

Matsuoka, T., Ahlberg, P. E., Kessaris, N., Iannarelli, P., Dennehy, U., Richardson, W. D., McMahon, A. P., and Koentges, G. (2005). Neural crest origins of the neck and shoulder. *Nature*, 436(7049):347–355.

Matthews, H. K., Broders-Bondon, F., Thiery, J. P., and Mayor, R. (2008a). Wnt11r is required for cranial neural crest migration. *Developmental Dynamics*, 237(11):3404–3409.

Matthews, H. K., Marchant, L., Carmona-Fontaine, C., Kuriyama, S., Larraín, J., Holt, M. R., Parsons, M., and Mayor, R. (2008b). Directional migration of neural crest cells in vivo is regulated by Syndecan-4/Rac1 and non-canonical Wnt signaling/RhoA. *Development*, 135(10):1771–80.

Mattila, P. K. and Lappalainen, P. (2008). Filopodia: molecular architecture and cellular functions. *Nature Reviews Molecuar Cell Biology*, 9(6):446–454.

Mayor, R. and Carmona-Fontaine, C. (2010). Keeping in touch with contact inhibition of locomotion. *Trends in Cell Biology*, 20(6):319 – 328.

Mayor, R., Guerrero, N., and Martnez, C. (1997). Role of fgf andnogginin neural crest induction. *Developmental Biology*, 189(1):1 – 12.

Mayor, R., Morgan, R., and Sargent, M. (1995). Induction of the prospective neural crest of Xenopus. *Development*, 121(3):767–777.

McCusker, C., Cousin, H., Neuner, R., and Alfandari, D. (2009). Extracellular Cleavage of Cadherin-11 by ADAM Metalloproteases Is Essential for Xenopus Cranial Neural Crest Cell Migration. *Mol. Biol. Cell*, 20(1):78–89.

McLennan, R., Teddy, J. M., Kasemeier-Kulesa, J. C., Romine, M. H., and Kulesa, P. M. (2010). Vascular endothelial growth factor (vegf) regulates cranial neural crest migration in vivo. *Developmental Biology*, 339(1):114 – 125.

McLin, V., Hu, C., Shah, R., and Jamrich, M. (2008). Expression of complement components coincides with early patterning and organogenesis in *Xenopus laevis*. *The International Journal of Developmental Biology*.

Milnor, J. (1985). On the concept of attractor. *Communications in Mathematical Physics*, 99:177–195.

Mitchell, M. (2009). *Complexity: A Guided Tour*. Oxford University Press, USA.

Montcouquiol, M., Crenshaw, E. B., and Kelley, M. W. (2006). Noncanonical wnt signalling and neural polarity. *Annual Review of Neuroscience*, 29(1):363–386.

Montell, D. J. (2008). Morphogenetic cell movements: Diversity from modular mechanical properties. *Science*, 322(5907):1502–1505.

Moore, B. (1980). A modification of the Rayleigh test for vector data. *Biometrika*, 67(1):175–180.

Moury, J. D. and Jacobson, A. G. (1990). The origins of neural crest cells in the axolotl. *Developmental Biology*, 141(2):243 – 253.

Muñoz, R., Moreno, M., Oliva, C., Orbenes, C., and Larraín, J. (2006). Syndecan-4 regulates non-canonical Wnt signalling and is essential for convergent and extension movements in *Xenopus* embryos. *Nat Cell Biol*, 8(5):492–500.

Nabeshima, K., Shimao, Y., Inoue, T., Itoh, H., Kataoka, H., and Koono, M. (1998). Hepatocyte growth factor/scatter factor induces not only scattering but also cohort migration of human colorectal-adenocarcinoma cells. *International Journal of Cancer*, 78(6):750–9.

Nair, S. and Schilling, T. F. (2008). Chemokine signaling controls endodermal migration during zebrafish gastrulation. *Science*, 322(5898):89–92.

Nakagawa, S. and Takeichi, M. (1995). Neural crest cell-cell adhesion controlled by sequential and subpopulation-specific expression of novel cadherins. *Development*, 121(5):1321–1332.

Nakagawa, S. and Takeichi, M. (1998). Neural crest emigration from the neural tube depends on regulated cadherin expression. *Development*, 125(15):2963–2971.

Nelson, C. M., Pirone, D. M., Tan, J. L., and Chen, C. S. (2004). Vascular endothelial-cadherin regulates cytoskeletal tension, cell spreading, and focal adhesions by stimulating rhoa. *Molecular Biology of the Cell*, 15(6):2943–53.

Nicolis, G. and Prigogine, I. (1977). *Self-organization in nonequilibrium systems from dissipative structures to order through fluctuations*. Wiley, New York.

Nieto, M., Bennett, M., Sargent, M., and Wilkinson, D. (1992). Cloning and developmental expression of Sna, a murine homologue of the Drosophila snail gene. *Development*, 116(1):227–237.

Nieto, M. A., Sargent, M. G., Wilkinson, D. G., and Cooke, J. (1994). Control of cell behavior during vertebrate development by slug, a zinc finger gene. *Science*, 264(5160):835–839.

Nietzsche, F. (1873). *Philosophy in the Tragic Age of the Greeks*. Gateway Editions, 1962.

Nieuwkoop, P. and Faber, J. (1967). *Normal Table of Xenopus laevis. A Systematical and Chronological Survey of the Development from the Fertilized Egg till the End of Metamorphosis*. North-Holland Publishing Co.

Ninomiya, H., Elinson, R. P., and Winklbauer, R. (2004). Antero-posterior tissue polarity links mesoderm convergent extension to axial patterning. *Nature*, 430(6997):364–367.

Nobes, C. D. and Hall, A. (1995). Rho, rac, and cdc42 gtpases regulate the assembly of multimolecular focal complexes associated with actin stress fibers, lamellipodia, and filopodia. *Cell*, 81(1):53–62.

Nowak, M. A. and Sigmund, K. (2004). Evolutionary Dynamics of Biological Games. *Science*, 303(5659):793–799.

Paddock, S. W. and Dunn, G. A. (1986). Analysing collisions between fibroblasts and fibrosarcoma cells: fibrosarcoma cells show an active invasionary response. *Journal of Cell Science*, 81:163–87.

Pearson, H. (2006). Genetics: What is a gene? *Nature*, 441(7092):398–401.

Perissinotto, D., Iacopetti, P., Bellina, I., Doliana, R., Colombatti, A., Pettway, Z., Bronner-Fraser, M., Shinomura, T., Kimata, K., Morgelin, M., Lofberg, J., and Perris, R. (2000). Avian neural crest cell migration is diversely regulated by the two major hyaluronan-binding proteoglycans PG-M/versican and aggrecan. *Development*, 127(13):2823–2842.

Perris, R. and Perissinotto, D. (2000). Role of the extracellular matrix during neural crest cell migration. *Mechanisms of Development*, 95(1-2):3 – 21.

Pertz, O., Hodgson, L., Klemke, R. L., and Hahn, K. M. (2006). Spatiotemporal dynamics of rhoa activity in migrating cells. *Nature*, 440(7087):1069–72.

Petrie, R. J., Doyle, A. D., and Yamada, K. M. (2009). Random versus directionally persistent cell migration. *Nature Reviews in Molecuar Cell Biology*, 10(8):538–549.

Pezeron, G., Mourrain, P., Courty, S., Ghislain, J., Becker, T. S., Rosa, F. M., and David, N. B. (2008). Live analysis of endodermal layer formation identifies random walk as a novel gastrulation movement. *Current Biology*, 18(4):276–81.

Pollard, T. D. and Borisy, G. G. (2003). Cellular motility driven by assembly and disassembly of actin filaments. *Cell*, 112(4):453–65.

Prigogine, I. and Stengers, I. (1977). *La Nueva Alianza / The New Alliance: Metamorfosis De La Ciencia / Metamorphosis Of Science*. Alianza Universidad (Spanish Edition), 2002 edition.

Rafelski, S. M. and Marshall, W. F. (2008). Building the cell: design principles of cellular architecture. *Nat Rev Mol Cell Biol*, 9(8):593–602.

Rafelski, S. M. and Theriot, J. A. (2004). Crawling toward a unified model of cell mobility: spatial and temporal regulation of actin dynamics. *Annual Review of Biochemistry*, 73:209–39.

Rao, C. V., Wolf, D. M., and Arkin, A. P. (2002). Control, exploitation and tolerance of intracellular noise. *Nature*, 420(6912):231–7.

Reichlin, M. (1980). Use of glutaraldehyde as a coupling agent for proteins and peptides. In Van Vunakis, H. and Langone, J., editors, *Methods in Enzymology*. Academic Press, New York.

Richardson, B. E., Beckett, K., Nowak, S. J., and Baylies, M. K. (2007). Scar/wave and arp2/3 are crucial for cytoskeletal remodeling at the site of myoblast fusion. *Development*, 134(24):4357–67.

Ridley, A. J., Schwartz, M. A., Burridge, K., Firtel, R. A., Ginsberg, M. H., Borisy, G., Parsons, J. T., and Horwitz, A. R. (2003). Cell migration: integrating signals from front to back. *Science*, 302(5651):1704–9.

Riento, K. and Ridley, A. J. (2003). Rocks: multifunctional kinases in cell behaviour. *Nature Reviews Molecular Cell Biology*, 4(6):446–56.

Rørth, P. (2009). Collective cell migration. *Annu Rev Cell Dev Biol*, 25:407–29.

Rottner, K., Hall, A., and Small, J. V. (1999). Interplay between rac and rho in the control of substrate contact dynamics. *Current Biology*, 9(12):640–8.

Sadaghiani, B. and Thibaud, C. H. (1987). Neural crest development in the xenopus laevis embryo, studied by interspecific transplantation and scanning electron microscopy. *Developmental Biology*, 124(1):91 – 110.

Sahu, A. and Lambris, J. D. (2001). Structure and biology of complement protein c3, a connecting link between innate and acquired immunity. *Immunological Reviews*, 180(1):35–48.

Sauka-Spengler, T. and Bronner-Fraser, M. (2008). A gene regulatory network orchestrates neural crest formation. *Nature Review Molecular Cell Biology*, 9(7):557–68.

Schraufstatter, I., Discipio, R., Zhao, M., and Khaldoyanidi, S. (2009). C3a and c5a are chemotactic factors for human mesenchymal stem cells, which cause prolonged erk1/2 phosphorylation. *The Journal of Immunology*, 182(6):3827–3836.

Schrödinger, E. (1964). *My View of the World*. Cambridge University Press.

Scott, J. D. and Pawson, T. (2009). Cell signaling in space and time: Where proteins come together and when they're apart. *Science*, 326(5957):1220–1224.

Selleck, M. and Bronner-Fraser, M. (1995). Origins of the avian neural crest: the role of neural plate-epidermal interactions. *Development*, 121(2):525–538.

Semenov, M. V., Habas, R., MacDonald, B. T., and He, X. (2007). Snapshot: Noncanonical wnt signaling pathways. *Cell*, 131(7):1378.e1 – 1378.e2.

Shattil, S. J., Kim, C., and Ginsberg, M. H. (2010). The final steps of integrin activation: the end game. *Nat Rev Mol Cell Biol*, 11(4):288–300.

Shnitsar, I. and Borchers, A. (2008). PTK7 recruits dsh to regulate neural crest migration. *Development*, 135(24):4015–4024.

Simons, M. and Mlodzik, M. (2008). Planar cell polarity signaling: From fly development to human disease. *Annual Review of Genetics*, 42(1):517–540.

Simpson, C. D., Anyiwe, K., and Schimmer, A. D. (2008). Anoikis resistance and tumor metastasis. *Cancer Letters*, 272(2):177 – 185.

Sohrmann, M. and Peter, M. (2003). Polarizing without a c(l)ue. *Trends in Cell Biology*, 13(10):526 – 533.

Srinivas, S., Rodriguez, T., Clements, M., Smith, J. C., and Beddington, R. S. (2004). Active cell migration drives the unilateral movements of the anterior visceral endoderm. *Development*, 131(5):1157–64.

Steventon, B. (2008). *A Temporal Modulation of FGF, Wnt, BMP and Retinoic Acid Signalling is Required for Neural Crest Induction*. PhD thesis, University College London, UK.

Steventon, B., Araya, C., Linker, C., Kuriyama, S., and Mayor, R. (2009). Differential requirements of BMP and Wnt signalling during gastrulation and neurulation define two steps in neural crest induction. *Development*, 136(5):771–779.

Steventon, B., Carmona-Fontaine, C., and Mayor, R. (2005). Genetic network during neural crest induction: from cell specification to cell survival. *Seminars in Cell and Developmental Biology*, 16(6):647–54.

Stramer, B., Moreira, S., Millard, T., Evans, I., Huang, C.-Y., Sabet, O., Milner, M., Dunn, G., Martin, P., and Wood, W. (2010). Clasp-mediated microtubule bundling regulates persistent motility and contact repulsion in Drosophila macrophages in vivo. *The Journal of Cell Biology*, 189(4):681–689.

Sumpter, D., Buhl, J., Biro, D., and Couzin, I. (2008). Information transfer in moving animal groups. *Theory in Biosciences*, 127(2):177–186.

Svetic, V., Hollway, G. E., Elworthy, S., Chipperfield, T. R., Davison, C., Adams, R. J., Eisen, J. S., Ingham, P. W., Currie, P. D., and Kelsh, R. N. (2007). Sdf1a patterns zebrafish melanophores and links the somite and melanophore pattern defects in choker mutants. *Development*, 134(5):1011–1022.

Tada, M. and Smith, J. C. (2000). Xwnt11 is a target of Xenopus Brachyury: regulation of gastrulation movements via Dishevelled, but not through the canonical Wnt pathway. *Development*, 127(10):2227–38.

Taneyhill, L. A., Coles, E. G., and Bronner-Fraser, M. (2007). Snail2 directly represses cadherin6B during epithelial-to-mesenchymal transitions of the neural crest. *Development*, 134(8):1481–1490.

Taulet, N., Comunale, F., Favard, C., Charrasse, S., Bodin, S., and Gauthier-Rouvire, C. (2009). N-cadherin/p120 catenin association at cell-cell contacts occurs in cholesterol-rich membrane domains and is required for rhoa activation and myogenesis. *Journal of Biological Chemistry*, 284(34):23137–23145.

Tawk, M., Araya, C., Lyons, D. A., Reugels, A. M., Girdler, G. C., Bayley, P. R., Hyde, D. R., Tada, M., and Clarke, J. D. W. (2007). A mirror-symmetric cell division that orchestrates neuroepithelial morphogenesis. *Nature*, 446(7137):797–800.

Teddy, J. M. and Kulesa, P. M. (2004). In vivo evidence for short- and long-range cell communication in cranial neural crest cells. *Development*, 131(24):6141–51.

Theveneau, E., Marchant, L., Kuriyama, S., Gull, M., Moepps, B., Parsons, M., and Mayor, R. (2010). Collective chemotaxis requires contact-dependent cell polarity. *Developmental Cell*, 19(1):39 – 53.

Thiery, J. P., Acloque, H., Huang, R. Y. J., and Nieto, M. A. (2009). Epithelial-mesenchymal

transitions in development and disease. *Cell*, 139(5):871–890.

Torney, C., Neufeld, Z., and Couzin, I. D. (2009). Context-dependent interaction leads to emergent search behavior in social aggregates. *Proceedings of the National Academy of Sciences of the United States of America*, 106(52):22055–60.

Trinkaus, J. P. (1985). Further thoughts on directional cell movement during morphogenesis. *Journal of Neuroscience Research*, 13(1-2):1–19.

Trbulo, C., Aybar, M. J., Snchez, S. S., and Mayor, R. (2004). A balance between the anti-apoptotic activity of slug and the apoptotic activity of msx1 is required for the proper development of the neural crest. *Developmental Biology*, 275(2):325 – 342.

Vasilyev, A., Liu, Y., Mudumana, S., Mangos, S., Lam, P.-Y., Majumdar, A., Zhao, J., Poon, K.-L., Kondrychyn, I., Korzh, V., and Drummond, I. A. (2009). Collective cell migration drives morphogenesis of the kidney nephron. *PLoS Biol*, 7(1):e1000009.

Veeman, M. T., Axelrod, J. D., and Moon, R. T. (2003). A second canon. Functions and mechanisms of beta-catenin-independent Wnt signaling. *Developmental Cell*, 5(3):367–77.

Vicente-Manzanares, M. (2005). Cell migration at a glance. *Journal of Cell Sciences*, 118(21):4917–4919.

Vielmetter, J., Stolze, B., Bonhoeffer, F., and Stuermer, C. A. (1990). In vitro assay to test differential substrate affinities of growing axons and migratory cells. *Experimental Brain Research*, 81(2):283–7.

Vladar, E. K., Antic, D., and Axelrod, J. D. (2009). Planar cell polarity signaling: The developing cell's compass. *Cold Spring Harbor Perspectives in Biology*, 1(3).

Waddington, C. (1956). *Principles of Embryology*. London: George Allen & Unwin Ltd.

Walport, M. J. (2001a). Complement. First of two parts. *New England Journal of Medicine*, 344(14):1058–66.

Walport, M. J. (2001b). Complement. Second of two parts. *New England Journal of Medicine*, 344(15):1140–4.

Wang, Y. and Nathans, J. (2007). Tissue/planar cell polarity in vertebrates: new insights and new questions. *Development*, 134(4):647–58.

Wedlich-Soldner, R., Altschuler, S., Wu, L., and Li, R. (2003). Spontaneous Cell Polarization Through Actomyosin-Based Delivery of the Cdc42 GTPase. *Science*, 299(5610):1231–1235.

Weijer, C. J. (2009). Collective cell migration in development. *Journal of Cell Science*, 122(18):3215–3223.

Weisstein, E. (2007). Random walk–2-dimensional.

Westerfield, M. (2000). *The zebrafish book. A guide for the laboratory use of zebrafish (Danio rerio)*. University of Oregon Press, Eugene, 4th edition edition.

Wheeler, A. P. and Ridley, A. J. (2004). Why three rho proteins? rhoa, rhob, rhoc, and cell motility. *Experimental Cell Research*, 301(1):43–9.

Wilensky, U. (1998). Netlogo random balls model.

Wilensky, U. (1999). Netlogo.

Wilkinson, P. C. (1998). Assays of leukocyte locomotion and chemotaxis. *Journal of Immunological Methods*, 216(1-2):139–153.

Winklbauer, R., Selchow, A., Nagel, M., and Angres, B. (1992). Cell interaction and its role in mesoderm cell migration during xenopus gastrulation. *Developmental Dynamics*, 195(4):290–302.

Witzel, S., Zimyanin, V., Carreira-Barbosa, F., Tada, M., and Heisenberg, C.-P. (2006). Wnt11 controls cell contact persistence by local accumulation of Frizzled 7 at the plasma membrane. *The Journal of Cell Biology*, 175(5):791–802.

Wolf, K., Wu, Y. I., Liu, Y., Geiger, J., Tam, E., Overall, C., Stack, M. S., and Friedl, P. (2007). Multi-step pericellular proteolysis controls the transition from individual to collective cancer cell invasion. *Nature Cell Biology*, 9(8):893–904.

Wolpert, L. (1969). Positional information and the spatial pattern of cellular differentiation. *Journal of Theoretical Biology*, 25(1):1 – 47.

Worthylake, R. A. and Burridge, K. (2003). Rhoa and rock promote migration by limiting membrane protrusions. *Journal of Biological Chemistry*, 278(15):13578–13584.

Xu, J., Wang, F., Van Keymeulen, A., Herzmark, P., Straight, A., Kelly, K., Takuwa, Y., Sugimoto, N., Mitchison, T., and Bourne, H. R. (2003). Divergent signals and cytoskeletal assemblies regulate self-organizing polarity in neutrophils. *Cell*, 114(2):201–14.

Yap, A. S. and Kovacs, E. M. (2003). Direct cadherin-activated cell signaling. *The Journal of Cell Biology*, 160(1):11–16.

Young, H. M., Hearn, C. J., Farlie, P. G., Canty, A. J., Thomas, P. Q., and Newgreen, D. F. (2001). Gdnf is a chemoattractant for enteric neural cells. *Developmental Biology*, 229(2):503 – 516.

Zarkadis, I. K., Mastellos, D., and Lambris, J. D. (2001). Phylogenetic aspects of the complement system. *Developmental & Comparative Immunology*, 25(8-9):745 – 762.

Zicha, D. and Dunn, G. (1995). Are growth factors chemotactic agents? *Experimental Cell Research*, 221:526–529.